

# Wnt Signalling in Endocrine Resistant Breast Cancer

A thesis submitted to Cardiff University in  
candidature for the degree of  
Doctor of Medicine (MD)

Rachel Antonia Micallef

June 2012

Breast Cancer (Molecular Pharmacology) Group  
Cardiff University

## Declaration and statements

This work has not previously been accepted in substance for any degree and is not concurrently submitted in candidature for any degree.

Signed..... (candidate) Date.....

### STATEMENT 1

This thesis is being submitted in partial fulfillment of the requirements for the degree of ..... (insert MCh, MD, MPhil, PhD etc, as appropriate)

Signed..... (candidate) Date.....

### STATEMENT 2

This thesis is the result of my own independent work/investigation, except where otherwise stated. Other sources are acknowledged by explicit references.

Signed..... (candidate) Date.....

### STATEMENT 3

I hereby give consent for my thesis, if accepted, to be available for photocopying and for inter-library loan, and for the title and summary to be made available to outside organisations.

Signed..... (candidate) Date.....

### STATEMENT 4: PREVIOUSLY APPROVED BAR ON ACCESS

I hereby give consent for my thesis, if accepted, to be available for photocopying and for inter-library loans **after expiry of a bar on access previously approved by the Graduate Development Committee.**

Signed..... (candidate) Date.....

## Summary

Wnt signalling components are reported to be deregulated in breast cancer but the contribution of this pathway in endocrine resistance is less clearly defined. Endocrine resistance is an important clinical challenge affecting up to a quarter of all breast cancer patients and is associated with a poorer clinical prognosis.

This project focussed on exploring the role of Wnt signalling in endocrine resistant breast cancer cell models. Wnt pathway elements were deregulated in the acquired tamoxifen resistant cell line (Tam-R) compared to tamoxifen sensitive parental cells (MCF-7), with changes supportive of Wnt signalling activation in this tamoxifen resistant model apparent from Affymetrix HGU-133A gene microarray data and Western blot analysis. In contrast, Wnt signalling appeared to be suppressed based on Affymetrix data for MCF-7 cells treated with oestradiol for 10 days, with equivocal changes in MCF-7 cells treated with tamoxifen for 10 days or a faslodex resistant cell model (Fas-R).

Excitingly, Tam-R cells were also more sensitive than MCF-7 cells to pharmacological manipulation of Wnt signalling. While Wnt activation using Wnt3a and LiCl did not affect cell growth or migration, inhibition of Wnt signalling using IWP2, PNU 74654 and iCRT14 suppressed Tam-R cell growth and migration.

There is mounting evidence of cross talk between Wnt and EGFR signalling in breast cancer, and EGFR activity is upregulated in Tam-R cells. The project's findings tentatively supported cross-talk between the two signalling pathways in this model. Thus, targeting of the Wnt pathway alongside EGFR blockade was superior in suppressing cell growth and migration in Tam-R cells. The effect appeared to be more pronounced when Wnt signalling was inhibited at the nuclear level using iCRT14.

Collectively, these data suggest that Wnt signalling may play an important role in tamoxifen resistance where it may offer an opportunity for more effective therapeutic intervention to control relapse and associated tumour aggressiveness.

## Acknowledgements

This work was generously funded by In The Pink: a charity founded by a group of remarkable women who, through their fundraising activities, have helped support breast cancer research in Wales: thank you for providing me with the opportunity to conduct this research.

I would like to thank my supervisors Professor Peter Barrett-Lee and Professor Malcolm Mason for their encouragement and support. I am particularly grateful to Dr Stephen Hiscox who conceived this project and guided me every step of the way; thank you for being so patient and supportive.

I would like to acknowledge all the members of the Breast Cancer Molecular Pharmacology Group at Cardiff University School of Pharmacy and Pharmaceutical Sciences for their help in this project. Special thanks go to Dr Julia Gee for her professional guidance and valuable support; Dr Nicola Jordan for showing me the ropes in the lab, Chris Smith for his assistance; Carol Dutkowski in tissue culture; Lynne Farrow for her help with statistical analysis and Richard McClelland and Carol Dutkowski for their proof reading skills. I would also like to thank Rebecca Goode for her wonderful administrative skills.

Finally, I would like to thank my family for their support every step of the way.





## **Poster presentation**

**RA Micallef**, C Smith, D Barrow, RI Nicholson, JMW Gee, PJ Barrett-Lee, and SE Hiscox.

Wnt Signalling: A New Target for Treatment and Prevention of Endocrine Resistant Breast Cancer?

San Antonio Breast Cancer Symposium, San Antonio, Texas, December 2011 (P3-01-05).

# Table of Contents

Declaration and statements .....	i
Summary .....	ii
Acknowledgements .....	iii
Poster presentation .....	iv
Table of Contents .....	v
List of Figures .....	xii
List of Tables.....	xvi
List of abbreviations.....	xviii
1 Introduction.....	2
1.1 Wnt signalling .....	2
1.1.1 The Planar Cell Polarity Pathway .....	3
1.1.2 The Wnt- Calcium Pathway .....	3
1.1.3 The Canonical Pathway.....	5
1.2 Wnt signalling and breast cancer .....	21
1.3 Endocrine therapy in breast cancer.....	27
1.3.1 The Oestrogen Receptor.....	27
1.3.2 Endocrine therapy .....	33
1.3.3 Tamoxifen Resistance in Breast Cancer .....	35
1.4 Project Objectives.....	42
2 Materials and Methods.....	44

2.1	Materials .....	44
2.2	Cell media.....	51
2.3	Cell lines.....	51
2.4	Cell culture .....	52
2.4.1	Cell passaging .....	53
2.4.2	Cell lysis for protein analysis.....	54
2.5	Protein Analysis .....	54
2.5.1	Protein Concentration Assay.....	54
2.5.2	SDS-PAGE Analysis.....	58
2.5.3	Western Blotting .....	60
2.5.4	Immuno-detection .....	62
2.5.5	Chemoluminescent detection .....	63
2.5.6	Validation of LRP6 and p-LRP6 antibodies .....	66
2.6	Cell growth assays.....	72
2.6.1	MTT assay.....	72
2.6.2	Cell counting.....	72
2.6.3	Estimation of half maximal inhibitory concentration (IC <sub>50</sub> ) for IWP2, PNU 74654 and iCRT14.....	73
2.7	Cell Migration Assays .....	75
2.8	Immunocytochemistry.....	77
2.8.1	Methanol fix for active $\beta$ - catenin staining .....	77
2.8.2	Formal Saline for Ki67 proliferation assays .....	78

2.8.3	Verification of active $\beta$ -catenin antibody.....	79
2.9	Semi-quantitative reverse transcription polymerase chain reaction.....	79
2.9.1	Extraction of RNA .....	80
2.9.2	RNA quantification .....	80
2.9.3	Agarose gel electrophoresis .....	81
2.9.4	Reverse Transcription (RT).....	82
2.9.5	RT Master Mix .....	82
2.9.6	Polymerase Chain Reaction (PCR) .....	83
2.9.7	Thermocycling program for PCR amplification .....	84
2.10	Affymetrix microarray analysis.....	87
2.11	TCF/LEF Reporter Assay .....	90
2.11.1	Transfection procedure.....	90
2.11.2	Cell lysis/ Reporter gene assay .....	91
2.11.3	Luciferase assay (Promega dual luciferase reporter assay kit) .....	92
2.12	Statistical analysis .....	94
3	Characterisation of Wnt signalling components in breast cancer cell lines .....	96
3.1	Affymetrix Analysis .....	96
3.1.1	Affymetrix HGU-133A gene microarray data analysis: Tam-R cells versus MCF-7 cells .....	97
3.1.2	Affymetrix HGU-133A gene microarray data analysis: tamoxifen treated MCF-7 cells versus MCF-7 cells .....	100

3.1.3	Affymetrix HGU-133A gene microarray data analysis: Fas-R cells versus MCF-7 cells (model for absence of ER activity).....	103
3.1.4	Affymetrix HGU-133A gene microarray data analysis: MCF-7 cells treated with oestradiol (E2) [ $10^{-9}$ M] for 10 days versus MCF-7 cells (model for enhanced ER activity).....	106
3.2	SDS-Page/ Western blot.....	109
3.3	Immunocytochemistry analysis of beta-catenin in endocrine sensitive versus resistant cells .....	111
3.4	Summary .....	114
3.4.1	Affymetrix HGU-133A gene microarray data .....	114
3.4.2	Western Blot.....	114
3.4.3	Immunocytochemistry analysis of beta-catenin in endocrine sensitive versus resistant cells.....	115
4	Activation of Wnt signalling in endocrine sensitive and endocrine resistant breast cancer cells .....	117
4.1	Activation of Wnt signalling in endocrine-sensitive and resistant cell models by Wnt3a.....	119
4.1.1	Changes in cell signalling when MCF-7 and Tam-R cells were treated with Wnt3a.....	119
4.1.2	Effect of Wnt3a on cell growth.....	121
4.2	Modulation of Wnt activity in endocrine-sensitive and resistant cell models by Lithium Chloride .....	123

4.2.1	Changes in cell signalling when MCF-7 and Tam-R cells were treated with LiCl.....	123
4.2.2	Effect of LiCl on cell growth .....	125
4.2.3	Effect of LiCl on gene transcription using TCF/LEF (luciferase) Reporter Assays .....	127
4.3	Summary for Wnt pathway activation.....	130
4.3.1	Wnt3a activity .....	130
4.3.2	LiCl activity .....	131
5	Inhibition of Wnt signalling in endocrine sensitive and endocrine resistant breast cancer cells.....	134
5.1	Changes in cell function when MCF-7 and Tam-R cells were treated with Wnt inhibitors.....	135
5.1.1	IWP2 and PNU 74654 inhibit cell growth .....	135
5.1.2	IWP2 and PNU 74654 inhibit cell migration.....	145
5.2	Changes in cell signalling when MCF-7 and Tam-R cells were treated with Wnt inhibitors.....	147
5.2.1	IWP2 .....	147
5.2.2	PNU 74654.....	165
5.3	Changes in signalling as assessed by PCR.....	186
5.4	PNU 74654 activity .....	189
5.5	Further Wnt signalling inhibition studies .....	193
5.5.1	iCRT14.....	193

5.6	Summary for Wnt inhibition .....	206
5.6.1	Activity of Wnt inhibitors .....	206
5.6.2	Effect of Wnt inhibitors on cell signalling.....	208
5.6.3	Targeting different levels of Wnt signalling pathway has the same effect on cell function .....	211
6	Exploration of Wnt and EGFR signalling pathway interplay in tamoxifen resistant breast cancer cells .....	214
6.1	Effect of dual EGFR and Wnt pathway inhibition on cell growth .....	214
6.2	Effect of dual inhibition on cellular proliferation: Ki-67 staining .....	219
6.3	Effect of EGFR inhibition on Wnt pathway activity and exploration of dual Wnt/ EGFR inhibition .....	222
6.3.1	Effect of Wnt inhibition on EGFR activity .....	223
6.3.2	Effect of EGFR inhibition on Wnt activity .....	223
6.3.3	Effect of dual inhibition on MAPK activity.....	223
6.3.4	Effect of dual inhibition on AKT activity .....	223
6.4	Affymetrix HGU-133A gene microarray data analysis: Tam-R cells treated with gefitinib [1 $\mu$ M] versus Tam-R cells .....	228
6.5	Summary .....	230
7	Discussion.....	233
8	References.....	256
9	Appendix.....	282
9.1	Affymetrix .....	282

9.2	Growth assays.....	317
9.2.1	DMSO does not affect cell growth of MCF-7 and Tam-R cells in concentrations below 5 $\mu$ M .....	317
9.2.2	Dose effects of iCRT14 on growth of MCF-7 and Fas-R cell lines were determined by MTT assays.....	320



## List of Figures

Figure 1.1 .....	4
Figure 1.2 .....	6
Figure 1.3 .....	9
Figure 1.4 .....	14
Figure 1.5 .....	18
Figure 1.6 .....	22
Figure 1.7 .....	29
Figure 1.8 .....	32
Figure 1.9 .....	41
Figure 2.1 .....	57
Figure 2.2 .....	61
Figure 2.3 .....	68
Figure 2.4 .....	71
Figure 2.5 .....	74
Figure 2.6 .....	76
Figure 2.7 .....	93
Figure 3.1 .....	110
Figure 3.2 .....	112
Figure 3.3 .....	113
Figure 4.1 .....	120
Figure 4.2 .....	122
Figure 4.3 .....	124
Figure 4.4 .....	126
Figure 4.5 .....	128

Figure 4.6 .....	129
Figure 5.1 .....	136
Figure 5.2 .....	137
Figure 5.3 .....	139
Figure 5.4 .....	141
Figure 5.5 .....	142
Figure 5.6 .....	144
Figure 5.7 .....	146
Figure 5.8 .....	148
Figure 5.9 .....	150
Figure 5.10 .....	151
Figure 5.11 .....	152
Figure 5.12 .....	153
Figure 5.13 .....	155
Figure 5.14 .....	156
Figure 5.15 .....	157
Figure 5.16 .....	158
Figure 5.17 .....	160
Figure 5.18 .....	161
Figure 5.19 .....	162
Figure 5.20 .....	163
Figure 5.21 .....	164
Figure 5.22 .....	166
Figure 5.23 .....	167
Figure 5.24 .....	168

Figure 5.25 .....	169
Figure 5.26 .....	171
Figure 5.27 .....	172
Figure 5.28 .....	173
Figure 5.29 .....	174
Figure 5.30 .....	176
Figure 5.31 .....	177
Figure 5.32 .....	178
Figure 5.33 .....	179
Figure 5.34 .....	181
Figure 5.35 .....	182
Figure 5.36 .....	183
Figure 5.37 .....	184
Figure 5.38 .....	185
Figure 5.39 .....	187
Figure 5.40 .....	188
Figure 5.41 .....	190
Figure 5.42 .....	191
Figure 5.43 .....	192
Figure 5.44 .....	194
Figure 5.45 .....	196
Figure 5.46 .....	198
Figure 5.47 .....	199
Figure 5.48 .....	200
Figure 5.49 .....	202

Figure 5.50 .....	203
Figure 5.51 .....	205
Figure 6.1 .....	216
Figure 6.2 .....	218
Figure 6.3 .....	220
Figure 6.4 .....	221
Figure 6.5 .....	224
Figure 6.6 .....	225
Figure 6.7 .....	226
Figure 6.8 .....	227
Figure 6.9 .....	229
Figure 6.10 .....	231
Figure 7.1 .....	243
Figure 7.2 .....	248
Figure 9.1 .....	289
Figure 9.2 .....	299
Figure 9.3 .....	309
Figure 9.4 .....	318
Figure 9.5 .....	319
Figure 9.6 .....	321

## List of Tables

Table 1.1.....	20
Table 1.2.....	26
Table 2.1.....	50
Table 2.2.....	56
Table 2.3.....	59
Table 2.4.....	59
Table 2.5.....	65
Table 2.6.....	67
Table 2.7.....	85
Table 2.8.....	86
Table 2.9.....	88
Table 3.1.....	98
Table 3.2.....	99
Table 3.3.....	101
Table 3.4.....	102
Table 3.5.....	104
Table 3.6.....	105
Table 3.7.....	107
Table 3.8.....	108
Table 5.1.....	209
Table 5.2.....	210
Table 7.1.....	251
Table 7.2.....	252
Table 7.3.....	253

Table 9.1.....	282
Table 9.2.....	292
Table 9.3.....	302
Table 9.4.....	312

## List of abbreviations

ABC	active $\beta$ - catenin
ABCB1	ATP-binding cassette, sub-family B (MDR/TAP), member 1
AF	activation function
AHR	Aryl hydrocarbon receptor
AI	Aromatase inhibitor
AIB1	Amplified in breast cancer 1
ANGPTL4	Angiopoietin-like 4
ANTXR1	Anthrax toxin receptor 1
AP-1	Activator protein-1
APC	Adenomatous Polyposis Coli
BCL2	B-cell lymphoma 2
BGLAP	Bone gamma-carboxyglutamate (gla) protein
BIRC5	Baculoviral IAP repeat containing 5
BMP4	Bone morphogenetic protein 4
$\beta$ -Trecp	beta-transducin repeat-containing protein
CACNA2D3	Calcium channel, voltage-dependent, alpha 2/delta subunit 3
CamK2	Calcium- calmodulin kinase 2
CCND1	Cyclin D1

CCND2	Cyclin D2
CD44	CD44 molecule (Indian blood group)
CDH1	Cadherin 1, type 1, E-cadherin (epithelial)
CDKN2A	Cyclin-dependent kinase inhibitor 2A (melanoma, p16, inhibits CDK4)
CDON	Cdon homolog (mouse)
CEBPD	CCAAT/enhancer binding protein (C/EBP), delta
CK1	Casein kinase 1
CtBP	C terminal binding protein 1
CTGF	Connective tissue growth factor
CUBN	Cubilin (intrinsic factor-cobalamin receptor)
DAB2	Disabled homolog 2, mitogen-responsive phosphoprotein (Drosophila)
DBD	DNA binding domain
Dkk	Dickkopf
DLK1	Delta-like 1 homolog (Drosophila)
DMEM	Dulbecco's Modified Eagle Medium
DPP10	Dipeptidyl-peptidase 10 (non-functional)
Dvl	Dishevelled
DSCR1	Down syndrome critical region gene 1
E2	Oestradiol
EFNB1	Ephrin-B1



EGFR	Epidermal growth factor receptor
EGR1	Early growth response 1
EnR	Endoplasmic Reticulum
ER	Oestrogen Receptor
ERE	Oestrogen responsive elements
ETS2	V-Ets erythroblastosis virus E26 oncogene homolog 2 (avian)
Fas-R	Fulvestrant resistant cell line derived from MCF-7
FGF	Fibroblast growth factor
FN1	Fibronectin 1
FCS	Foetal calf serum
FOSL1	FOS-like antigen 1
FST	Follistatin
Fz	Frizzled
GDF5	Growth differentiation factor 5
GDNF	Glial cell derived neurotrophic factor
GJA1	Gap junction protein, alpha 1
GSK-3	Glycogen synthase kinase 3
GnRH	Gonadotropin releasing hormone
HBD	Hormone binding domain
HDAC	Histone deacetylase

HMG	high mobility group
HER2	human epidermal growth factor receptor 2
ID2	Inhibitor of DNA binding 2, dominant negative helix-loop-helix protein
IGF	Insulin-like growth factor
IL6	Interleukin 6 (interferon, beta 2)
IRS1	Insulin receptor substrate 1
JAG1	Jagged 1
JNK	Jun kinase
KLF5	Kruppel-like factor 5 (intestinal)
LEF-1	Leukaemia enhancer binding factor
LRP	Lipoprotein receptor related protein
MET	Met proto-oncogene (hepatocyte growth factor receptor)
MMP	Matrix metalloproteinase
MMTV	Mouse mammary tumour virus
MYC	V-myc myelocytomatosis viral oncogene homolog (avian)
NANOG	Nanog homeobox
NRCAM	Neuronal cell adhesion molecule
NROR	Nuclear receptor co-repressor
NRP1	Neuropilin 1
NTRK2	Neurotrophic tyrosine kinase, receptor, type 2

PBS	phosphate- buffered saline
PCP	Planar Cell Polarity
PDGFRA	Platelet-derived growth factor receptor, alpha polypeptide
PITX2	Paired-like homeodomain 2
PKC	protein kinase C
PLAUR	Plasminogen activator, urokinase receptor
POU5F1	POU class 5 homeobox 1
PPAP2B	Phosphatidic acid phosphatase type 2B
PPARD	Peroxisome proliferator-activated receptor delta
PTCH1	Patched 1
PTGS2	Prostaglandin-endoperoxide synthase 2 (prostaglandin G/H synthase and cyclooxygenase)
Rac1	Ras-related C3 botulinum toxin substrate 1
RanBP3	Ran binding protein 3
ROCK	Rho- associated kinase
RPMI	RPMI 1640 containing phenol- red pH indicator
Rspo	R-Spondin
RUNX2	Runt-related transcription factor 2
S	Serine
SERD	Selective oestrogen receptor down regulators

SFRP	Secreted frizzled related protein
SIX	SIX homeobox
SMO	Smoothened, frizzled family receptor
SOST	Sclerostin
SOX	SRY (sex determining region Y)-box
SP- 1	Specificity protein- 1
SSRI	Selective serotonin reuptake inhibitors
T	Threonine
Tam-R	Tamoxifen resistant cell line derived from MCF-7
Tb	T, brachyury homolog (mouse)
TBST	Tris- Buffered Saline - Tween buffer solution
TLE1	Transducin-like enhancer protein 1
TCF	T-cell factor
TCF7L	Transcription factor 7-like
TF	Transcription factor
TGFB3	Transforming growth factor, beta 3
TRE	Transcriptional response element
TWIST	Twist homolog (Drosophila)
VEGF	Vascular endothelial growth factor
Wg	Wingless

WIF-1	Wnt inhibitory factor 1
WISP	WNT1 inducible signalling pathway protein
Wnt	Wingless-type MMTV integration site family member
WRE	Wnt responsive element
wRPMI	Phenol-red- free RPMI 1640

# Chapter 1

## Introduction

# 1 Introduction

## 1.1 Wnt signalling

Wnt signalling plays a key role in embryogenesis where it controls cell proliferation and stem cell fate. In mature tissues it is responsible for maintaining normal tissue architecture and function and regulates stem cell renewal. Germ line mutations of Wnt signalling have been linked to congenital defects; in mature tissues, somatic mutations resulting in Wnt activation can lead to cancer (Goss K 2011).

Wnt signalling came into prominence around thirty years ago from studies investigating a *Drosophila* mutant that lacked wings. The mutation was linked to a gene which determined anterior posterior polarity within individual embryonic segments. This gene was called wingless (Wg) (Sharma and Chopra 1976). It was also recognised that most cases of mice mammary tumours were caused by the mouse mammary tumour virus (MMTV). MMTV is a retrovirus that can be transmitted in milk. The MMTV viral genome is inserted into the host DNA. If this DNA is inserted inside or near an oncogene, it can alter the expression of that gene and cause cancer. In 1982, Roeland Nusse and Harold Varmus identified a mouse gene that was induced by MMTV called Int1 (Nusse and Varmus 1982). The two parts of the puzzle came together in 1987. Rij et al. (1987) isolated the *Drosophila* homolog of Int-1 (Dint-1). They found that Dint-1 was identical to Wg. The word Wnt was coined (Wg and Int-1) and the protein was called Wnt-1.

Three main branches of the Wnt pathway are described in the literature: the Planar Cell Polarity (PCP) pathway, the Wnt- Calcium Pathway and the Canonical/  $\beta$ -catenin pathway. The PCP pathway regulates cytoskeletal movements. The Wnt- Calcium pathway is important during the embryonic phase of gastrulation where it

regulates cell adhesion and cell movements. The canonical pathway regulates levels of cytoplasmic and nuclear  $\beta$ -catenin.

### **1.1.1 The Planar Cell Polarity Pathway**

The PCP pathway regulates cell movements during gastrulation and cell polarity. Signalling is initiated through the Frizzled (Fz) receptor at the cell membrane. Rho GTPases (including Rac) are recruited through the PDZ and DEP domains (see section 1.3.5) of Dishevelled (Dvl) and trigger two separate pathways. Daam1 (a formin homology protein) is required for activation of Rho, which in turn activates Rho- associated kinase (ROCK). Rac activation stimulates Jun kinase (JNK). The reactions lead to changes in the cell's actin cytoskeleton (see Figure 1.1).

### **1.1.2 The Wnt- Calcium Pathway**

Wnt- Calcium signalling is also initiated through Fz. G- proteins are activated and these interact with Dvl, phospholipase C, protein kinase C (PKC) and calcium-calmodulin kinase 2 (CamK2). This leads to intracellular release of calcium. The process is important for cell adhesions and cell movements during gastrulation (see Figure 1.1).



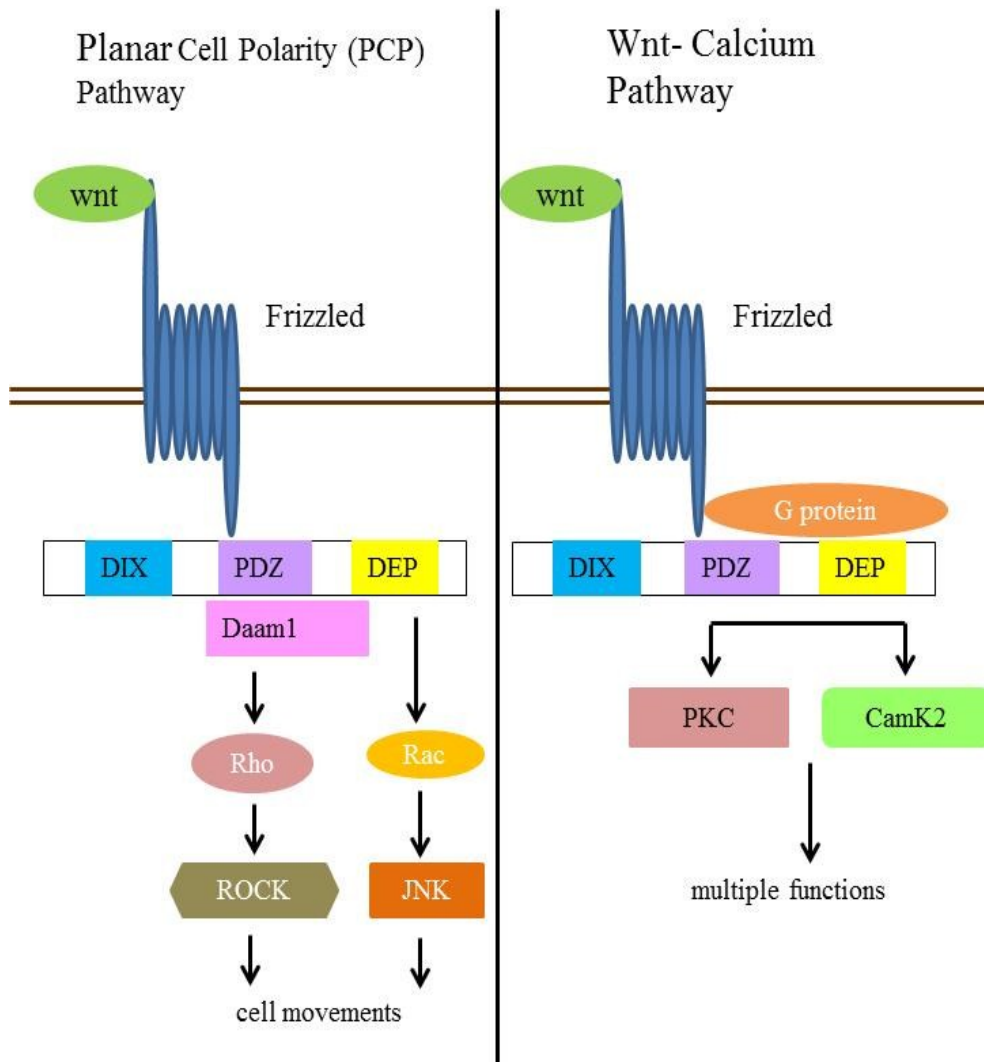


**Figure 1.1**  
**The Planar cell polarity (PCP) pathway and Wnt- Calcium Pathway. Adapted from Habas and Dawid (2005).**

PCP pathway: signalling is initiated through the Frizzled (Fz) receptor. Rho GTPases (including Rac) are activated through the PDZ and DEP domains of Dishevelled (Dvl) and the reaction leads to cytoskeletal changes.

Wnt- Calcium pathway: signalling is also initiated through Fz. G- proteins are activated and these interact with Dvl, phospholipase C (not shown), protein kinase C (PKC) and calcium- calmodulin kinase 2 (CamK2).

### **1.1.3 The Canonical Pathway**

An outline of the canonical/  $\beta$ -catenin pathway is described in Figure 1.2. In the 'OFF' state  $\beta$ -catenin forms a complex with adenomatous polyposis gene product (APC) and Axin. It is phosphorylated at the N-terminus by glycogen synthase kinase 3 (GSK-3) and casein kinase 1 (CK1). This forms a binding site for the E3 ubiquitin ligase  $\beta$ -Trcp ( $\beta$ -Transducin repeat containing protein) and triggers proteosomal degradation of  $\beta$ -catenin. The canonical Wnt pathway is activated through binding of Wnt ligands (see section 1.1.3.1.1) to the Fz receptor and lipoprotein receptor related protein 5 and 6 (LRP5/LRP6). This triggers phosphorylation of Dvl proteins which interact with Fz. LRP5/LRP6 aggregates form at the membrane and CK1 phosphorylates the intracellular portion of LRP5/LRP6. Axin is then recruited to the complex and proteosomal degradation of  $\beta$ -catenin is stopped. As a result,  $\beta$ -catenin accumulates in the cytoplasm. It is then free to enter the nucleus where it interacts with DNA-bound T-cell factor/lymphoid enhancer factor (TCF/LEF) and activates gene transcription.

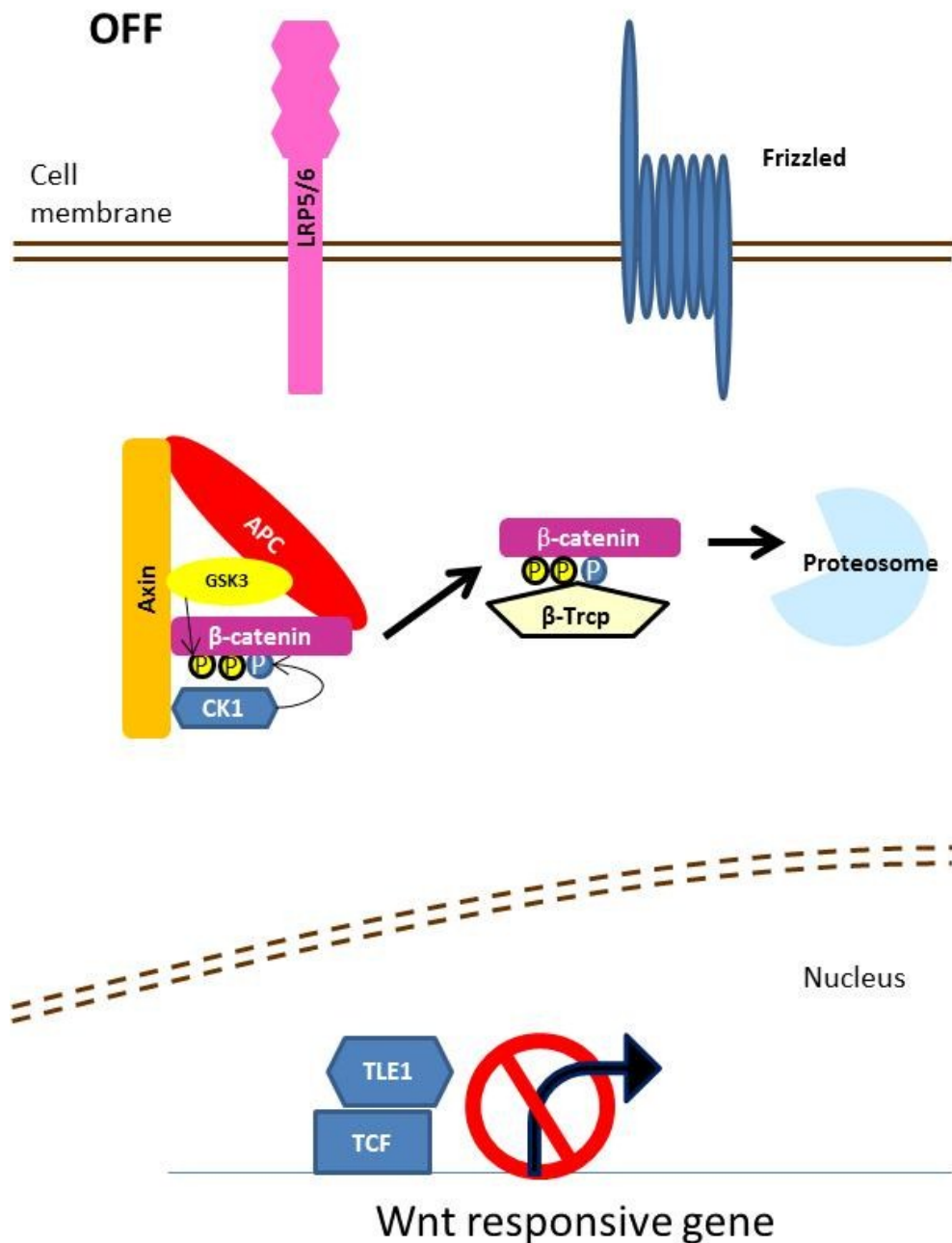


**Figure 1.2a**  
**Canonical Wnt signalling pathway (OFF state).**  
**Adapted from MacDonald, Tamai et al. (2009).**

OFF state:  $\beta$ -catenin forms a complex with Axin, APC, GSK-3A/B and CK1. It is then phosphorylated by CK-1 and GSK-3A/B in turn. The E3 ubiquitin ligase  $\beta$ -Trcp targets the phosphorylated  $\beta$ -catenin for degradation. Wnt gene expression is suppressed by TCF-TLE1/Groucho and histone deacetylase (HDAC).

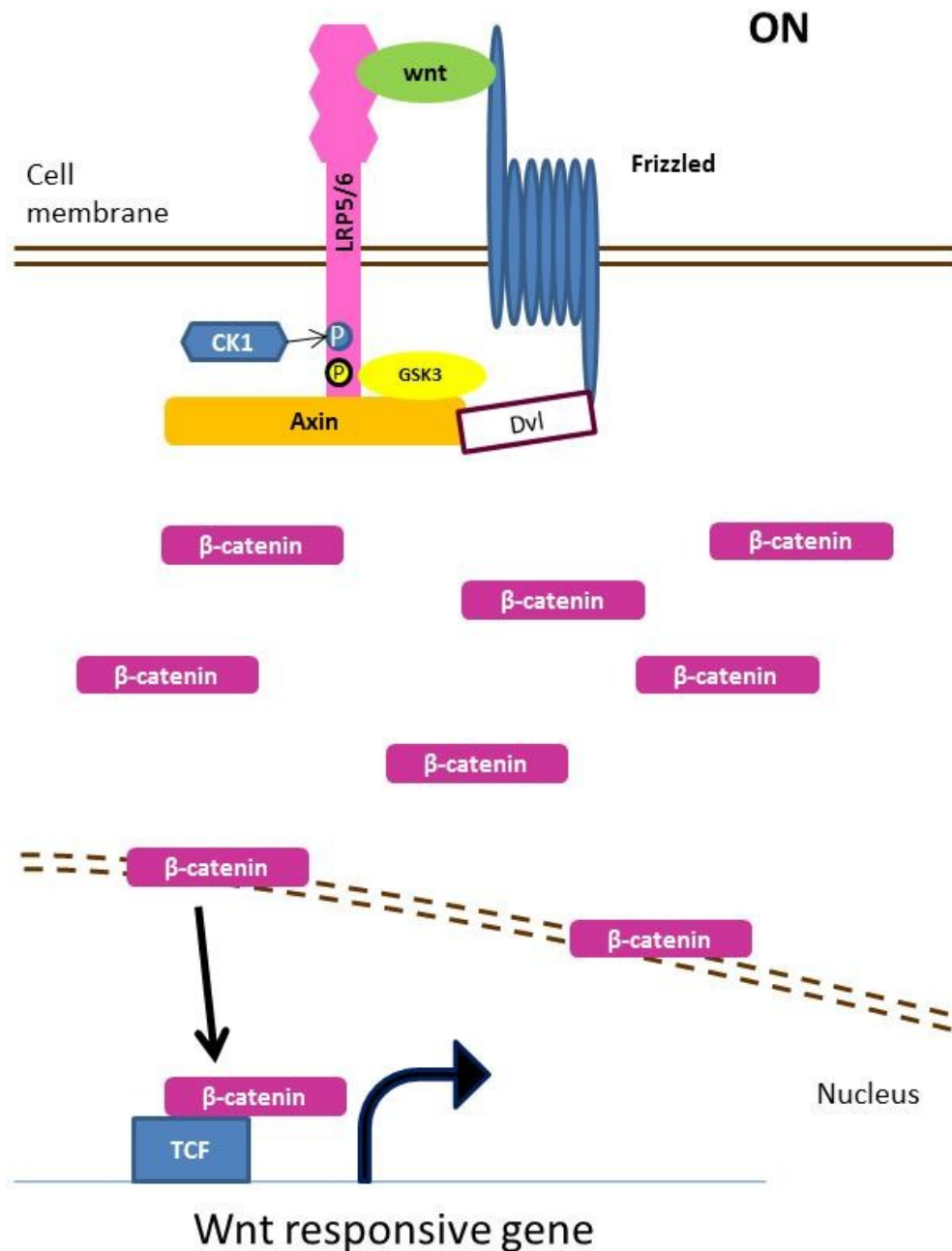


**Figure 1.2b**  
**Canonical Wnt signalling pathway (ON state).**  
**Adapted from MacDonald, Tamai et al. (2009).**

ON state: The Wnt ligand binds to Fz and LRP5/6 to form a complex. Dvl is recruited by Fz and this leads to phosphorylation of LRP5/6 by CK1 and GSK3. Axin joins the complex which in turn disrupts phosphorylation and degradation of β-catenin. β-catenin is free to accumulate in the nucleus where it acts as a co-activator for TCF and activates Wnt responsive genes.

### **1.1.3.1 At the cell surface**

#### **1.1.3.1.1 Wnt ligands**

Most of our current understanding on Wnt ligands comes from studies on the *Drosophila* Wingless. To date, nineteen Wnt ligands have been identified in mammals: they are highly conserved proteins containing about 350-400 amino acids. Some ligands will activate one pathway (e.g. Wnt5a activates non-canonical Wnt signalling); others (e.g. Wnt3) may activate both canonical and non-canonical Wnt signalling (Habas and Dawid 2005, Samarzija et al. 2009). In the cytoplasm, Wnt ligands undergo glycosylation and are lipid modified in the endoplasmic reticulum before being transported by the Golgi apparatus to the plasma membrane for secretion (Figure 1.3). Porcupine is a transmembrane protein in the endoplasmic reticulum with an O-acyl transferase domain and is important for lipid modification. Wntless is a protein complex in the Golgi, endoplasmic reticulum and plasma membrane and aids Wnt secretion (MacDonald et al. 2009).

Once secreted, Wnt proteins may act in an autocrine and paracrine fashion. It is thought that lipid modification of the protein may aid diffusion through the extracellular space. The exact mechanism for this is not fully understood and most of the research has been done for Wingless. Two separate secretory pathways can drive autocrine and paracrine signalling. Wingless may bind to lipoprotein particles (Panakova et al. 2005) or form multimers where lipid modifications are internalized (Katanaev et al. 2008) (long range signalling). Wingless receptors and heparan sulphate proteoglycans may be important for short range signalling (Lin 2004).

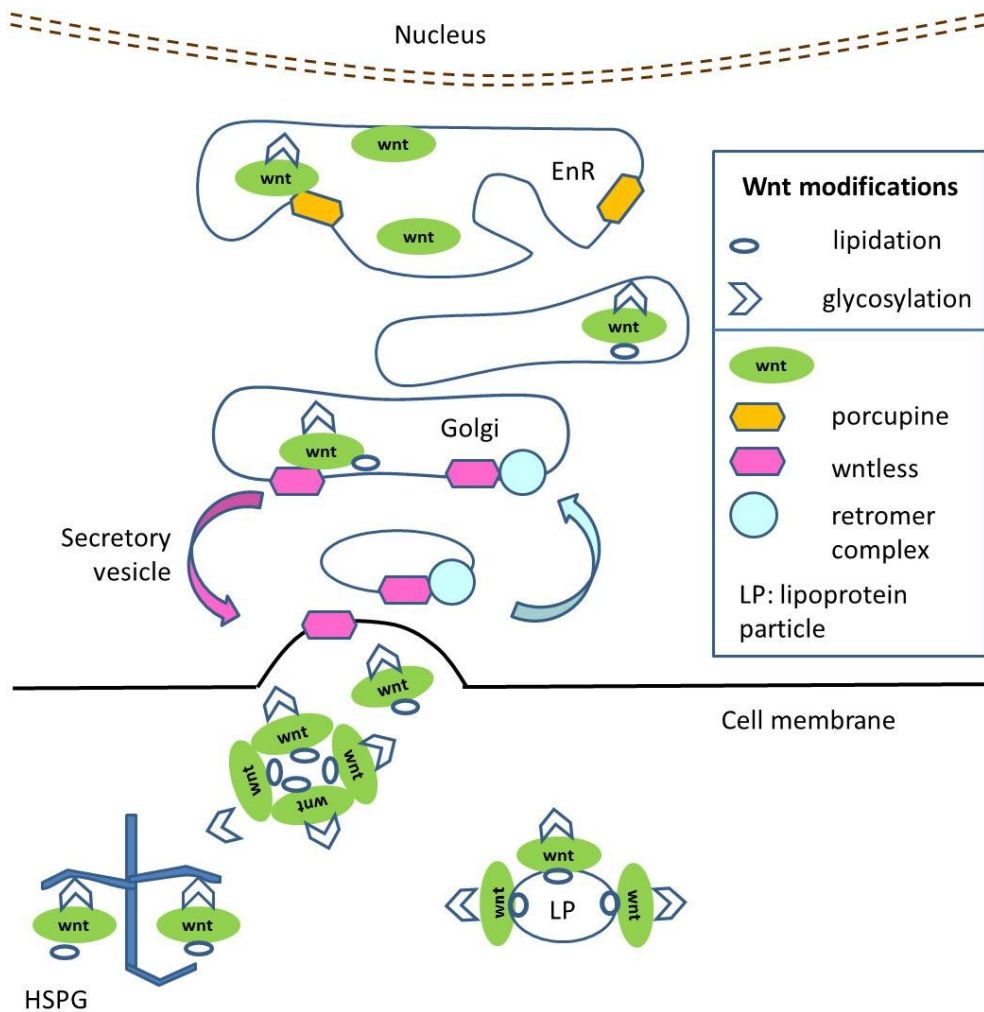


**Figure 1.3**  
**Wnt ligands: Post-translational modification and secretion. Adapted from MacDonald, Tamai et al. (2009).**

In the cytoplasm, Wnt ligands are glycosylated and lipid modified in the endoplasmic reticulum (EnR). This process involves Porcupine. Wntless in the Golgi apparatus transports the ligand to the plasma membrane for secretion. Once secreted, Wnt binds to heparan sulphate proteoglycans (HSPGs) and lipoprotein particles (LP) to form multimers.

#### **1.1.3.1.2 Endogenous Wnt agonists**

Norrin and members of the R-Spondin (Rspo) family are proteins which stimulate the Wnt pathway. Norrin protein activates the pathway by binding to Fz4 (Clevers 2004). LRP5 or LRP6 acts as a co-receptor in this process. There are four human Rspo proteins with Rspo2 and Rspo3 being the more active isoforms. Wnt ligands and LRP6 are required for their activity and Rspo proteins amplify Wnt3a, Wnt1, and Wnt7a signalling (Kim et al. 2008).

#### **1.1.3.1.3 Endogenous Wnt antagonists**

Wnt antagonist activity may broadly be divided into two (Kawano and Kypta 2003): Secreted frizzled related proteins (SFRPs) and Wnt inhibitory factor 1 (WIF-1) bind directly to Wnt proteins and thus prevent their binding to the Wnt receptor complex. There are five human SFRPs and have about 300 amino acids. They have a cysteine-rich domain similar to that in Fz but are encoded for by separate genes. WIF-1 binds Wnt ligands through a unique WIF domain. Dickkopf (Dkk) proteins and Sclerostin (SOST) on the other hand, inhibit Wnt signalling by binding to the LRP5/LRP6 component of the Wnt receptor complex. There are four human Dkk proteins. They share two cysteine-rich domains and have 250-350 amino acids (Glinka et al. 1998). Dkk forms a complex with LRP5/6 and Kremen and this is followed by endocytosis. LRP5/6 is thus removed from the cell surface.

The exceptions to this rule are Shisha proteins and Insulin-like growth factor binding protein 4. Shisha proteins trap Fz proteins in the endoplasmic reticulum and prevent maturation of the receptor (He 2005). Insulin-like growth factor binding protein 4 binds both Fz and LRP6.

#### **1.1.3.1.4 The Receptors**

##### **1.1.3.1.4.1 Frizzled**

There are ten known human Fz receptors (Fz1 to Fz10). They are seven trans-membrane receptors having an extracellular N-terminus, three extracellular loops, seven trans-membrane helices, three intracellular loops and an intracellular C-terminal domain. The N-terminal region is a cysteine rich domain; the C-terminus is important for signal transduction and recruitment of intracellular effectors (Gunnar Schulte 2012).

##### **1.1.3.1.4.2 Lipoprotein Receptor Related Proteins**

LRP6 is important in embryogenesis and LRP5 is essential for adult bone homeostasis. LRP5 and LRP6 act as co-receptors with Fz for Wnt ligands (MacDonald et al. 2009). A detailed LRP6 structure has been described in the literature (Chen et al. 2011): the extracellular part has four tandem  $\beta$ -propeller-EGF-like domain pairs that act as binding sites for Wnt ligands and Wnt antagonists such as Dkk1 (Bafico et al. 2001, Ahn et al. 2011) and Sclerostin (SOST) (Li et al. 2005). Antagonists prevent Wnt-LRP6 binding and thus Fz-LRP6 complex formation. Wnt3a and Dkk1 are believed to bind to the third  $\beta$ -propeller-EGF-like domain (Chen et al. 2011).

#### **1.1.3.2 In the Cytoplasm**

##### **1.1.3.2.1 Dishevelled**

There are three dishevelled proteins in mammals: Dvl- 1, Dvl- 2 and Dvl- 3. Each member has three conserved domains: an amino-terminal DIX domain (Dvl and



Axin); a central PDZ domain (Post-synaptic density-95, Discs large and Zonula occludens-1); and a carboxy-terminal DEP domain (Dvl, Egl-10 and Pleckstrin) (Habas and Dawid 2005). Dvl is a key component in all three Wnt signalling pathways. For the PCP and Wnt- Calcium pathways it functions at the cell membrane; for the canonical pathway it functions in the cytoplasm. Dvl may also be found in the nucleus: here it forms part of the TCF/  $\beta$ -catenin complex and facilitates TCF/  $\beta$ -catenin interaction (Gan et al. 2008).

#### **1.1.3.2.2 The Axin degradation complex**

The degradation complex has four key components: Axin, APC, GSK-  $3\alpha/\beta$ , CK1 $\alpha$ . It is important for both phosphorylation and proteosomal degradation of  $\beta$ -catenin (see Figure 1.4). Axin acts as a scaffolding protein at the heart of the destruction complex. It interacts with GSK-  $3\alpha/\beta$ , CK1 $\alpha$  and  $\beta$ -catenin at different sites and helps coordinate phosphorylation of  $\beta$ -catenin by the other two molecules (see section 1.3.8). It also interacts with APC via a regulator of G protein signalling domain. APC binds to Axin and  $\beta$ -catenin. GSK-  $3\alpha/\beta$  is a protein kinase; in mammals there are two isoforms: GSK-  $3\alpha$  and GSK-  $3\beta$ . Both isoforms need to be depleted for a decrease in  $\beta$ -catenin phosphorylation (S33/37). GSK-  $3\alpha/\beta$  is inactivated by phosphorylation (Vincan 2008). GSK-  $3\alpha/\beta$  and CK1 $\alpha$  phosphorylate Axin and APC and this helps further binding of Axin and APC to  $\beta$ -catenin. This stabilises the complex and enables degradation of  $\beta$ -catenin. PP1 and PP2A are two serine/ threonine phosphatases which help regulate the complex. They can bind to Axin and APC. PP1 dephosphorylates Axin and promotes complex destruction; PP2 dephosphorylates  $\beta$ -catenin. Both phosphatases thus decrease degradation of  $\beta$ -

catenin. APC in turn prevents PP2A activity. APC facilitates Axin degradation and vice versa.

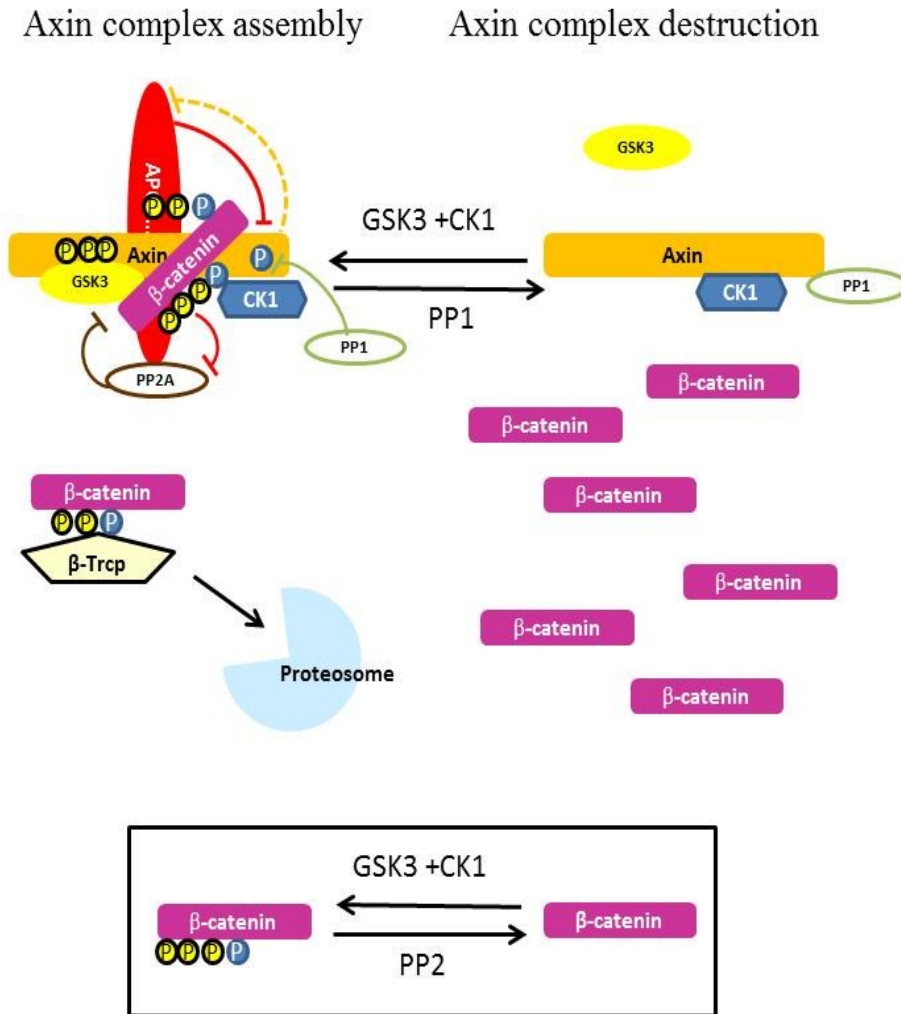


**Figure 1.4**  
**Regulation of degradation complex and  $\beta$ -catenin phosphorylation. Adapted from MacDonald, Tamai et al. (2009).**

The degradation complex consists of Axin, GSK3, CK1 and APC.  $\beta$ -catenin is phosphorylated by the complex and then destroyed by proteosomal degradation. GSK and CK1 also phosphorylate Axin and APC and stabilise the complex.  $\beta$ -catenin is dephosphorylated by PP2A. APC in turn prevents PP2A activity. APC facilitates Axin degradation and vice versa. PP1 dephosphorylates Axin and regulates binding of GSK to Axin resulting in complex destruction.

#### **1.1.3.2.3 Phosphorylation sites on $\beta$ -catenin**

The phosphorylation status of  $\beta$ -catenin is central to its intracellular functioning.  $\beta$ -catenin possesses a number of potential serine and tyrosine phosphorylation sites the phosphorylation of which can promote  $\beta$ -catenin degradation or signal activation. Phosphorylation at the amino terminus sites S33, S37, T41 and S45 favour degradation; phosphorylation at the armadillo domains S675, S552, Y654, Y487 and Y142 alters the adhesion of  $\beta$ -catenin to cadherins and promotes nuclear localization. GSK3 $\beta$  is responsible for phosphorylation at S33, S37, T41; CK1 $\alpha$  phosphorylates S45 (Heuberger J 2010). Activation of the Wnt pathway results in a decrease in levels of p-  $\beta$ -catenin in the cytoplasm (Vincan 2008).

#### **1.1.3.2.4 Movement of $\beta$ -catenin between cytoplasm and nucleus**

Stabilization of  $\beta$ -catenin results in increased cytoplasmic levels of  $\beta$ -catenin. This is free to translocate to the nucleus where it can activate gene transcription. Henderson (2002) showed that  $\beta$ -catenin can interact directly with nuclear pore proteins to enter the nucleus. Ras-related C3 botulinum toxin substrate 1 (Rac1- a member of the Rho GTPase family) is also important for nuclear translocation of  $\beta$ -catenin (Wu et al. 2008). Rac1 and JNK2 (Jun N-terminal kinase 2) form a complex with  $\beta$ -catenin. JNK2 phosphorylates  $\beta$ -catenin (serine 191 and 605 and  $\beta$ -catenin is then translocated to the nucleus).

APC (Henderson 2002), Axin (Cong and Varmus 2004) and RanBP3 (Ran binding protein 3) (Hendriksen et al. 2005) can export  $\beta$ -catenin out of the nucleus. Axin and APC also help retain  $\beta$ -catenin in the cytoplasm, while B- cell lymphoma 2 (BCL2)

and Pygopus increase nuclear levels of  $\beta$ -catenin. BCL2 and Pygopus are TCF and  $\beta$ -catenin co-activators.

#### **1.1.3.3 In the Nucleus**

The TCF/LEF family consists of four proteins: LEF-1, TCF1, TCF3 and TCF4. In the absence of nuclear  $\beta$ -catenin, TCF/LEF are coupled with transcription repressors such as Groucho, TLE1 and C-terminal binding protein 1 (CtBP1). When  $\beta$ -catenin enters the nucleus, it displaces Groucho and binds to TCF/LEF. TCF proteins are HMG (high mobility group) DNA-binding factors. They can bind to a DNA consensus sequence known as the WRE/ Wnt responsive element and this causes a change in the DNA chromatin structure. Both co-activators (e.g. BCL9 and Pygopus) and co-repressors (CtBP1, TLE1 and Histone deacetylase (HDAC)) are active during  $\beta$ -catenin-mediated transcription and help regulate the process (MacDonald et al. 2009).

Vlad et al. (2008) have proposed a three tiered cascade model of gene activation resulting from activation of  $\beta$ -catenin/TCF transcription. At the first level, TCF activation results in transcription of some genes including effectors (e.g. matrix metalloproteinase 7, MMP7), transcription regulators (e.g. c-myc) and pathway regulators (e.g. vascular endothelial growth factor, VEGF). These genes in turn regulate transcription of other effectors (e.g. the c-myc target gene p21) or target pathways (e.g. VEGF receptor tyrosine kinase pathway). The third level contains effectors of the target pathways (e.g. the VEGF target gene Down syndrome critical region gene 1, DSCR1). The original signal can thus be greatly amplified (see Figure 1.5). Table 1.1 is a list of the main Wnt pathway target genes. Key Wnt signalling

components are also regulated by TCF/ $\beta$ -catenin. Activation of Wnt induces Axin2, Dkk1 (Chamorro et al. 2005) and Naked (a dishevelled binding protein) and suppression of Fz and LRP6 (Khan et al. 2007) thus forming a negative feedback loop (Kazanskaya et al. 2004, Logan and Nusse 2004).

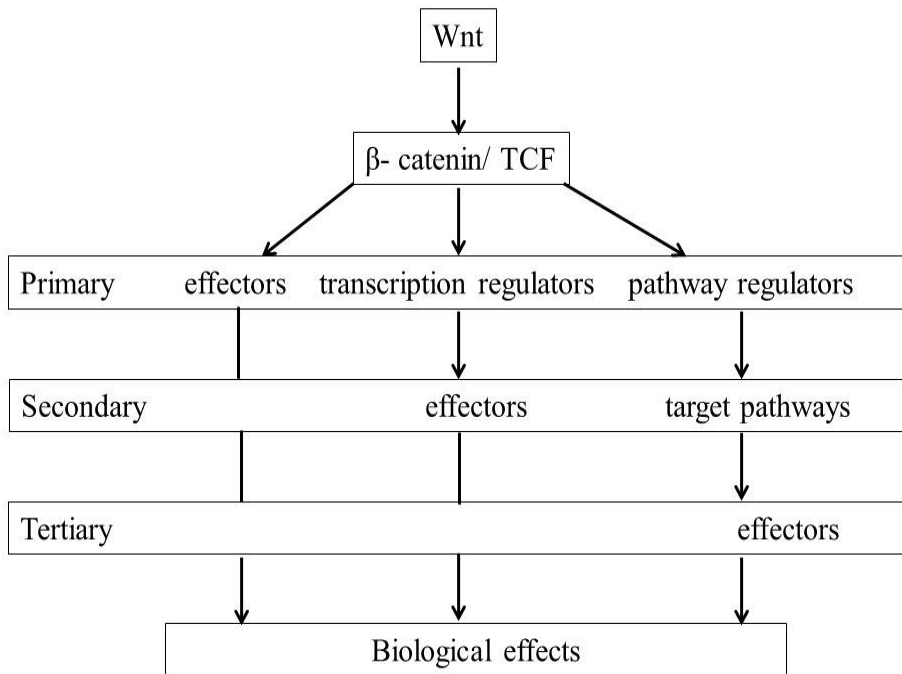


**Figure 1.5**  
**The three levels of the Wnt targetome. Adapted**  
**from Vlad, Röhrs et al. (2008).**

this image has been removed by the author for  
copyright reasons



this image has been removed by the author  
for copyright reasons

**Table 1.1**

Table of some Wnt target genes. (SABiosciences 2012)

## **1.2 Wnt signalling and breast cancer**

Wnt signalling is important in carcinogenesis. Most of our understanding of the Wnt pathway activity in breast tissue comes from work on mouse models which explored normal mammary embryonic development and postnatal development in puberty and around pregnancy (Figure 1.6). Changes are noted both in expression and function of individual Wnt pathway components in these contexts.

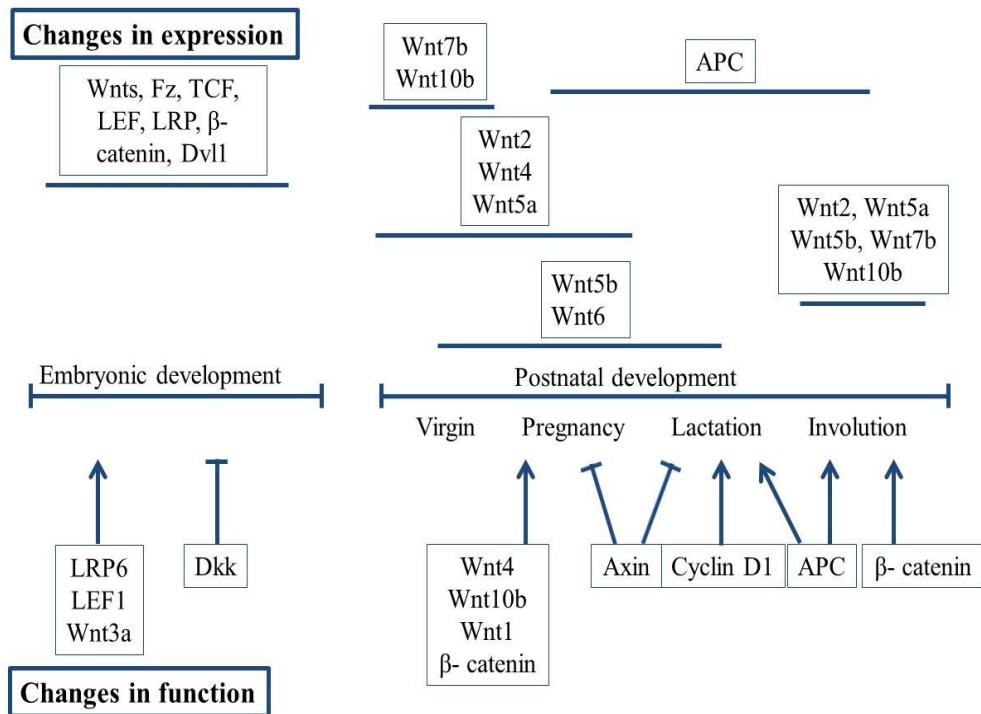


**Figure 1.6**  
**Expression and function of Wnt signalling pathway components during mammary gland development.**  
 Adapted from Prosperi and Goss (2010).

There has also been extensive research into the role of Wnt signalling in breast cancer; cell models, animal models and human breast cancer tissue have all been used. A selection of the important publications on the role of Wnt signalling in breast cancer are highlighted in Table 1.2 (Goss K 2011).

Wnt signalling may be altered in up to half of all breast cancers (Goss K 2011). Both up regulation of Wnt pathway activators and down regulation of pathway inhibitors have been identified in breast cancer. As in breast development, these changes may be functional changes or changes in expression. Some of these changes are discussed below.

Wnt1 ligand is important for breast carcinogenesis. Transgenic mice overexpressing Wnt1 develop spontaneous mammary adenocarcinoma and are used as models for studying breast cancer (Liu et al. 2010, Lawson et al. 2010, Baker et al. 2010, Yue et al. 2010, Prasad et al. 2009, Huang et al. 2008, Collu and Brennan 2007, Huang et al. 2006, Bocchinfuso et al. 1999, Li et al. 2000) . Wnt1 signalling is important for survival of MCF-7 cells (Wieczorek et al. 2008) and is also one of the target genes of oestrogen in MCF-7 cells (Kato 2003).

In a study of 1967 breast cancer samples, Dahl et al. (2005) showed that the negative Wnt regulator SFRP1 is downregulated in 73% of breast cancer cases and that loss of SFRP1 is associated with an unfavourable prognosis in early breast cancer. SFRP1 gene silencing was a result of promoter methylation.

Most of our understanding of APC comes from research in colorectal cancer where APC mutations are an important link in the adenoma- carcinoma chain. APC mutations in breast cancer are reported at 6%- 18% in selected series of sporadic human breast cancer (Furuuchi et al. 2000, Kashiwaba et al. 1994). Interestingly,

these breast cancer mutations were found outside the mutation cluster region - a 684-bp region described for colorectal cancers (Furuuchi et al. 2000, Abraham et al. 2002a, Ho et al. 1999, Kashiwaba et al. 1994). Hypermethylation of the APC promoter region (CpGsites) is more common and is reported in up to 70% of breast cancer cases and correlates with its epigenetic silencing (Dulaimi et al. 2004, Jin et al. 2001, Prasad et al. 2008, Sarrio et al. 2003, Van der Auwera et al. 2008, Virmani et al. 2001). Prasad et al. (2008) noted that these mutations were associated with an increase in nuclear localization of  $\beta$ -catenin in half the tumour samples. APC promoter hypermethylation has also been associated with increased methylation in the promoter region of the CDH-1 gene which codes for E-cadherin (Virmani et al. 2001, Van der Auwera et al. 2008), impacting on cell adhesion.

Different breast cancer subtypes have been reported to have specific changes in Wnt signalling. Khramtsov et al. (2010) showed that Wnt was upregulated in basal type cancers (also ER negative). LRP6 is upregulated in triple-negative breast cancers, human epidermal growth factor receptor 2 (HER2) negative and oestrogen receptor (ER) negative breast cancer cohorts (Liu et al. 2010).

Target	Study type	Key Summary Points	References
Wnt1	C   T A	Wnt and Notch Oestradiol and Wnt1 Wnt1 and cell survival Wnt1 and Her2 Wnt expression in cancer	(Collu and Brennan 2007) (Kato 2003) (Wieczorek et al. 2008) (Huang et al. 2006) (Wong et al. 2002)
Wnt2	T	Wnt and Twist	(Watanabe et al. 2004)
Wnt3, Wnt4, Wnt7b	C	gene expression	(Huguet et al. 1994)
Wnt2, Wnt3, Wnt4, Wnt7b	T	gene expression	(Huguet et al. 1994)
Wnt5a	T	mRNA expression	(Iozzo et al. 1995)
Wnt5a	T	gene expression	(Lejeune et al. 1995)
LRP6	A	breast development	(Lindvall et al. 2009)
LRP5	C/A/T	receptor as target	(Bjorklund et al. 2009)
$\beta$ -catenin	T   A C	basal type breast cancer cellular distribution and outcome interaction with APC mutations	(Khramtsov et al. 2010) (Nakopoulou et al. 2006) (López-Knowles et al. 2010) (Ryo et al. 2001) (Ueda et al. 2001)
$\beta$ -catenin, cyclin D1	C/T T	prognostic marker mutations	(Lin et al. 2000) (Kizildag et al. 2008)
$\beta$ -catenin, APC, Axin, WISP3	T	mutations	(Hayes et al. 2008)
$\beta$ -catenin, APC	T	mutations	(Abraham et al. 2002b)
$\beta$ -catenin, cyclin D1,	T	changes in cancer	(Ozaki et al. 2005)

c-myc			
β-catenin, APC, E-cadherin	T	genetic mutations	(Sarrio et al. 2003)
CK2	A	changes in cancer	(Landesman-Bollag et al. 2001)
WIF1, SFRP	C/T	epigenetic silencing	(Ai et al. 2006)
SFRP1,2,5; Dkk1	C	epigenetic silencing	(Suzuki et al. 2008)
SFRP1	C	prognosis	(Veeck et al. 2006, Veeck et al. 2008)
	T	type of breast cancer epigenetic silencing	(Ugolini et al. 2001) (Dahl, Veeck et al. 2005)
Dkk1	C/T	hormone resistance	(Forget et al. 2007)
Axin	C/T	mutations	(Webster et al. 2000)
Axin2	T	gene mapping	(Mai et al. 1999)
APC	T	mutations mutations mutations reduced protein expression mutations gene silencing gene silencing invasive ductal carcinoma lobular breast carcinoma inflammatory breast cancer signalling	(Abraham et al. 2002a) (Ozaki et al. 2005) (Furuuchi et al. 2000) (Ho et al. 1999) (Kashiwaba et al. 1994) (Dulaimi et al. 2004) (Jin et al. 2001) (Prasad et al. 2008) (Sarrio et al. 2003) (Van der Auwera et al. 2008) (Jönsson et al. 2000)
	C/T	epigenetic silencing	(Virmani et al. 2001)

**Table 1.2**

Table showing some of the Wnt signalling pathway components that have been studied in breast cancer (Goss K 2011). T= tissue; C= cell lines; A=animal models.

### **1.3 Endocrine therapy in breast cancer**

Breast cancer is the most common cancer in the UK and accounts for about 30% of all new female cancers (Cancer\_Research\_UK 2012). Early detection through breast screening programmes and improved treatments have led to improved survival rates. For 2005-2009, the age- standardised relative survival rate for breast cancer in the UK was 85% and 77% at five and ten years respectively. Despite this, there were nearly twelve thousand deaths from breast cancer in 2010 in the UK alone (Cancer\_Research\_UK 2012).

The oestrogen receptor (ER) is important for normal breast development but also plays a key role in breast cancer disease and progression. Endocrine therapies target the ER but their benefit in breast cancer is limited by intrinsic (*de novo*) and acquired resistance. In endocrine resistance, the ER pathway is deregulated and cell signalling mechanisms are altered. This leads to the activation of alternative escape pathways which provide the cells with alternative survival mechanisms.

#### **1.3.1 The Oestrogen Receptor**

The oestrogen receptor alpha (ER $\alpha$ ) is expressed in up to 70% of all breast cancers and levels are increased in malignant breast tissue compared to normal tissue (Allred and Mohsin 2000). There is also another receptor called ER $\beta$ . The genes are located on chromosome 6 and 14 respectively. The receptors show a differential distribution. ER $\alpha$  is mainly expressed in the pituitary gland, ovaries (thecal and interstitial cells), uterus, liver, kidneys, adrenals, and the mammary glands whilst ER $\beta$  is predominantly found in the prostate, bone, ovaries (granulosa cells), lungs, and in various parts of the central and peripheral nervous system (Zilli et al. 2009). The



ER $\alpha$  receptor is both a predictive and prognostic factor in clinical practise (Thorpe SM 1986, Thorpe 1988). The ER $\alpha$  is believed to be the dominant receptor in breast cancer (Osborne et al. 2000, Knowlden et al. 2000).

#### **1.3.1.1 Structure**

ER $\alpha$  is a steroid hormone receptor. It has six functional domains: A to F. The A/B domain is at the amino end and it contains a hormone independent transcription activation function region (AF-1). Key phosphorylation sites in AF-1 serve to maximise transcriptional responses following oestradiol binding to ER $\alpha$  (with AF-1 synergising with AF-2 in region E); these AF-1 sites can also mediate ER $\alpha$  activation by other growth signalling pathways. The C domain is the DNA binding domain (DBD) and has two zinc fingers which allow binding of the ER to oestrogen response elements (ERE) in target ER-regulated genes. The D domain, or hinge region, is important for co-regulatory protein binding, dimerization and heat shock protein 90 binding. The ligand dependent transcription activation function region (AF-2) and hormone binding domain (HBD) are found in the E domain. The carboxy- terminal F domain modulates function of anti-oestrogens (Figure 1.7) (Sommer and Fuqua 2001).

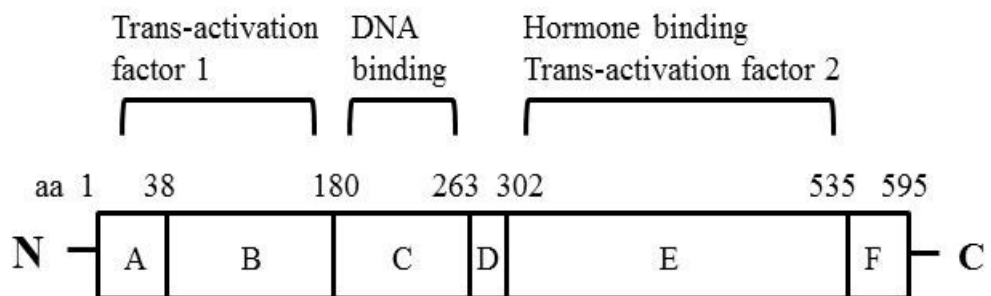


**Figure 1.7**

**Diagram showing structure of the oestrogen receptor and its separate functional domains. Adapted from Sommer and Fuqua (2001).**

### 1.3.1.2 Activation of the Oestrogen Receptor

ER signalling can be triggered by genomic and non-genomic mechanisms (see Figure 1.8).

In the absence of oestrogen, nuclear ER is maintained in an inactive state by chaperone proteins (e.g. heat shock protein 90). In **classical/ genomic ER signalling**, oestradiol (E2) can diffuse through the cell membrane and into the nucleus where it binds to the HBD of the ER. This triggers a conformational change in the ER protein and, as a result of this, the Hsp90 chaperone proteins are displaced. This is followed by dimerization of the E2-bound ER and the ER binds to the ERE on the DNA to initiate gene transcription of target genes, regulated by synergistic activity of AF-2 and AF-1. Additional co-activator proteins (Co-A) are also recruited to the ER/DNA complex and these can regulate cellular function by promoting or suppressing gene transcription (Osborne and Schiff 2005, Björnström and Sjöberg 2005, Osborne and Schiff 2011).

In **non-classical/ genomic ER signalling**, the E2-ER complex binds to DNA indirectly by forming protein-protein interactions with other transcription factors (TFs) such as activator protein- 1 (AP-1) or specificity protein- 1 (SP-1). This strengthens the binding of these transcription factors to their DNA responsive sites so ER acts as a co-regulator. This mechanism can thus serve to increase or reduce the transcriptional impact of the receptor. Activation of the AP-1 response elements has been linked to the development of tamoxifen resistance (Osborne and Schiff 2011). Other co-activators may be recruited to the complex: the co-activator SRC-3 is overexpressed in two thirds of breast cancer and overexpression of this gene has also been linked to tamoxifen resistance (Osborne and Schiff 2005, Björnström and Sjöberg 2005, Osborne and Schiff 2011).

ER signalling is also regulated by membrane growth factor receptor tyrosine kinases such as the epidermal growth factor receptor (EGFR) and insulin– like growth factor receptor (IGFR-1). These receptors can activate downstream kinase signalling mechanisms that result in AF-1 phosphorylation of the ER. This is **ligand independent ER signalling** (Osborne and Schiff 2005, Björnström and Sjöberg 2005, Osborne and Schiff 2011).

In addition, **Membrane activated ER signalling** can occur rapidly with oestrogens which is independent of genomic ER activity. E2-ER complexes at the cell membrane can activate protein kinases and these trigger signalling changes in the cytoplasm such as the PI3K/AKT and Ras/ MAPK pathways. Membrane ER binds directly to growth factor receptor tyrosine kinases (e.g. EGFR, IGF-1R) and with additional signalling molecules (such as src kinase) activates a cascade of downstream cellular kinase pathways (e.g. src, PI3K/AKT and Ras/MAPK). These kinases in turn phosphorylate various transcription factors to trigger alternative response elements (REs). (Osborne and Schiff 2005, Björnström and Sjöberg 2005, Osborne and Schiff 2011). However, these kinases may also feasibly interplay with nuclear ER (e.g. via AF-1 phosphorylation) to promote ERE-mediated gene expression.

this image has been removed by the author  
for copyright reasons

### **Figure 1.8**

#### **ER signalling mechanisms**

The oestrogen (E) - oestrogen receptor (ER) complex may bind to DNA sequences at the oestrogen responsive elements (ERE) or indirectly via protein- protein interactions with other transcription factors (TFs) at their DNA- responsive sites (classical and non-classical genomic ER signalling). Growth factor (GF) receptor tyrosine kinases (RTKs) can also activate protein kinases that result in phosphorylation of the ER (ligand independent ER signalling). Co-activator complexes (CoA) are recruited to modulate gene transcription including genes coding for RTKs and GFs.

The E-ER complex may also bind to GF RTKs (e.g. EGFR, IGF1-R) and other signalling molecules (e.g. src) to activate downstream kinase pathways (e.g. src, PI3K/ AKT, Ras/ MAPK (membrane activated ER signalling). These kinases in turn phosphorylate TFs and co-regulators including components of the ER pathway that promote gene expression on EREs and other responsive elements (REs).

Adapted from Osborne and Schiff (2011).

### **1.3.2 Endocrine therapy**

Given the importance of ER signalling for sustaining breast cancer cell growth, endocrine treatments for ER positive breast cancers seek to disrupt this pathway.

This may be achieved through the following:

- Selective oestrogen receptor modulators (SERM) e.g. tamoxifen, which act by competitive inhibition of the ER
- Selective oestrogen receptor down regulators (SERD) e.g. faslodex, which act by competitive inhibition of ER and deplete ER levels
- Gonadotropin releasing hormone (GnRH) agonists which act as chemical castration
- Aromatase inhibitors (e.g. anastrozole, exemestane, letrozole) which bring about severe oestrogen deprivation

Endocrine therapy plays an important role in the treatment of early, advanced and metastatic ER positive breast cancer. Following surgical excision of ER positive early breast cancer, adjuvant treatments have been shown to improve survival and reduce the risk of disease recurrence. Adjuvant endocrine treatment in ER positive disease may be used in combination with chemotherapy and radiotherapy. Endocrine therapy is also important in the primary treatment of locally advanced and metastatic ER positive breast cancer and in recurrent disease. Although aromatase inhibitors (AIs) are increasingly used as primary endocrine therapy in postmenopausal women, tamoxifen remains the treatment of choice in ER+ premenopausal women and in patients who are intolerant of AIs.

### **1.3.2.1 Tamoxifen**

Tamoxifen competes with oestradiol for the ER. On binding to the HBD, it induces a conformational change in the ER. This selectively promotes recruitment of co-repressors over co-activators and transcription of oestrogen responsive genes is inhibited. Tamoxifen inhibits AF-2 activity but genes regulated by AF-1 may still be expressed according to tissue context, and so the drug has been termed a partial antioestrogen (Osborne et al. 2000, Lewis and Jordan 2005). Tamoxifen is a pro-drug and is metabolized in the liver by cytochrome P450 to its active metabolites 4-hydroxytamoxifen and N-desmethyl-4-hydroxytamoxifen. The derivatives have 30-100 times more affinity to the ER than the parental drug (Jordan and Chen 1982) and both metabolites show anti-cancer activity. 4-hydroxytamoxifen acts as an ER antagonist in ER positive breast tissue and breast cancers; in the endometrium it exerts an agonistic effect and this is linked to the modest increased incidence of endometrial cancer.

Tamoxifen has been used in the treatment of ER positive breast cancer for over thirty years. Five years of adjuvant tamoxifen treatment in patients with ER positive breast cancers reduces the risk of local recurrence and the incidence of contralateral second primary breast cancers by about 40- 50% (Lewis and Jordan 2005). The benefit is seen in both pre- and post- menopausal women; in patients with node positive and node negative disease; and in patients having chemotherapy (Ravdin PM 1998, Early Breast Cancer Trialists' Collaborative 2011). This translates into a survival benefit and decreases mortality from breast cancer by about 30% (Early Breast Cancer Trialists' Collaborative 2011). The benefit of tamoxifen treatment is also seen in patients with ER positive advanced/ metastatic disease but less than half the patients will respond to tamoxifen treatment (Normanno et al. 2005). However, although

tamoxifen is clearly an invaluable therapeutic agent in ER+ breast cancer, all patients with metastatic disease and around 30%-40% of the patients receiving adjuvant tamoxifen will relapse having acquired resistance and ultimately die from their disease (Normanno et al. 2005).

### **1.3.3 Tamoxifen Resistance in Breast Cancer**

Endocrine resistance is an important clinical challenge affecting up to 25% of all breast cancer patients. It is associated with increased aggressiveness in tumours and a poorer clinical prognosis. In order to improve clinical outcome from endocrine agents, it is important to understand the underlying mechanisms of resistance (Johnston 2010, Ring and Dowsett 2004). Resistance may be *de novo* (before any treatment is given) or acquired (developing after a period of initial treatment response).

Diverse tamoxifen resistance mechanisms have been described, but may broadly be described under three main headings:

1. Modified ER status
2. Altered drug metabolism
3. Deregulation of the intracellular signalling environment

#### **1.3.3.1 Modified ER status**

##### **1.3.3.1.1 Loss of ER $\alpha$ expression**

Breast cancer cells must rely on ER activation to drive growth and proliferation in order for tamoxifen to exert its effect. Lack of ER expression is found in around 30%



of breast cancer patients and is the main cause of *de novo* endocrine resistance. Response to tamoxifen treatment also depends on levels of ER in ER positive tumours (Harris 2004). Tumours with high levels of ER show response rates to tamoxifen of about 75%, while tumours with low ER levels have a response rate of about 5%.

#### **1.3.3.1.2 Mutation of ER $\alpha$**

Point mutations which result in loss of ER function have been described by Schafer et al. (2000) and Wolf and Jordan (1994). Wolf and Jordan (1994) describe how a point mutation of tyrosine for aspartate at amino acid 351 leads to tamoxifen resistance in MCF-7 xenografts. Fuqua et al. (1993) describe how tamoxifen resistance can result from co-expression of wild type ER alongside a variant ER lacking exon 5 in the ligand binding domain which is unable to bind to oestrogen. However, such mutations are rare and are found in less than 1% of breast cancers (Herynk and Fuqua 2004) suggesting a limited contribution to endocrine resistance.

#### **1.3.3.1.3 Altered expression of ER $\beta$**

Expression of ER $\beta$  in breast cancer is associated with a better prognosis (Sugiura et al. 2007). This is due to a negative feedback on ER $\alpha$  driven transcription (Pettersson K 2000). Borgquist et al. (2008) and Hopp et al. (2004) showed that low levels of ER $\beta$  are predictive of tamoxifen resistance, and the relevance of ER $\beta$  remains highly controversial in the context of endocrine resistance.

### **1.3.3.2 Altered drug metabolism**

Tamoxifen is metabolised to 4-hydroxytamoxifen and 4-hydroxy-N-desmethyl tamoxifen (endoxifen). Endoxifen is up to ten times more abundant than 4-hydroxytamoxifen at steady state concentrations. It is predominantly metabolised by CYP2D6 via hydroxylation of N-desmethyl tamoxifen. Some relationships between altered tamoxifen metabolism and resistance have been reported, but in all instances these findings remain controversial.

#### **1.3.3.2.1 Pharmacogenomics**

Women with genomic variants for low or absent CYP2D6 activity will have lower levels of endoxifen during tamoxifen treatment (Jin et al. 2005). The most frequent null allele is 2D6 $\delta$ 4. It is found in about 25% of Caucasians (Zanger et al. 2004) but only 1% of Asians (Wang et al. 1993). Patients who are homozygous for CYP2D6  $\delta$ 4/ $\delta$ 4 genotype and who are receiving tamoxifen have been reported to be at a higher risk of disease recurrence (Goetz et al. 2005). Other variants associated with impaired enzyme function are CYP2D6 allele  $\delta$ 5,  $\delta$ 10 and  $\delta$ 41. This was confirmed in a recent clinical study by Teh et al. (2012). Patients having CYP2D6 $\delta$ 10 $\delta$ 10 and the heterozygous null allele had a higher risk of developing disease recurrence and metastases.

#### **1.3.3.2.2 Drug interactions affecting metabolising enzymes**

Some selective serotonin reuptake inhibitors (SSRIs) (paroxetine and fluoxetine) have been shown to inhibit CYP2D6 (Stearns et al. 2003) (Otton et al. 1996). Benefit

from tamoxifen use has been reported to be reduced in this setting (Goetz et al. 2007).

### **1.3.3.3 Deregulation of the intracellular signalling environment**

#### **1.3.3.3.1 Changes in co-regulators**

Several proteins cross talk with the ER to regulate transcription. Many are found in the nucleus and up-regulation of coactivators or downregulation of co-repressors may result in resistance (Smith et al. 1997). Osborne et al. (2003) have shown that patients receiving tamoxifen whose tumours overexpressed the co-activator amplified in breast cancer 1 (AIB1) as well as HER2 had a lowered five year disease free survival. Similar findings were reported by Kirkegaard et al. (2007) who showed that this was true for HER1, HER2 or HER3 overexpressing tumours. Low levels of nuclear receptor corepressor 1 (NCOR1) have also been associated with decreased relapse free survival in tamoxifen treated patients (Girault et al. 2003).

#### **1.3.3.3.2 Increased growth factor signalling**

Oestrogen can exert a negative feedback on transcription of proliferative genes such as EGFR and HER2 (Yarden et al. 2001). When tamoxifen blocks ER, EGFR and also HER2 expression increases (Figure 1.9). This activates downstream signalling via MAPK and AKT signalling pathways (Knowlden et al. 2003), which in turn activates nuclear ER through phosphorylation at activator protein-1 (AP-1) sites including Ser118 and Ser167 (Gee et al. 2003). There is increased expression of ER genes such as amphiregulin as a consequence. Amphiregulin is an EGFR ligand and completes the autocrine EGFR signalling loop. This results in increased growth of

cells in the presence of tamoxifen and is a mechanism behind the acquired tamoxifen resistance in breast cancer models including the tamoxifen resistant cell line, Tam-R, derived from MCF-7 (Knowlden et al. 2003).

Thus acquired tamoxifen resistance in MCF-7 cells has been linked to increased expression of EGFR/ HER2 in models such as Tam-R (Hutcheson et al. 2003, Jordan et al. 2004, Knowlden et al. 2003). MAPK and AKT signalling pathways are hyperactivated in this model, as is nuclear ER. Activated nuclear ER increases transcription not only of amphiregulin but also TGF- $\alpha$  which in turn activate EGFR. Insulin-like growth factor-2 (IGF-II) is produced as a further ER-regulated gene; and this also regulates EGFR/ MAPK signalling and cell proliferation via insulin-like growth factor-1 receptor (IGF-IR) cross-talk with EGFR.

However, interplay between growth factor signalling and membrane ER has also been implicated in tamoxifen resistance. Membrane ER can activate HER2 and downstream kinase signalling (Shou et al. 2004). Tamoxifen stimulates this cross talk leading to activation of the EGFR/ HER2 pathway. This effect may be a result of redistribution of ER from the nucleus to the cytoplasm and cell membrane (Fan et al. 2007). MCF-7/ HER2-18 cells overexpress HER2 and have been used as a model of *de novo* tamoxifen resistance. Tamoxifen has a stimulatory effect on these cells (Shou et al. 2004). It activates membrane ER, and EGFR/ HER2 signalling is substantially increased. Downstream MAPK and AKT signalling pathways are then activated and these in turn activate nuclear ER and the co-activator AIB1 to drive resistant growth.

Of note, EGFR and HER2 overexpression are prominent in both *de novo* and acquired tamoxifen resistance experimentally, with some evidence for increased

EGFR/HER2 signalling in clinical disease suggesting mechanistic relevance for increased growth factor signalling in endocrine resistance (Gee et al. 2005).

#### **1.3.3.3 Altered oestrogen sensitivity**

Some breast cancer cells can grow even in very low levels of oestrogen. These cells are thus hypersensitive or supersensitive to circulating oestrogen. Changes in growth factor signalling are again believed to be relevant in resistance to oestrogen deprivation, helping maximise membrane ER signalling and also ligand independent activity of the ER. This promotes cell growth even in the presence of very low oestradiol levels (Nicholson et al. 2004). This mechanism is potentially important in acquired resistance to aromatase inhibitors.

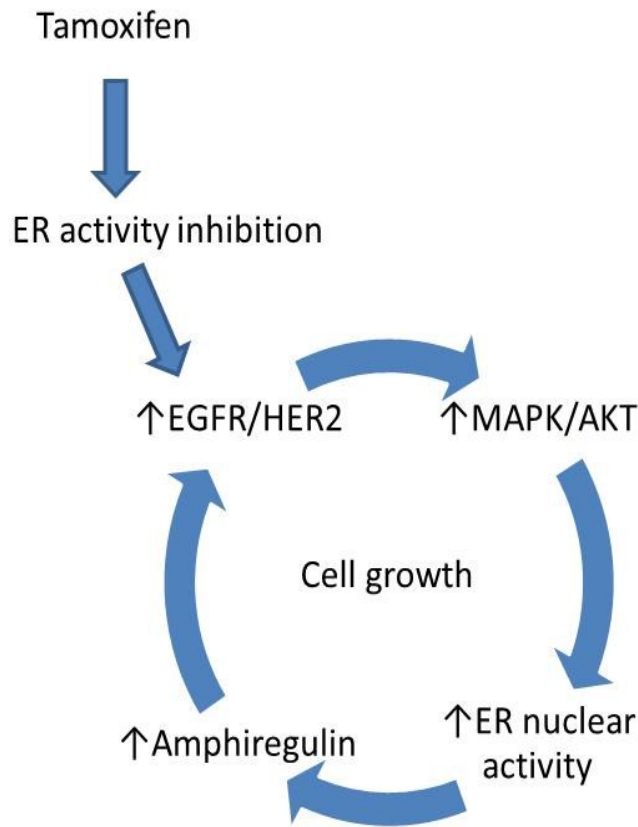


**Figure 1.9**  
**Autocrine proliferative loop.**

Antiproliferative effect of tamoxifen is limited by activation of autocrine signalling loop. Oestrogen activated ER regulates transcription of EGFR and HER2. Tamoxifen inhibits ER and transcription of EGFR and HER2 is increased. Downstream MAPK and AKT signalling pathways are activated and nuclear ER activity increases. Persistent ER activation leads to the transcription of ER-sensitive genes, including amphiregulin, a growth factor that can bind and activate EGFR. This completes the autocrine proliferative loop. Adapted from Britton et al. (2006).

## 1.4 Project Objectives

Despite the benefits of endocrine treatment, resistance remains a real clinical problem. A better understanding of the complex interactions between different growth signalling pathways may help us select targeted therapies to use alongside endocrine agents in the treatment of ER positive breast cancer. Considerable numbers of trials are exploring relevance of targeting erbB receptors and downstream kinases in this context, although it is already clear that many patients are *de novo* resistant to EGFR/HER2 blockade or rapidly acquire resistance to such treatment. Superior signalling targets and therapeutic strategies thus remain imperative.

Interestingly, previous work from our lab had shown that  $\beta$ -catenin is deregulated in the tamoxifen resistant breast cancer cell model derived from MCF-7 cells.  $\beta$ -catenin is also the key effector of canonical Wnt signalling. When Wnt signalling is activated,  $\beta$ -catenin accumulates in the nucleus where it acts a coactivator for transcription factors of the TCF/LEF family, leading to activation of Wnt responsive genes. Wnt signalling plays a role in breast cancer but its role in endocrine resistance is less well defined. The aim of this MD project was thus to explore whether Wnt signalling was deregulated in endocrine resistant breast cancer cell models and explore its potential as a therapeutic target in this setting. The main objectives were:

1. To characterise the Wnt signalling pathway in endocrine-sensitive MCF-7 cells and their endocrine-resistant tamoxifen resistant (Tam-R) and faslodex resistant (Fas-R) counterparts.
2. To explore the effect of pharmacological manipulation of the Wnt pathway on cell signalling in these cells.

# Chapter 2

## Materials and Methods



## 2 Materials and Methods

### 2.1 Materials

Materials/ Reagents	Supplier
3-(4,5- dimethylthiazol-2-yl)-2-5, diphenyl-tetrazolium bromide (MTT)	Sigma-Aldrich, Poole, Dorset, UK
Acrylamide/bis-acrylamide (30% solution, 29:1 ratio)	Sigma-Aldrich, Poole, Dorset, UK
Agarose	Bioline Ltd, London, UK
Ammonium Persulphate (APS)	Sigma-Aldrich, Poole, Dorset, UK
Amphotericin B (Fungizone)	Invitrogen, Paisley, UK
Ampicillin	Sigma-Aldrich, Poole, Dorset, UK
Antibiotics: Penicillin/Streptomycin	Life Technologies Inc, UK
Aprotinin	Sigma-Aldrich, Poole, Dorset, UK
AZD 0530	gift from Astra Zeneca, UK
Bijou vials - sterile (5ml)	Bibby Sterilin Ltd, Stone, UK
Bio-Rad Dc Protein Assay	Bio-Rad Laboratories Ltd, Herts, UK
Bovine serum albumin (BSA)	Sigma-Aldrich, Poole, Dorset, UK
Bromophenol Blue (BPB)	BDH Chemicals Ltd, Poole, UK
Cell culture medium: RPMI 1640 and Phenol-red –free RPMI 1640	Life Technologies Inc, UK
Cell culture medium: Phenol red free DCCM	Biological Industries Ltd, Israel
Sterile cell culture Corning plasticware (flasks, Petri-dishes, 24- and 96-well plates)	ThermoFisher Scientific, Leicestershire, UK
Cell scrapes	Greiner Bio-One Ltd,

	Gloucestershire, UK
Chemiluminescent Supersignal® West HRP Substrate (Pico, Dura , Femto)	Pierce and Warriner Ltd, Cheshire, UK
Cignal™ TCF/LEF Reporter Assay Kit cat no. 336841 CCS-018L	SA Biosciences, Qiagen Ltd, West Sussex, UK
Corning Standard Transwell® inserts (6.5mm diameter, 8um pore size)	Fisher Scientific, Leicestershire, UK
Coulter Counter counting cups and lids	Sarstedt AG and Co., Nümbrecht, Germany
Crystal Violet	Sigma-Aldrich, Poole, Dorset, UK
Di-butylphthalatexylene (DPX)	Raymond A Lamb Ltd, Eastbourne, UK
Dimethyl sulphoxide (DMSO)	Sigma-Aldrich, Poole, Dorset, UK
Di-potassium hydrogen orthophosphate anhydrous (K <sub>2</sub> HPO <sub>4</sub> )	Fisher Scientific UK Ltd, Loughborough, UK
Disposable cuvettes	Fisher Scientific UK Ltd, Loughborough, UK
Di-thiothreitol (DTT)	Sigma-Aldrich, Poole, Dorset, UK
Dual Luciferase Reporter Assay System E1910	Promega, Southampton, UK
Dynamo rPCR kit	Finnzymes Oy, Espoo, Finland
5% Ehrlich's haematoxylin solution	Sigma-Aldrich, Poole, Dorset, UK
Ethidium bromide (EtBr)	Sigma-Aldrich, Poole, Dorset, UK
Ethylene diamine tetraacetic acid (EDTA)	Sigma-Aldrich, Poole, Dorset, UK

Falcon tubes – sterile (15ml and 50ml)	Sarstedt AG and Co., Nümbrecht, Germany
Fibronectin (from human plasma; 1mg/ml in 0.05 TBS; pH 7.5)	Sigma-Aldrich, Poole, Dorset, UK
Filter paper (Grade 3)	Whatman, Maidstone, UK
Filter paper (Number 4)	Whatman, Maidstone, UK
Foetal calf serum (FCS)	Life Technologies Inc, UK
Gefitinib	gift from Astra Zeneca, UK
Gelatine	Sigma-Aldrich, Poole, Dorset, UK
General laboratory glass and plastic ware	Fisher Scientific UK Ltd., Loughborough, UK
Glacial Acetic Acid	Fisher Scientific UK Ltd., Loughborough, UK
Glass coverslips (thickness no. 2, 22mm <sup>2</sup> )	BDH Chemicals Ltd., Poole, Dorset, UK
Glass slides	Fisher Scientific UK Ltd., Loughborough, UK
Glycerol	Fisher Scientific UK Ltd., Loughborough, UK
Glycine	Sigma-Aldrich, Poole, Dorset, UK
Hydrochloric acid (HCl; 5M)	Fisher Scientific UK Ltd., Loughborough, UK
Hyperladder™ I and Hyperladder™ IV	Bioline Ltd, London, UK
Isoton® II azide-free balanced electrolyte solution	Beckman Coulter Ltd, High Wycombe, UK

IWP2	Tocris Bioscience, Bristol, UK
iCRT14	Tocris Bioscience, Bristol, UK
Ki-67 monoclonal antibody	DAKO, Cambridgeshire, UK
Kodak MXB Autoradiography film (blue sensitive; 18cm x 24cm)	Genetic Research Instrumentation (GRI), Rayne, UK
Leupeptin	Sigma-Aldrich, Poole, Dorset, UK
L-glutamine	Life Technologies Inc, UK
Liquid DAB <sup>+</sup> substrate chromogen system	DAKO, Cambridgeshire, UK
Lithium Chloride	Sigma-Aldrich, Poole, Dorset, UK
Lower buffer for SDS-PAGE Gels (Tris 1.5M, pH 8.8)	Bio-Rad Laboratories Ltd., HERTS, UK
LRP6 construct	gift from Professor Trevor Dale's Lab, Biosciences, Cardiff University, UK
p-LRP6 construct: GST-P3C-ΔNLRP6 His (20mM Hepes pH8 12.5 μM MgCl <sub>2</sub> )	gift from Professor Trevor Dale's Lab, Biosciences, Cardiff University, UK
Lipofectin® reagent	Invitrogen, Paisley, UK
Magnesium Chloride (MgCl <sub>2</sub> )	Sigma-Aldrich, Poole, Dorset, UK
Matrigel™ Basement Membrane Matrix	BD Biosciences, Oxford, UK
Methyl green	Sigma-Aldrich, Poole, Dorset, UK
Micro-centrifuge tubes (0.5 and 1.5ml)	Elkay Laboratory Products, Basingstoke, UK
N,N,N',N' - tetramethylene-diamine	Sigma-Aldrich, Poole, Dorset, UK

(TEMED)	
Nitrocellulose transfer membrane (Protan® BA85; 0.45µm pore size)	Thermo Fisher Scientific, Leicestershire, UK
pCR script	Promega, Southampton, UK
PD 98059	Merck Chemicals Ltd, Nottingham, UK
pH calibration buffer tablets (pH4, 7 and 10)	Fisher Scientific UK Ltd., Loughborough, UK
Phenylarsine oxide	Sigma-Aldrich, Poole, Dorset, UK
Phenylmethylsulfonyl fluoride (PMFS)	Sigma-Aldrich, Poole, Dorset, UK
Phosphate buffered saline – sterile (PBS)	Life Technologies Inc, UK
Pipette tips	Greiner Bio-One Ltd, Gloucestershire, UK
PNU 74654	Tocris Bioscience, Bristol, UK
Polyoxyethylene-sorbitan monolaurate (Tween 20)	Sigma-Aldrich, Poole, Dorset, UK
Ponceau S solution (0.1% in 5% acetic acid)	Sigma-Aldrich, Poole, Dorset, UK
Potassium Chloride (KCl)	Sigma-Aldrich, Poole, Dorset, UK
Potassium di-hydrogen orthophosphate (KH <sub>2</sub> PO <sub>4</sub> )	Fisher Scientific UK Ltd., Loughborough, UK
Precision Plus Protein™ All Blue Standards (10-250kDa)	Bio-Rad Laboratories Ltd., Herts, UK
Random Hexamers (RH)	Amersham, Little Chalfont, UK
Recombinant human wnt 3a (5036WN)	R and D systems, Abingdon, UK

RNase- free H <sub>2</sub> O	Sigma-Aldrich, Poole, Dorset, UK
RNasin® ribonuclease inhibitor	Promega, Southampton, UK
Serological pipettes - sterile, disposable (5ml, 10ml, 25ml)	Sarstedt AG and Co., Nümbrecht, Germany
Sodium Azide	Sigma-Aldrich, Poole, Dorset, UK
Sodium Chloride (NaCl)	Sigma-Aldrich, Poole, Dorset, UK
Sodium dodecyl sulphate (SDS)	Sigma-Aldrich, Poole, Dorset, UK
Sodium Fluoride (NaF)	Sigma-Aldrich, Poole, Dorset, UK
Sodium hydroxide (NaOH; 5M)	Fisher Scientific UK Ltd., Loughborough, UK
Sodium Molybdate (Na <sub>2</sub> MoO <sub>4</sub> )	Sigma-Aldrich, Poole, Dorset, UK
Solvents (acetone, chloroform, ethanol, formaldehyde, isopropanol, methanol)	Fisher Scientific UK Ltd., Loughborough, UK
Syringe filters - sterile (0.2µm)	Corning Inc., Corning, NY, USA
Syringe needles -sterile (BD Microbalance™ 3/ 25G x 5/8'')	Becton Dickenson (BD) UK Ltd, Oxford, UK
Syringe needles- sterile (Sherwood Medical Monoject; 21G x 1½'')	Sherwood- Davis and Geck, Gosport, Hampshire, UK
Syringes -sterile (BD Plastipak™; 1ml, 5ml, 10ml)	Becton Dickenson (BD) UK Ltd, Oxford, UK
Sucrose	Fisher Scientific UK Ltd., Loughborough, UK
Taq DNA polymerase (BioTaq™ ; 5U/µl)	Bioline Ltd, London, UK
Test tubes - sterile (5mls)	Fisher Scientific UK Ltd.,

	Loughborough, UK
TGF $\alpha$	Sigma-Aldrich, Poole, Dorset, UK
Topflash Reporter assay	SA Biosciences, UK
Tris HCl	Sigma-Aldrich, Poole, Dorset, UK
Triton X-100	Sigma-Aldrich, Poole, Dorset, UK
Trizma (Tris) base	Sigma-Aldrich, Poole, Dorset, UK
Trypsin/EDTA 10x solution	Life Technologies Inc, UK
Universal containers - sterile (30ml)	Greiner Bio-One Ltd, Gloucestershire, UK
Upper Buffer for SDS-PAGE gels (Tris 0.5M, pH 6.8)	Bio-Rad Laboratories Ltd., Herts, UK
VectorShield® hard-set mounting medium containing DAPI nuclear stain	Vector Laboratories, Inc., Peterborough, UK
Vybrant® Dil cell labeling solution	Invitrogen, Paisley, UK
Western Blocking Reagent	Roche Diagnostics, Mannheim, Germany
Wnt3a	R and D systems, Abingdon, UK
X-ray film developer solution (X-O-dev)	X-O- graph Imaging System, Tetbury, UK
X-ray film fixative solution (X-O-fix)	X-O- graph Imaging System, Tetbury, UK

**Table 2.1**  
**List of materials used and their suppliers.**

## **2.2 Cell media**

‘R5%’ media: RPMI 1640 supplemented with 5% foetal calf serum (FCS), penicillin (100units/ml), streptomycin (100µg/ml) and amphotericin B (2.5µg/ml).

‘W5%f’ media: Phenol-red- free RPMI 1640 (phenol red absent due to its oestrogenic action) supplemented with 5% FCS, L-Glutamine (200mM), penicillin (100units/ml), streptomycin (100µg/ml) and amphotericin B (2.5µg/ml)..

‘W5%s’: Phenol-red- free RPMI 1640 supplemented with 5% charcoal-stripped foetal calf serum (SFCS; charcoal-stripped to remove endogenous steroid hormones which may compete with endocrine agent for the ER), L-Glutamine (200mM), penicillin (100units/ml), streptomycin (100µg/ml) and amphotericin B (2.5µg/ml).

DMEM: Dulbecco's Modified Eagle Medium supplemented with 10% FCS, penicillin (100units/ml), streptomycin (100µg/ml) and amphotericin B (2.5µg/ml).

## **2.3 Cell lines**

The hormone sensitive MCF-7 wild-type cell line was a kind gift from AstraZeneca Pharmaceuticals (Macclesfield, Cheshire), and was originally obtained from ATCC® Number HTB-22™. The cells were maintained in R5%.

Initial characterisation of components of Wnt signalling pathway was done in MCF-7 cells grown in W5%s and W5%f. There was no difference in results for the two groups. Further experiments were carried out using W5%f. This was chosen to optimise growth conditions for MCF-7 cells.

Tamoxifen resistant MCF-7 cell line (Tam-R) is an in-house acquired resistant cell line as described by Knowlden et al. (2003). MCF-7 cells were grown in W5%s



supplemented with 4-hydroxytamoxifen (tamoxifen; 100nM concentration). Over a period of 2-3 months, resistant cells emerged. These cells were grown for a further 3 months until the fully stable resistant cell line was established. Tam-R cells were routinely grown in W5% supplemented with Tam (100nM).

Fulvestrant resistant MCF-7 cell line (Fas-R) is another acquired resistance in-house cell line as described by McClelland et al. (2001). MCF-7 cells were grown in W5% supplemented with Fulvestrant (Fas; 100nM concentration). Over a period of 2-3 months, resistant cells emerged. These cells were grown separately for a further 3 months until the resistant cell line was established. Long term faslodex resistant cells were studied at about two years (Nicholson et al. 2005). Fas-R cells were routinely grown in W5% supplemented with Fas (100nM).

SW480 cells were a gift from Trevor Dale's Lab (Biosciences, Cardiff University, UK). Cells were routinely grown in DMEM. This colorectal cancer cell line was used as a positive control for the nuclear protein  $\beta$ -catenin.

## **2.4 Cell culture**

Cell culture was carried out under sterile conditions in a MDH Class II laminar- flow safety cabinet (Bioquell UK Ltd, Andover, UK). All equipment and consumables were either purchased sterile for single use or sterilised at 119°C using a Denley BA852 autoclave (Thermoquest Ltd, Basingstoke, UK). Cells were grown in 25cm<sup>2</sup> flasks (T-25) or in 75cm<sup>2</sup> flasks (T-75) and grown in a Sanyo MCO-17AIC incubator (Sanyo E&E Europe BV, Loughborough, UK) at 37°C with a humidified atmosphere containing 5% CO<sub>2</sub>. Culture medium was changed every 3-4 days. The cells were passaged on reaching 80-90% confluence. A Nikon eclipse TE200 phase- contrast

microscope (Nikon UK Ltd, Kingston- upon- Thames, UK) was used to visually assess the cell cultures.

#### **2.4.1 Cell passaging**

The medium was removed and 10mls of trypsin (0.5%)/EDTA (0.02%) in warmed Dulbecco's phosphate-buffered saline (PBS) was added to the flask. The flask was then returned to the incubator for 3-5 minutes until the cells were in suspension. Trypsin/EDTA was neutralized with an equal volume of appropriate medium (as per cell line). Cells were then pelleted by centrifugation (Jouan C312 (Thermo Fischer Scientific Inc., MA, USA); 1000rpm for 5 min). The supernatant was aspirated off and the cell pellet was re-suspended in 10mls of the medium. A proportion of this suspension was diluted in further medium to seed additional flasks (usually 1:10 dilution). Cell-lines were passaged for up to 25 times and then discarded. Stocks of established cell- lines were stored in liquid nitrogen and thawed as necessary.

For cell seeding for experimental analysis, cells were washed twice with PBS prior to trypsin/EDTA dispersion, centrifugation and re-suspension as above. Cells were then passed through a sterile 25G syringe needle to obtain a single cell suspension. A 100µl aliquot of this suspension was added to 10mls of Isoton® II solution. Cell numbers were determined using a Coulter<sup>TM</sup> Multisizer (Beckman Coulter Ltd, High Wycombe, UK). Cells were then seeded at the appropriate density as suited to the experimental design.

### **2.4.2 Cell lysis for protein analysis**

Cells were seeded into 60mm or 100mm diameter Petri Dishes at an appropriate density and cultured to log- phase growth. For lysis, cells were washed twice with ice-cold PBS and lysed with Triton-X100 lysis buffer. This buffer contained the following protease and phosphatase inhibitors: sodium orthovanadate 2mM, phenylmethylsulfonyl fluoride 1mM, sodium fluoride 25mM, sodium molybdate 10mM, phenylarsine 20 $\mu$ M, leupeptin 10 $\mu$ g/ml and aprotinin 8 $\mu$ g/ml). Volume of lysis buffer was dependent on the size of the dish and cell confluency. The cells were then collected using a cell scraper and transferred to a 1.5ml micro-centrifuge tube. The lysate was then left on ice for 10-30 minutes before centrifugation (IEC Micromax RF micro-centrifuge (Thermo Electron Corporation, Hampshire, UK); 13000rpm, 15 minutes, 4°C). The supernatants were removed and stored at -20°C until required.

## **2.5 Protein Analysis**

### **2.5.1 Protein Concentration Assay**

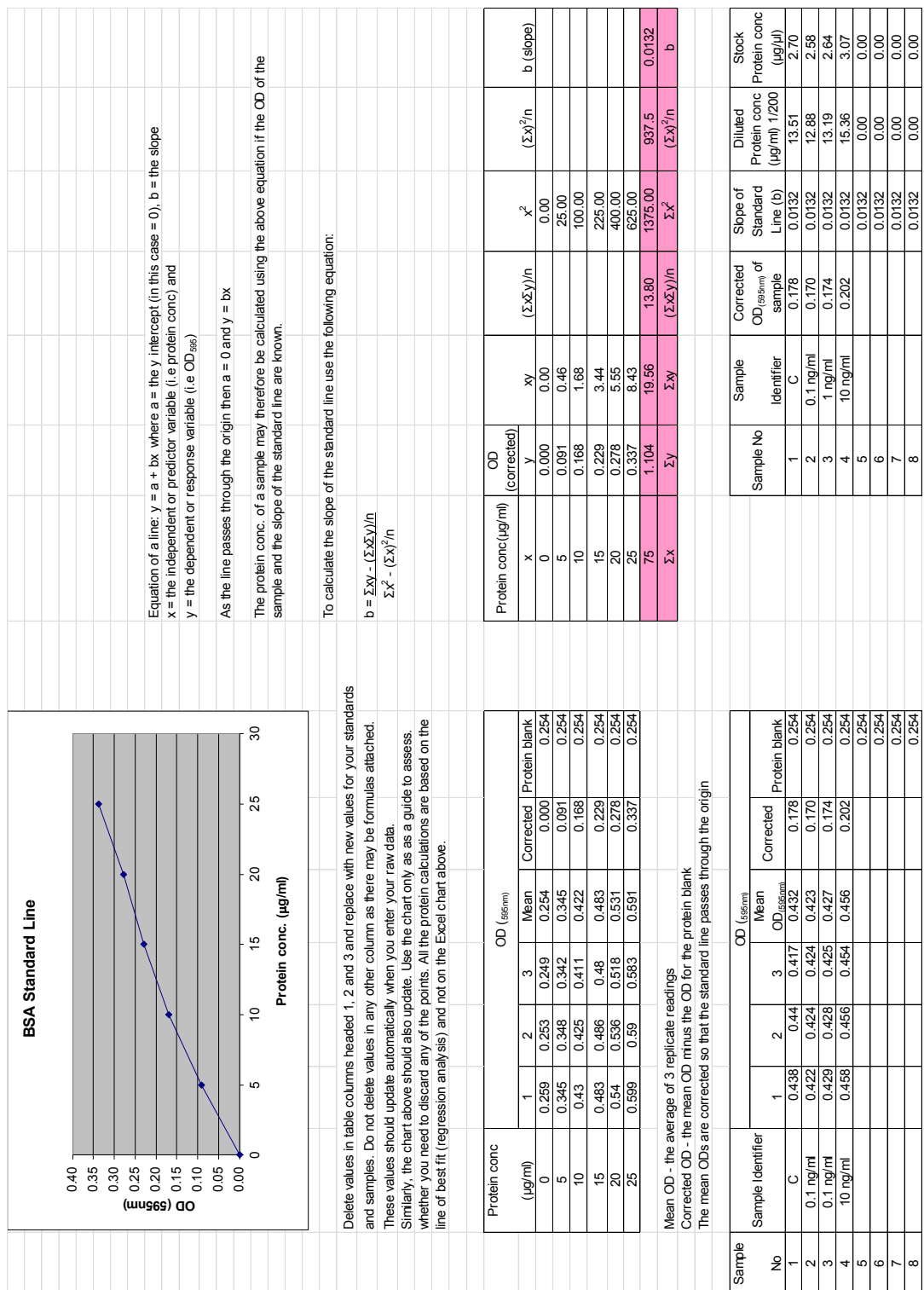
A BioRad microassay based on the Bradford Assay (Bradford 1976) was used to determine protein concentrations in lysate samples. Lysate samples were stored at -20°C until required. Bovine serum albumin (BSA) at concentration of 1mg/ml was used. This acted as protein standard against which samples were measured. A range of dilutions of the protein standard containing from 5 to 25 $\mu$ g/ml was prepared as outlined in the table below.

The test samples were then prepared at an appropriate dilution (usually 1/200); i.e. 2 $\mu$ l of cell lysate + 398 $\mu$ l of distilled water in an Eppendorf. If samples were very

dilute a dilution of 1/100 was used; for concentrated samples a dilution of 1/400 was used. 100µl of BioRad Dye Concentrate was then added to 400 µl of standard/test sample and vortexed to mix. After 10 min to 1hr, 3 x 150µl replicates of the standard/sample dye reaction mix were transferred to a 96 well plate and light absorbance was measured at 595nm (OD<sub>595</sub>) using a plate reader (Sunrise® microplate touch screen reader, Tecan, Reading, UK). The values were then transferred to an Excel spreadsheet template and protein concentration (µg/ml) versus the OD<sub>595</sub> was plotted. The protein concentration (µg/ml) was read from the standard line and the stock concentration of the sample was calculated by factoring in the dilution factor (Figure 2.1).

<b>BSA conc (µg/ml)</b>	<b>BSA Stock (µl)</b>	<b>dH<sub>2</sub>O (µl)</b>	
0	0	400	Blank
5	2	398	Protein Standards
10	4	396	
15	6	394	
20	8	392	
25	10	390	

**Table 2.2**  
**Serial concentrations for standard samples for BioRad Microassay.**



### 2.5.2 SDS-PAGE Analysis

Sodium-Dodecyl-Sulphate-Polyacrylamide Gel electrophoresis (SDS-PAGE) was performed using Bio-Rad Mini-Protean®III apparatus powered by a Powerpac Basic<sup>TM</sup> power pack (Bio-Rad Laboratories Ltd, Herts, UK) following the manufacturer's instructions. The gel system consisted of a 4% acrylamide/ bis-acrylamide stacking gel at pH 6.8 and a 6-10% acrylamide/ bis-acrylamide resolving gel at pH 8.8.

The apparatus was set up as per manufacturer's instructions. The glass plates were cleaned with ethanol (70%) before starting the experiment to prevent cross-contamination. The resolving gel was prepared (table 2.3); TEMED was only added to the mixture after mixing the other components of the gel. The solution was then added to the glass plate pair to about 1.5cm below the top. The gel was covered with ethanol and allowed to set. This helped prevent evaporation of various components of the gel as it polymerised. Once the gel had set, the ethanol was discarded and the surface was blotted dry using filter paper. The stacking gel was prepared (see table 2.4) and added to the top of the resolving gel. A 10- or 15-well comb was inserted at the top of the plates. The gel was then allowed to set. The set gel was assembled in the electrophoresis apparatus and SDS-PAGE running buffer was added to inner and outer reservoirs in the tank. The comb was then removed from the gel.

	6% gel	8% gel	10% gel	Final concentration in gel
acrylamide/ bis-acrylamide solution*	2ml	2.7ml	3.3ml	
H <sub>2</sub> O	5.3ml	4.6ml	4ml	
Tris (1.5M, pH 8.8)	2.5ml	2.5ml	2.5ml	375mM
SDS (10% solution in H <sub>2</sub> O)	100μl	100μl	100μl	0.1%
APS (10% solution in H <sub>2</sub> O)	100μl	100μl	100μl	0.1%
TEMED	20μl	20μl	20μl	0.2%

**Table 2.3**  
**Resolving gel used in SDS-PAGE**

	4% (for 10mls)	Final concentration in gel
acrylamide/ bis-acrylamide solution*	1.3ml	4%
H <sub>2</sub> O	6.1ml	
Tris (0.5M, pH 6.8)	2.5ml	125mM
SDS (10% solution in H <sub>2</sub> O)	100μl	0.1%
APS (10% solution in H <sub>2</sub> O)	50μl	0.05%
TEMED	6μl	0.06%

**Table 2.4**  
**Stacking gel used in SDS-PAGE**

\*Acrylamide solution used was a 30% solution and acrylamide: bis-acrylamide ratio was 29:1



### **2.5.2.1 Preparation of cell lysates**

Cell lysates with a known amount of protein were added to 2x or 3x Laemmli sample loading buffer. Samples were then denatured by heating for 5 min at 100°C. Cell samples and a protein molecular weight marker (precision Plus Protein™ All Blue standards 10-250kDa) were then loaded into the appropriate wells in the gel. Electrophoresis was carried out by running a voltage of 160V through the gel (about 90 minutes or until the blue dye had reached the bottom of the gel).

### **2.5.3 Western Blotting**

A Bio-Rad Mini-Protean® III apparatus powered by a Powerpac Basic™ power pack (Bio-Rad Laboratories Ltd, Herts, UK) was used to transfer the proteins onto a nitrocellulose membrane. For each gel, four pieces of filter paper and one piece of Protran B85 nitrocellulose membrane (0.45µM pore size) were cut to the same size as the gel plates. Two Teflon sponges of similar size, the filter paper and nitrocellulose membrane were soaked in Western blot transfer buffer for about 30 minutes. Once electrophoresis was ready, the gel plates were gently separated. The stacking gel was removed and the resolving gel carefully transferred to a tray containing transfer buffer. A transfer cassette was then set up as per manufacturer's instruction manual. (Figure 2.2) The cassette was then placed into the transfer apparatus and run at 100V for 1 hour to allow for transfer of proteins from the gel to the nitrocellulose membrane. An ice-block was added to the tank to prevent overheating in the process.

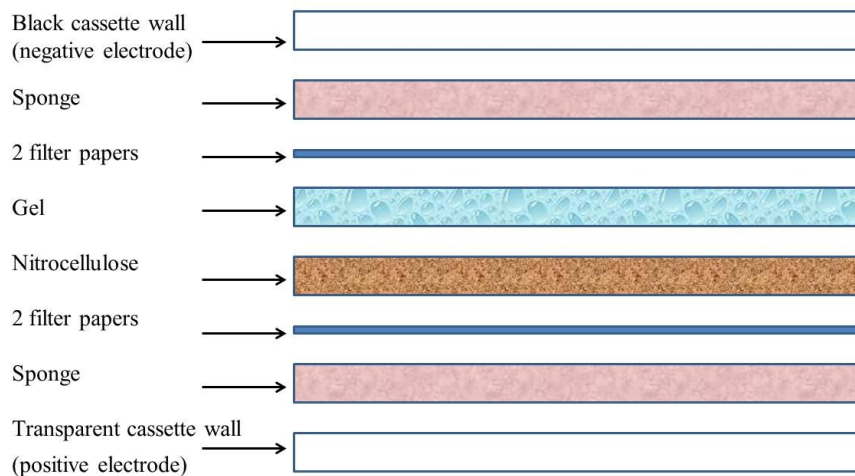


**Figure 2.2**  
**Assembly of Western blot transfer apparatus.**

#### **2.5.4 Immuno-detection**

The membrane was removed from the transfer apparatus and washed briefly in Ponceau S to stain proteins. This was then photocopied for a record of protein loading. The membrane was then rinsed with Tris- Buffered Saline - Tween (TBST) buffer solution to remove all traces of the stain. The membranes were incubated with 5% Marvel® skimmed milk powder/TBST in a lid for 30 minutes to 1 hour. This helped fix the protein onto the membrane. The membrane was washed briefly in TBST ((2x 5minutes) and then incubated overnight on a roller in the appropriate primary antibody at a temperature of 4°C.

Primary antibody: Dilutions of 1:1000 or 1:5000 were typically used for the primary antibody. For 1:1000 dilutions, 5 $\mu$ l of primary antibody, 5ml of TBST, 250 $\mu$ l of western blocking reagent and 50 $\mu$ l of sodium azide. For dilutions of 1:5000, 1 $\mu$ l of primary antibody was used instead.

The next day the membrane was washed briefly for three times in TBST at room temperature. It was then incubated with the secondary antibody for 1 hour before washing briefly in TBST for 5 times to remove any excess antibody.

Secondary antibody: Dilutions varied from 1:10 000 to 1:50 000 and mouse, rabbit or goat horseradish- peroxidase- linked secondary antibodies were used to match the primary antibody. For 1:10 000 dilutions, 1 $\mu$ l of secondary antibody was added to 10ml of 1% Marvel® skimmed milk powder/ TBST.

Primary and secondary antibodies are detailed in Table 2.5.

### **2.5.5 Chemoluminescent detection**

Chemoluminescence was performed using a luminol/peroxidase based enhanced chemoluminescence reagent (Supersignal<sup>TM</sup> PICO, Supersignal<sup>TM</sup> Dura or Supersignal<sup>TM</sup> Femto). The reagents were prepared as per manufacturer's instructions and added to the blot for five minutes. The reagent contained Luminol which was oxidised by HRP in the presence of hydrogen peroxide to produce an unstable product. This decayed to release photons of light which were captured on X-ray film. Exposures varied from one second to several hours depending on the strength of the signal. The X-ray films were developed using an X-O-graph Compact X2 x-ray developer (X-O-graph imaging system, Tetbury, UK). The films were scanned and analysed using a Bio-Rad GS-690 Imaging Densitometer (Bio-Rad Laboratories Ltd, Herts, UK) linked to a computer. Densitometry was measured using Molecular Analyst Version 1.5 (Bio-Rad Laboratories Ltd, Herts, UK).

<b>Primary Antibody</b>	<b>Company (see key in legend for company details)</b>	<b>Dilution</b>	<b>Antibody Incubation conditions</b>	<b>Source</b>	<b>Molecular mass</b>
$\beta$ -actin	Sigma A5316	1:20 000	1hr RT	Mouse	37 kDa
AKT total	cs #9272	1:4000	O/N 4°C	Rabbit	60 kDa
p-AKT	cs #9271 S473	1:1000	O/N 4°C	Rabbit	60 kDa
active $\beta$ - catenin (clone 8E7)	Millipore cat #05-665 lot #DAM 1614910	1:1000	O/N 4°C	Mouse	92 kDa
total $\beta$ - catenin	Sigma C2206 lot #059k454	1:1000	O/N 4°C	Mouse	92 kDa
p- $\beta$ - catenin (Ser 33/37 Thr 41)	cs #9561	1:1000	O/N 4°C	Rabbit	92 kDa
c-myc	sc 40 9E10	1:1000	O/N 4°C	Mouse	43-55 kDa
Cyclin D1	sc 718 lot F041	1:1000	O/N 4°C	Rabbit	37 kDa
EGFR total	cs #2232	1:1000	O/N 4°C	Rabbit	170 kDa
p-EGFR 1068	cs #2234 T1068	1:1000	O/N 4°C	Rabbit	170 kDa
GAPDH	sc32233 lot #D0408	1:15 000	1hr RT	Mouse	40 kDa
GSK- 3 $\alpha$ / $\beta$ total	sc 7291 (0011-A) lot #222	1:1000	O/N 4°C	Mouse	47,51 kDa
(Ser 21/9) p- GSK 3 $\alpha$ / $\beta$	cs #9331	1:1000	O/N 4°C	Rabbit	47,51 kDa
LRP6 total	cs #2560	1:1000	O/N 4°C	Rabbit	180-210

	C5C7				kDa
p-LRP6	cs #2568 S1490	1:1000	O/N 4°C	Rabbit	180-210 kDa
MAPK p44/42 total	cs #9102	1:2000	O/N 4°C	Rabbit	42-44 kDa
p- p44/42 MAPK	cs #9101L Thr 202/ Tyr 204	1:1000	O/N 4°C	Rabbit	42-44 kDa
src total	Biosorce 44-656G	1:1000	O/N 4°C	Rabbit	60 kDa
p-src	Biosorce 44-660G T418	1:1000	O/N 4°C	Rabbit	60 kDa
<b>Secondary</b>					
anti- rabbit horseradish- peroxidase- linked (HRP) IgG	cs # 7074	1:1000	1hr RT	from goat	
anti- mouse horseradish- peroxidase- linked (HPR) IgG	GE healthcare NXA931	1:1000	1hr RT	from sheep	

**Table 2.5**  
**Antibodies used for immune probing of western blots.**

Abbreviations:

cs: Cell Signalling; ab: Abcam; sc: Santa Cruz

O/N: overnight

RT: room temperature

### **2.5.6 Validation of LRP6 and p-LRP6 antibodies**

LRP6 and p-LRP6 constructs [GST-P3C- $\Delta$ NLRP6] (gift from Professor Trevor Dale's Lab, Biosciences, Cardiff University, UK) were used to validate secondary antibodies to LRP6 and p-LRP6. The  $\Delta$ NLRP6 (LRP6c) and p $\Delta$ NLRP6 (pLRP6c) constructs were about 53.2 kDa in size. LRP6 can be phosphorylated at multiple PPPSP sites including Thr1479, Ser1490 and Thr1493. (Figure 2.3, Table 2.6). The p $\Delta$ NLRP6 construct contained PPPSP motif A whereas the  $\Delta$ NLRP6 construct contained PPPSP motif B (Table 2.6).

The commercial total LRP6 antibody was produced by immunizing animals with a synthetic peptide corresponding to residues around Met1409 (cell\_signalling 2012a). The commercial p-LRP6 antibody targeted Ser1490 (present in PPPSP motif A) (cell\_signalling 2012b).

MCF-7 cells were cultured to log-phase growth and lysed as described in materials and methods. SDS-PAGE/ Western blot analyses was carried out using 30 $\mu$ g of MCF-7 total soluble protein and 1 $\mu$ g of  $\Delta$ NLRP6 and p $\Delta$ NLRP6 constructs (LRP6c and pLRP6c). The membranes were probed with antibodies specific to LRP6 or p-LRP6. The membrane containing p $\Delta$ NLRP6 construct was probed with antibodies specific to p-LRP6 and LRP6 antibodies (Figure 2.4). LRP6 and p-LRP6 in MCF-7 cell lysates were detected at 180-210 kDa. The  $\Delta$ NLRP6 construct was detected at 53-54 kDa; the p $\Delta$ NLRP6 construct was detected by the commercial p-LRP6 and LRP6 antibodies at 53-54 kDa (Figure 2.4).

Positions	Description
1487-1493	PPPSP motif A
1527-1534	PPPSP motif B
1568-1575	PPPSP motif C
1588-1593	PPPSP motif D
1603-1610	PPPSP motif E

**Table 2.6**

**PPPSP motifs for LRP6**

Accessed online on 19 April 2012

<http://www.uniprot.org/uniprot/O75581>



this image has been removed by the author  
for copyright reasons

this image has been removed by the author  
for copyright reasons

this image has been removed by the author  
for copyright reasons

**Figure 2.3**  
**Amino acid sequence for LRP6.**

Accessed online on 20 July 2011.  
<http://www.uniprot.org/uniprot/O75581>.

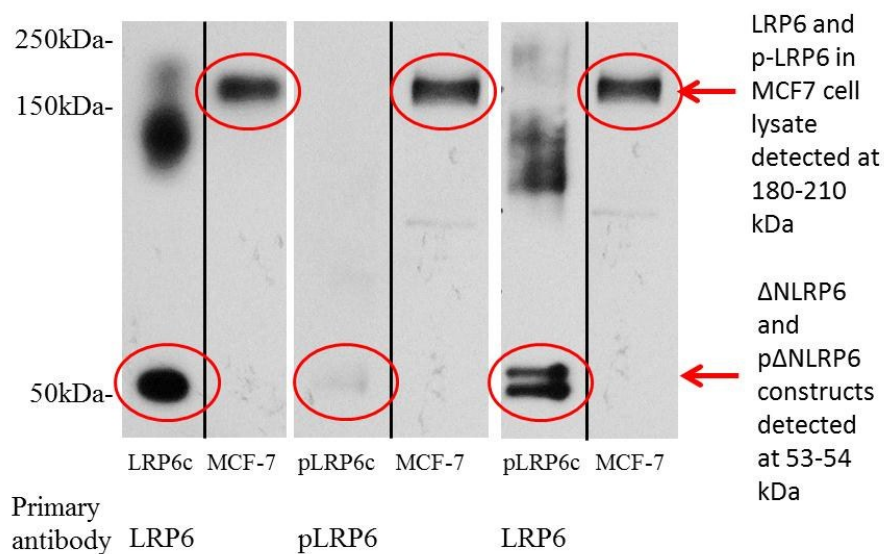


**Figure 2.4**  
**Validation of LRP6 and p-LRP6 constructs.**

MCF-7 cells were cultured to log-phase growth and lysed as described in materials and methods. SDS-PAGE/ Western blot analyses were carried out using 30 $\mu$ g of MCF-7 total soluble protein and 1 $\mu$ g of  $\Delta$ NLRP6 and p $\Delta$ NLRP6 construct (LRP6c and pLRP6c). The membranes were probed with antibodies specific to LRP6 or p-LRP6. The membrane for p $\Delta$ NLRP6c was probed with both p-LRP6 and LRP6 antibodies. LRP6 and p-LRP6 in MCF-7 cell lysate were detected at 180-210 kDa.  $\Delta$ NLRP6c and p $\Delta$ NLRP6c were detected at 53-54 kDa.

## **2.6 Cell growth assays**

### **2.6.1 MTT assay**

MTT growth assays rely on the metabolism of 3-(4, 5-dimethylthiazol-2-yl)-2,5-diphenyl-2H-tetrazolium (a soluble yellow compound) by mitochondrial dehydrogenase enzymes in the cell to produce insoluble formazan crystals (purple). The cells are then lysed to release these crystals and absorbance of the solution is proportional to the cell number.

Cells were harvested seeded in a 96 well plate at an appropriate density and using the appropriate medium. Treatment was added the following day (day 0). The plate was incubated at 37°C in humidified atmosphere containing 5% CO<sub>2</sub> for six days. Medium was changed after 3 days. On day six, the medium was removed, and cells were washed with PBS. 150µl of sterile filtered MTT in wRPMI (0.5mg/ml) were added to the cells and left in the incubator for four hours. The solution was then aspirated and 150µl of Triton-X100 in PBS (10%) was added to each well. This was left overnight at 4°C. The following day, the plate was allowed to reach room temperature and then read on a plate- reader (Sunrise® microplate touch screen reader, Tecan, Reading, UK) at 540nm.

### **2.6.2 Cell counting**

Cells were harvested using trypsin/EDTA and seeded in a 24 well plate (seeding density 40 000/well). Treatments were added after 24 hours. This allowed cells to settle in the wells. Cells were allowed to grow for 6-7 days and medium was changed every 3-4 days. The plate was incubated at 37°C in humidified atmosphere with 5% CO<sub>2</sub>. At the end of the experiment, the medium was removed and 1ml of

trypsin/EDTA was added to each well. Once the cells were in suspension, cells were drawn into a 5ml syringe through a 25G needle three times to obtain a single-cell suspension. The wells were then washed with 1ml of fresh Isoton II solution and this was then drawn up into the syringe. This final wash was repeated twice to give a total volume of 4mls in the syringe. The solution was then added to 6 mls of Isoton II solution in a counting cup to make up a volume of 10mls. Cells were then counted using a Coulter<sup>TM</sup> Multisizer II. Two counts were taken from each well. The values were multiplied by 20 to give the total number of cells per well.

### **2.6.3 Estimation of half maximal inhibitory concentration (IC<sub>50</sub>) for IWP2, PNU 74654 and iCRT14**

Data from MTT assays was used to determine the half maximal inhibitory concentration (IC<sub>50</sub>) for IWP2, PNU 74654 and iCRT14. A linear effect of the drug on cell growth was assumed, and a linear model of interpolation was used (template is shown in Figure 2.5).

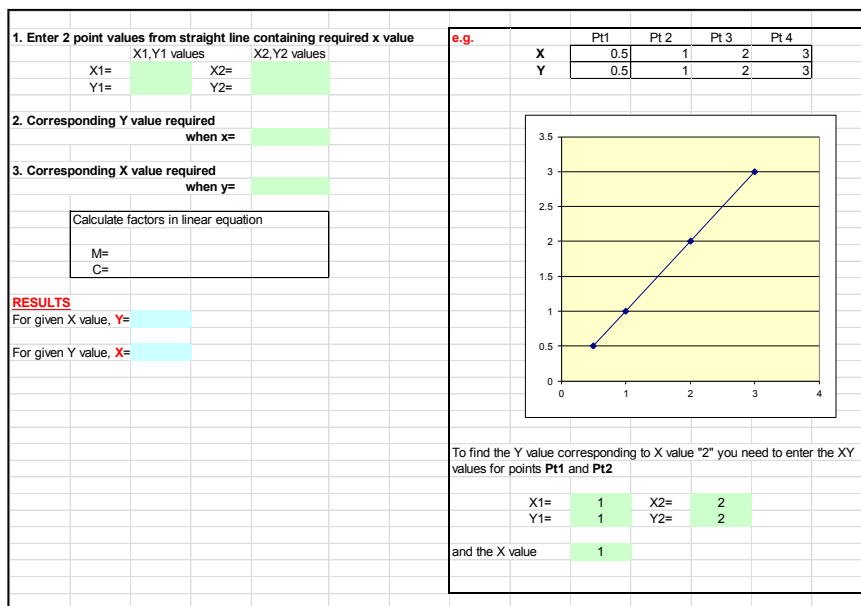


**Figure 2.5**  
**Linear model of interpolation template.**

The half maximal inhibitory concentration (IC50) for pharmacological Wnt inhibitors IWP2, PNU 74654 and iCR14 was estimated using this model.

## 2.7 Cell Migration Assays

Cell migration assays were carried out using Corning Transwell® inserts with 6.5mm diameter and 8µm membrane pore size. The undersides of the Transwell® insert membranes were coated with fibronectin. Fibronectin was diluted to 10µg/ml in wRPMI (with no additives) and 200µl was added to each well. The inserts were then placed in the well, so that the bottoms of the inserts were just submerged in the matrix solution (Figure 2.6). The plate was then incubated at 37°C for 2 hours. After this, the inserts were removed, washed with PBS and allowed to air dry. Cells were harvested using Trypsin/EDTA as previously described and seeded into the upper Transwell® compartment at a density of  $5 \times 10^4$  +/- Tamoxifen (100nM) +/- treatments (650µl) and then added to the lower compartment of the insert. The plate was then incubated at 37°C for 24 hours. The medium in the upper compartment of the inserts was then removed and the cells on the top of the membrane (i.e. the non-migratory cells) were removed using a cotton swab. The cells on the under surface of the membrane (i.e. migratory cells) were fixed in 3.7% formaldehyde in PBS for 10 minutes. The cells were washed with PBS and stained with crystal violet (0.5% in water) for 15-30 minutes. The inserts were then washed in PBS to remove excess crystal violet stain and air dried at room temperature. Cells were counted in five random fields of view at 10x magnification using an Olympus BH-2 phase contrast microscope and data was presented as mean cell count/field.



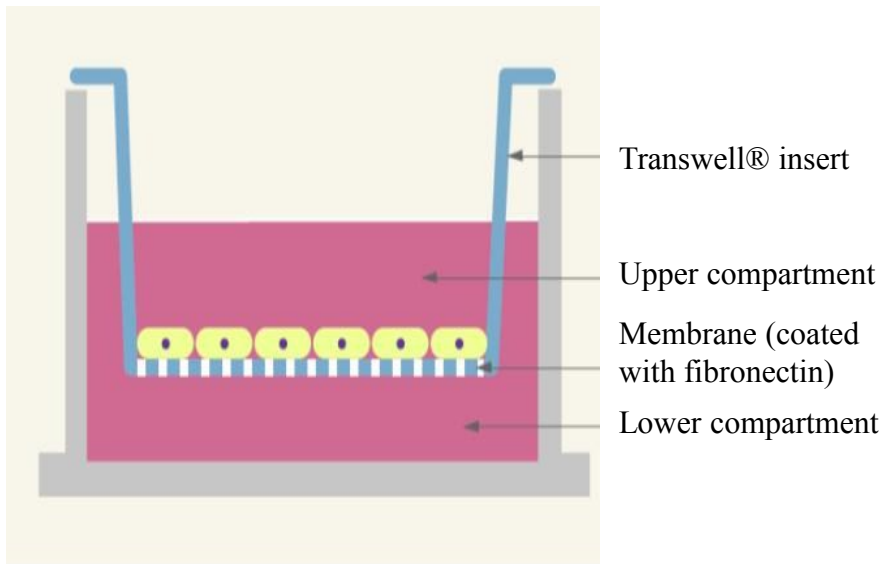


**Figure 2.6**  
**Diagram of Corning Transwell® insert in a 24-well plate.**

Figure accessed online on 19 April 2012 and adapted from [http://catalog2.corning.com/Lifesciences/media/pdf/transwell\\_guide.pdf](http://catalog2.corning.com/Lifesciences/media/pdf/transwell_guide.pdf) (Corning 2012).

## **2.8 Immunocytochemistry**

### **2.8.1 Methanol fix for active $\beta$ -catenin staining**

Cells were seeded on TESPA-coated coverslips and grown to 70- 80% confluence. The cells were then fixed using ice-cold methanol for 10 minutes (for active  $\beta$ -catenin assay) followed by immunochemical staining. The coverslips were placed in a rack and submerged in a bath containing methanol for ten minutes at  $-10^{\circ}\text{C}$  to  $-30^{\circ}\text{C}$  and then air dried for twenty minutes before storing at  $-70^{\circ}\text{C}$ . For immunostaining, coverslips were washed with 0.01M PBS (2 x five minutes) and rinsed with 0.02% Tween/ PBS for a further five minutes. Primary antibody for active  $\beta$ -catenin was diluted in PBS (dilution optimized for each sample) and 50 $\mu\text{l}$  added to each coverslip. Samples were incubated overnight in a humidified atmosphere at  $23^{\circ}\text{C}$ . The next day the coverslips were washed with PBS (2x five minutes) and incubated with one drop of the appropriate HRP- labeled mouse or rabbit antibody (Dako EnVision<sup>TM</sup> system, peroxidase (DAB) kit) for 60 minutes at  $23^{\circ}\text{C}$ . The coverslips were washed again in PBS for three minutes and then in Tween/PBS (2 x five minutes). 2,3-diaminobenzidine (DAB), a chromogenic HRP substrate solution, was added to the coverslips for ten minutes, which were then washed in distilled water (2 x two minutes). They were counterstained with 5% haematoxylin in water for four minutes, rinsed with tap water and submerged in tap water for another four minutes. The samples were then air dried and affixed to a microscope slide using di-butylphthalatexylene (DPX) adhesive. Slides were assessed on an Olympus BH-2 phase- contrast microscope fitted with Olympus DP-12 digital camera system (eyepiece magnification x10). Representative images were taken at x40 magnifications.

H-scores (histological scores) were also calculated for nuclear, cytoplasmic and membrane expression of active  $\beta$ -catenin. The score ranged from 0 to 300 for each localisation. Percentage positive cells for a localisation were noted and staining intensity was subdivided into low, medium or high. The final score was calculated using the following formula: (% low) + (% moderate x2) + (% high x3). For example, for a 90% positive nuclear stain that was 40% low, 40% moderate and 10% high, the H-score would be 40+80+30=150. The experiments were repeated in triplicate and the average H-score for each localisation was calculated.

### **2.8.2 Formal Saline for Ki67 proliferation assays**

To accompany MTT viability assays, we then stained for Ki67, a surrogate for cellular proliferation. Cells were seeded on TESPA-coated coverslips and grown to 70- 80% confluence, following which they were fixed in formal saline (3.7%) for ten minutes and stored at -20°C. The coverslips were washed with PBS (3 x two minutes) and then rinsed with 0.02% Tween/ PBS for a few seconds. Excess buffer was removed before applying the primary antibody (Ki-67) which was diluted in PBS (optimised for each sample; 1:100 for Dako Ki67 clone MIB-1 (M7240)) and then added to each coverslip. After 90 minutes, the samples were washed in PBS for three minutes and in PBS/Tween (2 x five minutes). The coverslips were incubated with one drop of appropriate HRP- labeled mouse or rabbit antibody (Dako EnVision™ system, peroxidase DAB kit) for seventy- five minutes at 23°C. They were washed again in PBS for three minutes and then in Tween/PBS (2 x five minutes). 2,3-diaminobenzidine (DAB), a chromogenic HRP substrate solution, was added to the coverslips for ten minutes which were then washed in distilled water (2 x two minutes). An aqueous solution of 0.5% methyl green was applied to the

sections for one minute and sections were then rinsed with distilled water (2 x three minutes). The samples were affixed to a microscope slide using di-butylphthalatexylene (DPX) adhesive. Slides were assessed on an Olympus BH-2 phase-contrast microscope fitted with Olympus DP-12 digital camera system (eyepiece magnification x10). Representative images were taken at x40 magnifications.

### **2.8.3 Verification of active $\beta$ -catenin antibody**

Active  $\beta$ -catenin (ABC) localisation in the human colon adenocarcinoma cell line SW480, is reported to be predominantly nuclear (Maher et al. 2010) and thus SW480 cells were chosen as a positive control for nuclear  $\beta$ -catenin. Staining of nuclear  $\beta$ -catenin was performed as follows: SW480 cells were cultured on cover slips until they reached log-phase growth. They were then fixed with methanol as described in the materials and methods section and assayed for active  $\beta$ -catenin using a specific monoclonal antibody. Representative images were taken at x40 magnification (Figure 3.2) using an Olympus BH-2 phase contrast microscope fitted with Olympus DP-12 digital camera system (eyepiece magnification x10).

## **2.9 Semi-quantitative reverse transcription polymerase chain reaction**

This was used to investigate mRNA expression of canonical Wnt target genes, cyclin D1 and c-myc, in MCF-7 and Tam-R cell lines (Saiki et al. 1988, Saiki et al. 1985).

### **2.9.1 Extraction of RNA**

Cells were seeded into 100mm petri dishes at an appropriate density and grown to log phase. Total RNA was extracted under sterile conditions in a fume cupboard using Sigma TRI reagent (Sigma, UK). Cell culture medium was removed and cells were washed twice with PBS. 1ml of TRI reagent was added to each dish and cells were homogenised with a cell scraper. This was then allowed to stand for five minutes at room temperature. 1ml of the sterile lysate was then pipetted into a sterile eppendorf. Chloroform was added (0.2ml chloroform per ml of TRI reagent) and the tube was shaken vigorously for fifteen seconds. The lysate was allowed to stand for fifteen minutes at room temperature before being centrifuged at 12000g for fifteen minutes at 4°C. The aqueous upper phase was then removed to a fresh eppendorf tube. 0.5ml isopropanol (2-propanol) per ml TRI reagent was added and this was again shaken and allowed to settle at room temperature for ten minutes. The sample was then centrifuged at 7500g for five minutes at 4°C. The supernatant was discarded and the pellet was washed with 1ml 75% ethanol. Following a quick vortex, it was then centrifuged at 7500g for five minutes at 4°C. This was then stored at -70°C till further use.

### **2.9.2 RNA quantification**

The pellet was air dried in a fume cupboard to remove as much ethanol as possible. The dry pellet was solubilised in 20-50µl of sterile water. Quantitative spectrometry was performed. 0.5-2µl of sample was added to 500µl RNase free water for each reading. Optical density (OD) readings were taken at 260 and 280nm (for calculation of nucleic acid and phenol/ protein concentrations respectively). A ratio of 1.8-2.0 was taken to represent pure preparations of RNA.

For RNA concentration in  $\mu\text{g/ml}$ :  $[\text{RNA}] = \text{OD}_{260} \times 40 \times \text{dilution factor}$

Samples were diluted to  $1\mu\text{g}/\mu\text{l}$  using RNase free water.

RNA integrity (18S and 28S) was also checked by agarose gel electrophoresis (see section 2.9.3).

### **2.9.3 Agarose gel electrophoresis**

Samples were resolved on 2% agarose gel in Tris-acetate-EDTA buffer (TAE pH 8.3) containing ethidium bromide ( $1\mu\text{l}$  of a  $10\text{mg/ml}$  solution per  $50\text{ml}$  gel solution). Gels were run using a Sub-cell® Agarose Electrophoresis system connected to Powerpac 1000 power pack (Bio-Rad Laboratories Ltd, HERTS, UK) according to the manufacturer's instructions.  $1\mu\text{l}$  RNA samples were added to  $5\mu\text{l}$  loading dye before loading. A standard marker ladder (Hyperladder™ IV 100-1000bp; Bioline, London, UK) was also used. The gel was run at 100V for about twenty- thirty minutes. Gels were visualised under UV light using a FOTODYNE 3-3002 UV transilluminator and photographed with a Polaroid Gel Cam Camera (both GRI, Rayne, UK) for densitometry. The images were scanned using a Bio-Rad GS-690 Imaging Densitometer (Bio-Rad Laboratories Ltd, HERTS, UK) connected to a computer running molecular Analyst Version 1.5 (Bio-Rad Laboratories Ltd, HERTS, UK). This enabled us to check the integrity of ribosomal RNA (18S and 28S).

### 2.9.4 Reverse Transcription (RT)

Complementary DNA (cDNA) was prepared by reverse transcription (RT) using M-MLV (Molony-murine leukaemia virus) reverse transcriptase enzyme (Invitrogen).

The reaction mixture was as follows:

	<b>Stock</b>	<b>Final</b>	<b>Volume Added</b>
1µg RNA	1µg/µl	1µg/tube	1µl
Pd(N) <sub>6</sub> random hexamers	100µM	10µM	2µl
*dNTP mix	2.5mM	0.5mM	4µl
RNase free water			5µl

\*dNTP mix (0.625mM each of dGTP, dCTP, dATP and dTTP)

This mixture was denatured by heating in a PTC-100 programmable thermal controller (MJ Research Ltd, Massachusetts, USA) at 65°C for five minutes and then rapidly chilled on ice.

### 2.9.5 RT Master Mix

	<b>Stock</b>	<b>Final</b>	<b>Volume Added</b>
5x First strand buffer	5x	1x	4µl
DTT	0.1M	10mM	2µl
RNAsin	40U/µl	40U/tube	1µl
M-MLV (kit)	200U/µl	200U/tube	1µl

8µl of the RT master mix was added to each denatured sample. The final mixture was incubated at 37°C for fifty minutes, followed by heat inactivation at 70°C for fifteen minutes. Samples were stored in the freezer until required.

### 2.9.6 Polymerase Chain Reaction (PCR)

All PCR reaction mixes were set up under sterile conditions. The PCR master mix was prepared as outlined below (0.5µl cDNA in 25µl reaction solution):

	Stock	Final	Volume added
RNase free water			17.8µl
dNTP mix	2.5mM	0.2mM	2µl
PCR buffer	10x	1x	2.5µl
F primer*	20µM	500nM	0.625µl
R primer**	20µM	500nM	0.625µl
F actin primer	20µM	500µM	0.2µl (if used)
R actin primer	20µM	500nM	0.2µl (if used, 0.4µl water removed)
Biotaq***	5U/µl	1U/tube	0.2µl
Mg <sup>2+</sup>		1.5mM	0.75µl

\*F primer: forward primer

\*\*R primer: reverse primer

\*\*\*Biotaq<sup>TM</sup> (DNA polymerase)

All primers and sequences are described in Table 2.7 and Table 2.8.

The mix was vortexed and centrifuged for a few seconds. 24.5µl of this master mix was added to a PCR tube and 0.5µl of cDNA template was then added. The mix was again vortexed and centrifuged. A negative control in which cDNA was substituted with an equal volume of DNase free water was used for each experiment.



### **2.9.7 Thermocycling program for PCR amplification**

This was carried out in the PTC-100 programmable thermal controller (MJ Research Ltd, Massachusetts, USA)

#### **Step 1**

- 1) Initial denaturation 95°C for 2 min
- 2) 55°C for 1 min
- 3) 72°C 2 min

#### **Step 2**

Step 2 was repeated for 23- 24 cycles depending on the target

- 1) Denaturation 94°C 1 min
- 2) Annealing 56°C 30 sec
- 3) Elongation/extension 72°C 1 min

23 Cycles for actin 55°C

24 Cycles for c-myc 58°C (co amplified with actin at same conditions)

24 Cycles for cyclin D1 58°C

#### **Step 3**

- 1) Denaturation 94°C 1 min
- 2) Final extension 60°C 7min

#### Step 4

1) Hold 12°C ∞

Samples were resolved using 2% agarose gel as described previously (see Section 2.9.3). 8µl of PCR product was mixed with 10µl gel loading buffer.

primer used for PCR (amplicon size)	Supplier
β- actin (204bp)	MWG biotech, London, UK
c-myc (468bp)	Invitrogen, Paisley, UK
cyclin D1 (515bp)	Invitrogen, Paisley, UK

**Table 2.7**  
**primers used for PCR.**

Target gene	Primer sequence	Conditions (annealing temperature and cycle number)
β- actin F 204bp	5'-GGAGCAATGATCTTGATCTT-3'	55 °C 23 cycles
β- actin R 204bp	5'-CCTTTCTGGGCATGGAGTCCT-3'	55 °C 23 cycles
c-myc F	5'-TTGCAGCTGCTTAGACGCTG-3'	58 °C 24 cycles
c-myc R	5'-CCACATACAGTCCTGGATGA-3'	58 °C 24 cycles
Cyclin D1 F	5'-GGATGCTGGAGGTCTGCGAG-3'	58 °C 24 cycles
Cyclin D1 R	5'-GAGAGGAAGCGTGTGAGGCG-3'	58 °C 24 cycles

**Table 2.8**  
**Primer sequences and reaction conditions used for semi-quantitative RT-PCR.**

## **2.10 Affymetrix microarray analysis**

The Breast Cancer Molecular Pharmacology Group has an extensive database of Affymetrix derived gene expression data sets for endocrine resistant breast cancer cell models which was accessed for Wnt pathway profiling in this study. Biological replicates were used: RNA had been isolated from triplicate cultures of MCF-7, Tam-R, Fas-R cells (during log phase growth), MCF-7 cells treated for 10 days with tamoxifen [MCF-7 (tam)] and Tam-R cells treated with gefitinib [Tam-R (gefitinib)] using TriReagent with subsequent minicolumn-based DNaseI treatment and RNA clean-up. Following quantification and determination of RNA integrity using denaturing gel electrophoresis, samples were used in Affymetrix U133A Genechip analysis (Central Biotechnology Services, Cardiff University, Cardiff, UK). Hybridised arrays were scanned and data output generated using Microarray Suite MAS5.0 software (Affymetrix) and data quality confirmed through analyses of internal control gene expression before uploading it onto a Genesifter® analysis software package.

In this project, an online search was done to select genes identified with Wnt signalling. An on-line commercially available database of genes (SABiosciences 2012) was selected for this purpose. This contained 84 genes related to Wnt signalling (Table 2.9).

this image has been removed by the author  
for copyright reasons

**Table 2.9**

List of Wnt gene probe set (adapted from  
SABiosciences, 2012).

The database was cross referenced with genes on GeneCards (2012) to identify Affymetrix U133A probe sets matching these genes were identified. A total of 76 genes had U133A probes and all probes for the genes were included. A total of 111 gene probes were identified (see Appendix).

The in-house database of Affymetrix U133A Genechip data was then assessed for these genes in the following models:

- Log phase MCF-7 cells versus Tam-R cells (stable; 1year)
- MCF-7 cells +/- 10 days of tamoxifen [ $10^{-7}$ M]
- Log-phase MCF-7 cells versus Fas-R cells (stable; 2 years)
- MCF-7 cells +/- 10 days of oestradiol [ $10^{-9}$ M]
- Tam-R cells +/- 10 days of gefitinib [ $1\mu$ M].

Comparative gene expression was performed by Lynne Farrow (Breast Cancer Molecular Pharmacology Group) on data for each cell model using median-normalised, log-transformed data using the on-line software package ([www.genesifter.net](http://www.genesifter.net)). Heatmaps were generated (see Table 9.1, Table 9.2, Table 9.3, Table 9.4, Figure 9.1, Figure 9.2, Figure 9.3) and probes with expression  $>1.5$ x control were selected (i.e. Tam-R vs. MCF-7, tamoxifen treated MCF-7 vs. MCF-7, Fas-R versus MCF-7, oestradiol treated MCF-7 vs. MCF-7). For gefitinib treated Tam-R versus Tam-R cells, only genes which were differentially expressed in Tam-R cells compared to MCF-7 cells (see Table 3.2) were explored (see Figure 6.9). Red signalled increased expression; green showed decreased expression of mRNA compared to MCF-7 or Tam-R controls (black). T-testing was also carried out for each probe and a p value  $\leq 0.05$  was taken to be significant.

## 2.11 TCF/LEF Reporter Assay

### 2.11.1 Transfection procedure

Cells were plated at an appropriate density into 12 well plates in normal basal medium for 24 hours prior to transfection. Volumes of media, lipid, and plasmids required for experiment were calculated based on instructions outlined below. DCCM with 2% glutamine was prepared for the experiment. For each construct used, three 15ml falcon tubes were required (A, B, C).

Signal® TCF/LEF reporter (luc) assay kit was used to evaluate the Wnt pathway (Biosciences).

TCF/LEF Reporter	A mixture of inducible TCF/LEF-responsive firefly luciferase construct and constitutively expressing Renilla luciferase construct (40:1).
Negative control	A mixture of non-inducible firefly luciferase construct and constitutively expressing Renilla luciferase construct (40:1).
Positive control	A mixture of constitutively expressing GFP, constitutively expressing firefly luciferase, and constitutively expressing Renilla luciferase constructs (40:1:1).

For each reporter gene construct (see Figure 2.7):

Tube A: 60µl of DCCM/well was added to tube A. 3µl/well of transfection lipid (Lipofectin®) was then added.

Tube B: 60µl of DCCM/well was added to tube B. A total of 1µg of plasmid DNA per well was then added comprising 500ng of TCF/LEF construct and 500ng (0.9µg) of pCR script bulk plasmid per well.

Tubes A and B were gently shaken to mix and left to equilibrate at 37°C for 45 minutes.

Tube C: Enough DCCM was added to bring the final volume to 500µl (380µl of DCCM+ 60µl A +60µl B per well). 5µl per well DMSO was then added to tube C (final concentration of 1%).

The procedure was then repeated for negative and positive constructs. After 45 minutes, tubes A and B were mixed and allowed to stand at 37°C for 15 minutes. Tube C was then added to combined contents of A and B to produce the final transfection medium (Figure 2.7: rows 1, 2 and 3). The cell medium was then aspirated and the cells were washed with 1ml of DCCM. The medium was then removed and 500µl of appropriate transfection medium was added to each well. Plates were incubated at 37°C for 6 hours. Treatment media were prepared (wRPMI+ 5%SFCS + 2%glutamine+ pharmacological treatments). Treatments used were lithium chloride [10 and 20mM], PNU74654 [10µM] and iCRT14 [6.25µM]. Antibiotics and antifungals were excluded. After 6 hours, the transfected cells were washed with 1.5mls of basal medium and then this was replaced with treatment medium. Cells were treated for 16-24 hours before proceeding to cell lysis.

## **2.11.2 Cell lysis/ Reporter gene assay**

### **2.11.2.1 Cell lysis**

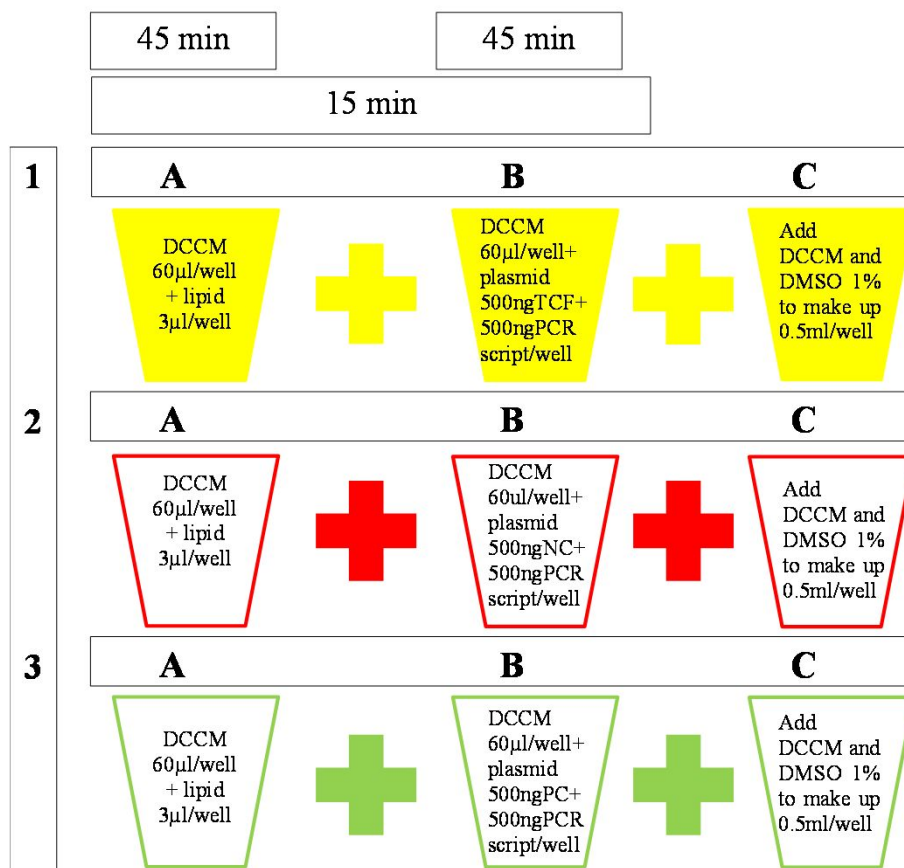
Treatment medium was removed and cells were washed with sterile PBS. This was then aspirated and replaced with 200µl of 1xPromega Passive Lysis Buffer for dual luciferase assay. Cells were scraped into lysis buffer using the barrel of a 1ml syringe and then transferred to a 1.5ml eppendorf tube and kept on ice for 10



minutes. Lysates were frozen at -80°C for at least 1 hour prior to thawing for reporter assay. This freeze-thaw step acted as part of the lysis process.

### **2.11.3 Luciferase assay (Promega dual luciferase reporter assay kit)**

100µl of assay reporter buffer was added to 100µl of thawed lysate and read for 10 seconds on the luminometer (Lumet LB 9507; EG and G Berthold). The tube was removed and 100µl of Stop and Glo reagent was then added to quench the initial reaction and initiate the second phase of the dual luciferase assay. Tubes were again read using the luminometer and the process was repeated for each sample. Luminometer signal levels were comparable with other signal levels validated in the lab (Jarno 2003, Madden 2004). Transfection efficacy information was obtained from readout of positive control (GFP) samples using fluorescent microscope. Cells were counterstained with Dil cell labelling solution to assess percentage transfection. Our transfection rates were 30-40% and these were comparable with other reporter assays validated in the lab (Jarno 2003, Madden 2004).



1	TCF/LEF construct
2	Negative control
3	Positive control

**Figure 2.7**  
Flow chart outlining transfection process for reporter assay.

## **2.12 Statistical analysis**

Statistical analysis of results was carried out where data allowed. In comparing treatment against suitable control, paired student's t-test was used and significance was determined at  $p < 0.05$ . For multiple data points, analysis of variance (ANOVA) was done followed by post hoc analysis using Tamhane (for unequal variance), Dunnett or Tukey tests (for equal variance).

# Chapter 3

Characterisation of Wnt signalling components in  
breast cancer cell lines

### **3 Characterisation of Wnt signalling components in breast cancer cell lines**

Based on existing data supporting deregulation of beta-catenin in cell models of acquired endocrine resistance (Hiscox et al. 2006), we hypothesised that this may reflect deregulation of the Wnt pathway, of which beta-catenin is a key downstream effector. Thus, we initially interrogated our in-house microarray database for Wnt pathway gene changes.

#### **3.1 Affymetrix Analysis**

A list of genes coding for different elements in canonical Wnt signalling were selected for detailed analysis from the list in Table 2.9.

AES (TLE/Groucho), APC, AXIN1, BCL9 , CSNK1A1, CSNK1D, CSNK1G1, CSNK2A1, CTBP1, CTBP2, CTNNB1, CTNNBIP1 (ICAT), CXXC4, DIXDC1, DKK1, DVL1, DVL2, EP300, FRAT1, FZD1, FZD2, FZD3, FZD4, FZD5, FZD6, FZD7, FZD8, GSK3A, GSK3B, LEF1, LRP5, LRP6, NKD1, PORCN, PPP2CA, PPP2R1A, PYGO1, SENP2, SFRP1, SFRP4, SOX17, TCF7, TCF7L1, WIF1, WNT1, WNT10A, WNT16, WNT2, WNT2B, WNT3, WNT3A, WNT4, WNT6, WNT7A, WNT7B, WNT8A.

### **3.1.1 Affymetrix HGU-133A gene microarray data analysis: Tam-R cells versus MCF-7 cells**

The genes in section 3.1 were cross- referenced with the Affymetrix data set for probes showing >1.5 times differences compared to control (Table 3.1) and a separate list was generated consisting of twenty-three gene probes (Table 3.2). CTBP2 and EP300 were not included in this table as their effect on canonical Wnt signalling is not clear. Ten gene probes coding for genes which stimulate canonical Wnt signalling were up-regulated and two were down- regulated; five gene probes coding for genes that inhibit canonical Wnt signalling were up-regulated and one was down- regulated. AXIN1, CSNK1G1 and CSNK1A1 have a dual effect and may act as co-suppressors or co-activators. Of the twenty-three genes in this selected list, changes in seven probes were significant by t-testing (\*). These were WNT4, WNT6, APC, CTNNB1, EP300, DKK1 and Axin1. WNT4, WNT6, CTNNB1, EP300, DKK1 and Axin1 had only 1 probe set; EP300 had two probe sets; APC had four probe sets. Of the two EP300 gene probes, only one probe reached statistical significance at >1.5 control. Of the four APC genes probes, only one probe reached significance at >1.5 control and by t-testing. The other probes listed in Table 3.2 showed >1.5 difference compared to control but they failed to reach significance by t-testing. This was probably due to inter-sample variation. Assuming equal contribution from each gene probe which reached statistical significance, there was activation of canonical Wnt signalling in Tam-R cells compared to MCF-7 cells.

Row	Other ID	Gene ID	Fold Difference
1	208606_s_at	WNT4*	10.39
2	221609_s_at	WNT6*	9.01
3	221558_s_at	LEF1	5.29
4	203525_s_at	APC*	3.35
5	220277_at	CXXC4	3.02
6	205990_s_at	WNT5A	2.83
7	201533_at	CTNNB1*	2.29
8	200951_s_at	CCND2	1.97
9	204420_at	FOSL1	1.88
10	212073_at	CSNK2A1	1.86
11	34697_at	LRP6	1.81
12	221455_s_at	WNT3	1.78
13	202210_x_at	GSK3A	1.7
14	213425_at	WNT5A	1.69
15	206459_s_at	WNT2B	1.63
16	201700_at	CCND3	1.61
17	204129_at	BCL9	1.57
18	219993_at	SOX17	1.55
19	208867_s_at	CSNK1A1	1.55
20	203698_s_at	FRZB	1.53
21	209468_at	LRP5	1.52
22	221245_s_at	FZD5	1.51
96	202221_s_at	EP300*	1.5
97	218665_at	FZD4	1.51
98	218759_at	DVL2	1.54
99	218941_at	FBXW2	1.63
100	204901_at	BTRC	1.7
101	215377_at	CTBP2	1.86
102	206796_at	WISP1	1.98
103	212849_at	AXIN1*	2
104	201466_s_at	JUN	2.05
105	220640_at	CSNK1G1	2.1
106	214489_at	FSHB	2.21
107	216060_s_at	DAAM1	2.23
108	204602_at	DKK1*	2.35
109	203220_s_at	TLE1	3.22
110	201465_s_at	JUN	3.89
111	203222_s_at	TLE1	4.44

yellow: canonical Wnt signalling
red: increased expression
green: decreased expression

**Table 3.1**

Gene probes for Tam-R cells versus MCF-7 cells showing  $\geq 1.5$  fold difference. \* Significant by t-test at  $p \leq 0.05$ . Genes associated with canonical Wnt signalling (see section 3.1) are highlighted in yellow. Genes above red line show increased expression (red), genes below red line show decreased expression (green). Highlighted probes (yellow) were identified for further analysis (see Table 3.2).

	upregulated	reported impact on Wnt signalling	downregulated	reported impact on Wnt signalling
<b>Ligands/effectors</b>	WNT4*	increased	DKK1*	decreased
	WNT6*	increased		
	WNT3	increased		
	WNT2B	increased		
<b>Receptors</b>	LRP6	increased	FZD4	increased
	LRP5	increased		
	FZD5	increased		
<b>Destruction complex</b>	APC*	decreased	DVL2	increased
	CXXC4	decreased	Axin 1*	equivocal
	CK1alpha1 (CSNK1A1)	equivocal	CK1gamma1 (CSNK1G1)	equivocal
	CK2alpha1 (CSNK2A1)	decreased		
	GSK3A	decreased		
	β- catenin (CTNNB1)*	increased		
<b>Nuclear</b>	LEF1	increased		
	BCL9	increased		
	SOX17	decreased		

**Table 3.2**

Table showing canonical Wnt signalling genes that are differentially expressed in Tam-R cells versus MCF-7 cells (highlighted yellow in Table 3.1). \* Significant by t-test at  $p \leq 0.05$ .



The process was repeated for each comparison group.

### **3.1.2 Affymetrix HGU-133A gene microarray data analysis: tamoxifen treated MCF-7 cells versus MCF-7 cells**

Table 3.3 is a list of the gene probes that showed >1.5 difference compared to control for this analysis. The highlighted probes (yellow) were referenced to the list for canonical Wnt signalling (see section 3.1). A list of twenty- six probes was identified (see Table 3.4). In the probes which were upregulated, seven probes coded for genes which increase canonical Wnt activity, two coded for genes that decrease canonical Wnt activity; CSNK1A1 may either increase or decrease canonical Wnt signalling. The list of downregulated gene probes included seven probes coding for genes that increase canonical signalling, five probes coding for genes down-regulating canonical Wnt signalling and three coding for genes that may both increase or decrease canonical Wnt signalling. Of the twenty- six probes, eight probes were significant when compared to MCF-7 controls by t-testing. These were LEF1, DVL2, SFRP1, SFRP4, FZD5, LRP5, TCF7L1 and GSK3A. Genes coding for LRP5 and TCF7L1 had only one probe, the other genes had two probes. Assuming equal contribution from each gene probe which reached statistical significance, these changes were equivocal for changes in canonical Wnt signalling components between MCF-7 cells treated with  $[10^{-7}\text{M}]$  tamoxifen for ten days and MCF-7 cells.

Row	Other ID	Gene ID	Fold Difference
1	221558_s_at	LEF1*	3.22
2	203525_s_at	APC	3.21
3	214724_at	DIXDC1	3.07
4	216060_s_at	DAAM1	2.61
5	203987_at	FZD6	2.53
6	209630_s_at	FBXW2	2.42
7	201465_s_at	JUN	2.38
8	212073_at	CSNK2A1	2.18
9	34697_at	LRP6	2.13
10	213425_at	WNT5A	2.05
11	200951_s_at	CCND2	1.94
12	219683_at	FZD3	1.92
13	201219_at	ZRANB1	1.82
14	201349_at	SLC9A3R1	1.74
15	208865_at	CSNK1A1	1.65
16	208606_s_at	WNT4	1.61
17	202431_s_at	MYC	1.59
18	215517_at	PYGO1	1.58
19	206524_at	T	1.5
89	57532_at	DVL2*	1.51
90	202037_s_at	SFRP1*	1.54
91	208774_at	CSNK1D	1.57
92	212849_at	AXIN1	1.64
93	203081_at	CTNNBIP1	1.65
94	221609_s_at	WNT6	1.65
95	204051_s_at	SFRP4*	1.66
96	206136_at	FZD5*	1.7
97	217729_s_at	AES	1.71
98	210248_at	WNT7A	1.77
99	220277_at	CXXC4	1.78
100	206459_s_at	WNT2B	1.81
101	204420_at	FOSL1	1.83
102	209468_at	LRP5*	1.94
103	203698_s_at	FRZB	2.05
104	221016_s_at	TCF7L1*	2.1
105	203222_s_at	TLE1	2.27
106	202210_x_at	GSK3A*	2.38
107	203697_at	FRZB	2.39
108	40837_at	TLE2	2.41
109	221029_s_at	WNT5B	2.54
110	220640_at	CSNK1G1	2.54
111	214489_at	FSHB	2.74

yellow: canonical Wnt signalling
red: increased expression
green: decreased expression

**Table 3.3**

Gene probes for MCF-7 cells treated with tamoxifen [ $10^{-7}$ M] for 10 days versus MCF-7 cells showing  $\geq 1.5$  fold difference. \* Significant by t-test at  $p \leq 0.05$ . Genes associated with canonical Wnt signalling (see section 3.1) are highlighted in yellow. Genes above red line show increased expression (red), genes below red line show decreased expression (green). Highlighted probes (yellow) were identified for further analysis (see Table 3.4).

	upregulated	reported impact on Wnt signalling	downregulated	reported impact on Wnt signalling
<b>Ligands/effectors</b>	WNT4	increased	WNT6	increased
			WNT2B	increased
			WNT7A	increased
			SFRP1*	decreased
			SFRP4*	decreased
<b>Receptors</b>	FZD6	increased	FZD5*	increased
	LRP6	increased	LRP5*	increased
	FZD3	increased		
<b>Destruction complex</b>	APC	decreased	DVL2*	increased
	DIXDC1	increased	CXXC4	decreased
	CK2alpha1 (CSNK2A1)	decreased	AXIN1	equivocal
	CK1alpha1 (CSNK1A1)	equivocal	GSK3A*	decreased
			CK1delta (CSNK1D)	equivocal
			CK1gamma1 (CSNK1G1)	equivocal
<b>Nuclear</b>	LEF1*	increased	AES	decreased
	PYGO1	increased	TCF7L1*	increased
			CTNNBIP1	decreased

**Table 3.4**

Table showing canonical Wnt signalling genes that are differentially expressed in [10<sup>-7</sup>M] tamoxifen treated MCF-7 cells versus MCF-7 cells (highlighted yellow in Table 3.3). \* Significant by t-test at p<= 0.05.

### **3.1.3 Affymetrix HGU-133A gene microarray data analysis: Fas-R cells versus MCF-7 cells (model for absence of ER activity)**

Similar analysis was done for the data comparing Fas-R versus MCF-7 cells (Table 3.5). Twenty- three probes were identified for further analysis (Table 3.6). The list of up-regulated probes was sub-divided as follows: four probes coded for genes that increased canonical Wnt activity; six probes coded for genes decreasing canonical Wnt signalling. For the list of down-regulated probes, seven probes coded for genes that increased canonical Wnt activity, one coded for a gene that decreased canonical Wnt signalling and three probes coded for genes that could increase or decrease canonical Wnt signalling. CTBP1 and CTBP2 were not included in this table as their effect on canonical Wnt signalling is not clear. The changes identified between MCF-7 versus Fas-R were significant by t-testing for eight probes (\*): these coded for CTNNB1, DVL2, CSNK1D, AXIN1, FZD7 and FZD2. Both probes for CSNK1D and DVL2 were positive. CTNNB1, AXIN1, FZD7 and FZD2 had only one probe. Assuming equal contribution from each gene probe which reached statistical significance, these changes were equivocal for activation of canonical Wnt signalling in Fas-R compared to MCF- cells.

Row	Other ID	Gene ID	Fold Difference
1	201700_at	CCND3	5.84
2	204712_at	WIF1	2.99
3	221609_s_at	WNT6	2.95
4	208606_s_at	WNT4	2.39
5	40837_at	TLE2	2.25
6	215310_at	APC	2.04
7	206737_at	WNT11	1.83
8	210248_at	WNT7A	1.79
9	212073_at	CSNK2A1	1.66
10	201533_at	CTNNB1*	1.65
11	208652_at	PPP2CA	1.65
12	220277_at	CXXC4	1.61
13	203525_s_at	APC	1.57
14	209630_s_at	FBXW2	1.54
86	221455_s_at	WNT3	1.5
87	206524_at	T	1.5
88	211312_s_at	WISP1	1.5
89	204452_s_at	FZD1	1.52
90	57532_at	DVL2*	1.6
91	207683_at	FOXM1	1.61
92	201465_s_at	JUN	1.69
93	215377_at	CTBP2	1.71
94	202221_s_at	EP300	1.79
95	214489_at	FSHB	1.86
96	203698_s_at	FRZB	1.97
97	216060_s_at	DAAM1	1.97
98	221558_s_at	LEF1	2.03
99	203220_s_at	TLE1	2.05
100	213980_s_at	CTBP1	2.16
101	208774_at	CSNK1D*	2.2
102	218759_at	DVL2*	2.2
103	220640_at	CSNK1G1	2.22
104	212849_at	AXIN1*	2.39
105	207945_s_at	CSNK1D*	2.63
106	208712_at	CCND1	2.86
107	203705_s_at	FZD7*	2.88
108	203222_s_at	TLE1	3.29
109	210220_at	FZD2*	3.51
110	208711_s_at	CCND1	4.59
111	204420_at	FOSL1	9.46

**yellow: canonical  
Wnt signalling**

**red: increased  
expression**

**green: decreased  
expression**

**Table 3.5**

Gene probes for MCF-7 cells versus Fas-R cells showing  $\geq 1.5$  fold difference.

\* Significant by t-test at  $p \leq 0.05$ . Genes associated with canonical Wnt signalling (see section 3.1) are highlighted in yellow. Genes above red line show increased expression (red), genes below red line show decreased expression (green). Highlighted probes (yellow) were identified for further analysis (see Table 3.6).

	upregulated	reported impact on Wnt signalling	downregulated	reported impact on Wnt signalling
<b>Ligands/effectors</b>	WIF1	decreased	WNT3	increased
	WNT6	increased	DVL2*	increased
	WNT4	increased	DVL2*	increased
	WNT7A	increased		
<b>Receptors</b>			FZD7*	increased
			FZD2*	increased
			FZD1	increased
<b>Destruction complex</b>	APC	decreased	CK1delta (CSNK1D)*	equivocal
	APC	decreased	CK1delta (CSNK1D)*	equivocal
	CK2 $\alpha$ 1 (CSNK2A1)	decreased	AXIN1*	decreased
	PPP2CA	decreased	CK1gamma1 (CSNK1G1)	equivocal
	$\beta$ -catenin (CTNNB1)*	increased		
	CXXC4	decreased		
<b>Nuclear</b>			LEF1	increased

**Table 3.6**

Table showing canonical Wnt signalling genes that are differentially expressed in MCF-7 cells versus Fas-R cells (highlighted yellow in Table 3.5. \* Significant by t-test at  $p \leq 0.05$ .

### **3.1.4 Affymetrix HGU-133A gene microarray data analysis: MCF-7 cells treated with oestradiol (E2) [ $10^{-9}$ M] for 10 days versus MCF-7 cells (model for enhanced ER activity)**

Table 3.7 is a list of the gene probes that showed  $>1.5$  difference compared to control for this analysis. The highlighted probes (yellow) were referenced to the list for canonical Wnt signalling (see section 3.1). A list of twenty- seven probes was identified (see Table 3.8). In the probes which were upregulated, two probes coded for genes which increase canonical Wnt activity, two coded for genes that decrease canonical Wnt activity; CSNK1A1 and CSNK2A1 may both increase or decrease canonical Wnt signalling. The list of downregulated gene probes included eight probes coding for genes that increase canonical signalling, six probes coding for genes down-regulating canonical Wnt signalling and two coding for genes that may both increase or decrease canonical Wnt signalling. Of the twenty- seven probes, ten probes were significant when compared to MCF-7 controls by t-testing. These were FZD6, DKK1, FZD2, FZD4, LRP5, CSNK1D, FRAT1, PYGO1, AES and TCF7L1. Genes coding for FZD6, PYGO1, FRAT1, FZD4, LRP5, AES, TCF7L1, FZD2 and DKK1 had only one probe, CSNK1D had two probes. Assuming equal contribution from each gene probe which reached statistical significance, there was inhibition of canonical Wnt signalling components between MCF-7 cells treated with [ $10^{-9}$ M] oestradiol for ten days and MCF-7 cells.

Row	Other ID	Gene ID	Fold Difference
2	203525 s at	APC	3.59
3	34697 at	LRP6	3.01
4	208712 at	CCND1	2.53
5	213425 at	WNT5A	2.45
6	203987 at	FZD6*	2.44
7	200952 s at	CCND2	2.21
8	208711 s at	CCND1	2.08
9	201466 s at	JUN	1.98
10	202431 s at	MYC	1.97
11	212073 at	CSNK2A1	1.96
12	216060 s at	DAAM1	1.91
13	206562 s at	CSNK1A1	1.8
14	209630 s at	FBXW2	1.78
15	208865 at	CSNK1A1	1.58
16	201219 at	ZRANB1	1.56
17	213086 s at	CSNK1A1	1.55
18	201349 at	SLC9A3R1	1.54
19	208867 s at	CSNK1A1	1.52
81	202037 s at	SFRP1	1.5
82	202221 s at	EP300	1.53
83	208606 s at	WNT4	1.53
84	218941 at	FBXW2	1.54
85	212849 at	AXIN1	1.54
86	208774 at	CSNK1D*	1.54
87	215517 at	PYGO1*	1.57
88	219889 at	FRAT1*	1.59
89	205254 x at	TCF7	1.62
90	207683 at	FOXN1	1.63
91	204712 at	WIF1	1.71
92	218665 at	FZD4*	1.72
93	208570 at	WNT1	1.76
94	205648 at	WNT2	1.78
95	209468 at	LRP5*	1.79
96	217729 s at	AES*	2.02
97	221029 s at	WNT5B	2.04
98	202210 x at	GSK3A	2.07
99	221016 s at	TCF7L1*	2.08
100	203698 s at	FRZB	2.11
101	207558 s at	PITX2	2.21
102	210220 at	FZD2*	2.23
103	203697 at	FRZB	2.24
104	202036 s at	SFRP1	2.25
105	40837 at	TLE2	2.48
106	203222 s at	TLE1	2.8
107	220640 at	CSNK1G1	2.88
108	214489 at	FSHB	2.89
109	206796 at	WISP1	3.3
110	205990 s at	WNT5A	4.43
111	204602 at	DKK1*	4.63

yellow: canonical Wnt signalling
red: increased expression
green: decreased expression

**Table 3.7**

Gene probes for MCF-7 cells versus MCF-7 cells treated with E2 [ $10^{-9}$ M] showing  $\geq 1.5$  fold difference. \* Significant by t-test at  $p \leq 0.05$ . Genes associated with canonical Wnt signalling are highlighted in yellow. Genes above red line show increased expression (red), genes below red line show decreased expression (green). Highlighted probes (yellow) were identified for further analysis (see Table 3.8).



	upregulated	reported impact on Wnt signalling	downregulated	reported impact on Wnt signalling
<b>Ligands/effectors</b>			SFRP1	decreased
			SFRP1	decreased
			WIF1	decreased
			Wnt1	increased
			Wnt2	increased
			Wnt4	increased
			DKK1*	decreased
<b>Receptors</b>	LRP6	increased	FZD2*	increased
	FZD6*	increased	FZD4*	increased
			LRP5*	increased
<b>Destruction complex</b>	APC	decreased	Axin 1	decreased
	CK2alpha1 (CSNK2A1)	decreased	CK1delta (CSNK1D)*	equivocal
	CK1alpha1 (CSNK1A1)	equivocal	GSK3A	decreased
	CK1alpha1 (CSNK1A1)	equivocal	CK1gamma1 (CSNK1G1)	equivocal
	CK1alpha1 (CSNK1A1)	equivocal	FRAT1*	increased
	CK1alpha1 (CSNK1A1)	equivocal		
<b>Nuclear</b>			PYGO1*	increased
			TCF7	increased
			AES*	decreased
			TCF7L1*	increased

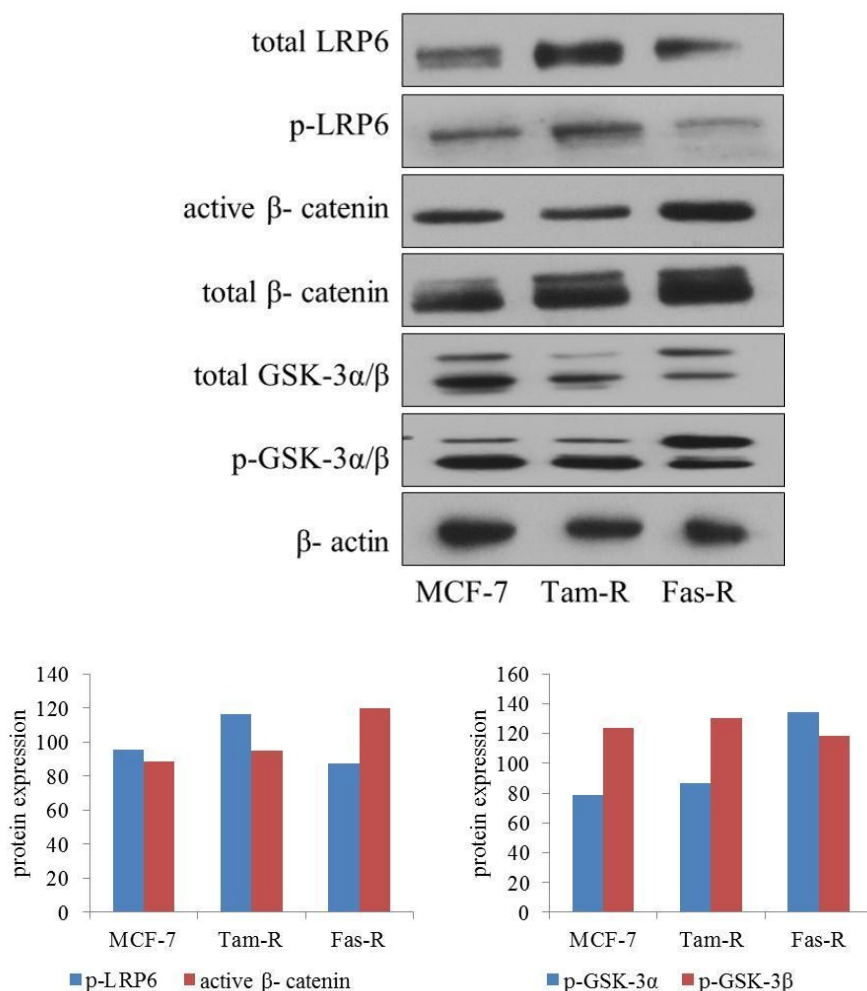
**Table 3.8**

Table showing canonical Wnt signalling genes that are differentially expressed in MCF-7 cells versus MCF-7 cells treated with E2 [ $10^{-9}$ M] for 10 days (highlighted yellow in Table 3.7). \* Significant by t-test at  $p \leq 0.05$ .

### 3.2 SDS-Page/ Western blot

Affymetrix data suggested differences in mRNA expression for Wnt signalling components between the different cell lines. The main focus of the project centred on pharmacological manipulation of Wnt signalling. We set out to explore signalling changes resulting from such modulation by SDS-Page/ Western blot. It was thus important to explore baseline expression and activity of Wnt signalling components. We focused on LRP6 (receptor), GSK-  $3\alpha/\beta$  (component of the destruction complex) and  $\beta$ - catenin (main effector of Wnt signalling).

Western Blot analysis showed up regulation of LRP6 and p-LRP6 in Tam-R compared to MCF-7 replicating data suggested by heatmaps (Figure 3.1). Total  $\beta$ -catenin was raised in Tam-R cells consistent with previously published data (Hiscox et al. 2006) and the mRNA profile (Table 3.2). Analysis of Fas-R cells was also done (Figure 3.2). p-LRP6 expression appeared to be reduced compared to parental MCF-7 cells, but total  $\beta$ - catenin was raised (as for mRNA data, Table 3.8) suggesting a possible role for Wnt signalling in this setting too. This was also supported by active  $\beta$ - catenin (dephosphorylated on S33 or T41; see Section 1.1.3.2.3 and Section 3.3) expression which was highest in Fas-R cells. Total GSK-  $3\alpha/\beta$  was highest in MCF-7 cells and lowest in Tam-R cells. Levels of expression for total (active) GSK-  $3\alpha/\beta$  relative to (inactive) p- GSK-  $3\alpha/\beta$  were lower in Tam-R cells compared to MCF-7 cells. This would be consistent with more activated Wnt activity in Tam-R cells (see Section 1.1.3.2.2). However, p- GSK-  $3\alpha/\beta$  level was highest in Fas-R cells suggesting decreased  $\beta$ - catenin phosphorylation in this cell line. A representative blot for Western blot analysis is shown in Figure 3.1.



**Figure 3.1**  
**Profiling different components of Wnt pathway in MCF-7, Tam-R and Fas-R cell lines as determined by Western blotting.**

MCF-7, Tam-R and Fas-R cells were cultured to log-phase growth. The cells were then lysed. SDS-PAGE/ Western blot analyses was carried out using 30 $\mu$ g of total soluble protein and the membranes were probed with antibodies specific to LRP6, p-LRP6, active  $\beta$ -catenin, total  $\beta$ -catenin, GSK-3 $\alpha/\beta$ , p-GSK-3 $\alpha/\beta$  and  $\beta$ -actin. There are differences in the levels of protein expression between the three cell lines. Representative blot for  $\beta$ -actin is shown. Densitometry was done and data were corrected for  $\beta$ -actin.

### **3.3 Immunocytochemistry analysis of beta-catenin in endocrine sensitive versus resistant cells**

$\beta$ -catenin is a key effector of canonical Wnt signalling. Transcriptionally active  $\beta$ -catenin is  $\beta$ -catenin dephosphorylated at serine 37 (S37) or threonine 41 (T41). It is free to migrate to the nucleus where it can bind to TCF/LEF and activate gene transcription. Localisation of active  $\beta$ -catenin in MCF-7 and Tam-R cell lines was explored using immunocytochemistry. H score for active  $\beta$ -catenin was calculated (Figure 3.2, Figure 3.3). Data represents collated data from three separate experiments. The average H score for nuclear active  $\beta$ -catenin in Tam-R cells was particularly high at 225 and about 40% greater than in MCF-7 cells. This difference was significant by paired t-test analysis ( $p=0.01$ ). This finding supports prominent active Wnt signalling in Tam-R cells. SW480 cells were used as a control for nuclear  $\beta$ -Catenin staining (see Section 2.8.3).

Active  $\beta$  - catenin (mouse monoclonal  
antibody: 1:30 for MCF-7 and Tam-R;  
1:120 for SW480 ) methanol fix

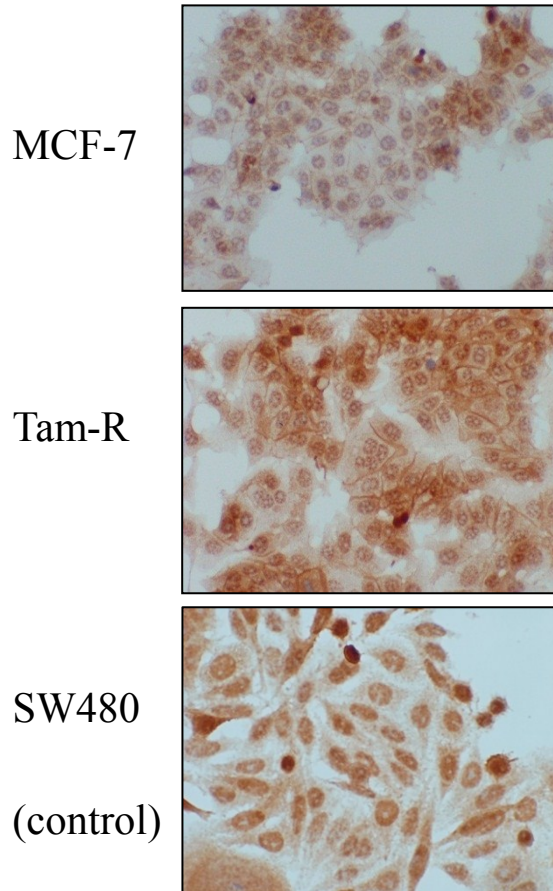


**Figure 3.2**  
**Localisation of active  $\beta$ - catenin in MCF-7 and**  
**Tam-R cell lines as determined by**  
**immunocytochemistry.**

MCF-7, Tam-R and SW480 cells were cultured on cover slips until they reached log- phase growth. They were then fixed with methanol as described in the materials and methods section. The cells were then assayed for active (dephosphorylated)  $\beta$ -catenin using a specific monoclonal antibody. SW480 cells were used as control. Representative images were taken using Olympus BH-2 phase contrast microscope fitted with Olympus DP-12 digital camera system. Original magnifications x40.

(A)

	MCF-7	Tam-R
Nuclear	167.7	225.0
Membrane	91.7	126.7
Cytoplasm	88.3	136.7

(B)

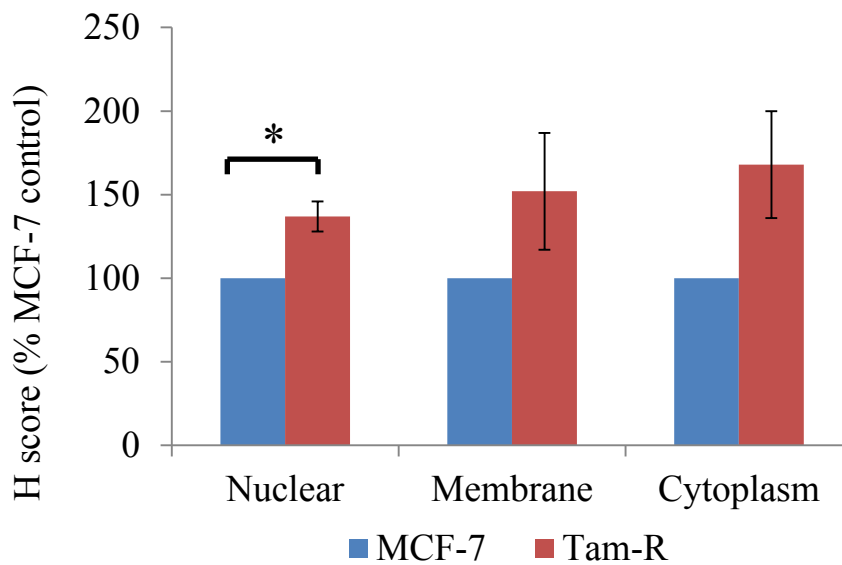


**Figure 3.3**

**H score for active  $\beta$ -catenin in MCF-7 and Tam-R cells as determined by immunocytochemistry.**

H score for active  $\beta$ -catenin in MCF-7 and Tam-R cells was calculated (see Figure 3.3). Table (A) shows average H score values for the two cell lines. Graph (B) shows H score as % MCF-7 control. The difference between the two cell lines was significant for nuclear expression of active  $\beta$ -catenin \* ( $p=0.01$ ). Error bars show SEM ( $n=3$ ).

## **3.4 Summary**

### **3.4.1 Affymetrix HGU-133A gene microarray data**

Findings from the Affymetrix HGU-133A gene microarray data analysis of Tam-R, Fas-R, MCF-7 cells treated with tamoxifen and MCF-7 cells treated with oestradiol showed changes in mRNA expression for Wnt signalling compared to MCF-7 controls. This difference was most pronounced for Tam-R cells compared to MCF-7 cells, and MCF-7 cells treated with oestradiol compared to MCF-7 cells. The changes supported a role for increased Wnt signalling in tamoxifen resistance and suggested that Wnt signalling may be repressed by oestradiol.

The on-line gene list selected was chosen as it provided a broad overview of various components of Wnt signalling (SABiosciences 2012). More detailed analysis was focused on the canonical Wnt pathway of which  $\beta$ -catenin is a main effector. We appreciate that a limitation of the analysis is that only t-testing was done. False discovery rate (FDR) may be reduced by Bonferroni or Benjamini-Hochberg testing (Reiner et al. 2003, Dudoit et al. 2003). Our Affymetrix analysis looked at variations in mRNA expression of selected genes. A change in mRNA expression does not always translate into altered protein activity, but data are often used as a surrogate to help direct further investigations. The data could be further validated using PCR and this gives scope for future work.

### **3.4.2 Western Blot**

Western blotting was used to explore protein levels for LRP6, p-LRP6, GSK- $3\alpha/\beta$ , p-GSK- $3\alpha/\beta$ , total  $\beta$ -catenin and active  $\beta$ -catenin. LRP6 and p-LRP6 antibodies were verified with respective constructs (gift from Professor Trevor Dale's Lab,

School of Biosciences, Cardiff University, UK); see Methods section 2.5.6). p-LRP6 appeared to be increased in Tam-R cells compared to MCF-7 cells as was total  $\beta$ -catenin. GSK-3 $\alpha/\beta$  activity appears to be reduced in both Tam-R cells and Fas-R cells suggesting decreased activation of the degradation complex. This would support increased nuclear  $\beta$ -catenin activity and enhanced Wnt signalling. Wnt signalling is transmitted through dephosphorylated  $\beta$ -catenin (Staal FJ 2002): the active  $\beta$ -catenin is dephosphorylated at S37 or T41.

Western blotting is a qualitative test. Semi-quantitative analysis was possible by running a house-keeping gene ( $\beta$ -actin), and using densitometry as a quantification measure for the image.

### **3.4.3 Immunocytochemistry analysis of beta-catenin in endocrine sensitive versus resistant cells**

Staining for active  $\beta$ -catenin was more pronounced in Tam-R cells compared to MCF-7 cells and nuclear staining is more prominent. Antibody activity was verified using SW480 cells (gift from Professor Trevor Dale's lab, School of Biosciences, Cardiff University, UK; see section 2.8.3).



# Chapter 4

Activation of Wnt signalling in endocrine sensitive  
and endocrine resistant breast cancer cells

## **4 Activation of Wnt signalling in endocrine sensitive and endocrine resistant breast cancer cells**

Our previous gene and protein analysis pointed to a deregulation of Wnt pathway elements in tamoxifen resistant versus tamoxifen sensitive breast cancer cells. To further explore the importance of this pathway in these cells, we sought to induce Wnt pathway activation in Tam-R and MCF-7 cell models using the Wnt ligand, Wnt3a, and also lithium chloride.

Use of Wnt3a ligand to stimulate Wnt activity is widely reported in the literature. It may be used in purified form or as enriched conditioned medium. A commercially available purified Wnt3a ligand was used in this project. Both GSK-  $3\beta$  and  $\beta$ -catenin represent suitable endpoints with which to monitor Wnt pathway activity. Wnt3a has been shown to activate Wnt signalling (Yun et al. 2005) with resultant increase in  $\beta$ -catenin as evidenced by Western blot. GSK-  $3\beta$  activity has also been reported to change as a result of Wnt3a stimulation (Sonderegger et al. 2010). Work on HEK 293 cells by Gujral and MacBeath (2010) traced changes in  $\beta$ -catenin from as early as 5 minutes. The authors observed two phases of transcription following stimulation by Wnt3a: an early phase (at 1 hour) where signalling antagonists were downregulated and a late phase (at 24 hours) where some of these antagonists were upregulated. Changes were correlated to increased proliferation.

Similarly, activation of Wnt signalling using lithium chloride (LiCl) results in modulation of GSK-  $3\alpha/\beta$  activity which in turn may act to stabilise  $\beta$ -catenin. LiCl is a GSK-  $3\alpha/\beta$  inhibitor. The exact mechanism of action remains unknown; it is not specific to Wnt signalling as GSK-  $3\alpha/\beta$  interacts with other pathways. GSK-  $3\alpha/\beta$  is inactivated by phosphorylation (serine-9 in GSK- $3\beta$  and serine-21 in GSK- $3\alpha$ )

(Vincan 2008). LiCl exposure should result in an increase in total  $\beta$ -catenin but these changes can be difficult to see in cells expressing high levels of  $\beta$ -catenin (Vincan 2008). O'Brien et al. (2009) quote  $IC_{50}$  for lithium inhibition of GSK3 at about 1.0 mM whereas Vincan (2008) indicates that 20-30mM levels are required for GSK3 inhibition. A range of concentrations up to 40mM were used in these experiments.

We also wanted to explore whether modulation of Wnt pathway signalling would affect cellular proliferation in these cells. Thus, MTT assays were used to monitor changes in cell growth in response to both Wnt3a and LiCl.

When Wnt signalling is activated,  $\beta$ -catenin translocates to the nucleus where it is free to bind with TCF/LEF and activate gene transcription. This activity may be measured using TCF/LEF Reporter assays and these are widely used to explore Wnt signalling modulation (Molenaar et al. 1996). Reporter assays were used to assess response to LiCl stimulation in this project.

## **4.1 Activation of Wnt signalling in endocrine-sensitive and resistant cell models by Wnt3a**

Wnt signalling activation by Wnt3a ligand in MCF-7 and Tam-R cells was assessed using Western blot and growth assays.

### **4.1.1 Changes in cell signalling when MCF-7 and Tam-R cells were treated with Wnt3a**

MCF-7 and Tam-R cells were treated with Wnt3a ligand (0 to 200ng/ml concentrations) for 1 hour. Wnt3a activation should result in increased phosphorylation of GSK-  $3\alpha/\beta$ , an increase in active  $\beta$ - catenin (due to decreased  $\beta$ - catenin phosphorylation) and an increase in total  $\beta$ - catenin levels. Changes in signalling protein expressions were determined by Western blot (see Figure 4.1).

There was no change in GSK-  $3\alpha$  or active  $\beta$ - catenin expression when MCF-7 cells were treated with Wnt3a. Total  $\beta$ - catenin expression fell at Wnt3a concentration of 100ng/ml. There was a fall in GSK-  $3\beta$  expression after treatment at Wnt3a concentrations of 100 and 200ng/ml. p-GSK -  $3\alpha$  expression fell at Wnt3a concentration of 200ng/ml; there was a rise in p-GSK -  $3\beta$  expression at Wnt3a concentrations of 50ng/ml and 100ng/ml and a fall at Wnt3a concentration of 200ng/ml.

When Tam-R cells were treated with Wnt3a, there was no change in total GSK-  $3\alpha/\beta$  and total  $\beta$ - catenin expression. There was a rise in active  $\beta$ - catenin expression at Wnt3a concentrations of 50, 100 and 200ng/ml. There was a rise in p- GSK-  $3\alpha$  expression at Wnt3a concentration of 100ng/ml and a fall in p- GSK-  $3\beta$  expression at Wnt3a concentration of 200ng/ml.

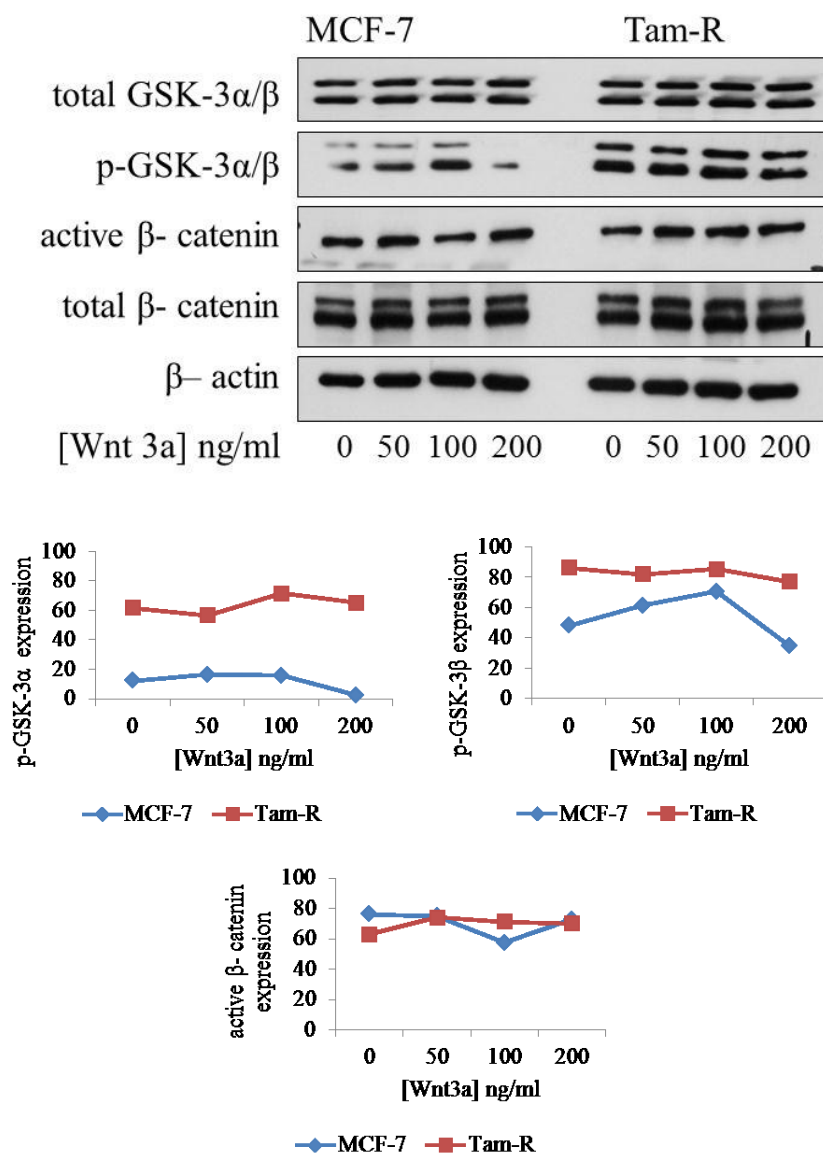


**Figure 4.1**  
**Effects of Wnt3a ligand (1 hour) on components of Wnt signalling in MCF-7 and Tam-R cell lines as determined by Western blotting.**

MCF-7 and Tam-R cells were cultured to log-phase growth and then treated with Wnt3a ligand (0- 200ng/ml concentrations) for 1 hr. The cells were then lysed as described in materials and methods. SDS-PAGE/ Western blot analyses was carried out using 30µg of total soluble protein and the membranes were probed with antibodies specific to GSK-3α/β, p- GSK-3α/β, active β- catenin, total β- catenin and β- actin. The representative blot for β- actin is shown. Densitometry was done and data were corrected for β- actin. (n=1)

#### **4.1.2 Effect of Wnt3a on cell growth**

MCF-7 and Tam-R cells were treated with Wnt3a ligand (200ng/ml) for seven days following which an MTT assay was performed to determine effects of Wnt3a on cell growth. Various concentrations of Wnt3a have been reported in the literature. The chosen concentration for this growth assay was 200ng/ml as this was the concentration corresponding to greatest signalling changes in MCF-7 cells (see Figure 4.1). The data suggested that there were no significant effects on cell growth over this period. This was true for both MCF-7 cells and Tam-R cells (Figure 4.2).

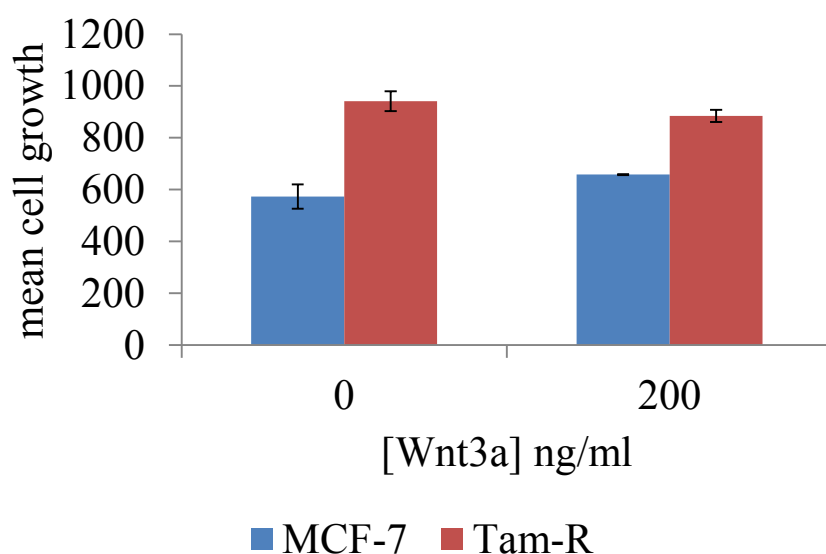


**Figure 4.2**  
**Effects of Wnt3a ligand (7 days) on growth of MCF-7 and Tam-R cells as determined by MTT assay.**

MTT assay using MCF-7 and Tam-R cells treated with Wnt3a ligand (0- 200ng/ml) for 7 days was done as described in materials and methods section. No significant difference in growth was noted. Error bars show SD (n=1; 24 samples).

## **4.2 Modulation of Wnt activity in endocrine-sensitive and resistant cell models by Lithium Chloride**

Wnt signalling activation by LiCl in MCF-7 and Tam-R cells was assessed using Western blot, growth assays and reporter assays.

### **4.2.1 Changes in cell signalling when MCF-7 and Tam-R cells were treated with LiCl**

MCF-7 and Tam-R cells were treated with LiCl (0 to 40mM concentrations) for 1 hour and signalling changes were determined by Western blot (Figure 4.3). When MCF-7 cells were treated with LiCl, total  $\beta$ -catenin expression was stable; total GSK-3 $\alpha/\beta$  expression fell at LiCl concentrations of 10, 20 and 40mM; p-GSK-3 $\alpha/\beta$  and active  $\beta$ -catenin expression rose at LiCl concentrations of 10, 20 and 40mM. When Tam-R cells were treated with LiCl, total GSK-3 $\alpha/\beta$  and total  $\beta$ -catenin expression were stable; p-GSK-3 $\alpha/\beta$  and active  $\beta$ -catenin expressions were increased at LiCl concentrations of 10, 20 and 40mM.



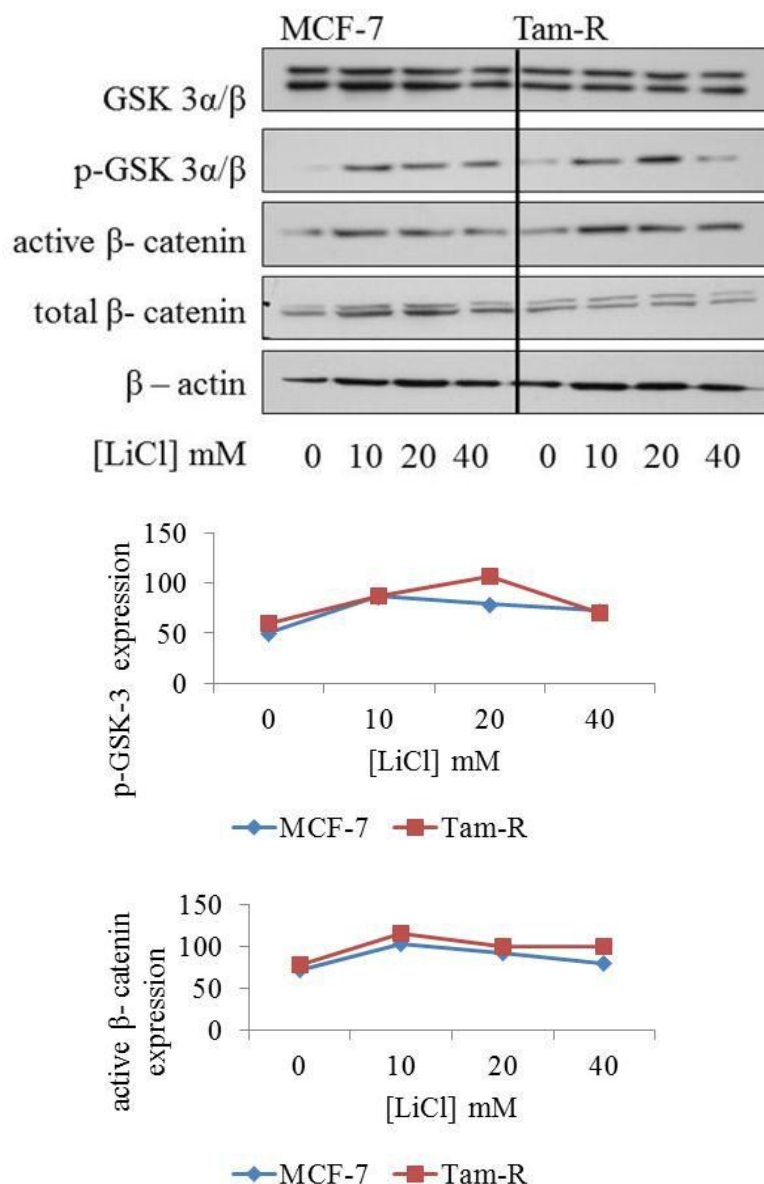


**Figure 4.3**  
**Effect of Lithium Chloride (1 hour) on components of Wnt signalling in MCF-7 and Tam-R cell lines as determined by Western blotting.**

MCF-7 and Tam-R cells were cultured to log-phase growth and then treated with Lithium Chloride (LiCl) 0- 40mM concentrations for 1 hour. The cells were then lysed as described in materials and methods. SDS-PAGE/Western blot analyses was carried out using 30 $\mu$ g of total soluble protein and the membranes were probed with antibodies specific to GSK-3 $\alpha/\beta$ , p- GSK-3 $\alpha/\beta$  , active  $\beta$ - catenin, total  $\beta$ - catenin and  $\beta$ -actin. Densitometry was done and data were corrected for  $\beta$ -actin. (n=1)

#### **4.2.2 Effect of LiCl on cell growth**

MCF-7 and Tam-R cells were treated with LiCl (0, 10 and 20mM concentrations) for four days and MTT assays were performed to determine effects of LiCl on cell growth. The data suggested that there were no significant effects on cell growth over this period. This was true for both MCF-7 cells and Tam-R cells (Figure 4.4).

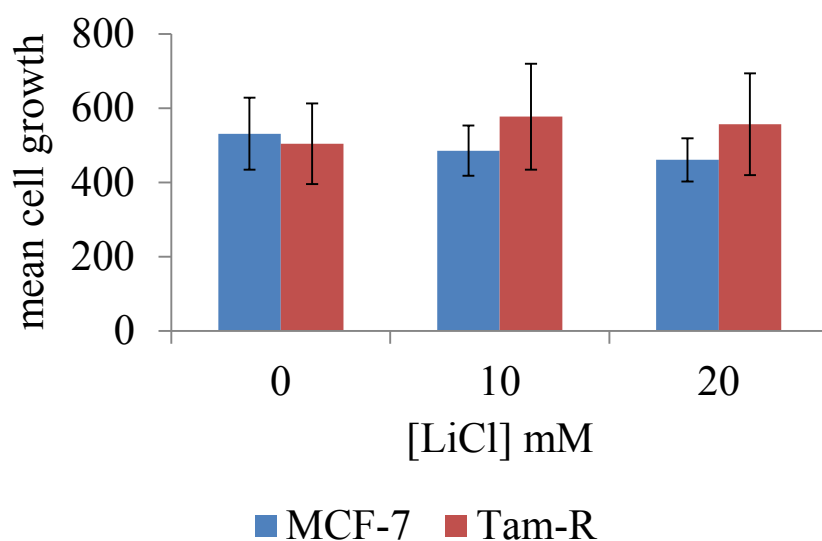


**Figure 4.4**  
**Effects of LiCl (4 days) on growth of MCF-7 and Tam-R cells as determined by MTT assay.**

MTT assay using MCF-7 and Tam-R cells treated with LiCl (0-20mM) for 4 days was done as described in materials and methods section. No significant difference in cell growth was noted. Error bars show SEM (n=3; 72 samples).

### **4.2.3 Effect of LiCl on gene transcription using TCF/LEF (luciferase)**

#### **Reporter Assays**

Tam-R cells were treated with LiCl (0, 10 and 20mM concentrations) and TCF/ LEF reporter assays were done as described in materials and methods section. There were three parallel wells for each treatment and experiments were repeated three times.

The Renilla luciferase serves as an internal control for normalizing transfection efficiencies and monitoring cell viability. Transfection efficiency in Tam-R cells was about 30%. Representative images of Tam-R cells were captured using fluorescent microscopy at 20x magnification. Green fluorescence indicates transfected cells which have taken up and are expressing the green fluorescent protein (GFP). Non-transfected cells were counterstained red with Dil cell labelling solution (Figure 4.5).

The TCF/LEF-responsive luciferase construct encodes the firefly luciferase reporter gene under the control of a minimal (m)CMV promoter and tandem repeats of the TCF/LEF transcriptional response element (TRE). Luciferase activities were expressed as fold stimulation and were related to respective reporter activities obtained with control vector plasmid. There was increased luciferase expression in Tam-R cells treated with LiCl. This was in keeping with Wnt pathway activation as a result of inhibition of GSK-  $3\alpha/\beta$  by LiCl and correlates with signalling data (Figure 4.3). A dose response was observed and the change was significant (Figure 4.6). TCF/ LEF reporter assays support Wnt pathway activation by LiCl treatment.

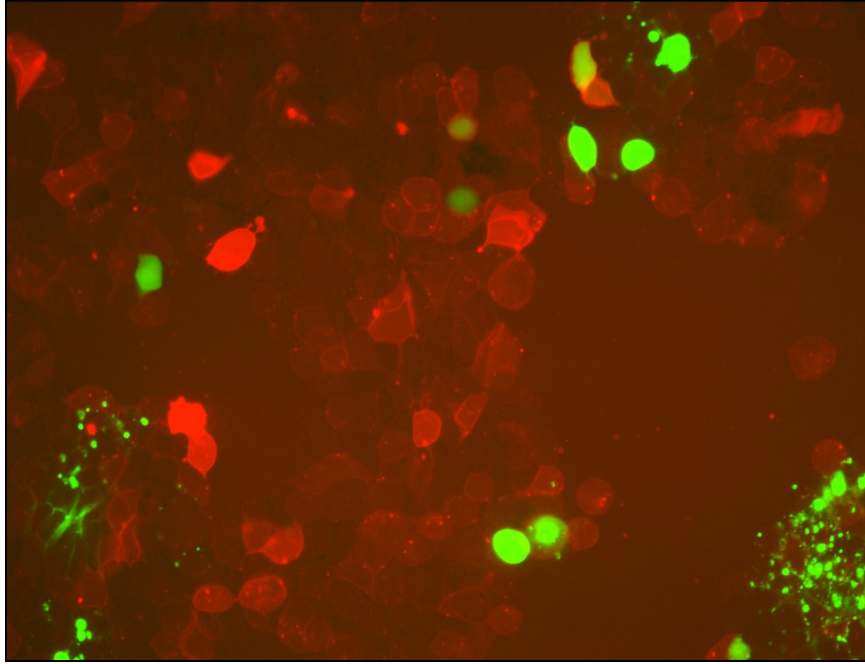


**Figure 4.5**  
**Picture of Tam-R cells following TCF/LEF reporter assay transfection.**

Representative images of Tam-R cells were captured using a fluorescent microscopy at 20x magnification. Green dye show cells which have taken up the green fluorescent protein (GFP) which is coupled to Renilla (about 30%). Non- transfected cells were counterstained red with Dil cell labelling solution.

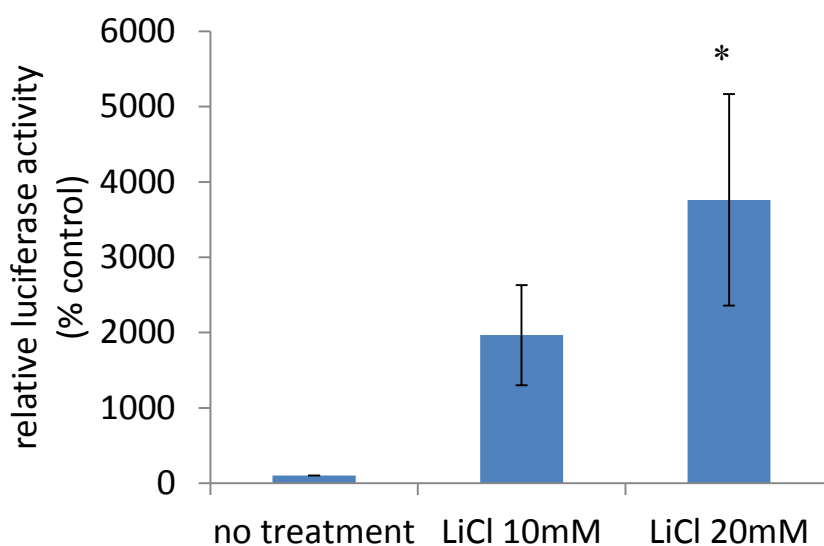


**Figure 4.6**  
**Graph showing results of TCF/LEF reporter assay for Tam-R cells after treatment with LiCl for 16 hours.**

Reporter assay was done as described in materials and methods section, and Tam-R cells were treated with LiCl (0- 20mM concentrations). Luciferase activity was expressed as fold stimulation and was related to respective reporter activity obtained with control vector plasmid.

Error bars show SD. \*test was significant compared to control (<0.05) by post hoc Dunnett 2-sided t-test. (n=2 for LiCl 10mM; n=3 for LiCl 0 and 20 mM).

### **4.3 Summary for Wnt pathway activation**

#### **4.3.1 Wnt3a activity**

Previous gene and protein expression data on Tam-R cells suggested a deregulation of Wnt signalling activity.

When Tam-R cells were treated with Wnt3a, the rise in active  $\beta$ -catenin expression at Wnt3a concentrations of 50, 100 and 200ng/ml would support Wnt activation by the ligand, but expression of GSK-3 $\alpha/\beta$ , p-GSK-3 $\alpha/\beta$  and total  $\beta$ -catenin were again inconclusive. Protein expression data for MCF-7 cells is also inconclusive.

MTT growth assay data was negative for both MCF-7 and Tam-R cells treated with Wnt3a ligand.

A number of limitations need to be considered when interpreting the results:

1. Number of experiments:

The experiments were only done once and data cannot be confirmed to be a true reflection of Wnt3a activity.

2. Choice of ligand:

The subtle changes seen in protein expression in Tam-R cells would suggest that these cells were responsive to the ligand. This was however not confirmed with the growth assay. MCF-7 cells failed to respond to the ligand. The ligand may not be appropriate for the cell model. Alternatively, Tam-R cells may have a higher baseline activity of Wnt activity and cannot achieve further stimulation of activity.

### 3. Timing:

Cells were exposed to ligand for 1 hour in signalling experiments. Shorter time points/ time course experiments may be more suited to pick out earlier signalling changes.

### 4. Other experiments:

The use of purified conditioned media is widely reported in the literature and may be better suited for investigating Wnt activity. Enriched conditioned medium is produced from L-cells. L- cells are located in the mucosa of the distal ileum and colon (Goss K 2011) and exhibit constitutive Wnt pathway activation. They are used to produce Wnt3a medium (ATCC#CRL-2647) and parental L-cells (ATCC#2648) produce control conditioned medium for comparison.

Reporter assays for transcription activity may add further insight into baseline Wnt activity and response to Wnt3a ligand in either cell line.

#### **4.3.2 LiCl activity**

LiCl stimulated Wnt activity in MCF-7 and Tam-R cells: p- GSK-3 $\alpha/\beta$  and active  $\beta$ -catenin expression were increased with increasing concentrations of LiCl. Reporter assay activity confirmed activation of Wnt signalling by LiCl in Tam-R cells. MTT growth assay data was negative for MCF-7 and Tam-R cells treated with LiCl.

The limitations of this experiment were as follows.

#### 1. Number of experiments:



The experiments were only done once and data cannot be confirmed to be a true reflection of LiCl activity.

## 2. Timing:

Cells were exposed to ligand for 1 hour in signalling experiments. Shorter time points may be more suited to pick out earlier signalling changes.

## 3. Method:

Tam-R cells have increased expression of  $\beta$ -catenin compared to the endocrine sensitive MCF-7 cells. Work reported by Vincan (2008, pg69) highlights that baseline expression of  $\beta$ -catenin is very important in interpreting signalling changes by western blotting.  $\beta$ -catenin is highly expressed in Panc04.03 cells. Even though they showed depletion of GSK-3 $\alpha\beta$  after transfection of the cells by GSK-3 $\alpha$  and GSK-3 $\beta$  vectors, the authors failed to show a corresponding increase in levels of  $\beta$ -catenin by Western blotting. They suggest that reporter assay may be more appropriate to look at Wnt pathway activation in this setting. In contrast when they used MiaPaCa2 cells (low levels of baseline  $\beta$ -catenin), they were able to show an increase in total  $\beta$ -catenin after similar transfection and inhibition of GSK-3 $\alpha\beta$ . Our findings would support this hypothesis as we did not show changes in  $\beta$ -catenin levels in our Western blotting experiments.

# Chapter 5

Inhibition of Wnt signalling in endocrine sensitive  
and endocrine resistant breast cancer cells

## **5 Inhibition of Wnt signalling in endocrine sensitive and endocrine resistant breast cancer cells**

Having identified that elements of the Wnt signalling pathway are deregulated in a model of tamoxifen-resistant breast cancer versus their endocrine sensitive counterparts, we next wished to investigate whether Wnt signalling played a dominant role in the Tam-R cells. To pursue this objective, we used two inhibitors of the Wnt pathway, IWP2 and PNU 74654 which act at different levels in the pathway. IWP2 is an inhibitor of Wnt processing and secretion and thus blocks Wnt ligand production (Chen et al. 2009). It is reported to inactivate Porcn, a membrane-bound O-acyltransferase (MBOAT), and selectively inhibits palmitoylation of Wnt. It also blocks Wnt-dependent phosphorylation of LRP6 receptor and Dvl2, and  $\beta$ -catenin accumulation (Chen et al. 2009). LRP6 and Dvl2 gene probes were both deregulated in the Affymetrix data set for Tam-R cells compared to MCF-7 cells (Table 3.1). Chen et al. (2009) used L-cells to demonstrate IWP2 activity and as yet there is no published work on the effect of IWP2 on breast cancer cells. PNU 74654 is reported to bind to  $\beta$ -catenin. It inhibits the interaction between  $\beta$ -catenin and T cell factor 4 (TCF4) and disrupts the Wnt signalling pathway (Trosset et al. 2006).

We set out the following objectives:

- to investigate functional activity of Wnt inhibition by looking at growth and migration.
- to investigate underlying mechanisms and signalling pathways.
- to confirm reported activity of IWP2 and PNU 74654.

## **5.1 Changes in cell function when MCF-7 and Tam-R cells were treated with Wnt inhibitors**

### **5.1.1 IWP2 and PNU 74654 inhibit cell growth**

To determine the importance of Wnt signalling to MCF-7 and Tam-R cells, we first performed growth assays in the presence of the two inhibitors of Wnt signalling.

Data from MTT assays revealed that both IWP2 and PNU 74654 had significantly suppressed the growth of Tam-R cells by about 50% but had no effect on MCF-7 cell growth at 10 $\mu$ M (Figure 5.1). Both drugs were superior in the Tam-R model. Cell counting assays using PNU 74654 showed a reduction in cell growth for both MCF-7 cells and Tam-R cells, but the effect was again greater in Tam-R cells (Figure 5.2). IWP2 growth inhibition in cell counting assays replicated findings in MTT assays (Figure 5.2).

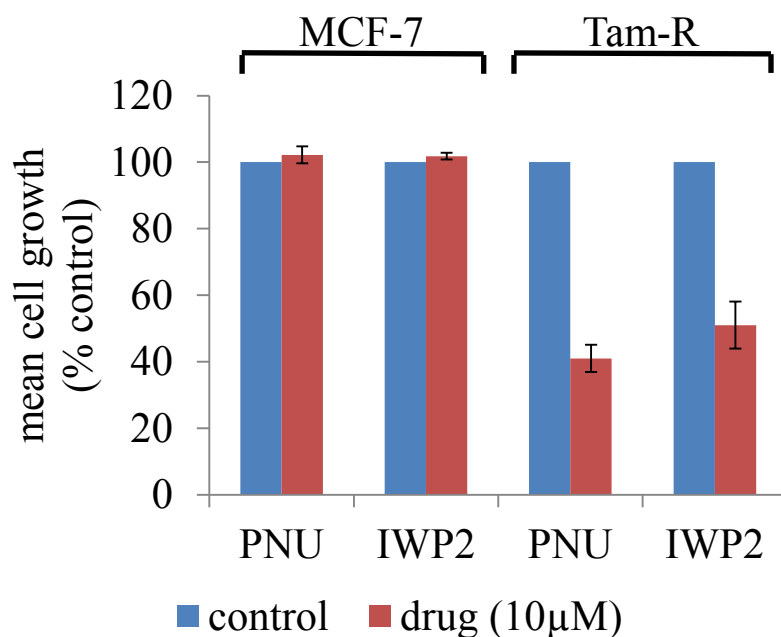


**Figure 5.1**  
**Effects of IWP2 and PNU 74654 (6 days) on growth of MCF-7 and Tam-R cells as determined by MTT assay.**

MTT assay using MCF-7 and Tam-R cells treated with IWP2 and PNU 74654 (control and 10μM concentrations) for 6 days was done as described in materials and methods section. Error bars show SD (n=2, 16 samples). Growth suppression by Wnt inhibitors is greater in Tam-R than in MCF-7 cells.

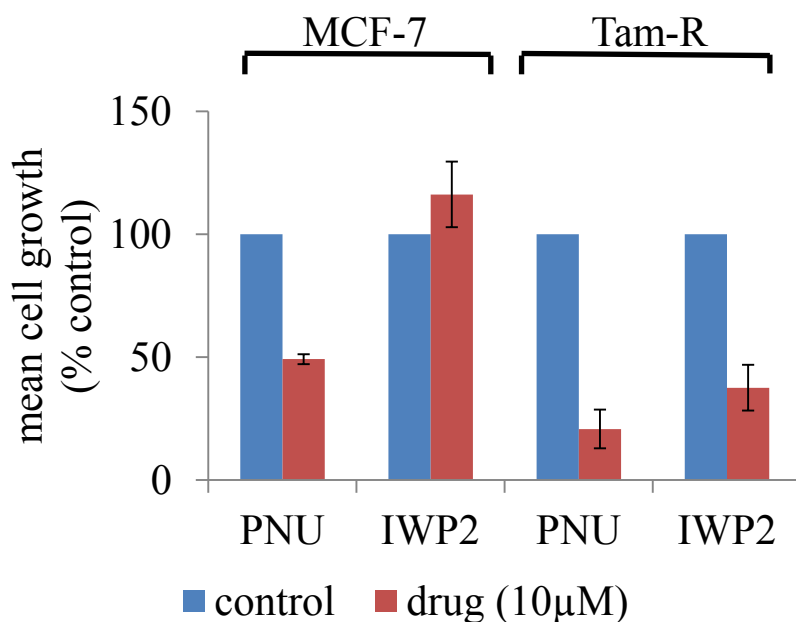


**Figure 5.2**  
**Effects of IWP2 and PNU 74654 (6 days) on growth of MCF-7 and Tam-R cells as determined by cell counting assay.**

Cell counting assay using MCF-7 and Tam-R cells treated with IWP2 and PNU 74654 (control and 10μM concentrations) for 6 days was done as described in materials and methods section. Error bars show SD (n=2 experiments, 6 samples). Growth suppression by Wnt inhibitors is greater in Tam-R than in MCF-7 cells.

We wanted to explore if tamoxifen had any interaction with the Wnt inhibitors and the effects outlined above could have been a result of this interaction. Previous work in the lab suggested that Tam-R cells have intracellular tamoxifen reserves for about two weeks. Tam-R cells were deprived of tamoxifen supplementation for two weeks and MTT assay was repeated. Growth in Tam-R cells was again reduced by half after treatment with IWP2 and PNU 74654. This suggested there was no interaction between tamoxifen and Wnt inhibitors in these cells (Figure 5.3).

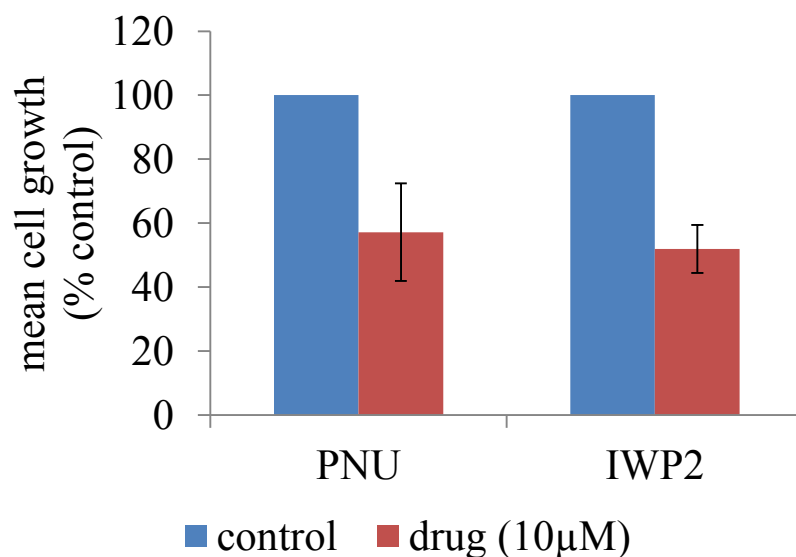


**Figure 5.3**  
**Effects of IWP2 and PNU 74654 (6 days) on growth of Tamoxifen deprived Tam-R cells as determined by MTT assay.**

Tam-R cells were grown in Tamoxifen deprived medium for two weeks before starting MTT assay. These cells were treated with IWP2 and PNU 74654 (control and 10μM concentrations) for 6 days as described in materials and methods section. Error bars show SD (n=2 experiments, 16 samples). Growth of Tam-R cells was reduced by half after treatment with Wnt inhibitors.



Dose effects of IWP2 and PNU 74654 on growth of MCF-7 and Tam-R cell lines was determined by MTT assays. MCF-7 and Tam-R cells were treated with IWP2 and PNU 74654 (0- 10 $\mu$ M concentrations) for 6 days. There was no significant effect on growth inhibition in MCF-7 cells treated with the two drugs (Figure 5.4). Maximum growth inhibition occurred at 10 $\mu$ M concentration of drugs in Tam-R cells (Figure 5.5). The maximum DMSO concentration used in these experiments was 2 $\mu$ M (see Appendix).

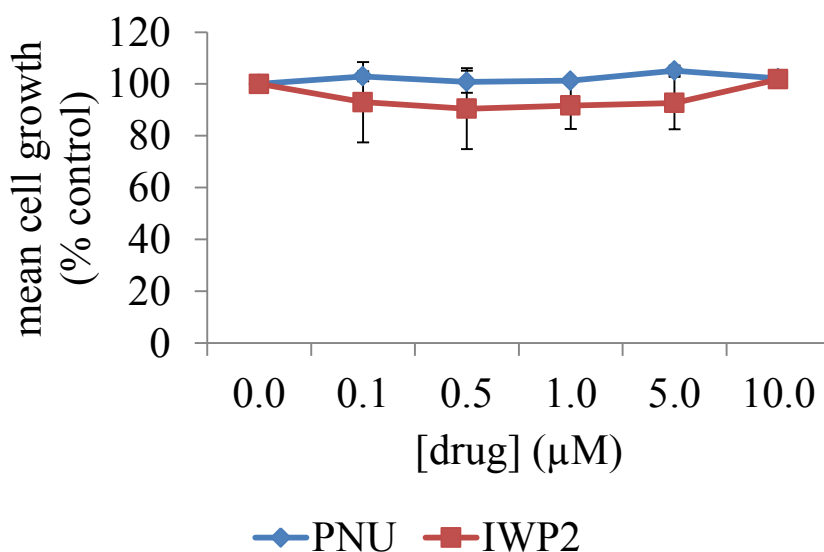


**Figure 5.4**  
**Effects of IWP2 and PNU 74654 (6 days) on growth of MCF-7 cells as determined by MTT assay.**

MTT assays using MCF-7 cells treated with IWP2 and PNU 74654 (0- 10μM concentrations) for 6 days were done as described in materials and methods section. There was no significant change in cell growth. Error bars show SEM (n=2, 16 samples).

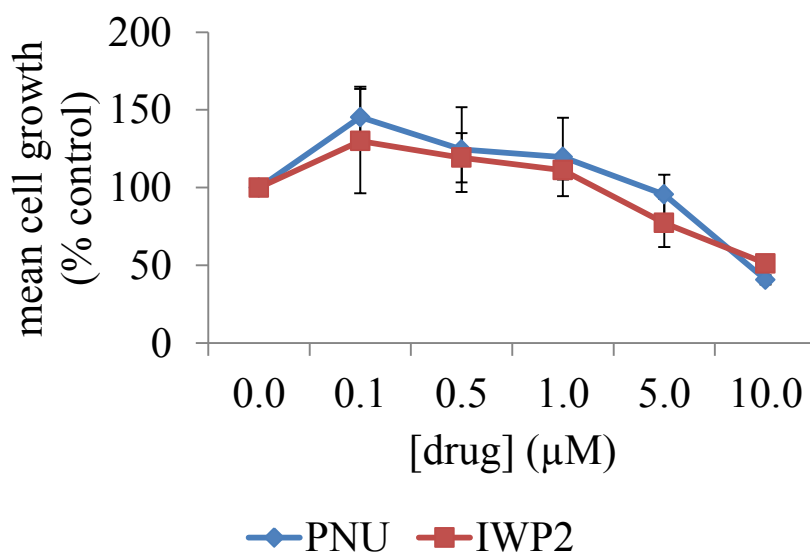


**Figure 5.5**  
**Effects of IWP2 and PNU 74654 (6 days) on growth of Tam-R cells as determined by MTT assay.**

MTT assays using Tam-R cells treated with IWP2 and PNU 74654 (0- 10μM concentrations) for 6 days were done as described in materials and methods section. The greatest reduction in cell growth is seen at 10μM concentrations. Error bars show SEM (n=2, 16 samples).

Using data from MTT assays, the half maximal inhibitory concentration (IC<sub>50</sub>) for IWP2 and PNU 74654 was calculated for Tam-R cells (Figure 5.6) using linear interpolation (see Section 2.6.3). An IWP2 IC<sub>50</sub> of 27nM is quoted for L-cells (Chen, Dodge et al. 2009). IWP2 IC<sub>50</sub> for Tam-R cells was 10.2μM. There is no IC<sub>50</sub> data in the literature for PNU 74654. Our results showed an IC<sub>50</sub> of 8.5μM in Tam-R cells. IWP2 and PNU 74654 did not have a significant effect on growth of MCF-7 cells. This model assumes a linear effect of the drug on the cells: an exponential model may be better alternative approach.

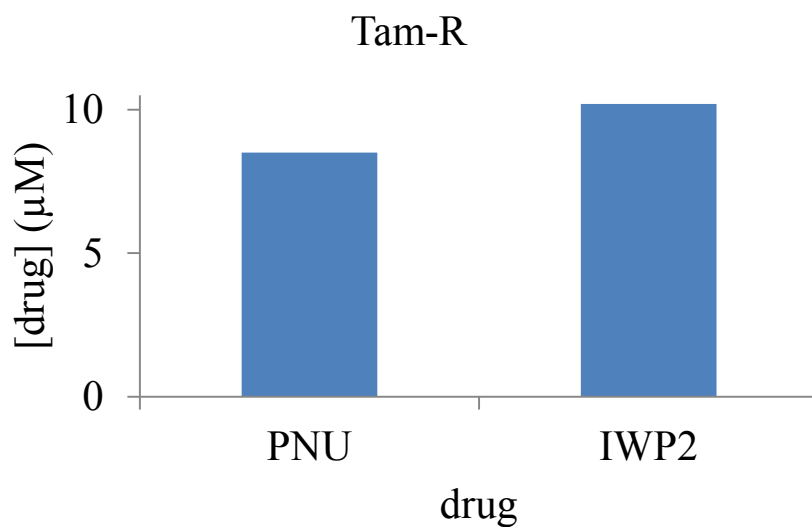


**Figure 5.6**  
**The half maximal inhibitory concentration for**  
**Tam-R cells treated with IWP2 and PNU 74654.**

The half maximal inhibitory concentration (IC<sub>50</sub>) for Tam-R cells treated with IWP2 and PNU 74654 as determined by linear interpolation of data from MTT assays.

### 5.1.2 IWP2 and PNU 74654 inhibit cell migration

We set out to explore changes in cell migration in Tam-R cells after treatment with Wnt inhibitors. Previous experiments done in the lab had shown that MCF-7 cells have limited migratory properties, and were therefore not included in these experiments. In contrast, Tam-R cells have increased migratory behaviour.

Migratory capacity of Tam-R cells following treatment with IWP2 and PNU 74654 was assessed using *in vitro* migration assays. Representative images of migratory cells were captured using light microscopy at 20x magnification. Cells were stained purple with crystal violet. For quantification, the number of migratory cells in 5 random fields of view were counted using a light microscope and presented as % of Tam-R untreated control (Figure 5.7). IWP2 and PNU 74654 both significantly decreased cell migration in Tam-R cells ( $p < 0.05$ ).

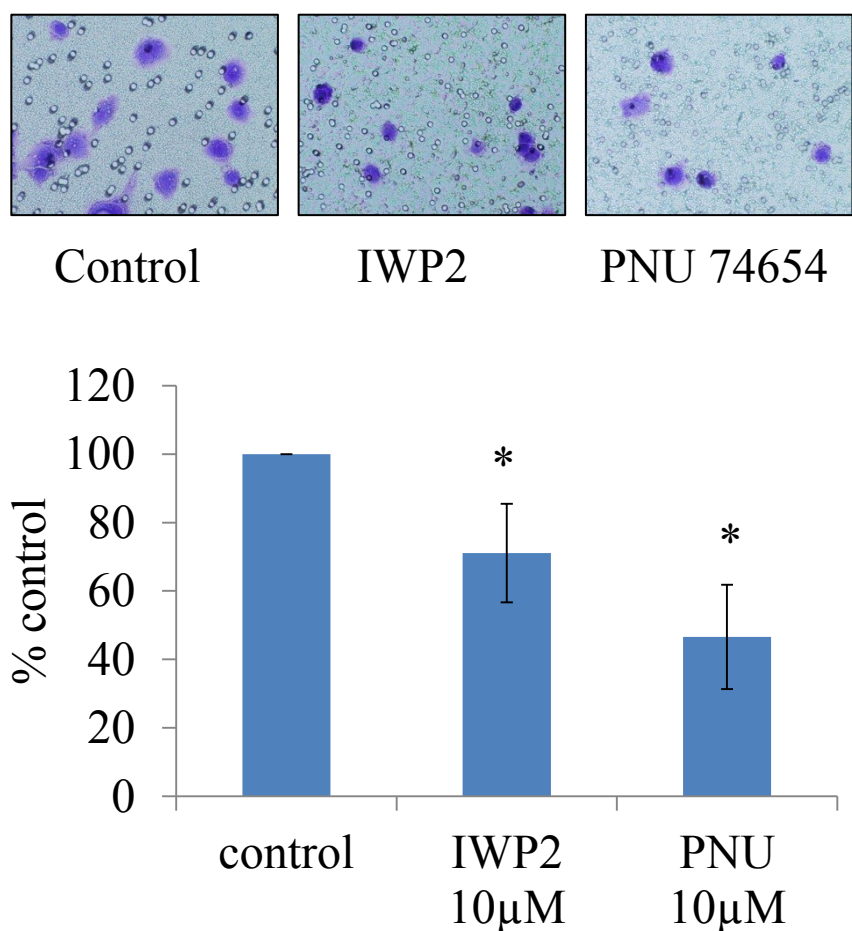


**Figure 5.7**  
**Effects of IWP2 and PNU 74654 at 24 hours on migration in Tam-R cells as determined by cell migration assay.**

Migratory capacity of Tam-R following treatment with IWP2 and PNU 74654 was assessed using *in vitro* migration assays. Representative images of migratory cells were captured using a light microscopy at 20x magnification. Cells are stained purple with crystal violet. For quantification, the number of migratory cells in 5 random fields of view were counted using a light microscope and presented as % of Tam-R control.

Error bars show SD for n=3.  $p < 0.05$  (\*) for both IWP2 and PNU 74654 compared to control using post hoc 2 sided Dunnett t- test.

## **5.2 Changes in cell signalling when MCF-7 and Tam-R cells were treated with Wnt inhibitors**

Having established functional activity of Wnt inhibitors, we set out to explore underlying mechanisms and signalling pathways using Western Blotting. MCF-7 and Tam-R cells were treated with IWP2 and PNU 74654 at concentrations of 0 to 10 $\mu$ M. Experiments were repeated at 5 minutes and at 1 hour. Equal loading was confirmed by Ponceau S staining. Unfortunately, we had persistent problems with  $\beta$ -actin and we were unable to obtain a signal in some experiments. GAPDH was used in other experiments

### **5.2.1 IWP2**

#### **5.2.1.1 IWP2 activity**

We wanted to establish proof of activity for IWP2 by Western blotting. As previously mentioned, IWP2 blocks Wnt-dependent phosphorylation of LRP6 receptor. MCF-7 and Tam-R cells were treated with IWP2 for 5 minutes. As expected, IWP2 decreased p-LRP6 expression (Figure 5.8). This confirmed IWP2 activity in both cell lines.



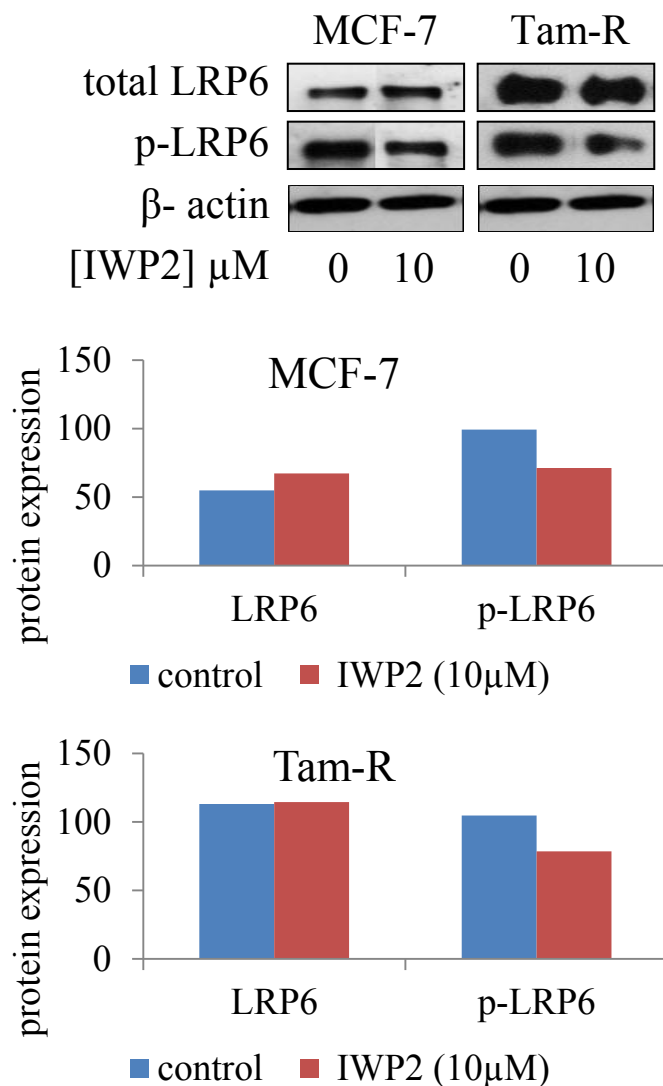


**Figure 5.8**  
**Effect of IWP2 on LRP6 in MCF-7 and Tam-R**  
**cells as determined by Western Blotting.**

MCF-7 and Tam-R cells were cultured to log-phase growth and then treated with IWP2 (10  $\mu$ M concentration) and DMSO for 5 minutes. The cells were then lysed. SDS-PAGE/ Western blot analyses was carried out using 30  $\mu$ g of total soluble protein and the membranes were probed with antibodies specific to LRP6, p-LRP6 and  $\beta$ -actin. Densitometry data was corrected for  $\beta$ -actin. IWP2 decreased p-LRP6 in both MCF-7 and Tam-R cells.

#### **5.2.1.2 Effect of IWP2 on Wnt signalling components**

Inhibition of Wnt signalling at the receptor level should result in increased activity in the destruction complex of which GSK-  $3\alpha/\beta$  is a key component. This leads to increased phosphorylation of  $\beta$ - catenin at S33, S37, T41 and a decrease in total  $\beta$ -catenin.

When MCF-7 cells were treated with IWP2 (Figure 5.9, Figure 5.10), there was no consistent change in expression of total  $\beta$ - catenin and p- $\beta$ - catenin (S33/37/T41) for the two time points and a small drop was noted in p-GSK-  $3\alpha/\beta$  expression at 1 hour. There was a fall in GSK-  $3\alpha$  expression with increasing IWP2 concentrations at 5 minutes, but a rise was noted at 1 hour (Figure 5.9, Figure 5.10).

The process was repeated using Tam-R cells. There was no change in expression of p-GSK-  $3\alpha/\beta$ , total  $\beta$ - catenin for the two time points. At five minutes, p- $\beta$ - catenin (S33/37/T41) expression was decreased from 5 $\mu$ M and total GSK- $3\alpha/\beta$  expression was decreased from 1 $\mu$ M (Figure 5.11, Figure 5.12).

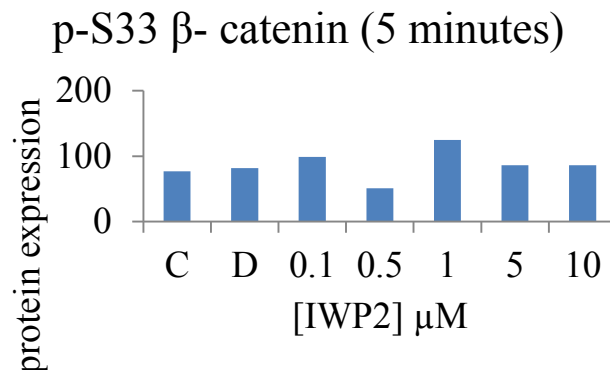
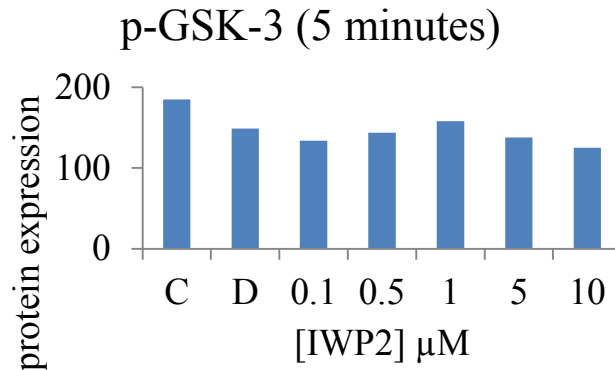
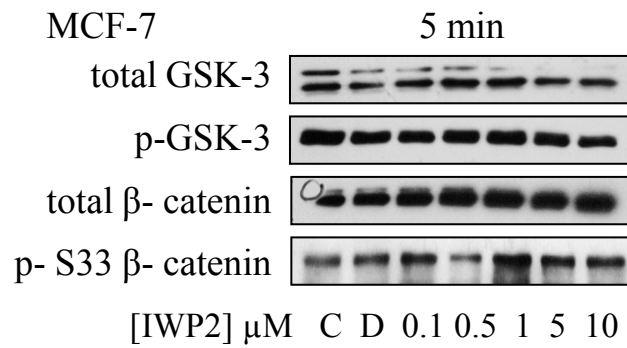


**Figure 5.9**

**Dose dependent effect of IWP2 on GSK-3 $\alpha$ / $\beta$  and  $\beta$ -catenin in MCF-7 cells at 5 minutes as determined by Western Blotting.**

C=control D=DMSO (n=1)

MCF-7 cells were cultured to log-phase growth and then treated with IWP2 (0 to 10  $\mu$ M concentrations) for 5 minutes. The cells were then lysed. SDS-PAGE/ Western blot analyses was carried out using 30  $\mu$ g of total soluble protein and the membranes were probed with antibodies specific to GSK-3 $\alpha$ / $\beta$ , p- GSK-3 $\alpha$ / $\beta$ ,  $\beta$ -catenin and p-S33  $\beta$ -catenin. Densitometry data are shown. GSK-3 $\alpha$  expression decreases with IWP2 treatment.

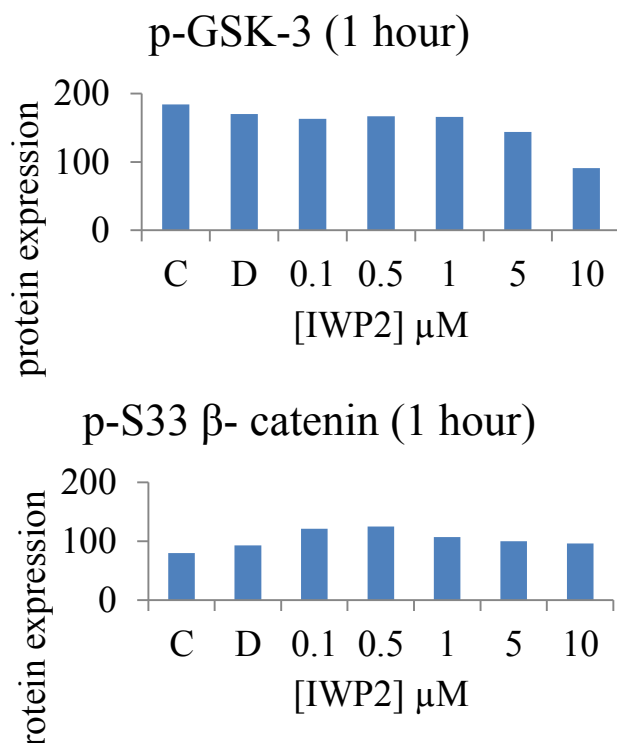
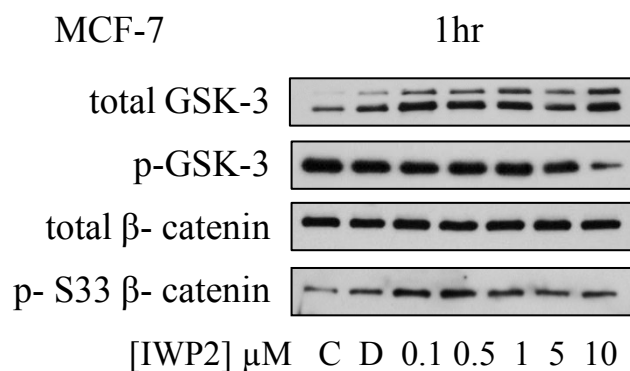


**Figure 5.10**

**Dose dependent effect of IWP2 on GSK-3 $\alpha/\beta$  and  $\beta$ -catenin in MCF-7 cells at 1 hour as determined by Western Blotting.**

C=control D=DMSO (n=1)

MCF-7 cells were cultured to log-phase growth and then treated with IWP2 (0 to 10  $\mu$ M concentrations) for 1 hour. The cells were then lysed. SDS-PAGE/ Western blot analyses was carried out using 30  $\mu$ g of total soluble protein and the membranes were probed with antibodies specific to GSK-3 $\alpha/\beta$ , p- GSK-3 $\alpha/\beta$ ,  $\beta$ -catenin and p-S33  $\beta$ -catenin. Densitometry data are shown. IWP2 increased p- GSK-3 $\alpha/$  expression at 1 hour.

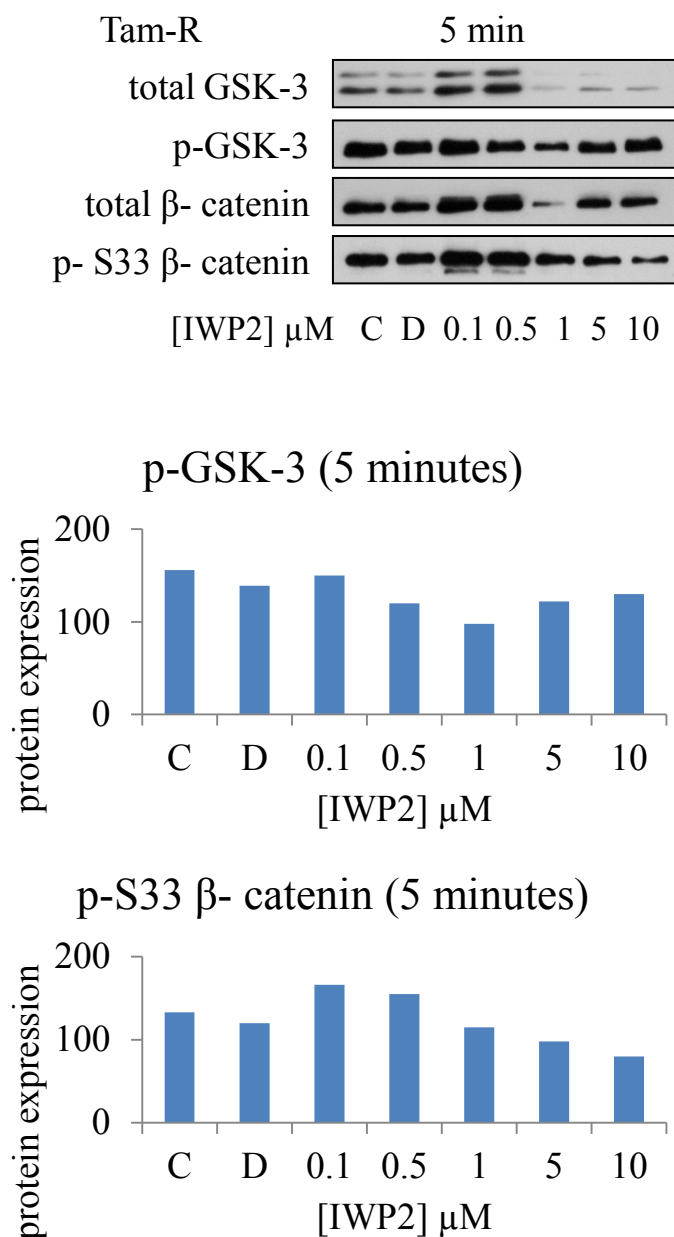


**Figure 5.11**

**Dose dependent effect of IWP2 on GSK-3 $\alpha/\beta$  and  $\beta$ - catenin in Tam-R cells at 5 minutes as determined by Western Blotting.**

C=control D=DMSO (n=1)

Tam-R cells were cultured to log-phase growth and then treated with IWP2 (0 to 10  $\mu$ M concentrations) for 5 minutes. The cells were then lysed. SDS-PAGE/ Western blot analyses was carried out using 30  $\mu$ g of total soluble protein and the membranes were probed with antibodies specific to GSK-3 $\alpha/\beta$ , p- GSK-3 $\alpha/\beta$ ,  $\beta$ -catenin, and p-S33  $\beta$ - catenin. Densitometry data are shown. IWP2 decreased p-S33  $\beta$ - catenin and total GSK-3 $\alpha/\beta$  expression at 5 minutes.

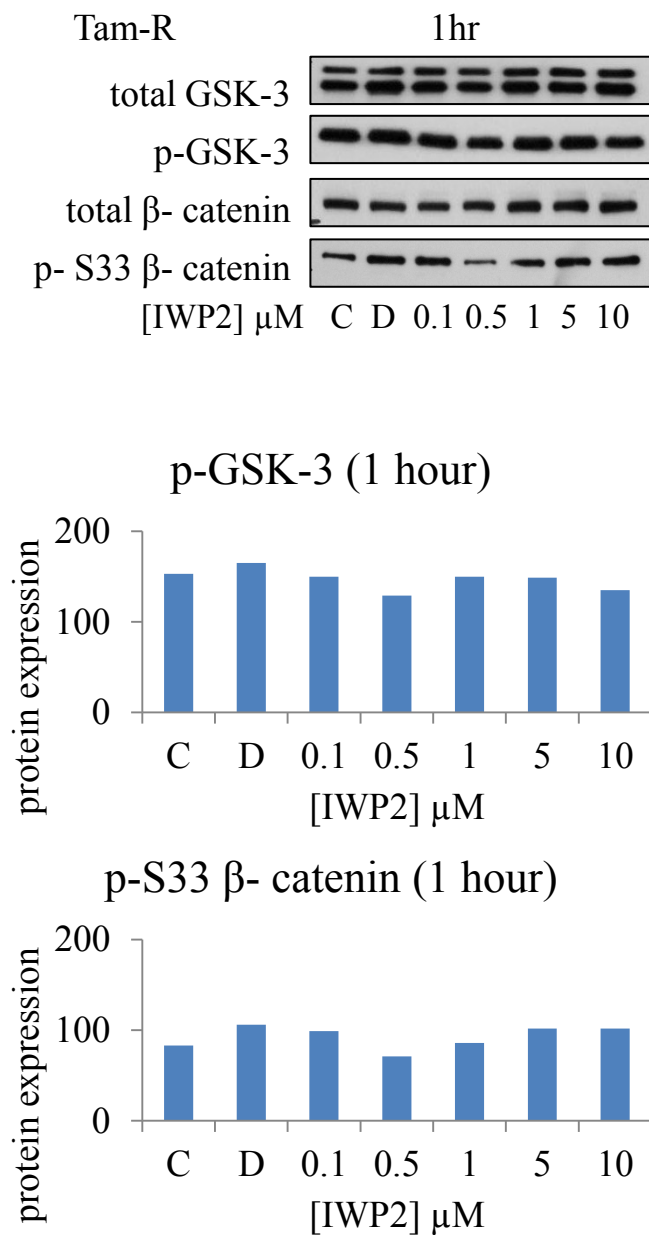


**Figure 5.12**

**Dose dependent effect of IWP2 on GSK-3 $\alpha/\beta$  and  $\beta$ -catenin in Tam-R cells at 1 hour as determined by Western Blotting.**

C=control D=DMSO (n=1)

Tam-R cells were cultured to log-phase growth and then treated with IWP2 (0 to 10  $\mu$ M concentrations) for 1 hour. The cells were then lysed. SDS-PAGE/ Western blot analyses was carried out using 30  $\mu$ g of total soluble protein and the membranes were probed with antibodies specific to GSK-3 $\alpha/\beta$ , p- GSK-3 $\alpha/\beta$ ,  $\beta$ -catenin, and p-S33  $\beta$ -catenin. Densitometry data are shown.

### **5.2.1.3 Effect of IWP2 on cell cycle proteins**

Binding of  $\beta$ -catenin to TCF/LEF results in transcription of several genes, including c-myc and cyclin D1 (Lepourcelet et al. 2004). Cell cycle proteins were assessed through cyclin D1 and c-myc expression.

Following treatment of MCF-7 with IWP2, c-myc expression was decreased at 5 minutes (from 5  $\mu$ M) and increased at 1 hour (from 0.1  $\mu$ M). Cyclin D1 expression was decreased at 1 hour from 5  $\mu$ M (Figure 5.13, Figure 5.14).

When Tam-R cells were treated with IWP2, c-myc expression decreased at 5 minutes (from 0.5  $\mu$ M), but increased at 1 hour (from 0.1  $\mu$ M). There was a fall in cyclin D1 expression at 5 minutes (from 0.5  $\mu$ M) but no change was noted at 1 hour (Figure 5.15, Figure 5.16).

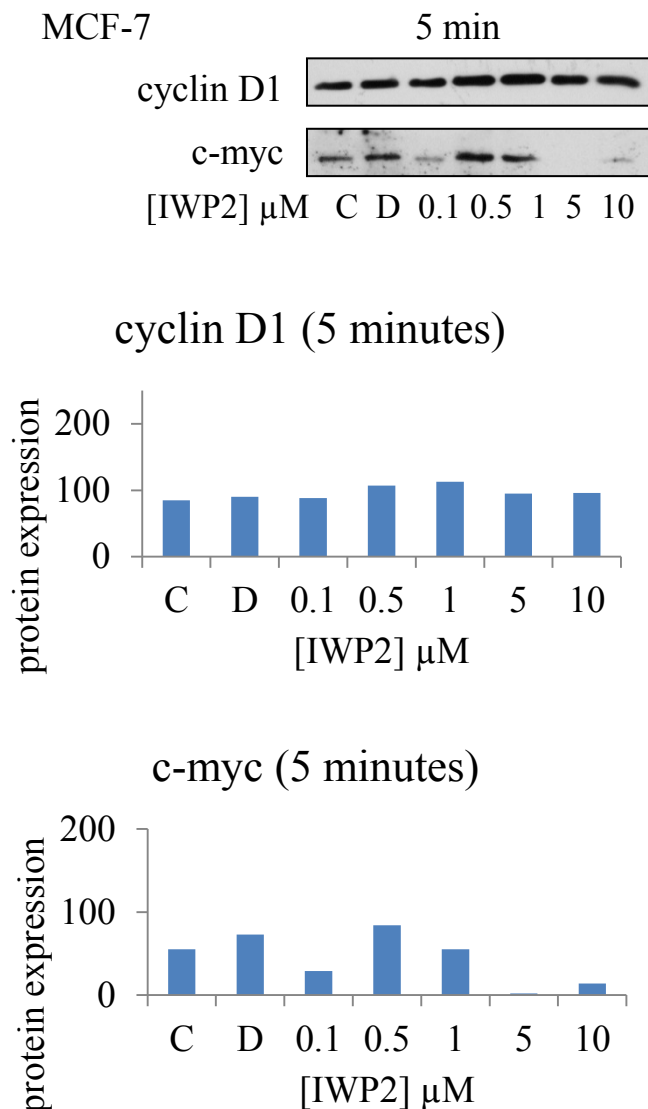


**Figure 5.13**

**Dose dependent effect of IWP2 on cyclin D1 and c-myc in MCF-7 cells at 5 minutes as determined by Western Blotting.**

C=control D=DMSO (n=1)

MCF-7 cells were cultured to log-phase growth and then treated with IWP2 (0 to 10  $\mu$ M concentrations) for 5 minutes. The cells were then lysed. SDS-PAGE/ Western blot analyses was carried out using 30  $\mu$ g of total soluble protein and the membranes were probed with antibodies specific to cyclin D1 and c-myc. Densitometry data are shown. IWP2 decreased c-myc expression at 5 minutes (from 5  $\mu$ M).



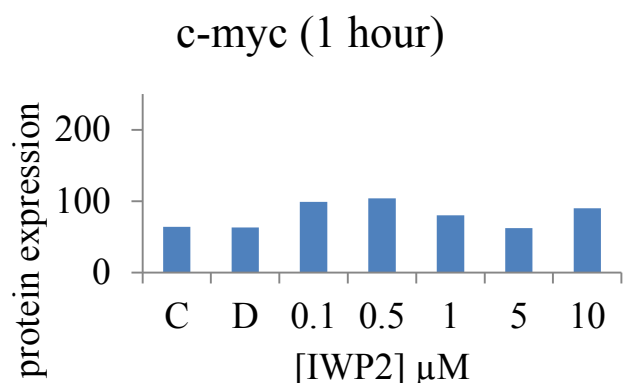
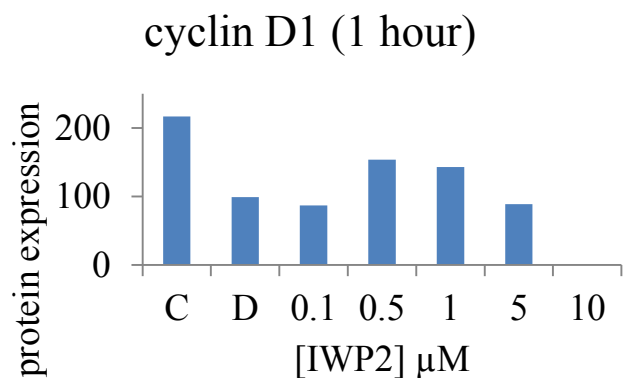
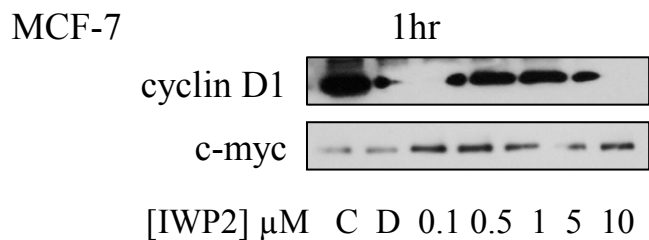


**Figure 5.14**

**Dose dependent effect of IWP2 on cyclin D1 and c-myc in MCF-7 cells at 1 hour as determined by Western Blotting.**

C=control D=DMSO (n=1)

MCF-7 cells were cultured to log-phase growth and then treated with IWP2 (0 to 10  $\mu$ M concentrations) for 1 hour. The cells were then lysed. SDS-PAGE/ Western blot analyses was carried out using 30  $\mu$ g of total soluble protein and the membranes were probed with antibodies specific to cyclin D1 and c-myc. Densitometry data are shown. At 1 hour, IWP2 decreased cyclin D1 (10  $\mu$ M) and increased c-myc expression (from 0.1  $\mu$ M).

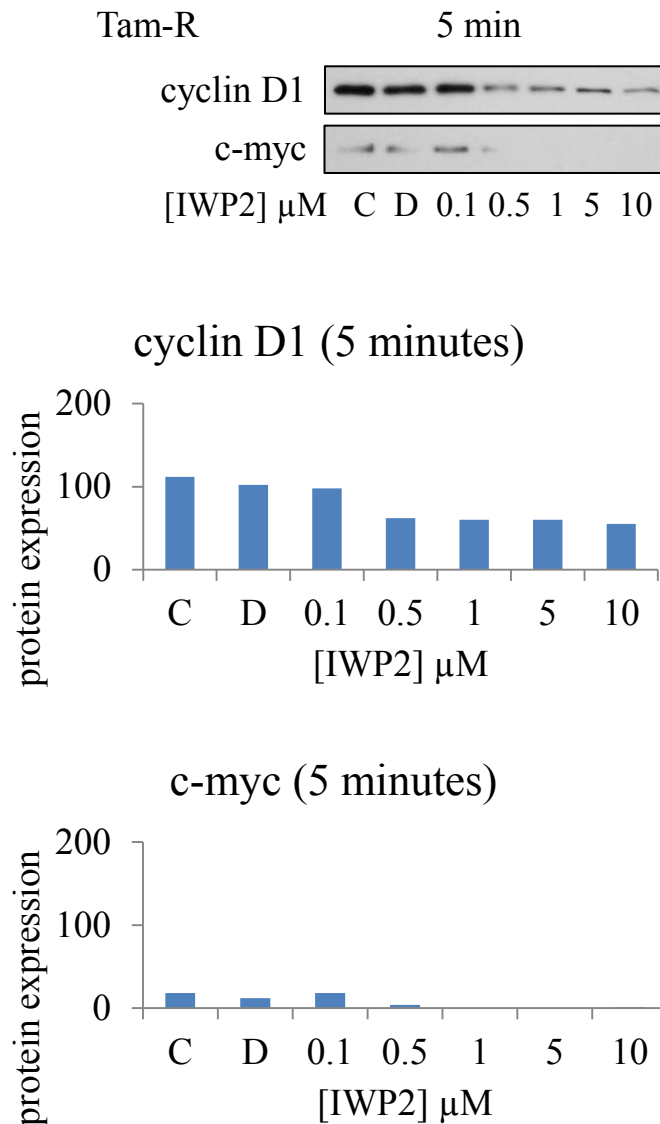


**Figure 5.15**

**Dose dependent effect of IWP2 on cyclin D1 and c-myc in Tam-R cells at 5 minutes as determined by Western Blotting.**

C=control D=DMSO (n=1)

Tam-R cells were cultured to log-phase growth and then treated with IWP2 (0 to 10  $\mu$ M concentrations) for 5 minutes. The cells were then lysed. SDS-PAGE/ Western blot analyses was carried out using 30  $\mu$ g of total soluble protein and the membranes were probed with antibodies specific to cyclin D1 and c-myc. Densitometry data are shown. IWP2 decreased c-myc expression at 5 minutes.

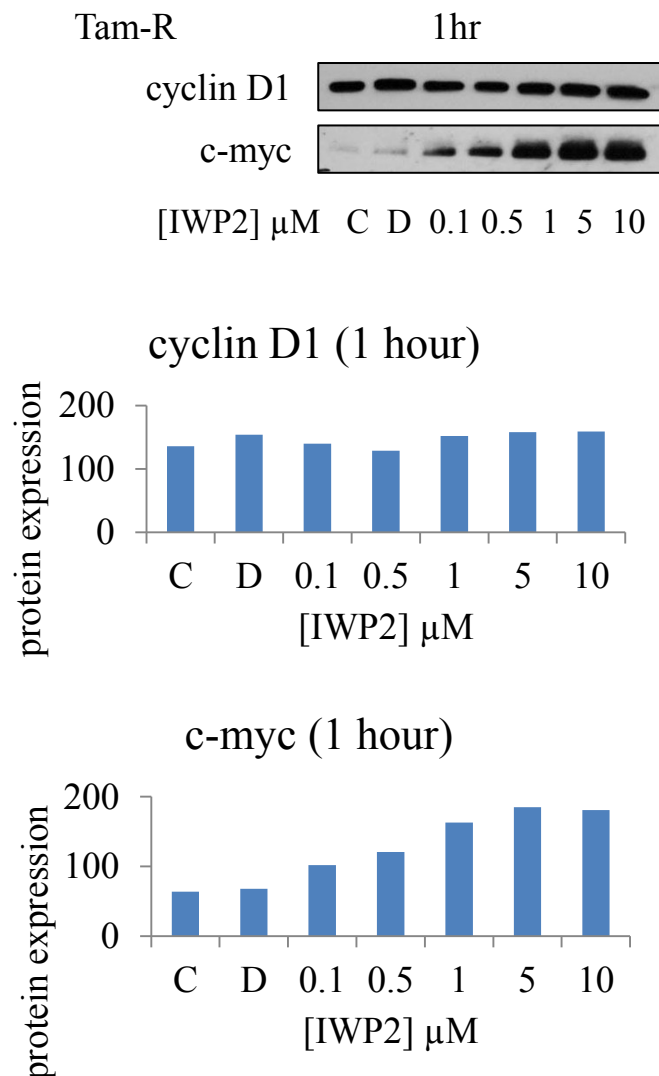


**Figure 5.16**  
**Dose dependent effect of IWP2 on cyclin D1 and c-myc in Tam-R cells at 1 hour as determined by Western Blotting.**

C=control D=DMSO (n=1)

Tam-R cells were cultured to log-phase growth and then treated with IWP2 (0 to 10  $\mu$ M concentrations) for 1 hour. The cells were then lysed. SDS-PAGE/ Western blot analyses was carried out using 30  $\mu$ g of total soluble protein and the membranes were probed with antibodies specific to cyclin D1 and c-myc. Densitometry data are shown. IWP2 increased c-myc expression at 1 hour.

#### **5.2.1.4 Additional signalling mechanisms**

Previous experiments had shown that Wnt inhibition reduced growth and migration in Tam-R cells. We next looked at src and MAPK activity which help drive these two processes and are substantial in these cells (Hiscox S 2009, Hutcheson et al. 2003).

Following treatment of MCF-7 cells with IWP2, p-src expression was decreased at 5 minutes (from 5 $\mu$ M). The rise in p-src expression at 1 hour (from 0.1 $\mu$ M) was paralleled by changes in total src expression (Figure 5.17, Figure 5.18).

For Tam-R cells treated with IWP2, there was a decrease in p-src expression at 5 minutes (at 10  $\mu$ M) and a rise at 1 hour (at 1 and 10  $\mu$ M) (Figure 5.19, Figure 5.20). There was a decrease in p-MAPK expression by 10 $\mu$ M (Figure 5.21).

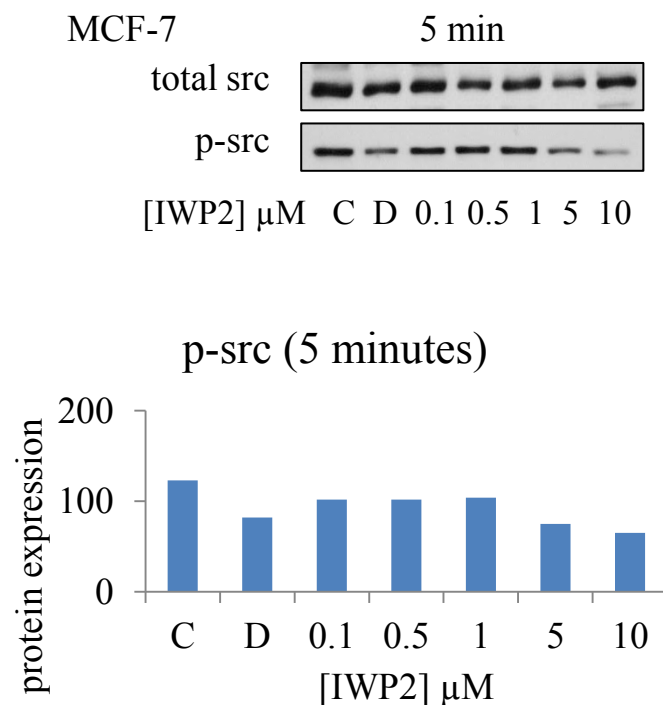


**Figure 5.17**  
**Dose dependent effect of IWP2 on src in MCF-7 cells**  
**at 5 minutes as determined by Western Blotting.**

C=control D=DMSO (n=1)

MCF-7 cells were cultured to log-phase growth and then treated with IWP2 (0 to 10  $\mu\text{M}$  concentrations) for 5 minutes. The cells were then lysed. SDS-PAGE/ Western blot analyses was carried out using 30  $\mu\text{g}$  of total soluble protein and the membranes were probed with antibodies specific to src and p-src. Densitometry data are shown. IWP2 decreased p-src expression at 5 minutes from 5  $\mu\text{M}$ .

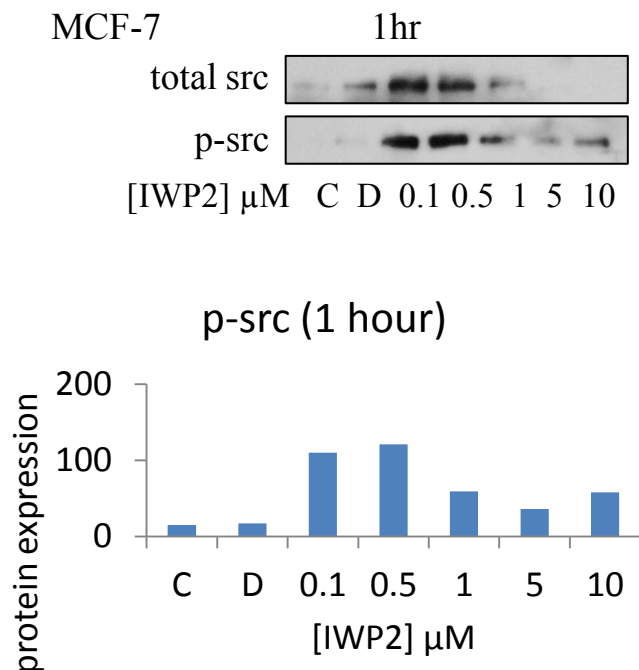


**Figure 5.18**  
**Dose dependent effect of IWP2 on src in MCF-7 cells at 1 hour as determined by Western Blotting.**

C=control D=DMSO (n=1)

MCF-7 cells were cultured to log-phase growth and then treated with IWP2 (0 to 10  $\mu$ M concentrations) for 1 hour. The cells were then lysed. SDS-PAGE/ Western blot analyses was carried out using 30  $\mu$ g of total soluble protein and the membranes were probed with antibodies specific to src and p-src. Densitometry data are shown. IWP2 increased p-src expression at 1 hour but these changes were paralleled by changes in total src expression.

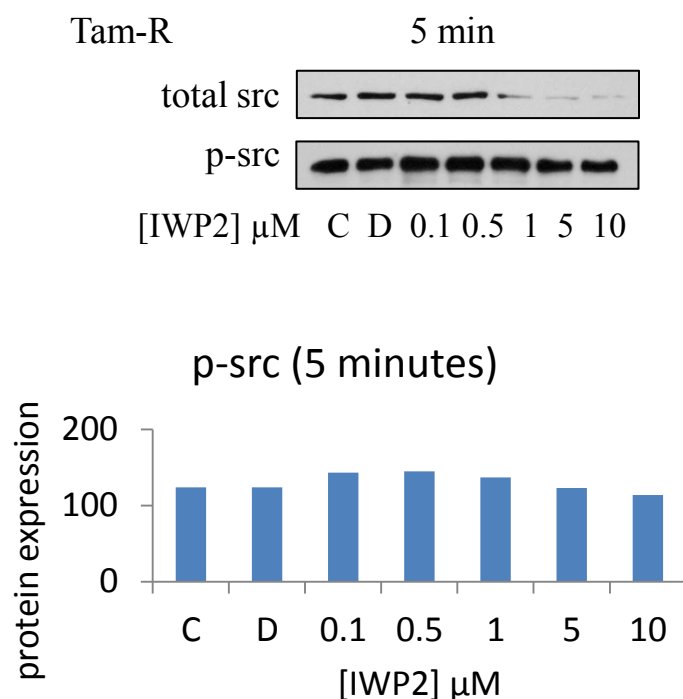


**Figure 5.19**

**Dose dependent effect of IWP2 on src in Tam-R cells at 5 minutes as determined by Western Blotting.**

C=control D=DMSO (n=1)

Tam-R cells were cultured to log-phase growth and then treated with IWP2 (0 to 10  $\mu\text{M}$  concentrations) for 5 minutes. The cells were then lysed. SDS-PAGE/ Western blot analyses was carried out using 30  $\mu\text{g}$  of total soluble protein and the membranes were probed with antibodies specific to src and p-src. Densitometry data are shown. There was no change in p-src expression.

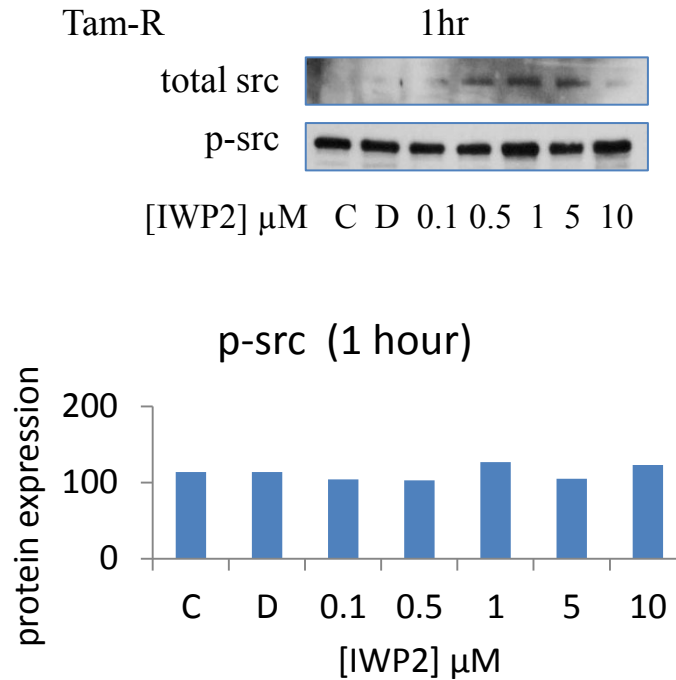


**Figure 5.20**  
**Dose dependent effect of IWP2 on src in Tam-R cells at 1 hour as determined by Western Blotting.**

C=control D=DMSO (n=1)

Tam-R cells were cultured to log-phase growth and then treated with IWP2 (0 to 10  $\mu\text{M}$  concentrations) for 1 hour. The cells were then lysed. SDS-PAGE/ Western blot analyses was carried out using 30  $\mu\text{g}$  of total soluble protein and the membranes were probed with antibodies specific to src and p-src. Densitometry data are shown. There was no change in p-src expression.



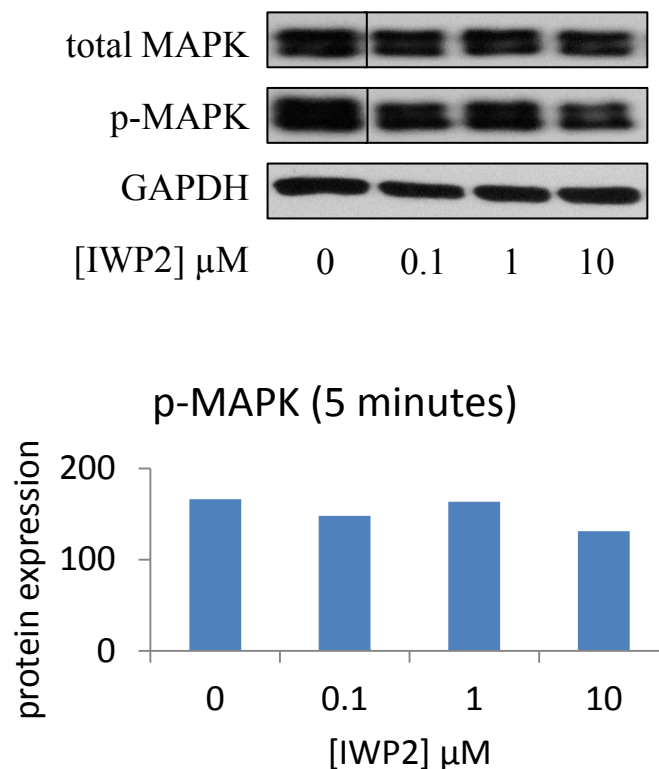


**Figure 5.21**

**Dose dependent effect of IWP2 on MAPK in Tam-R cells at 5 minutes as determined by Western Blotting.**

C=control D=DMSO (n=1)

Tam-R cells were cultured to log-phase growth and then treated with IWP2 (0 to 10  $\mu\text{M}$  concentrations) for 5 minutes. The cells were then lysed. SDS-PAGE/ Western blot analyses was carried out using 30  $\mu\text{g}$  of total soluble protein and the membranes were probed with antibodies specific to MAPK, p-MAPK and GAPDH. Densitometry data are shown and is corrected for GAPDH. Expression of p-MAPK decreased when cells were treated with IWP2 (10  $\mu\text{M}$ ) .

### **5.2.2 PNU 74654**

PNU 74654 binds to  $\beta$ -catenin. It is reported to inhibit the interaction between  $\beta$ -catenin and TCF4.

#### **5.2.2.1 Effect of PNU 74654 on Wnt signalling components**

PNU 74654 acts in the nucleus. We wanted to explore if its activity would have an effect on Wnt signalling components. We looked at receptor activity (LRP6), destruction complex activity (through GSK3 activity) and p- $\beta$ -catenin (S33/37/T41).

When MCF-7 cells were treated with PNU 74654,  $\beta$ -catenin expression remained unchanged at the two time points. p- $\beta$ -catenin (S33/37/T41) expression was decreased at 5 minutes (at 10 $\mu$ M) and increased at 1 hour (at 10 $\mu$ M). There was decreased p-LRP6 and p-GSK3 (by 10 $\mu$ M) expression after treatment with PNU 74654 for 5 minutes and decreased p-LRP6, p-GSK-3 $\alpha$  and p-GSK-3 $\beta$  expression (from 0.1 $\mu$ M) after treatment with PNU 74654 for 1 hour (Figure 5.22, Figure 5.23, Figure 5.24, Figure 5.25). This suggested that Wnt inhibition at a nuclear level by PNU 74654 resulted in feedback to upstream components of Wnt signalling.

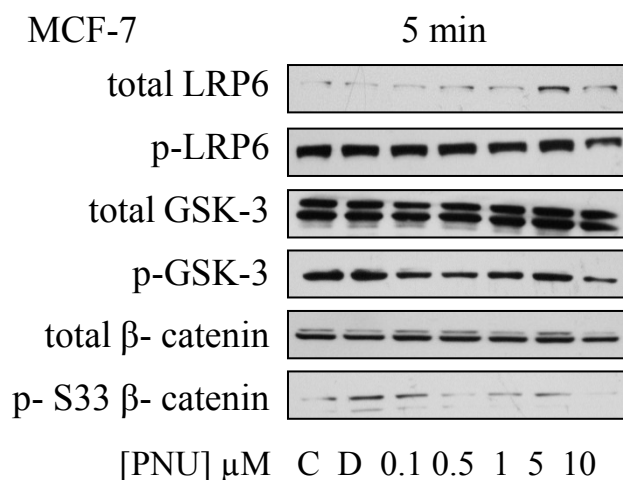


**Figure 5.22**  
**Dose dependent effect of PNU 74654 on GSK-3 $\alpha/\beta$  and  $\beta$ - catenin in MCF-7 cells at 5 minutes as determined by Western Blotting.**

C=control D=DMSO (n=1)

MCF-7 cells were cultured to log-phase growth and then treated with PNU 74654 (0 to 10  $\mu$ M concentrations) for 5 minutes. The cells were then lysed. SDS-PAGE/ Western blot analyses was carried out using 30  $\mu$ g of total soluble protein and the membranes were probed with antibodies specific to LRP6, p-LRP6, GSK-3 $\alpha/\beta$ , p- GSK-3 $\alpha/\beta$ ,  $\beta$ - catenin and p-S33  $\beta$ -catenin.

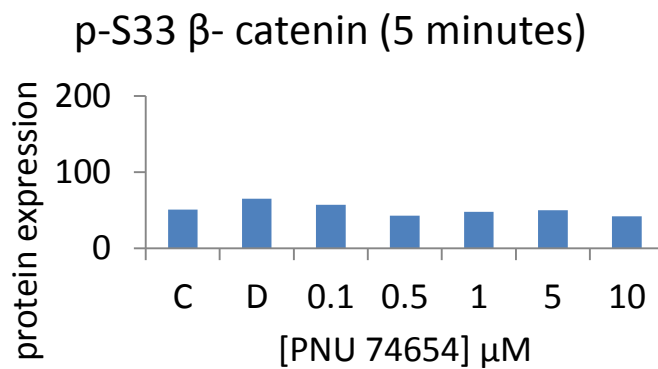
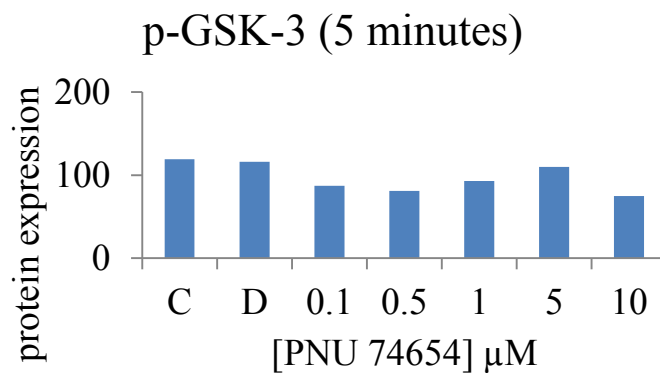
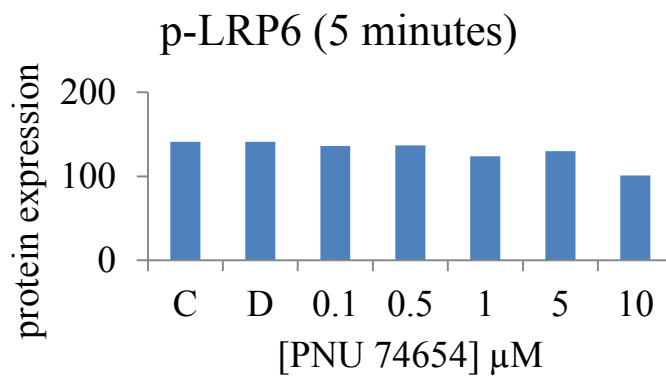


**Figure 5.23**  
**Densitometry data.**

Densitometry data for MCF-7 cells treated with PNU 746654 for 5 minutes are shown. (see figure 5.20). PNU 74654 decreased p-LRP6 and p-GSK-3 expression (by 10 $\mu\text{M}$ ) .

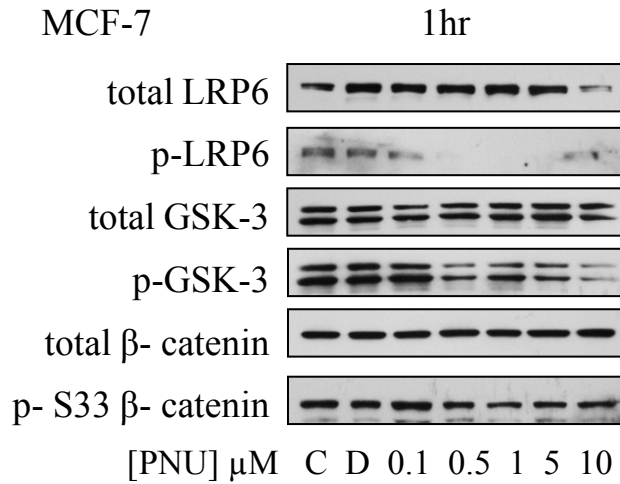


**Figure 5.24**  
**Dose dependent effect of PNU 74654 on GSK-3 $\alpha/\beta$  and  $\beta$ -catenin in MCF-7 cells at 1 hour as determined by Western Blotting.**

C=control D=DMSO (n=1)

MCF-7 cells were cultured to log-phase growth and then treated with PNU 74654 (0 to 10  $\mu$ M concentrations) for 1 hour. The cells were then lysed. SDS-PAGE/ Western blot analyses was carried out using 30  $\mu$ g of total soluble protein and the membranes were probed with antibodies specific to LRP6, p-LRP6, GSK-3 $\alpha/\beta$ , p-GSK-3 $\alpha/\beta$ ,  $\beta$ -catenin and p-S33  $\beta$ -catenin.

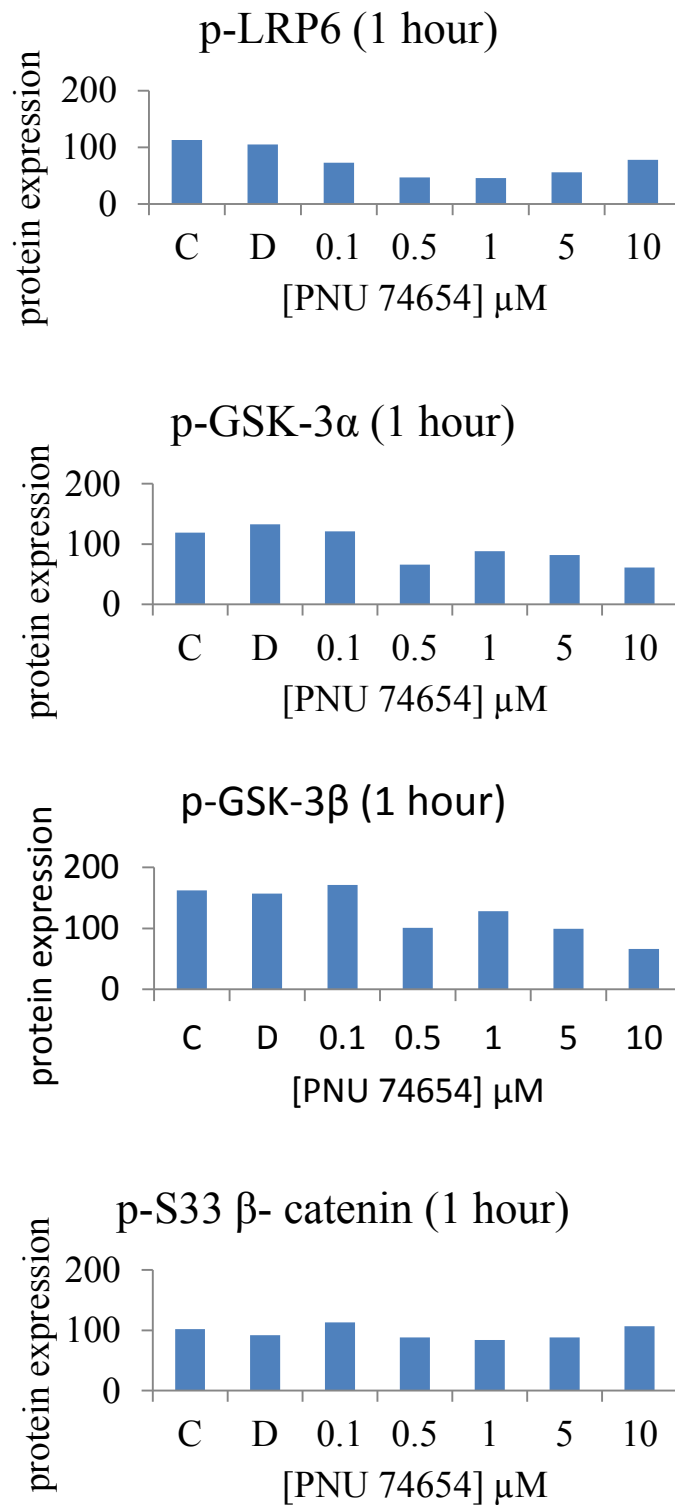


**Figure 5.25**  
**Densitometry data.**

Densitometry data for MCF-7 cells treated with PNU 746654 for 1 hour are shown. (see figure 5.22). PNU 74654 decreased p-LRP6, p-GSK-3 $\alpha$  and p-GSK-3 $\beta$  expression (from 0.5 $\mu$ M) but had no impact on p-S33  $\beta$ -catenin expression.

The process was repeated using Tam-R cells (Figure 5.26, Figure 5.27, Figure 5.28, and Figure 5.29). PNU 74654 decreased p-LRP6 (from 0.5 $\mu$ M) and p-GSK3 expression (from 0.1 $\mu$ M) at 5 minutes; expression of p-GSK3 was decreased at 1 hour (from 0.5 $\mu$ M) as was expression of p- $\beta$ -catenin (S33/37/T41) (from 0.5 $\mu$ M). This supported findings with MCF-7 cells and the suggestion that Wnt inhibition at a nuclear level by PNU 74654 resulted in feedback to upstream components of Wnt signalling.

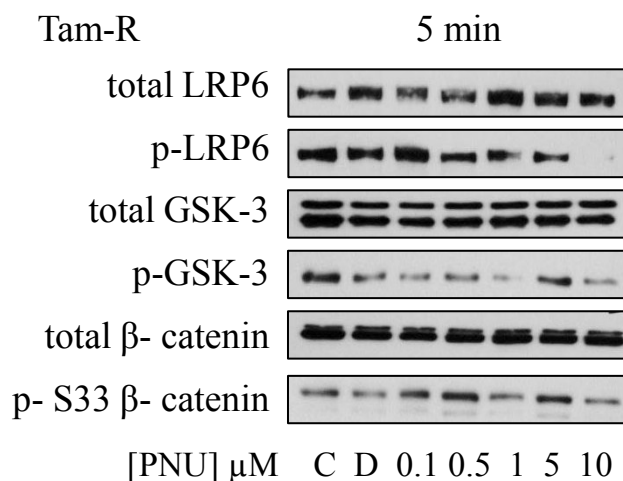


**Figure 5.26**  
**Dose dependent effect of PNU 74654 on GSK-3 $\alpha/\beta$  and  $\beta$ -catenin in Tam-R cells at 5 minutes as determined by Western Blotting.**

C=control D=DMSO (n=1)

Tam-R cells were cultured to log-phase growth and then treated with PNU 74654 (0 to 10  $\mu$ M concentrations) for 5 minutes. The cells were then lysed. SDS-PAGE/ Western blot analyses was carried out using 30  $\mu$ g of total soluble protein and the membranes were probed with antibodies specific to LRP6, p-LRP6, GSK-3 $\alpha/\beta$ , p-GSK-3 $\alpha/\beta$ ,  $\beta$ -catenin and p-S33  $\beta$ -catenin.



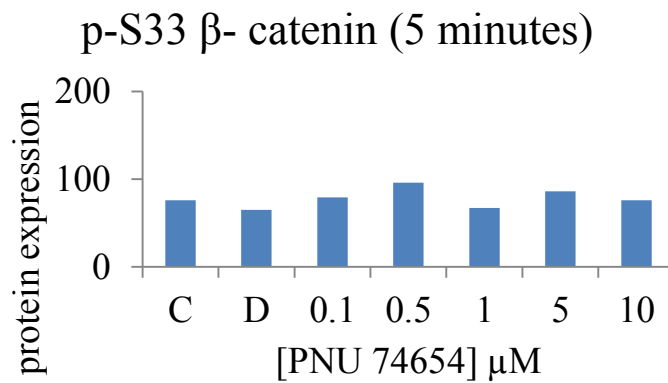
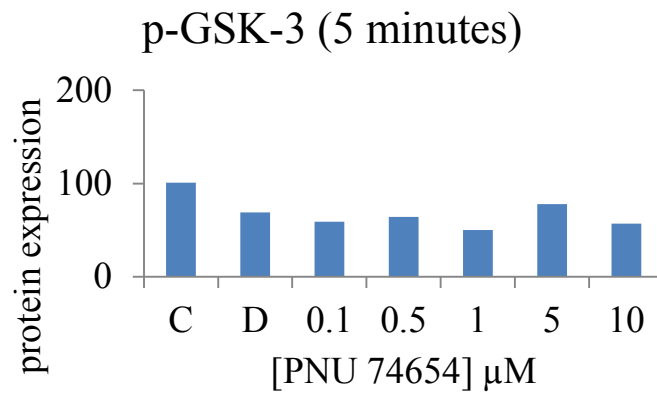
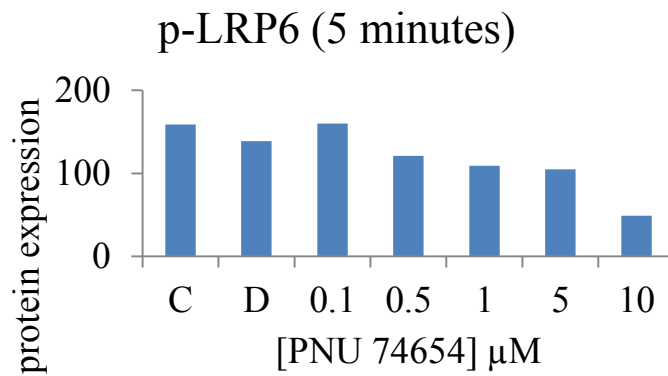


**Figure 5.27**  
**Densitometry data.**

Densitometry data for Tam-R cells treated with PNU 74654 for 5 minutes are shown (see figure). PNU 74654 decreases p-LRP6 and p-GSK-3 expression had no impact on p-S33  $\beta$ -catenin expression.

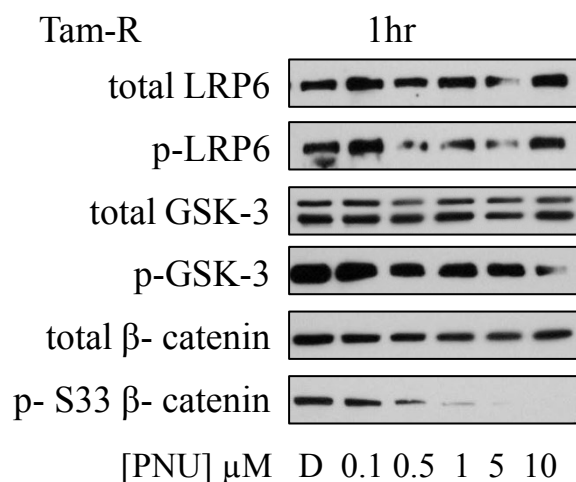


**Figure 5.28**

**Dose dependent effect of PNU 74654 on GSK-3 $\alpha/\beta$  and  $\beta$ - catenin in Tam-R cells at 1 hour as determined by Western Blotting.**

C=control D=DMSO (n=1)

Tam-R cells were cultured to log-phase growth and then treated with PNU 74654 (0 to 10  $\mu$ M concentrations) for 1 hour. The cells were then lysed. SDS-PAGE/ Western blot analyses was carried out using 30  $\mu$ g of total soluble protein and the membranes were probed with antibodies specific to LRP6, p-LRP6, GSK-3 $\alpha/\beta$ , p- GSK-3 $\alpha/\beta$ ,  $\beta$ - catenin and p-S33  $\beta$ -catenin.

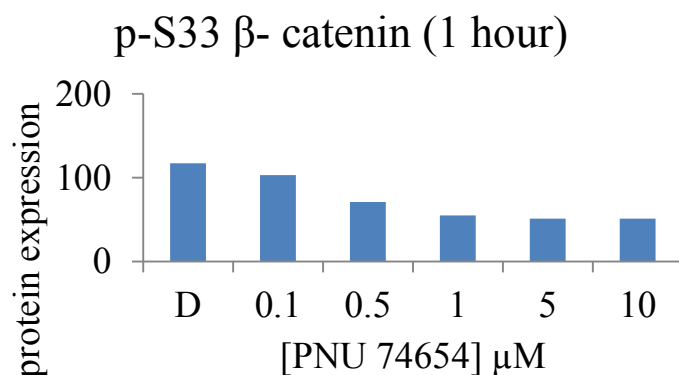
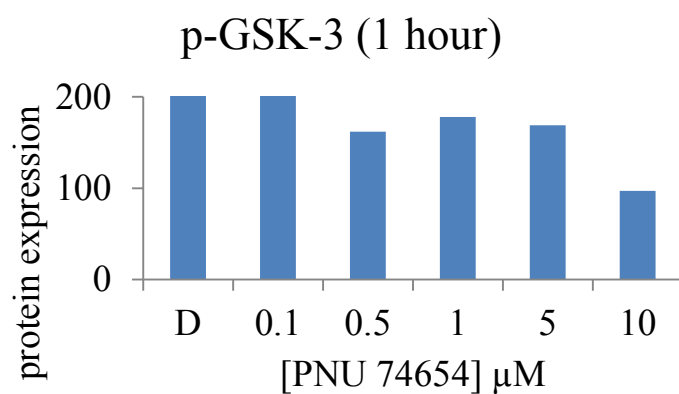
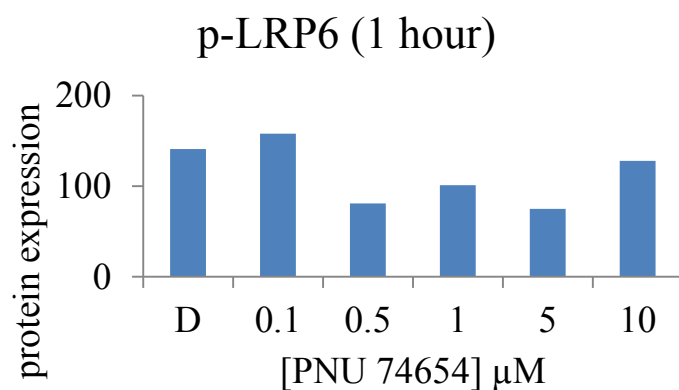


**Figure 5.29**  
**Densitometry data**

Densitometry data for Tam-R cells treated with PNU 746654 for 1 hour are shown. (see figure 5.28). PNU 74654 decreased p-GSK-3 and p-S33  $\beta$ -catenin expression (from 0.5 $\mu\text{M}$ ).

#### **5.2.2.2 Effect of PNU 74654 on growth signalling**

The impact of PNU 74654 on growth signalling was assessed through cyclin D1 and c-myc expression.

Following treatment of MCF-7 cells with PNU 74654, c-myc expression was decreased by 1 hour at 10 $\mu$ M. There was no change in cyclin D1 expression at 5 minutes and 1 hour (Figure 5.30, Figure 5.31).

Tam-R cells treated with PNU 74654 had decreased expression of c-myc at 5 minutes (from 0.1 $\mu$ M) and 1 hour (10 $\mu$ M); cyclin D1 expression fell at the two time points with 10 $\mu$ M (Figure 5.32, Figure 5.33).

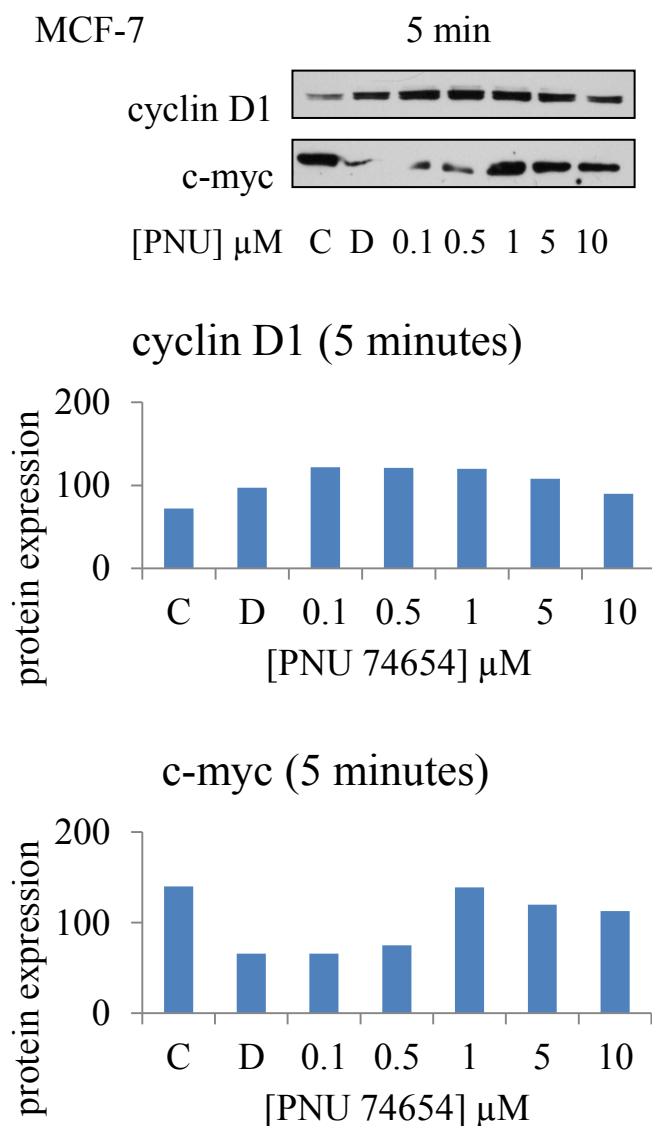


**Figure 5.30**  
**Dose dependent effect of PNU 74654 on cyclin D1 and c-myc in MCF-7 cells at 5 minutes as determined by Western Blotting.**

C=control D=DMSO (n=1)

MCF-7 cells were cultured to log-phase growth and then treated with PNU 74654 (0 to 10  $\mu$ M concentrations) for 1 hour. The cells were then lysed. SDS-PAGE/ Western blot analyses was carried out using 30  $\mu$ g of total soluble protein and the membranes were probed with antibodies specific to cyclin D1 and c-myc. Densitometry data are shown.

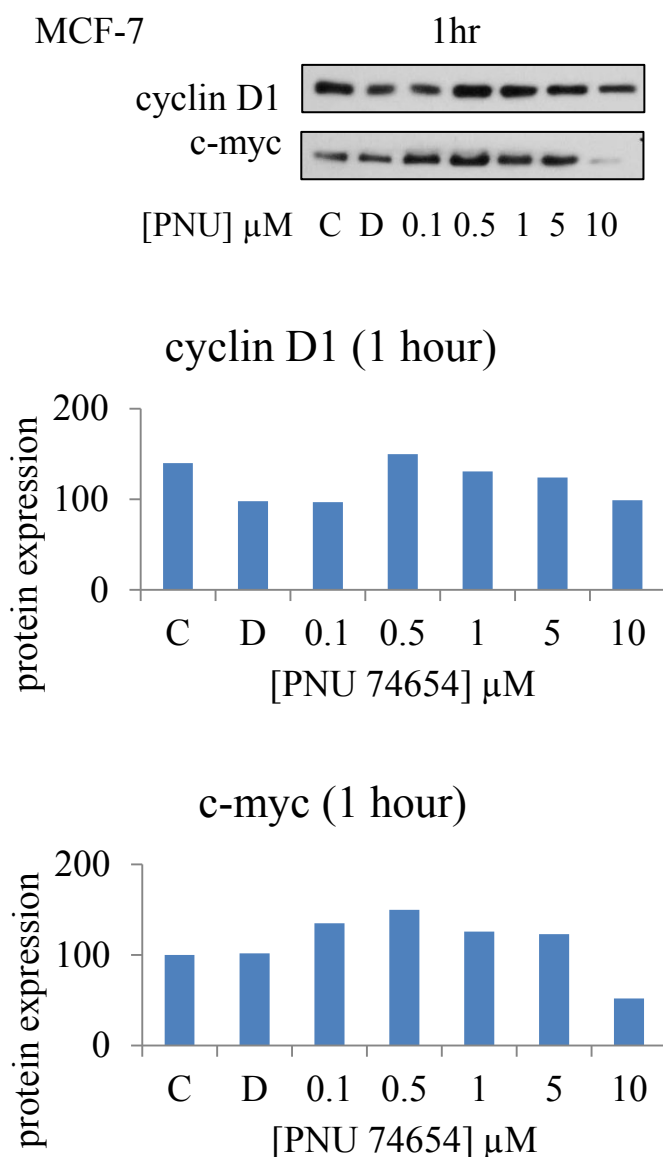


**Figure 5.31**

**Dose dependent effect of PNU 74654 on cyclin D1 and c-myc in MCF-7 cells at 1 hour as determined by Western Blotting.**

C=control D=DMSO (n=1)

MCF-7 cells were cultured to log-phase growth and then treated with PNU 74654 (0 to 10  $\mu$ M concentrations) for 1 hour. The cells were then lysed. SDS-PAGE/ Western blot analyses was carried out using 30  $\mu$ g of total soluble protein and the membranes were probed with antibodies specific to cyclin D1 and c-myc. Densitometry data are shown. PNU 74654 decreased c-myc expression by 1 hour at 10  $\mu$ M.

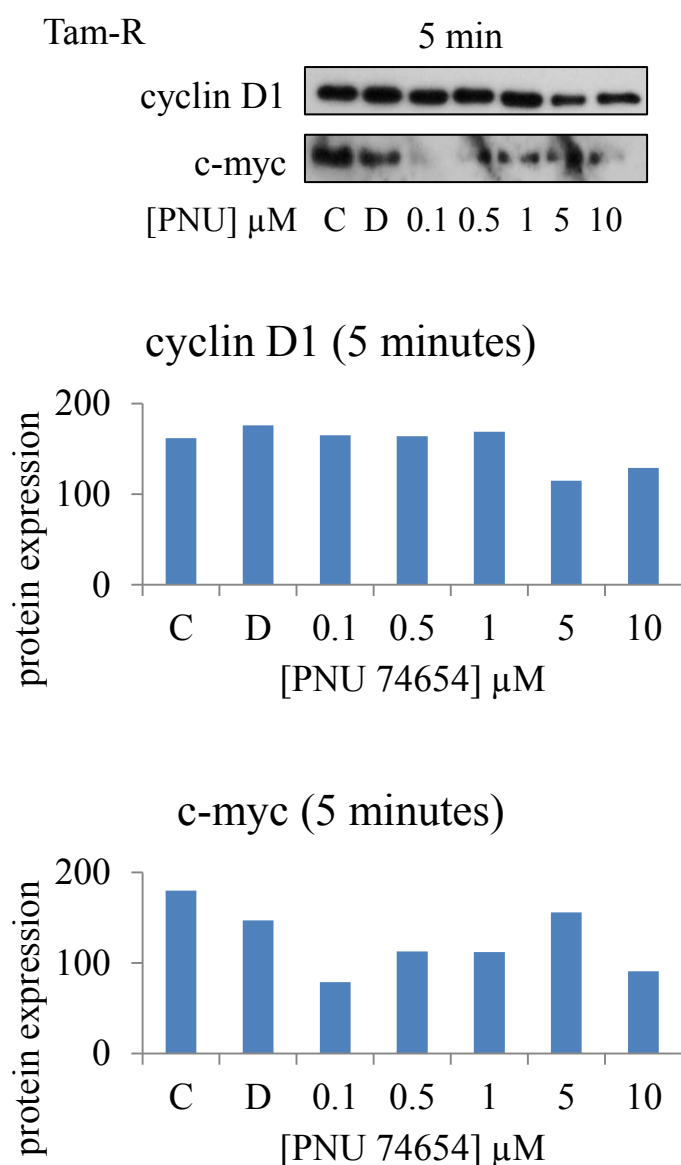


**Figure 5.32**  
**Dose dependent effect of PNU 74654 on cyclin D1 and c-myc in Tam-R cells at 5 minutes as determined by Western Blotting.**

C=control D=DMSO (n=1)

Tam-R cells were cultured to log-phase growth and then treated with PNU 74654 (0 to 10  $\mu$ M concentrations) for 1 hour. The cells were then lysed. SDS-PAGE/ Western blot analyses was carried out using 30  $\mu$ g of total soluble protein and the membranes were probed with antibodies specific to cyclin D1 and c-myc. Densitometry data are shown. PNU 74654 decreased cyclin D1 expression (10  $\mu$ M) and c-myc expression (from 0.1  $\mu$ M) at 5 minutes.

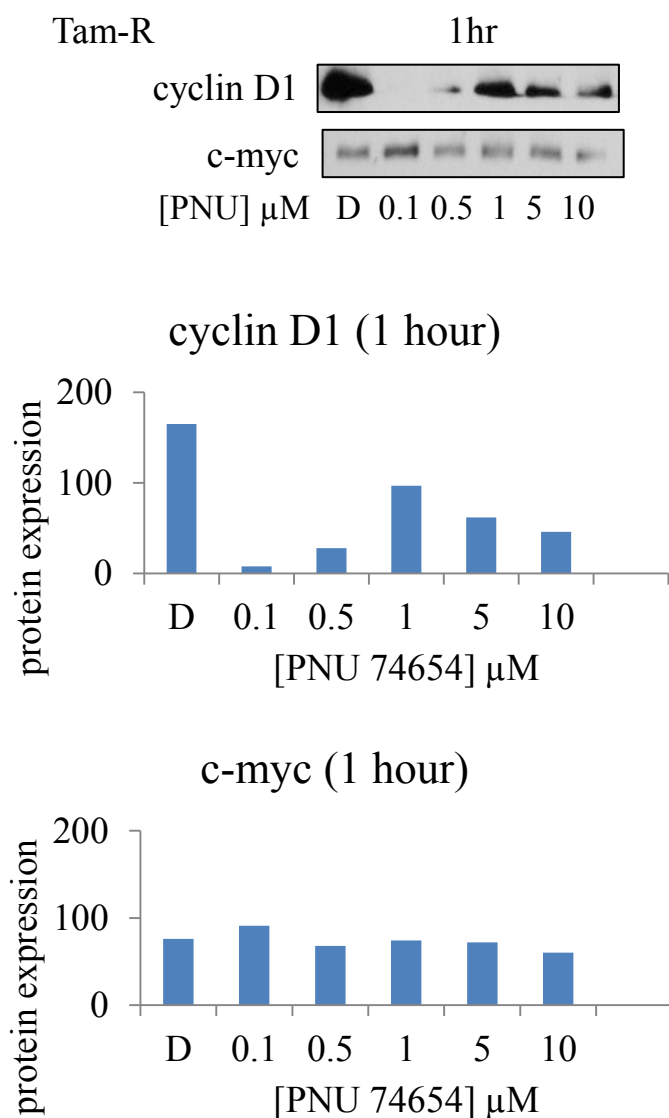


**Figure 5.33**  
**Dose dependent effect of PNU 74654 on cyclin D1 and c-myc in Tam-R cells at 1 hour as determined by Western Blotting.**

C=control D=DMSO (n=1)

Tam-R cells were cultured to log-phase growth and then treated with PNU 74654 (0 to 10  $\mu$ M concentrations) for 1 hour. The cells were then lysed. SDS-PAGE/ Western blot analyses was carried out using 30  $\mu$ g of total soluble protein and the membranes were probed with antibodies specific to cyclin D1 and c-myc. Densitometry data are shown. PNU 74654 decreased cyclin D1 (5  $\mu$ M) and c-myc expression at 1 hour (10  $\mu$ M).



### **5.2.2.3 Additional signalling mechanisms.**

As with IWP2, we looked at src and MAPK activity following treatment with PNU 74654.

When MCF-7 cells were treated with PNU 74654, p-src expression was increased at 5 minutes (from 0.5 $\mu$ M) but there was no consistent change at 1 hour (Figure 5.34, Figure 5.35).

Similarly, when Tam-R cells were treated with PNU 74654, p-src expression was decreased at 5 minutes (from 0.1 $\mu$ M), but there was no change in p-src expression at 1 hour (Figure 5.36, Figure 5.37). There was a decrease in p-MAPK expression (from 0.1 $\mu$ M) following treatment with PNU 74654 for 5 minutes (Figure 5.38).

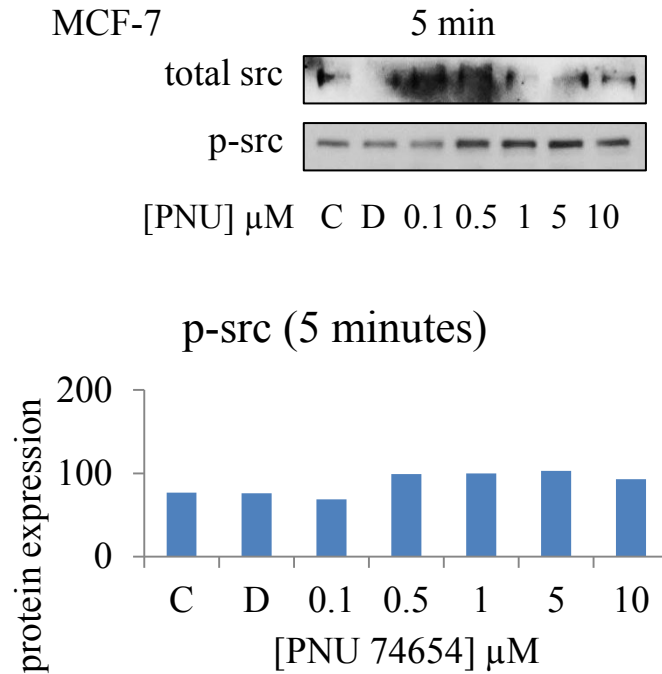


**Figure 5.34**  
**Dose dependent effect of PNU 74654 on src in MCF-7 cells at 5 minutes as determined by Western Blotting.**

C=control D=DMSO (n=1)

MCF-7 cells were cultured to log-phase growth and then treated with PNU 74654 (0 to 10  $\mu$ M concentrations) for 5 minutes. The cells were then lysed. SDS-PAGE/ Western blot analyses was carried out using 30  $\mu$ g of total soluble protein and the membranes were probed with antibodies specific to src and p-src. Densitometry data are shown. PNU 74654 increased p-src expression (0.5  $\mu$ M).

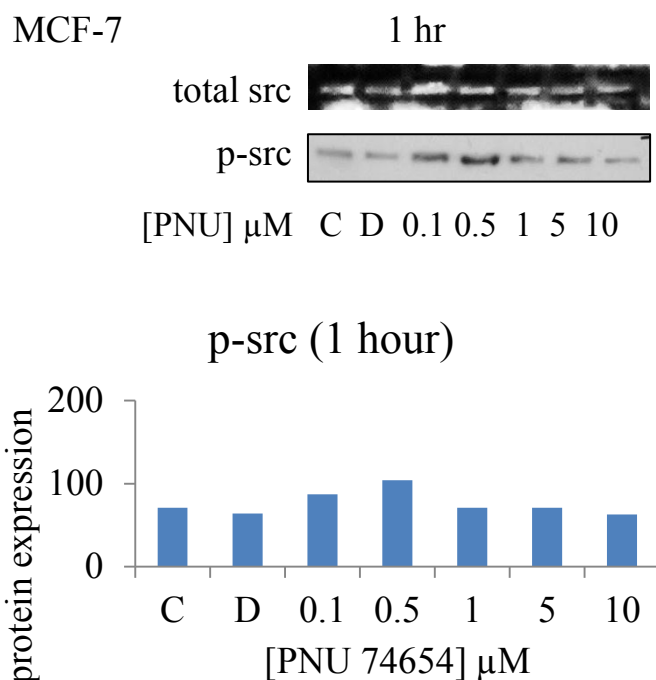


**Figure 5.35**  
**Dose dependent effect of PNU 74654 on src in MCF-7 cells at 1 hour as determined by Western Blotting.**

C=control D=DMSO (n=1)

MCF-7 cells were cultured to log-phase growth and then treated with PNU 74654 (0 to 10  $\mu$ M concentrations) for 1 hour. The cells were then lysed. SDS-PAGE/ Western blot analyses was carried out using 30  $\mu$ g of total soluble protein and the membranes were probed with antibodies specific src and p-src. Densitometry data are shown. There was no consistent change in p-src expression.

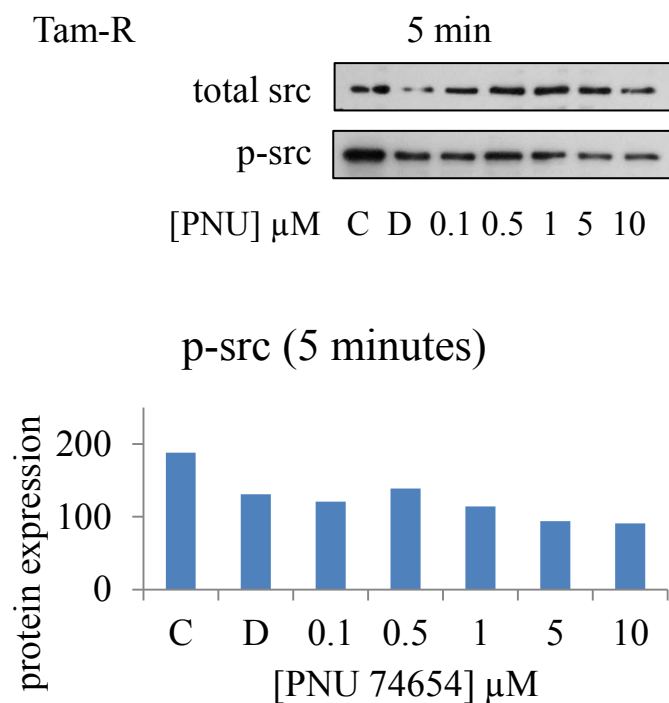


**Figure 5.36**

**Dose dependent effect of PNU 74654 on src in Tam-R cells at 5 minutes as determined by Western Blotting.**

C=control D=DMSO (n=1)

Tam-R cells were cultured to log-phase growth and then treated with PNU 74654 (0 to 10  $\mu$ M concentrations) for 5 minutes. The cells were then lysed. SDS-PAGE/ Western blot analyses was carried out using 30  $\mu$ g of total soluble protein and the membranes were probed with antibodies specific to src and p-src. Densitometry data are shown. PNU 74654 decreased p-src expression.

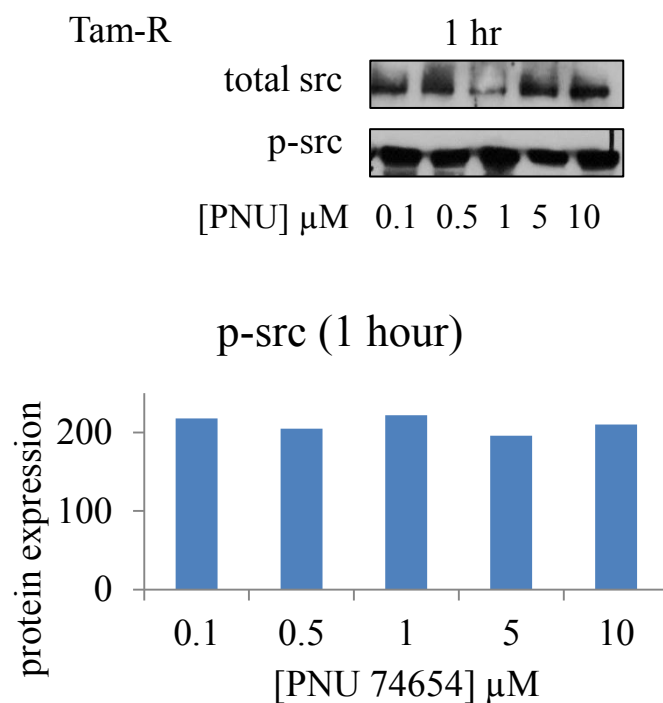


**Figure 5.37**  
**Dose dependent effect of PNU 74654 on src in Tam-R cells at 1 hour as determined by Western Blotting.**

C=control D=DMSO (n=1)

Tam-R cells were cultured to log-phase growth and then treated with PNU 74654 (0 to 10  $\mu\text{M}$  concentrations) for 1 hour. The cells were then lysed. SDS-PAGE/ Western blot analyses was carried out using 30  $\mu\text{g}$  of total soluble protein and the membranes were probed with antibodies specific to src and p-src. Densitometry data are shown.

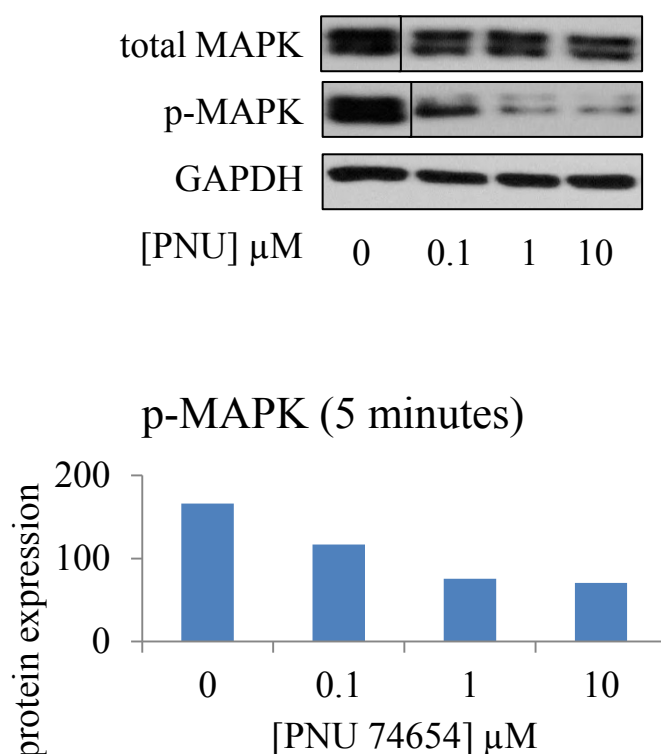


**Figure 5.38**  
**Dose dependent effect of PNU 74654 on MAPK in Tam-R cells at 5 minutes as determined by Western Blotting.**

C=control D=DMSO (n=1)

Tam-R cells were cultured to log-phase growth and then treated with PNU 74654 (0 to 10  $\mu\text{M}$  concentrations) for 5 minutes. The cells were then lysed. SDS-PAGE/ Western blot analyses was carried out using 30  $\mu\text{g}$  of total soluble protein and the membranes were probed with antibodies specific MAPK, p-MAPK and GAPDH. Densitometry data are shown. PNU 74654 decreased p-MAPK expression at 5 minutes (from 0.1  $\mu\text{M}$ ).

### **5.3 Changes in signalling as assessed by PCR**

Western blot analysis had suggested changes in c-myc and cyclin D1 expression when Tam-R cells were treated with IWP2 and PNU 74654 (see section 5.2.1.3 and 5.2.2.2). We set out to explore this further by using semi-quantitative reverse transcription polymerase chain reaction (RT-PCR) over a longer time frame.

Tam-R cells were treated with IWP2 and PNU 74654 for 24 and 72 hours respectively and expression of these gene targets was examined using RT-PCR. Disappointingly, results failed to show a sustained significant change in expression of cyclin D1 or c-myc at 24 and 72 hours (Figure 5.39, Figure 5.40).

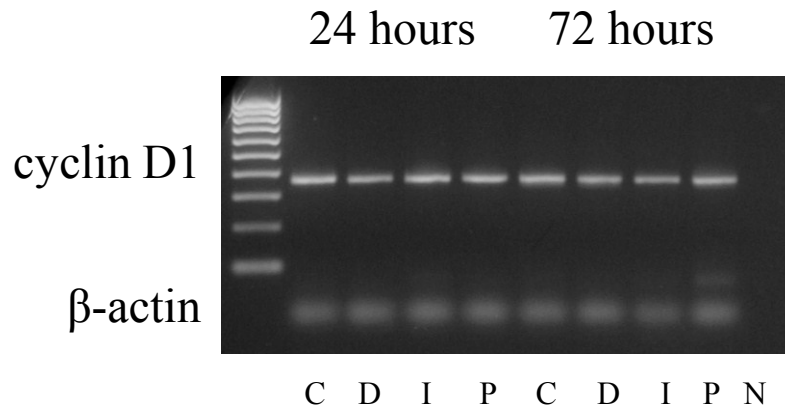


**Figure 5.39**  
**Semi-quantitative reverse transcription polymerase chain reaction for cyclin D1.**

C=control; D=DMSO; I= IWP2 10μM; P=PNU 74654 10μM; N=negative control. (n=1)

Tam-R cells were cultured to log-phase growth and then treated with IWP2, PNU 74654 (10μM concentration) or DMSO for 24 or 72 hours. The cells were then lysed as described in materials and methods section, and semi-quantitative reverse transcription polymerase chain reaction was carried out. Probes for cyclin D1 and β-actin were used. Densitometry data was corrected for β-actin.



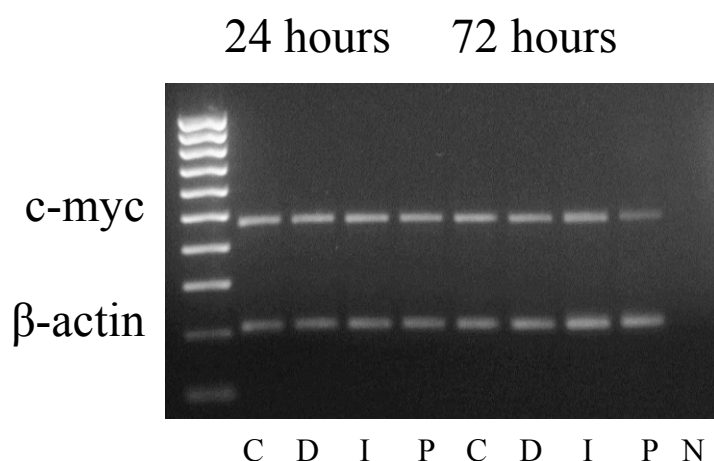


**Figure 5.40**

**Semi-quantitative reverse transcription polymerase chain reaction for c-myc.**

C=control; D=DMSO; I= IWP2 10 $\mu$ M; P=PNU 74654 10 $\mu$ M; N=negative control. (n=2)

Tam-R cells were cultured to log-phase growth and then treated with IWP2, PNU 74654 (10 $\mu$ M concentration) or DMSO for 24 or 72 hours. The cells were then lysed as described in materials and methods section, and semi-quantitative reverse transcription polymerase chain reaction was carried out. Probes for c-myc and  $\beta$ -actin were used. Densitometry data was corrected for  $\beta$ -actin.

## 5.4 PNU 74654 activity

PNU 74654 is reported to inhibit the interaction between  $\beta$ -catenin and TCF4. We used TCF/LEF reporter assays to assess PNU 74654 activity in Tam-R cells.

TCF/ LEF (luciferase) reporter assays were done as described in materials and methods section, and Tam-R cells were treated with PNU 74654 and combination LiCl- PNU 74654 treatments. Results were normalised to internal control. Transfection efficacy was about 35% as assessed by GFP coupled to Renilla (Figure 5.41).

There was no corresponding drop in luciferase expression when Tam-R cells were treated with PNU 74654 (Figure 5.42). There was an increase in luciferase activity suggesting an activation of Wnt signalling by PNU 74654. The experiment was repeated using combination LiCl- PNU 74654 in an attempt to stimulate Wnt activity prior to PNU 74654 impact on Tam-R cells: again there was no significant drop in luciferase activity by PNU 74654 compared to LiCl control (Figure 5.43).

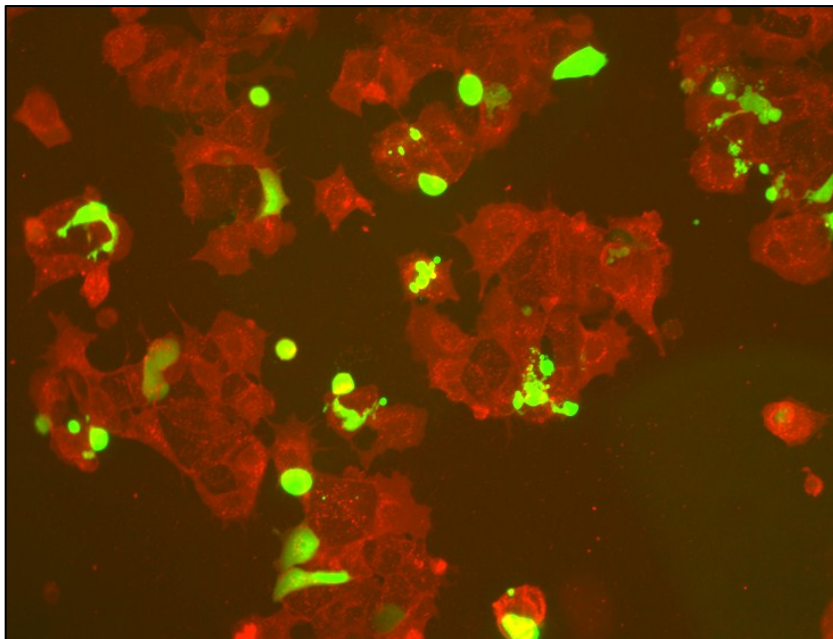


**Figure 5.41**  
**Tam-R cells following reporter assay transfection.**

Reporter assay (TCF/LEF) was done in Tam-R cells as described in materials and methods section. Representative image of Tam-R cells was captured using fluorescent microscopy at 20x magnification. Green dye show cells which have taken up the green fluorescent protein (GFP). Non-transfected cells were counterstained red with Dil cell labelling solution.

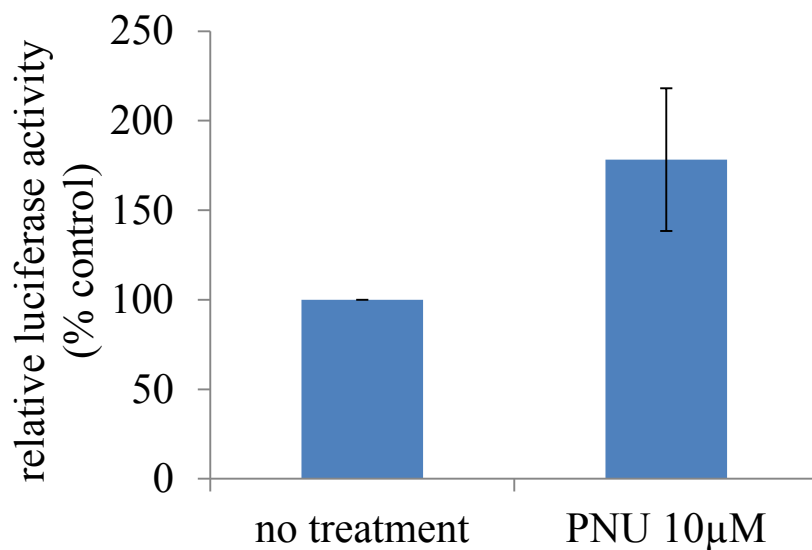


**Figure 5.42**  
**TCF/LEF reporter assay for Tam-R cells treated with PNU 74654.**

TCF/LEF reporter assay was done as described in materials and methods section, and Tam-R cells were treated with PNU 74654 (0 and 10 $\mu$ M concentrations). Luciferase activities are expressed as fold stimulation and are related to respective reporter activities obtained with control vector plasmid. Error bars show SD (n=2).

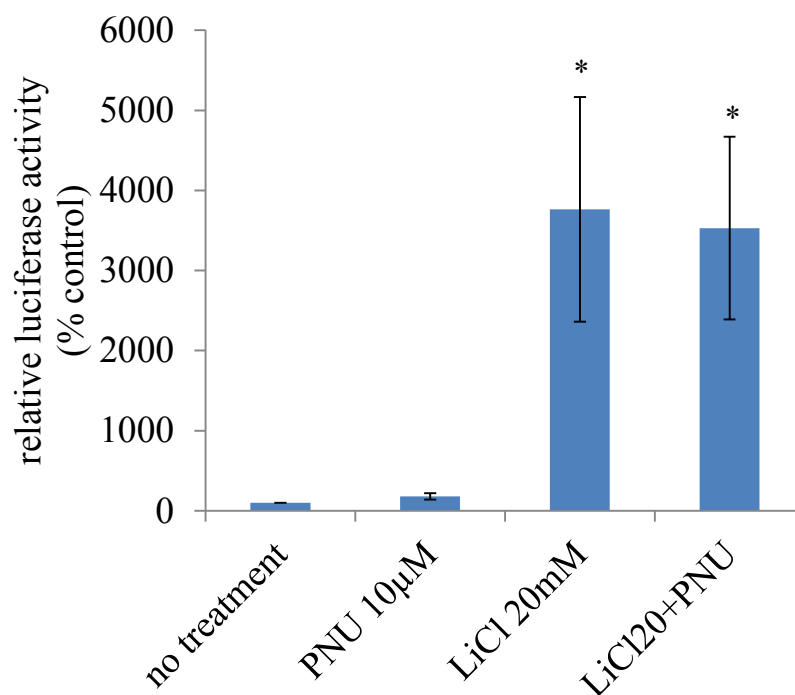


**Figure 5.43**  
**TCF/LEF reporter assay for Tam-R cells treated with LiCl and PNU 74654.**

TCF/LEF reporter assay was done as described in materials and methods section, and Tam-R cells were treated with LiCl (0 and 20mM concentrations), PNU 74654 10μM and combination treatments. Luciferase activities are expressed as fold stimulation and are related to respective reporter activities obtained with control vector plasmid.

Error bars show SD (n=3).

\* changes were significant compared to no treatment arm (<0.05) as determined by post hoc Dunnett t-test.

## **5.5 Further Wnt signalling inhibition studies**

Work done on IWP2 and PNU 74654 was encouraging and supported the role for Wnt signalling in endocrine resistance. However PNU 74654 activity was difficult to interpret. It was disappointing that the reporter assay activity in Tam-R cells treated with PNU 74654 did not support published data (Trosset et al. 2006). Further signalling modulation was thus done by using another Wnt inhibitor acting at nuclear level of the pathway: iCRT14.

### **5.5.1 iCRT14**

iCRT14 is a commercially available inhibitor which inhibits the  $\beta$ -catenin-responsive element (CRT). It is thought to influence the interaction between  $\beta$ -catenin and TCF4 possibly by binding to  $\beta$ -catenin. TCF and E-cadherin bind to overlapping sites on  $\beta$ -catenin (Bienz and Clevers 2003) (Figure 5.44). Gonsavales et al. (2011) showed that the interactions between E-cadherin,  $\alpha$ -catenin and  $\beta$ -catenin were not affected by iCRT14, thus showing specificity of drug activity.

The aims were:

- to establish activity of iCRT14 using reporter assays
- to further investigate functional activity of Wnt inhibition by looking at the effect of iCRT14 on growth and migration.

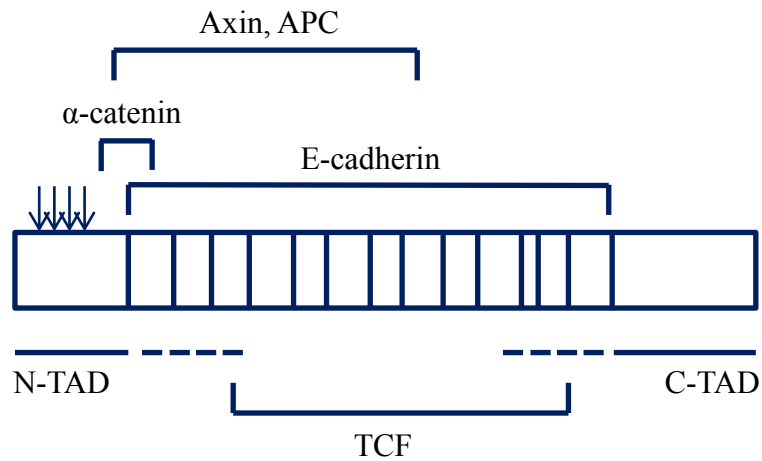


**Figure 5.44**  
**Diagram showing structure of  $\beta$ -catenin (adapted from Bienz and Clevers (2003)).**

Phosphorylation sites for GSK3 and CKI phosphorylation sites (small arrows) are found at the N terminus and are required for proteasome-mediated destruction; the C-terminal domain is required for signalling. Binding sites on  $\beta$ -catenin for cytoplasmic APC, Axin,  $\alpha$ -catenin and E-Cadherin and nuclear TCF are overlapping.

TAD: transcriptional activation domains

#### **5.5.1.1 iCRT14 activity**

Tam-R cells were treated with LiCl (20mM) or combination LiCl (20mM) and iCRT14 (6.25 $\mu$ M) and TCF/ LEF (luciferase) reporter assays were done as described in materials and methods section 2.11. Luciferase activity was expressed as fold stimulation and was related to respective reporter activity obtained with control vector plasmid. When Tam-R cells were treated with LiCl there was increased TCF/LEF activity (expressed by increased luciferase activity); treatment of Tam-R cells with combination LiCl - iCRT14 decreases this activity (Figure 5.45). This supports modulation of Wnt signalling at the nuclear level by iCRT14. Transfection efficacy was about 30% as determined by GFP coupled to Renilla (similar to Figure 5.41).



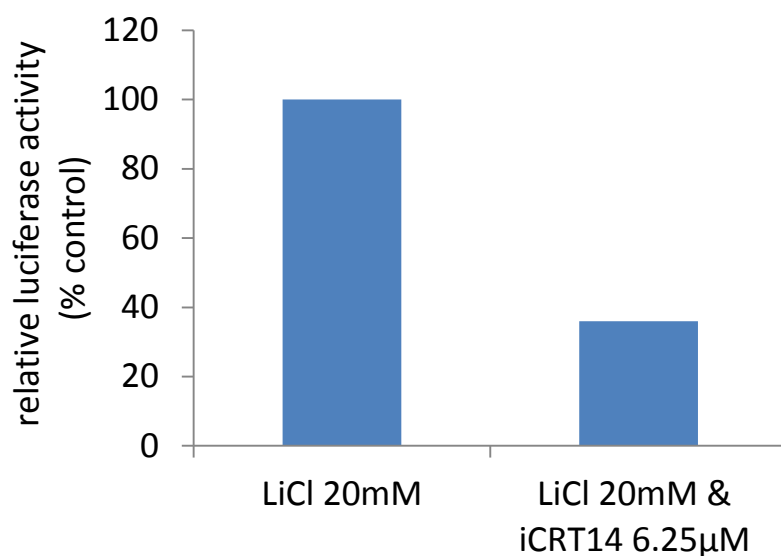


**Figure 5.45**  
**Effects of LiCl and iCRT14 on Wnt signalling transduction pathways in Tam-R cells as determined by TCF/LEF reporter assay.**

TCF/LEF reporter assay for Tam-R cells treated with LiCl (20mM) and iCRT14 (6.25µM). Activities are expressed as fold stimulation and are related to respective reporter activities obtained with control vector plasmid. LiCl stimulates TCF/LEF activity and iCRT14 reduces this activity in the presence of LiCl (n=1).

### **5.5.1.2 Effects of iCRT14 on cell growth**

Having established iCRT14 activity, we wanted to explore its effect on cell growth and proliferation. Cell growth was assessed by MTT assays and cellular proliferation was assessed by ICC through Ki-67 staining.

#### **5.5.1.2.1 MTT assays**

iCRT14 had a differential growth inhibitory effect in MCF-7 cells and Tam-R cell lines as assessed by MTT assays. Growth after treatment with inhibitor for 6 days was reduced by more than half in Tam-R cells, but there was no corresponding drop in MCF-7 cells (Figure 5.46).

Dose effects of iCRT14 on growth of MCF-7 and Tam-R cell lines were determined by MTT assays. Cells were treated with iCRT14 (0- 25 $\mu$ M concentrations) for 6 days. Growth inhibition was greater in Tam-R cells compared to MCF-7 cells (Figure 5.47).

Using data from growth assays, the half maximal inhibitory concentration (IC<sub>50</sub>) for iCRT14 was determined by interpolation (see section 2.6.3). IC<sub>50</sub> for iCRT14 in Tam-R cells was 5.5 $\mu$ M and IC<sub>50</sub> in MCF-7 cells was 23 $\mu$ M (Figure 5.48).

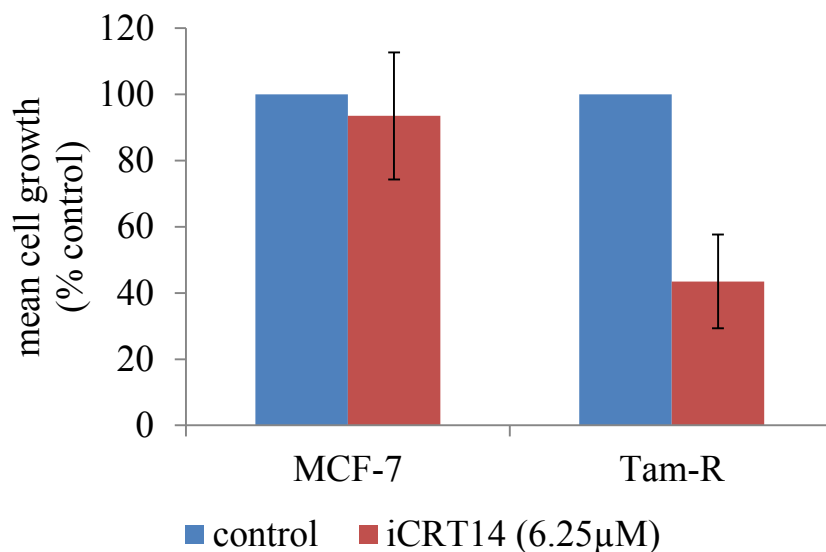


**Figure 5.46**  
**Effects of iCRT14 (6 days) on growth of MCF-7 and Tam-R cells as determined by MTT assay.**

MTT assay was done as described in materials and methods section using MCF-7 and Tam-R cells treated with iCRT14 (control and 6.25 μM concentrations) for 6 days. Error bars show SD for n=2, 16 samples. Growth suppression by iCRT14 is greater in Tam-R than in MCF-7 cells.

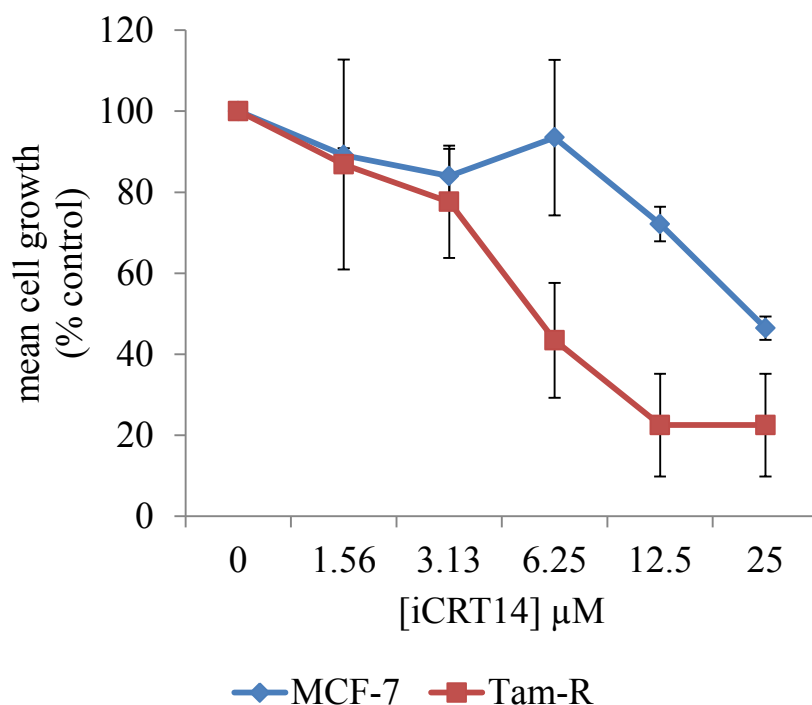


**Figure 5.47**  
**Effects of iCRT14 (6 days) on growth of MCF-7 and Tam-R cells as determined by MTT assay.**

MTT assays using MCF-7 and Tam-R cells treated with iCRT14 (0- 25 $\mu\text{M}$  concentrations) for 6 days were done as described in materials and methods section. Tam-R cells were more sensitive to growth inhibition than MCF-7 cells. Error bars show SD (n=3, 24 samples).

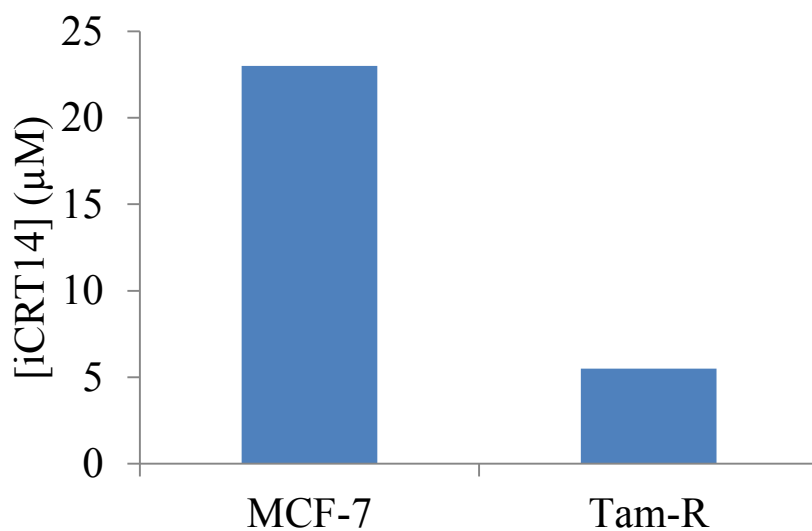


**Figure 5.48**  
**The half maximal inhibitory concentration for**  
**MCF-7 and Tam-R cells treated with iCRT14.**

The half maximal inhibitory concentration (IC<sub>50</sub>) for iCRT14 in MCF-7 and Tam-R cells was determined by interpolation from cell growth data.

#### **5.5.1.2.2 Effects of iCRT14 on cellular proliferation.**

Next we explored the effects of iCRT14 on cellular proliferation. MCF-7 and Tam-R cells were treated with iCRT14 6.35 $\mu$ M for 3 days and then stained for Ki-67 as described in the materials and methods section. There was about 40% decreased percentage positive staining in Tam-R cells compared to MCF-7 following iCRT14 treatment (Figure 5.49, Figure 5.50). This is coupled by weaker nuclear staining.

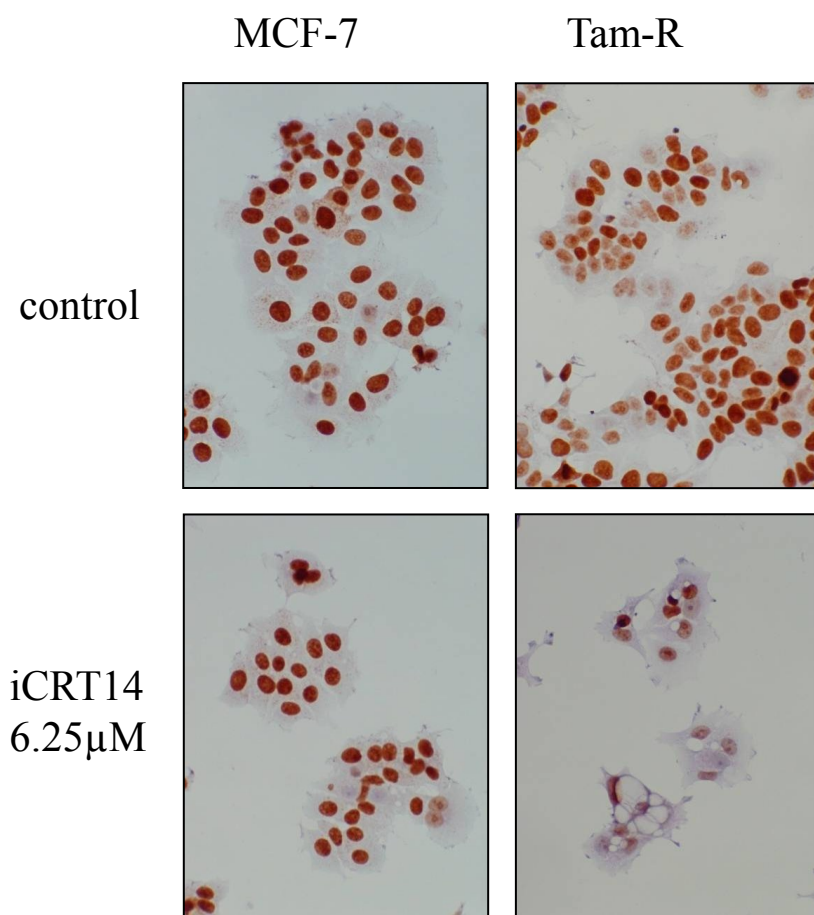


**Figure 5.49**  
**Effects of iCRT14 treatment on proliferation of MCF-7 and Tam-R cells as determined by Ki-67 antigen staining.**

MCF-7 and Tam-R cells were treated with iCRT14 6.25 $\mu$ M for 3 days as described in the methods section. Cellular proliferation was assessed by staining for Ki-67 antigen. Representative images of cells were captured using a light microscopy at 20x magnification (n=2).

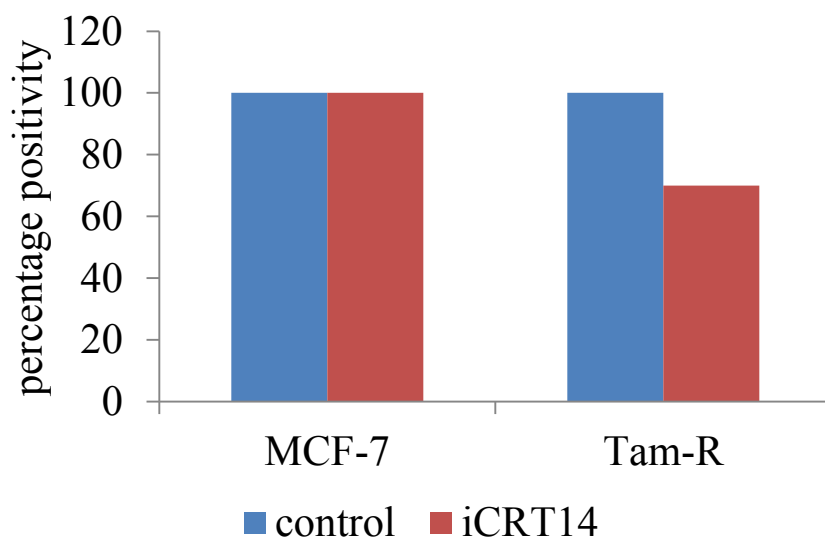


**Figure 5.50**  
**Percentage positivity for Ki67 antigen staining in**  
**MCF-7 and Tam-R cells.**

Percentage positivity for Ki67 staining in MCF-7 and Tam-R cells treated with iCRT14 (0 or 6.25 $\mu$ M). (see Figure 5.49).



#### **5.5.1.3 iCRT14 inhibits cell migration in Tam-R cells**

Migratory capacity of Tam-R cells following treatment with iCRT14 was assessed using *in vitro* migration assays. For quantification, the number of migratory cells in 5 random fields of view were counted using a light microscope and presented as % of Tam-R control. Treatment with iCRT14 significantly reduced migration of Tam-R cells ( $p < 0.001$ ) (Figure 5.51).

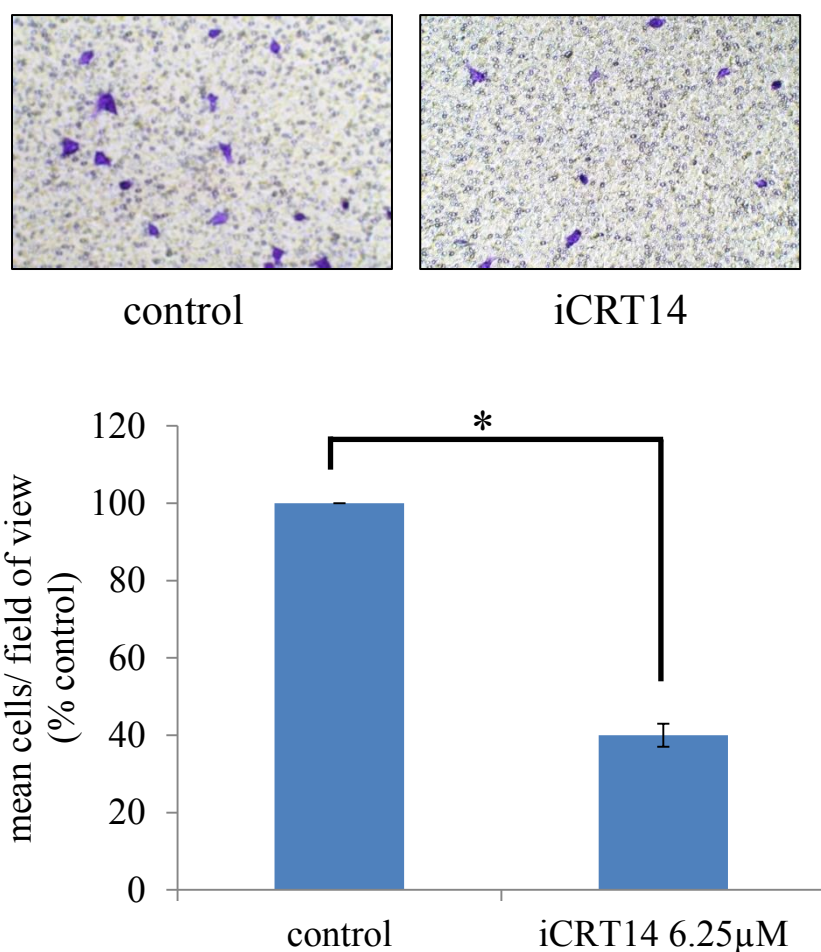


**Figure 5.51**  
**Effects of iCRT14 on migration in Tam-R cells as determined by cell migration assay at 24 hours.**

Migratory capacity of Tam-R following treatment with iCRT14 was assessed using *in vitro* migration assays. Representative images of migratory cells were captured using a light microscopy at 20x magnification. Cells are stained purple with crystal violet. For quantification, the number of migratory cells in 5 random fields of view were counted using a light microscope and presented as % of Tam-R control. Error bars show SD for n=3 (p< 0.001).

## 5.6 Summary for Wnt inhibition

### 5.6.1 Activity of Wnt inhibitors

- IWP2 is reported to inhibit phosphorylation of p-LRP6 (Chen et al. 2009). This was demonstrated for both MCF-7 and Tam-R cells (Figure 5.8). Phosphorylation of LRP6 was taken as internal control for proof of drug activity in further experiments.
- PNU 74654 is reported to bind to  $\beta$ -catenin and inhibit the interaction between  $\beta$ -catenin and (TCF4). Our experiments have failed to show consistent modulation of  $\beta$ -catenin or transcriptional activity (as assessed by Western blotting, PCR and TCF/LEF (luciferase) reporter assay). As described previously, changes in protein expression for  $\beta$ -catenin as determined by Western blotting can be difficult to demonstrate in cells having a high baseline expression of  $\beta$ -catenin (see Chapter 4). Western blotting experiments showed a decrease in c-myc and cyclin D1 expression when Tam-R cells were treated with PNU 74654 for 1 hour (Figure 5.33); but these results were not reproducible with RT-PCR (Figure 5.39, Figure 5.40). Cyclin D1 and c-myc expression are not exclusive to Wnt signalling modulation and this may explain why we failed to show a change in transcription for both IWP2 and PNU 74654. Leproucelet et al. (2004) analysed a number of compounds which inhibit  $\beta$ -catenin and TCF interaction. Interestingly, they report a selective inhibition of c-myc and cyclin D1 by different compounds and one compound did not show inhibition

of either target. They also failed to show a reduction in cellular levels of  $\beta$ -catenin by Western Blot analysis. This selectivity may explain why IWP2 and PNU 74654 failed to reduce expression of c-myc and cyclin D1 by RT-PCR.

TCF/LEF (luciferase) assays failed to confirm PNU 74654 activity (Figure 5.42, Figure 5.43). Initial drug characterisation experiments with this drug suggested a dose dependent effect of the drug on Tam-R cell growth, with lower concentrations having a stimulatory effect (Figure 5.5). The reporter assay process involves addition of RNA material to the cell. One possible explanation is that this results in a dilution of PNU 74654 concentrations relative to  $\beta$ -catenin/TCF binding site. This could be further explored by dose response reporter activity. Another explanation may be a differential effect of PNU 74654 on different cell lines. This could be further investigated by repeating reporter assays with human colorectal adenocarcinoma cell lines (e.g. SW480 [APC mutation] or HCT116 [Ser45-mutant  $\beta$ -catenin]).

- iCRT14 is reported to inhibit the  $\beta$ -catenin- responsive element (CRT). It is thought to influence the interaction between  $\beta$ -catenin and TCF4. TCF/LEF (luciferase) reporter assays showed decreased activity following treatment with iCRT14 (Figure 5.45). Regretably the reporter assay experiments could only be performed once. Repeat experiments will help confirm iCRT14 activity.

### **5.6.2 Effect of Wnt inhibitors on cell signalling**

Signalling experiments were only done once and data cannot be confirmed to be a true reflection of IWP2 and PNU 74654 activity. Effects of iCRT14 on cell signalling were not explored due to time constraints and this is scope for future work.

Western blotting experiments were challenging. We noted that baseline expression of signalling components such as GSK-  $3\alpha/\beta$ , p-GSK-  $3\alpha/\beta$ , LRP6, p-LRP6, p- $\beta$ -catenin (S33/37/T41), src and p-src in MCF-7 and Tam-R cells was not always consistent among controls. Immunoblotting for  $\beta$ - actin was particularly troublesome.

Treatments were given for 5 minutes or 1 hour. Wnt activation can occur quickly though exact time schedules are difficult to determine and can vary between different cell lines. Compensatory mechanisms complicate interpretation of results for longer time schedules.

Whilst signalling changes could reflect a hierarchical relationship with the Wnt pathway, it more probably revealed inherent variability of individual blots. This would be explored by further experiments. The general changes following treatment of MCF-7 and Tam-R cells with IWP2 and PNU 74654 are summarised in Table 5.1 and Table 5.2.

[10μM]	IWP2-MCF-7	IWP2-MCF-7	IWP2-Tam-R	IWP2-Tam-R
	5 minutes	1 hour	5 minutes	1 hour
<b>Wnt signalling</b>				
p-LRP6	decreased		decreased	
p-GSK- 3α/β	NC	decreased	NC	decreased
p- β- catenin (S33/37/T41)	NC	NC	decreased	NC
<b>growth signalling</b>				
cyclin D1	NC	decreased	decreased	NC
c- myc	decreased	increased	decreased	increased
<b>other signalling</b>				
p-src	decreased	increased	decreased	increased
p-MAPK			decreased	

**Table 5.1**

Summary of signalling changes in MCF-7 and Tam-R cells following treatment with IWP2 (10μM) for 5 minutes and 1 hour as determined by Western blotting. green= decreased protein expression; pink= increased protein expression; NC= no change.

Decreased Wnt activity following treatment with IWP2 is supported by decreased expression of p-LRP6. Changes in cyclin D1 and c-myc expression at 5 minutes cannot as yet be explained. Decreased p-MAPK expression in Tam-R cells supports findings in growth and migration assays.

[10 $\mu$ M]	PNU-MCF-7	PNU-MCF-7	PNU-Tam-R	PNU-Tam-R
	5 minutes	1 hour	5 minutes	1 hour
<b>Wnt signalling</b>				
p-LRP6	decreased	decreased	decreased	NC
p-GSK- 3 $\alpha$ / $\beta$	decreased	decreased	decreased	decreased
p- $\beta$ - catenin (S33/37/T41)	decreased	increased	NC	decreased
<b>growth signalling</b>				
cyclin D1	NC	NC	decreased	decreased
c- myc	decreased	decreased	decreased	decreased
<b>other signalling</b>				
p-src	increased	NC	decreased	NC
p-MAPK			decreased	

**Table 5.2**

Summary of signalling changes in MCF-7 and Tam-R cells following treatment with PNU 74654 (10 $\mu$ M) for 5 minutes and 1 hour as determined by Western blotting. green= decreased protein expression; pink= increased protein expression; NC= no change.

PNU 74654 acts in the nucleus. Surprisingly there appears to be feedback to components higher up in the signalling pathway and Wnt inhibition is supported by decreased expression of p-LRP6, cyclin D1 and c-myc. Decreased p-MAPK expression in Tam-R cells supports findings in growth and migration assays.

### **5.6.3 Targeting different levels of Wnt signalling pathway has the same effect on cell function**

Wnt signalling can be targeted at different levels with similar effect. Differential growth and migration were observed in MCF-7 and Tam-R cells after treatment with IWP2, PNU 74654 and iCRT14, with Tam-R cells being more sensitive to Wnt inhibition than MCF-7 cells. In the seminal paper by Hanahan and Weinberg (2000) on the hallmarks of cancer, growth and migration are two major features of cancer cells. This highlights the potential clinical benefit for use of Wnt inhibitors in this setting.

Cell growth for IWP2 and PNU 74654 was assessed using MTT and cell counting assays (Figure 5.1, Figure 5.2). Each experiment was carried out twice, but results from MTT and cell counting assays were complementary. There are no models for direct comparison of the two growth assays. In cell counting assays, the final cellular concentration exceeded seeding density, suggesting that IWP2 and PNU 74654 had a cytostatic rather than a cytotoxic effect. We noted that cell counting assays were particularly challenging as drug treatment seemed to affect cell viscosity. We were worried about reproducibility of these results and further growth assays were done using MTT assays. Tamoxifen did not appear to affect activity of IWP2 or PNU74654. When Tam-R cells were deprived of tamoxifen and treated with the two inhibitors, a similar pattern of growth inhibition was observed. Cell growth inhibition was significant in Tam-R cells treated with iCRT14 ( $p < 0.001$ ) as assessed by MTT assays (Figure 5.46). Cellular proliferation was also reduced in Tam-R cells following treatment with iCRT14 and this was reflected in the percentage positivity (Figure 5.49, Figure 4.50).



IWP2, PNU 74654 and iCRT14 all inhibited cell migration in Tam-R cells. Results were statistically significant at  $<0.05$  (Figure 5.7, Figure 5.51). The effects on cell migration could also occur via cell growth inhibition. However migration was assessed at 24 hours and growth inhibition/ cell viability was assessed at 6 days. The data supports suppression of cell migratory capacity following treatment with Wnt inhibitors.

## Chapter 6

Exploration of Wnt and EGFR signalling pathway  
interplay in tamoxifen resistant breast cancer cells

## **6 Exploration of Wnt and EGFR signalling pathway interplay in tamoxifen resistant breast cancer cells**

The Wnt signalling pathway is known to interact with a number of other pathways including those mediated by growth factors, the resultant effect of which may be receptor transactivation and/or elevated activity of downstream signalling elements (Goss K 2011). In breast cancer, there is evidence of cross talk between Wnt and the human epidermal growth factor receptor (EGFR) pathway. This is of particular interest in the context of tamoxifen resistance, as EGFR activity is known to be upregulated in Tam-R cells (Hutcheson et al. 2006) and also clinical material from tamoxifen resistant tumours (Gee et al. 2005). In this chapter, we wished to determine whether crosstalk between the EGFR and Wnt pathways represented a mechanism for increased Wnt activity in Tam-R cells.

### **6.1 Effect of dual EGFR and Wnt pathway inhibition on cell growth**

All three Wnt inhibitors (IWP2, PNU 74654 and iCRT14) had shown significant effects on Tam-R cell growth (see Figure 5.1, Figure 5.44). However we were unable to reliably determine the effect of PNU 74654 on Wnt signalling. IWP2 and iCRT14 were therefore used for further experiments. Gefitinib (an EGFR kinase inhibitor and kind gift from Astra Zeneca, UK) was used to inhibit EGFR signalling and will subsequently be referred to as TKI.

MCF-7 and Tam-R cells were exposed to IWP (10 $\mu$ M) and TKI (1 $\mu$ M) as monotherapies and as combined agents and cellular growth determined by MTT

assay (Figure 6.1). IWP2, TKI and TKI – IWP2 treatments all significantly reduced Tam-R cell growth. There was a significant further growth inhibition for TKI when IWP2 was compared to TKI, and between IWP2 and TKI- IWP2, but the difference between TKI and TKI – IWP2 was not significant. The findings support an additive rather than a synergistic effect.

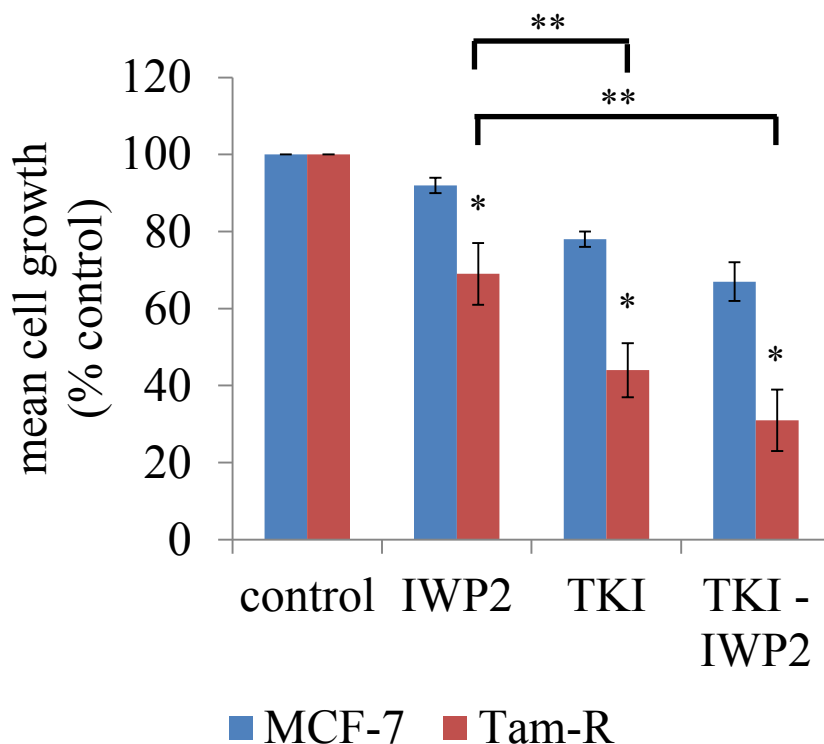


**Figure 6.1**  
**Effects of IWP2 and EGFR tyrosine kinase inhibition (TKI/ gefitinib) on growth of MCF-7 and Tam-R cells as determined by MTT assay.**

MCF-7 and Tam-R cells were treated with IWP2 (10 $\mu$ M), TKI (1 $\mu$ M) or combination TKI - IWP2 treatments for 3 days. Inhibition of cell growth was assessed using MTT assays as described in the materials section. IWP2 and TKI both inhibit cell growth. Tam-R cells were more sensitive to inhibition than MCF-7 cells.

Error bars show SD for n=3 experiments. \*test was significant compared to untreated control by post hoc statistical analysis. Other significant comparisons in Tam-R cells were IWP2 compared to IWP2 – TKI and TKI compared to IWP2 (\*\*).

MCF-7 and Tam-R cells were treated with iCRT14 (6.25 $\mu$ M), TKI (1 $\mu$ M) or combination TKI – iCRT14 (Figure 6.2). Again, Tam-R cells were more sensitive to single and dual inhibition than MCF-7 cells. In MCF-7 cells, TKI and TKI – iCRT14 treatments had a significant effect on cell growth. For Tam-R cells, all three treatment arms were significant. Combined inhibition of Wnt and EGFR resulted in a greater suppression of cell proliferation versus inhibition of each of these pathways alone (iCRT14 alone versus TKI – iCRT14 and TKI versus TKI – iCRT14) in Tam-R cells. The findings support a synergistic effect.

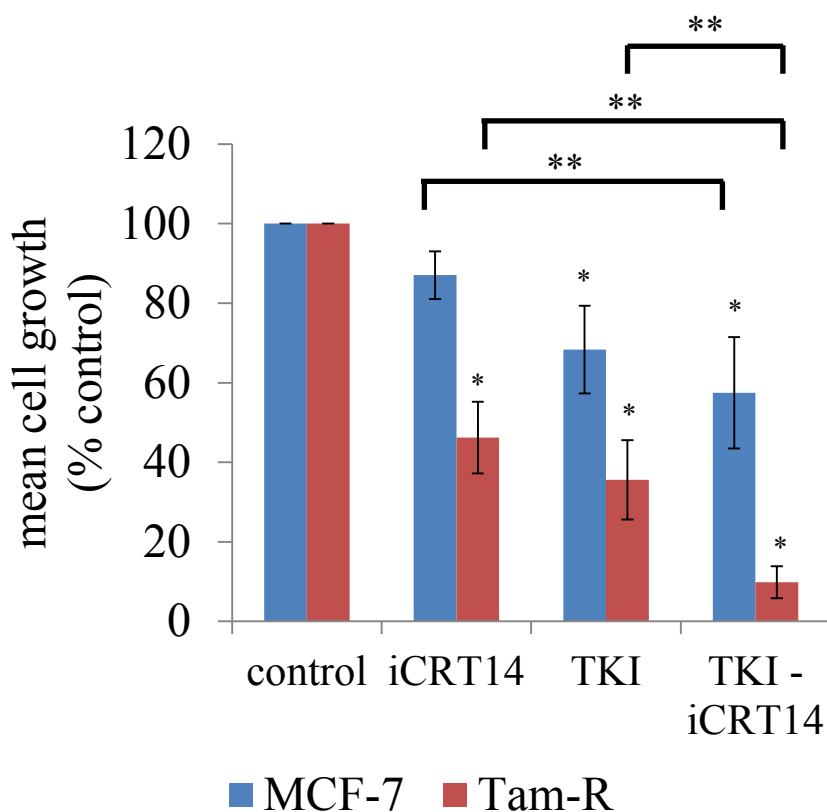


**Figure 6.2**  
**Effects of iCRT14 and EGFR tyrosine kinase inhibition (TKI/ gefitinib) on growth of MCF-7 and Tam-R cells as determined by MTT assay.**

MCF-7 and Tam-R cells were treated with iCRT14 (6.25 $\mu$ M), TKI (1 $\mu$ M) or combination TKI - iCRT14 treatments for 3 days. Inhibition of cell growth was assessed using MTT assays as described in the methods section. iCRT14 and TKI both inhibit cell growth and the effect with combination treatments is additive. Tam-R cells were more sensitive to this inhibition than MCF-7 cells.

Error bars show SD for n=3 experiments. \* post hoc statistical analysis was significant compared to untreated control. For MCF-7 cells, difference between iCRT14 and TKI - iCRT14 was also significant (\*\*); for Tam-R cells, difference between iCRT14 and TKI - iCRT14 and difference between TKI and TKI - iCRT14 were also significant (\*\*).

## **6.2 Effect of dual inhibition on cellular proliferation: Ki-67 staining**

Having investigated the effect of dual inhibition on cell growth using MTT assays, subsequent experiments were performed in order to confirm these observations by looking at changes in cellular proliferation through Ki-67 staining.

In these experiments, MCF-7 and Tam-R cells were treated with TKI (1 $\mu$ M), iCRT14 (6.25 $\mu$ M) or the two agents in combination for a period of 3 days. The resulting cells were then stained for Ki-67. MCF7 cells showed little change in Ki-67 staining with any of the treatments over this time period with the percentage positivity being approximately 100% for all treatment arms (Figure 6.3). In contrast to this, Tam-R cells exposed to TKI or iCRT14 as single agents lost Ki-67 positivity whereas the combination treatment substantially reduced this to 20% (Figure 6.4).



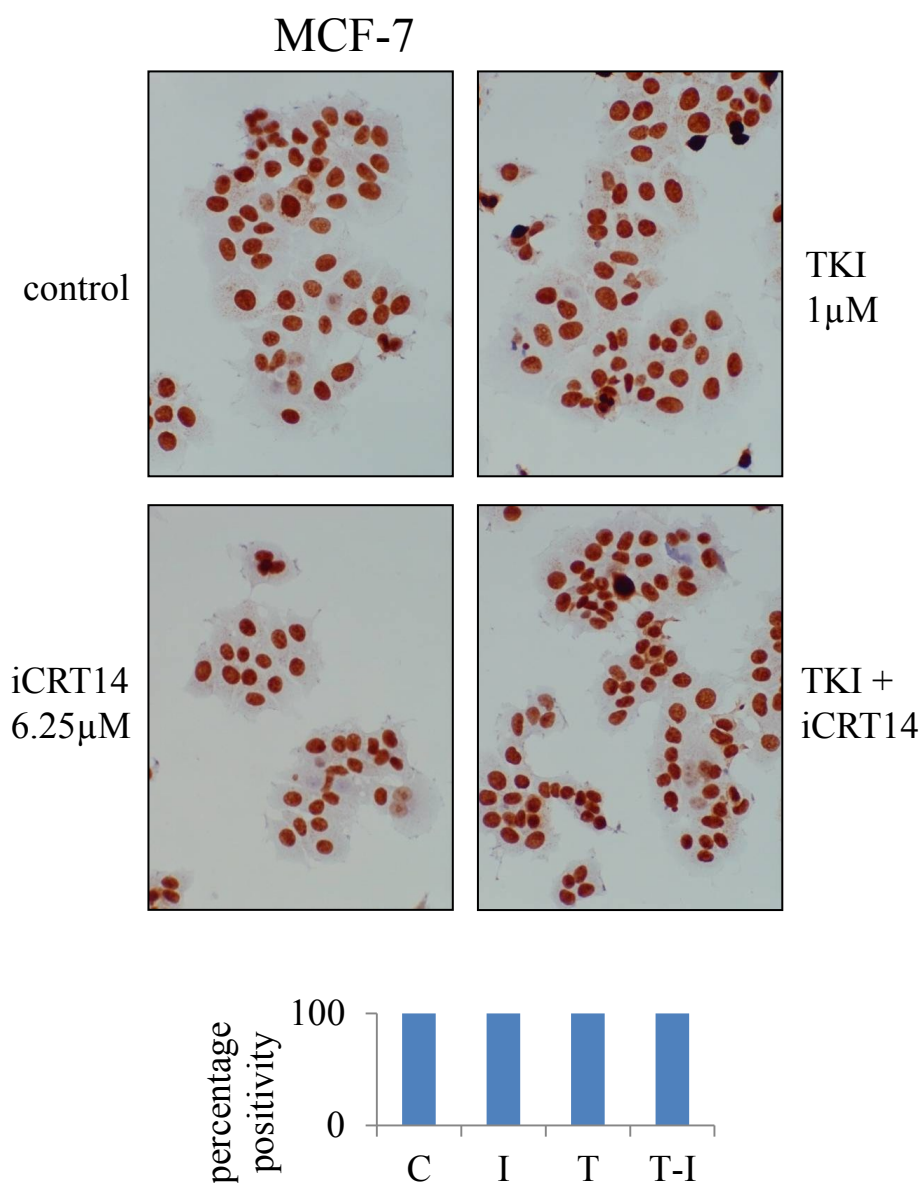


**Figure 6.3**  
**Effects of iCRT14 and EGFR tyrosine kinase inhibition (TKI/ gefitinib) on proliferation of MCF-7 cells as determined by Ki-67 antigen staining.**

MCF-7 cells were treated with iCRT14 (I, 6.25  $\mu$ M), TKI (T, 1  $\mu$ M) or combination TKI - iCRT14 (T-I) treatments for 3 days as described in the methods section. Cellular proliferation was assessed by staining for Ki-67 antigen. Representative images of cells were captured using a light microscopy at 20x original magnification (n=2). Percentage positivity for Ki-67 antigen staining is shown in the graph.

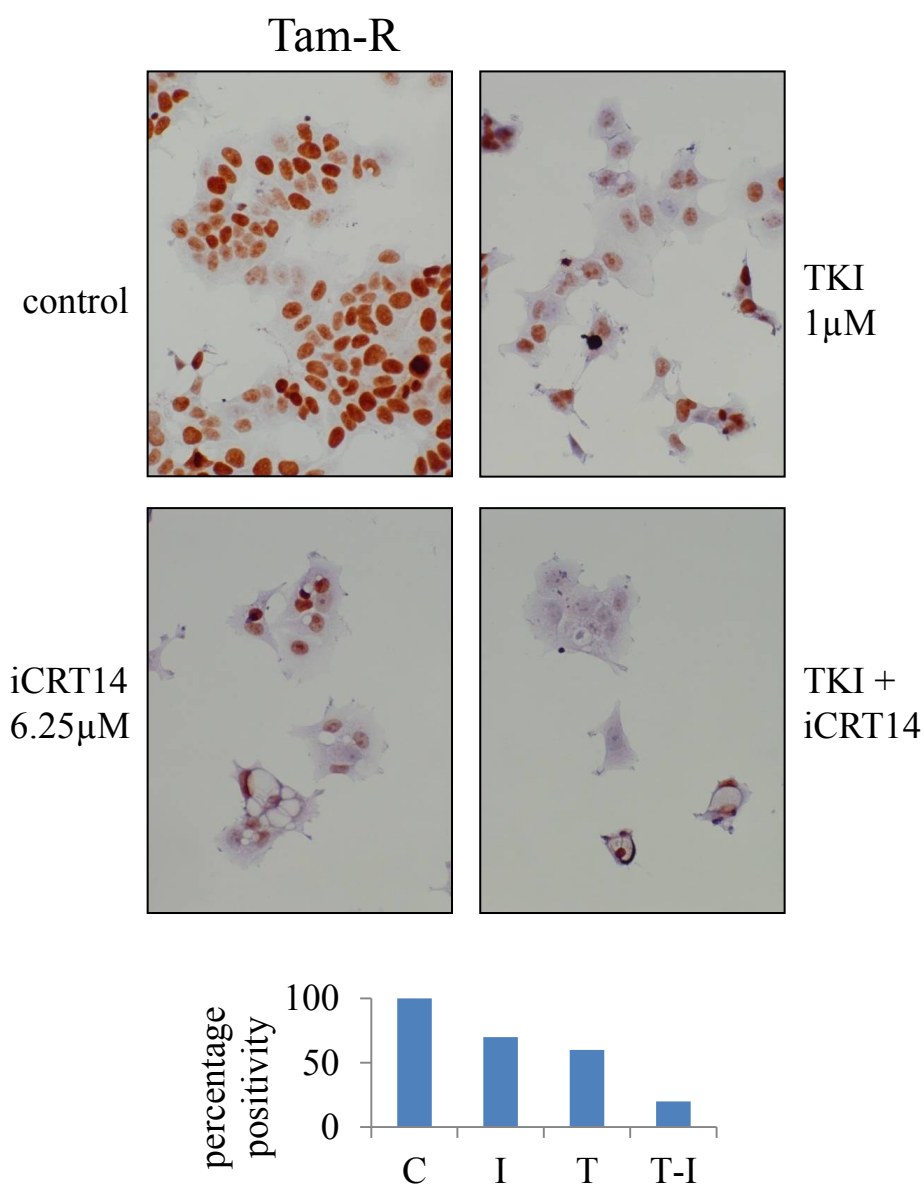


**Figure 6.4**  
**Effects of iCRT14 and EGFR tyrosine kinase inhibition (TKI/ gefitinib) on proliferation of Tam-R cells as determined by Ki-67 antigen staining.**

Tam-R cells were treated with iCRT14 (I, 6.25μM), TKI (T, 1μM) or combination TKI - iCRT14 (T-I) treatments for 3 days as described in the methods section. Cellular proliferation was assessed by staining for Ki-67 antigen. Representative images of cells were captured using a light microscopy at 20x magnification (n=2). Percentage positivity for Ki-67 antigen staining is shown in graph.

### **6.3 Effect of EGFR inhibition on Wnt pathway activity and exploration of dual Wnt/ EGFR inhibition**

Growth data supported interaction between Wnt and EGFR signalling in Tam-R cells. We next set out to explore

- (i) whether Wnt inhibition affected EGFR pathway activity;
- (ii) whether EGFR inhibition affected Wnt pathway activity and
- (iii) whether combined Wnt and EGFR inhibition resulted in a greater suppression of EGFR and Wnt pathways than when these treatments were used as single agents.

Tam-R cells were treated with IWP2 (10 $\mu$ M), gefitinib/ TKI (1 $\mu$ M) or combination of these agents (TKI - IWP2) for 5 minutes. Signalling changes were determined by Western blotting. We used LRP6 and p-LRP6 as read out for Wnt signalling modulation. MAPK and AKT were identified as downstream signalling elements common to the two pathways.

Having previously established activity of IWP2 in Tam-R cells (see Section 5.2.1.1), a fall in expression of p-LRP6 was used as control for IWP2 activity. We have also shown that IWP2 inhibits MAPK activity in Tam-R cells (see section 5.2.1.4). Gefitinib [4-(3-chloro-4-fluoroanilino)-7-methoxy-6-(3-morpholinopropoxy)quinazoline] selectively inhibits the EGFR tyrosine kinase (Wakeling et al. 2002) and its activity on Tam-R cells has been previously described by Knowlden et al. (2003). A fall in p-EGFR expression was used as a control for gefitinib (TKI) activity. Gefitinib also inhibits MAPK and AKT activity in Tam-R cells (Knowlden et al. 2003).

### **6.3.1 Effect of Wnt inhibition on EGFR activity**

When Tam-R cells were treated with combination TKI- IWP2, there was a fall in p-EGFR expression but this was not substantially different to the effect seen following treatment with either IWP2 or TKI alone (Figure 6.5).

### **6.3.2 Effect of EGFR inhibition on Wnt activity**

Treatment of Tam-R cells with IWP2, TKI and combination TKI- IWP2 all resulted in a fall in p-LRP6 expression (Figure 6.6). The change in expression following treatment with IWP2 was greater than that seen following treatment with TKI; and treatment with combination TKI- IWP2 showed similar activity to IWP2 treatment alone.

### **6.3.3 Effect of dual inhibition on MAPK activity**

When Tam-R cells are treated with IWP2, TKI or combination TKI- IWP2, there is a fall in p-MAPK expression (Figure 6.7). This is greater for TKI than IWP2, but the effect following combination TKI or TKI- IWP2 is similar.

### **6.3.4 Effect of dual inhibition on AKT activity**

Treatment of Tam-R cells with IWP2, TKI and combination TKI- IWP2 resulted in a fall in p-AKT expression and the effect was similar in all treatment groups (Figure 6.8).

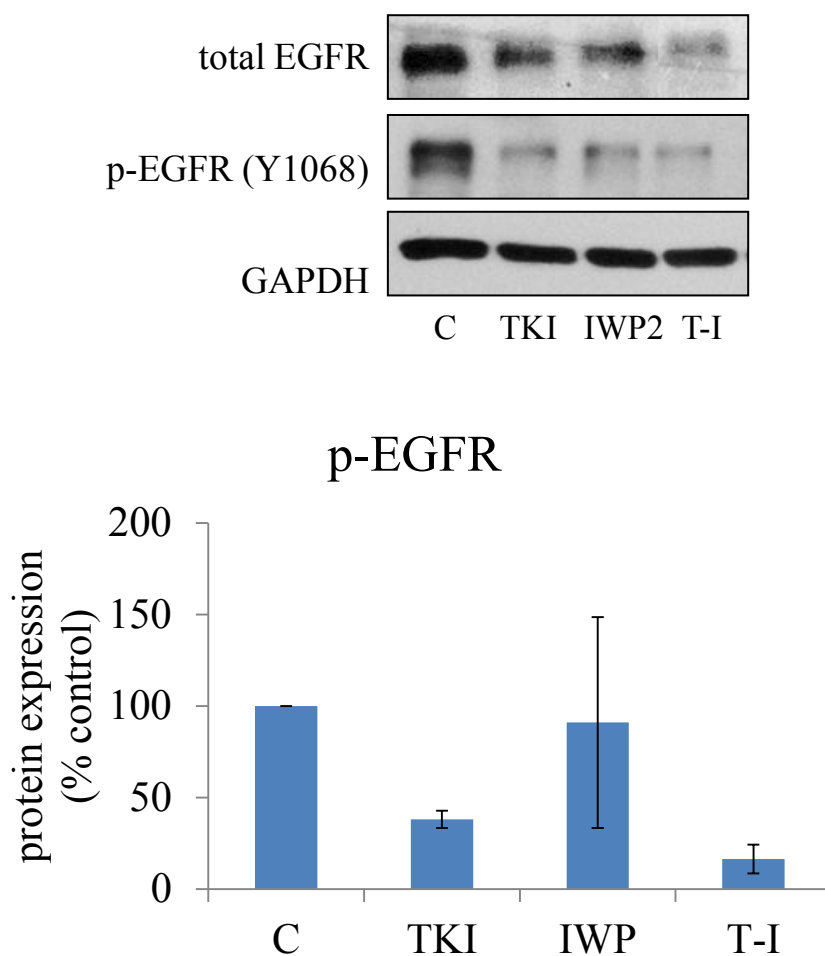


**Figure 6.5**  
**Effect of IWP2, gefitinib and combination**  
**treatments on EGFR activity in Tam-R cells.**

C=control, T-I = sequential TKI and IWP2

Tam-R cells were cultured to log-phase growth and then treated with IWP2 10 $\mu$ M, TKI (gefitinib) 1 $\mu$ M, or sequentially with TKI and IWP2 for 5 minutes. The cells were then lysed as described in materials and methods. SDS-PAGE/ Western blot analyses was carried out using 30 $\mu$ g of total soluble protein and the membranes were probed with antibodies specific to EGFR. p-EGFR and GAPDH. Densitometry data is shown and corrected for GAPDH. Error bars show SEM (n=2).

EGFR activity was suppressed with single and dual inhibition.

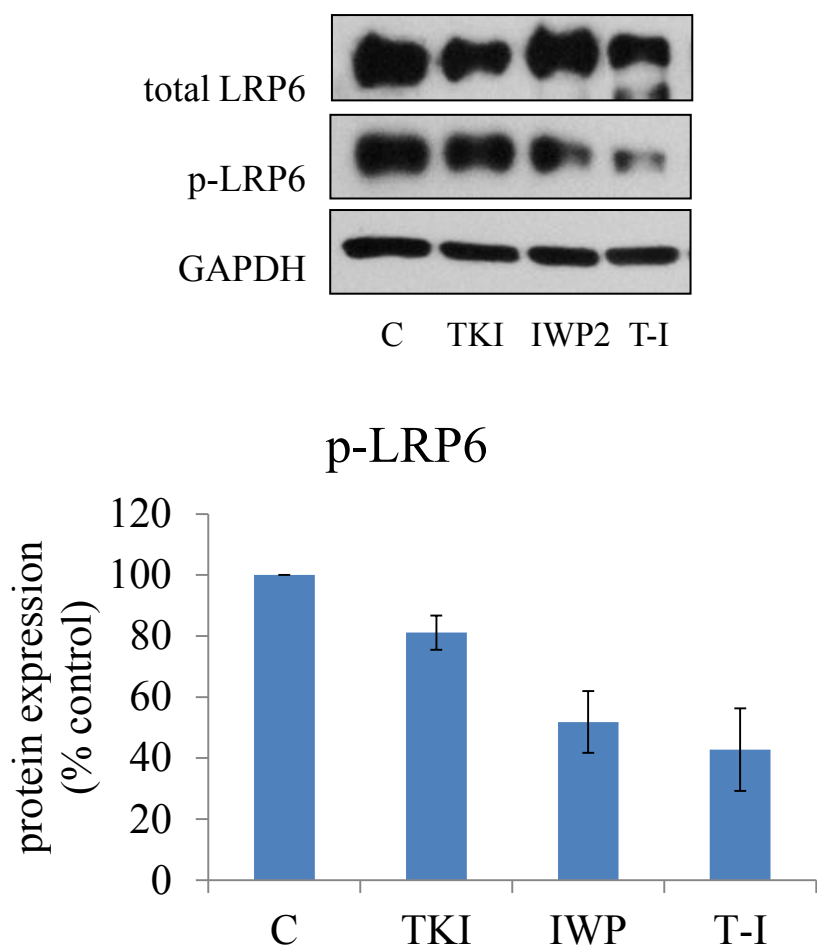


**Figure 6.6**  
**Effect of IWP2, gefitinib and combination treatments on LRP6 activity in Tam-R cells.**

C=control, T-I = sequential TKI and IWP2

Tam-R cells were cultured to log-phase growth and then treated with IWP2 10 $\mu$ M, TKI (gefitinib) 1 $\mu$ M, or sequentially with TKI and IWP2 for 5 minutes. The cells were then lysed as described in materials and methods. SDS-PAGE/ Western blot analyses was carried out using 30 $\mu$ g of total soluble protein and the membranes were probed with antibodies specific to LRP6, p-LRP6 and GAPDH. Densitometry data is shown and corrected for GAPDH. Error bars show SEM (n=2).

LRP6 activity was suppressed with IWP2 and dual inhibition.

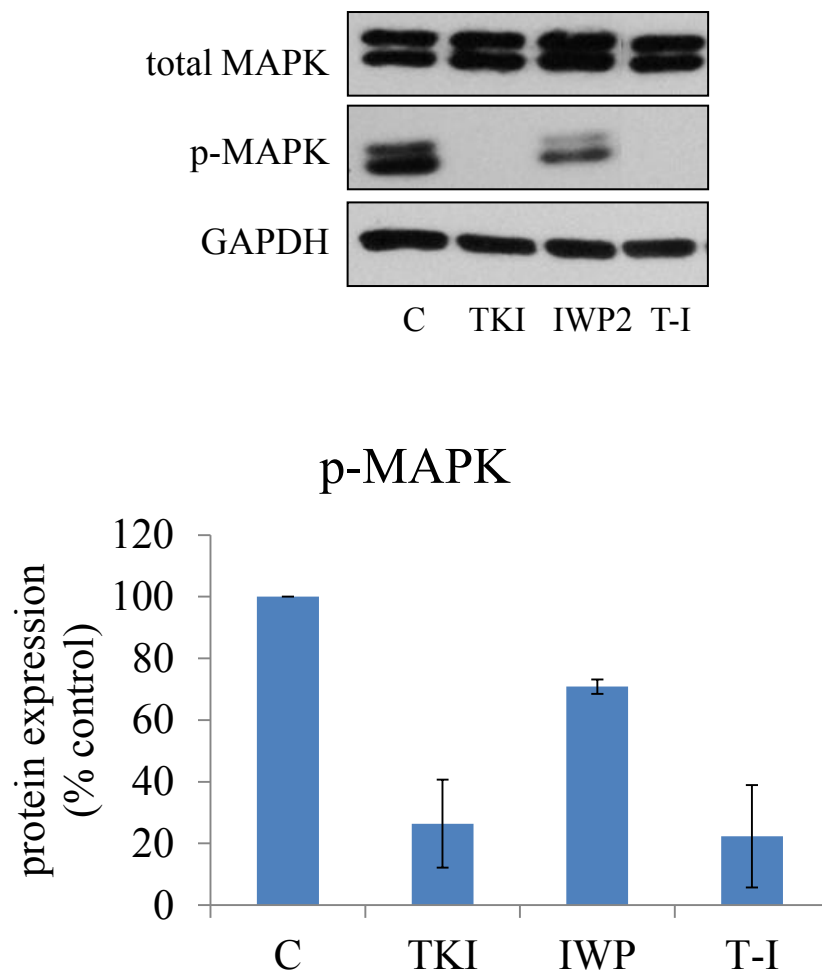


**Figure 6.7**  
**Effect of IWP2, gefitinib and combination treatments on MAPK activity in Tam-R cells.**

C=control, T-I = sequential TKI and IWP2

Tam-R cells were cultured to log-phase growth and then treated with IWP2 10 $\mu$ M, TKI (gefitinib) 1 $\mu$ M, or sequentially with TKI and IWP2 for 5 minutes. The cells were then lysed as described in materials and methods. SDS-PAGE/ Western blot analyses was carried out using 30 $\mu$ g of total soluble protein and the membranes were probed with antibodies specific to MAPK, p-MAPK and GAPDH. Densitometry data is shown and corrected for GAPDH. Error bars show SEM (n=2).

MAPK activity was suppressed with TKI and dual inhibition.

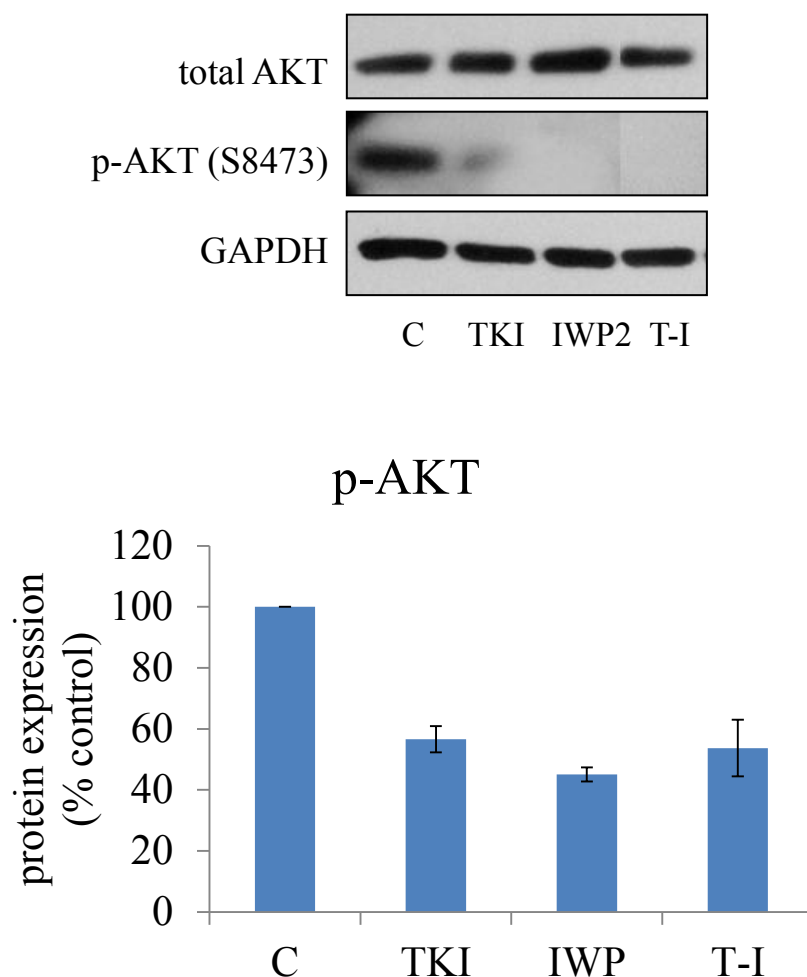


**Figure 6.8**  
**Effect of IWP2, gefitinib and combination treatments on AKT activity in Tam-R cells.**

C=control, T-I = sequential TKI and IWP2

Tam-R cells were cultured to log-phase growth and then treated with IWP2 10 $\mu$ M, TKI (gefitinib) 1 $\mu$ M, or sequentially with TKI and IWP2 for 5 minutes. The cells were then lysed as described in materials and methods. SDS-PAGE/ Western blot analyses was carried out using 30 $\mu$ g of total soluble protein and the membranes were probed with antibodies specific to AKT, p-AKT and GAPDH. Densitometry data is shown and corrected for GAPDH. Error bars show SEM (n=2).

AKT activity was suppressed with single and dual inhibition.



## **6.4 Affymetrix HGU-133A gene microarray data analysis: Tam-R cells treated with gefitinib [1 $\mu$ M] versus Tam-R cells**

Encouraged by these data, we looked at Affymetrix HGU-133A gene microarray data for Tam-R cells treated with gefitinib [1 $\mu$ M] for 10 days (Figure 6.9). Our search was guided by previous findings in Tam-R cells (see Section 3.1.1) and was limited to probes identified in Table 3.2.

DKK1, Wnt6 and Wnt4 probe sets were upregulated in gefitinib treated Tam-R cells versus Tam-R cells (>1.5 fold change compared to control). These changes were significant by t-testing ( $p < 0.05$ ). DKK1 inhibits Wnt signalling; Wnt6 and Wnt4 promote Wnt signalling. These changes support Wnt activation in Tam-R cells following treatment with gefitinib and this activation is in addition to changes previously reported between Tam-R cells and MCF-7 cells.

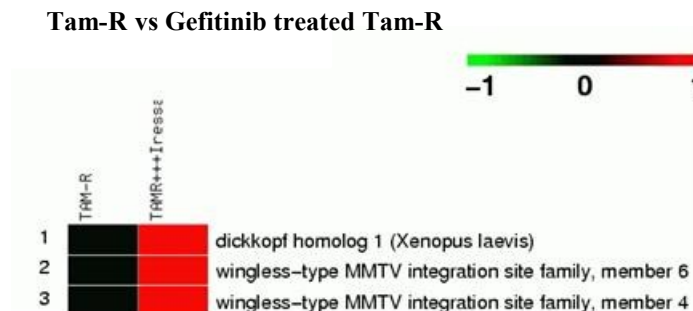


**Figure 6.9**  
**Heatmap for Wnt signalling probe set showing changes in gene expression between Tam-R cells treated with Gefitinib and Tam-R cells.**

Red signalled increased expression compared to Tam-R control (black).

DKK1, Wnt6 and Wnt4 probes were upregulated in Gefitinib treated Tam-R cells versus Tam-R cells (>1.5 fold change compared to control) . These changes were significant by t-testing ( $p < 0.05$ ).

## 6.5 Summary

Growth assays showed that Wnt and EGFR inhibitors were inhibitory both as single agents and particularly in combination in Tam-R cells. These findings suggested increased Wnt activity in Tam-R cells compared to MCF-7 cells. Affymetrix HGU-133A gene microarray data for Tam-R cells treated with gefitinib [1 $\mu$ M] for 10 days also supported a link between the two pathways in this model. Growth suppression by Wnt inhibition may represent indirect targeting of EGFR signalling given the cross talk between the two pathways. Growth data using IWP2 and TKI would support this. However, combination iCRT14 and TKI had greater inhibitory effect on Tam-R growth than either inhibitor alone. This may be due to a degree of independent pathway activity. Data also suggests that targeting Wnt activity at the nuclear level (iCRT14) may be more effective than targeting Wnt signalling at the ligand/ receptor level (IWP2). These findings were supported by Ki-67 staining. Further evidence for cross- talk between the two signalling pathways comes from Affymetrix HGU-133A gene microarray data for Tam-R cells treated with gefitinib for 10 days, where changes suggest increased Wnt activation following gefitinib treatment.

Early signalling data suggests that the interaction between EGFR and LRP6 may be bi-directional. This has led to the proposed model of Wnt and EGFR signalling in Tam-R cells (Figure 6.10). Unfortunately we were unable to explore the effect of signalling changes with iCRT14 and TKI combinations due to time constraints and this provides scope for further work.

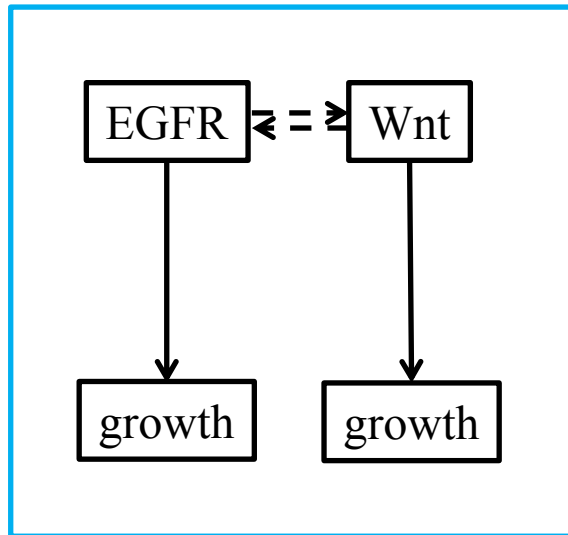


**Figure 6.10**  
**Possible interaction between EGFR and Wnt signalling pathways.**

# Chapter 7

## Discussion

## 7 Discussion

The data in this study shows that:

- (i) Wnt pathway elements are deregulated in a cell model of acquired tamoxifen resistance (Tam-R) compared to their tamoxifen sensitive parental cells (MCF-7).
- (ii) Tamoxifen resistant breast cancer cells are sensitive to pharmacological Wnt inhibitors, resulting in suppression of growth and migration; these agents have no effect on tamoxifen sensitive cells.
- (iii) A level of cross-talk appears to exist between the EGFR and the Wnt pathway in tamoxifen resistant cells.

Collectively, these data suggest that Wnt signalling may play an important role in tamoxifen resistance where it may offer an opportunity for therapeutic intervention to control relapse and associated tumour aggressiveness.

Human breast cancer cell lines represent important tools in breast cancer research to study signalling pathways and mechanisms that can promote an endocrine-insensitive state and identify potential means to circumvent these phenomena and/ or to treat it (Lacroix M 2004). The tamoxifen resistant MCF-7 cell line (Tam-R) has been extensively characterised and has been shown to be a good model for acquired clinical endocrine resistance (Simstein et al. 2003, Gee et al. 2005b). Tam-R cells have a more aggressive phenotype accompanied by deregulated  $\beta$ -catenin (Hiscox et al. 2006). It has also been reported that there is increased coupling of  $\beta$ -catenin to LEF-1 with increased basal expression of c-myc, cyclin-D1 and CD44 catenin (Hiscox et al. 2006).  $\beta$ -catenin is a major effector of canonical Wnt signalling where it acts as a cofactor to modulate TCF/LEF transcription factor activity. This model was chosen to evaluate the importance of Wnt signalling in the context of tamoxifen resistance in this project.

Initial observations from Affymetrix microarray data using the established Tam-R cells revealed changes in the expression of Wnt signalling components in these cells versus their parental, tamoxifen sensitive MCF-7 cells. These data therefore suggested that Wnt pathway activity might also be deregulated in these resistant cells, and thus might represent a mechanism which contributed to their resistant growth and aggressive behaviour.

We subsequently wanted to explore if Wnt pathway deregulation occurred in response to tamoxifen treatment or if this was only present in the resistant phenotype, since tamoxifen is known to induce changes in signalling pathway

activity (e.g. EGFR) in response to short term treatment (Hiscox et al. 2006). Although some Wnt signalling components were deregulated in MCF-7 cells following 10 days of tamoxifen treatment, assuming an equal contribution from each gene change observed, the overall effect on canonical Wnt signalling remained equivocal during the endocrine response, contrasting with more prevalent changes by the time resistance emerges in Tam-R cells.

Since both MCF-7 and Tam-R cells are ER positive breast cancer models, possible changes in Affymetrix data for Wnt signalling following modulation of ER activity over and above treatment with tamoxifen were explored. MCF-7 cells treated with oestradiol (E2) [ $10^{-9}$ M] for 10 days were chosen as a model for enhanced ER activity; faslodex resistant MCF-7 (Fas-R) cells are ER negative and were used as a model for absence of ER activity (*de novo* tamoxifen resistance). Affymetrix data for MCF-7 cells treated with  $10^{-9}$ M E2 for 10 days suggested a reduction in Wnt signalling compared to MCF-7 cells. This is supported by data from Katoh (2002) who showed that in MCF-7 cells, Wnt3a was downregulated after treatment with oestradiol. This confirms some aspect of Wnt signalling may be repressed by oestradiol. To further investigate whether there might be a link between ER expression and Wnt pathway regulation, Wnt pathway expression in Fas-R cells (which are ER negative) was investigated. Although a number of changes were observed in Wnt pathway components in Fas-R cells when compared to the parental MCF-7 cell model, the overall effect on canonical Wnt signalling remained equivocal in this model. The data implies that ER must be present for Wnt signalling. Increases seen in acquired endocrine resistance begin during early



treatment with tamoxifen and are maintained after development of tamoxifen resistance.

An on-going working collaboration has been established with the Bioinformatics group at Philips Research Laboratories, Eindhoven, Netherlands. They have developed a computational model of the Wnt pathway using Affymetrix U133Plus2.0 gene microarrays and this has been validated in clinical material (Verhaegh et al. 2012). Preliminary exploration of our Affymetrix U133 gene microarray data for MCF-7 and Tam-R cells on their model, predicted that the probability of Wnt activation in Tam-R cells was higher than in MCF-7 cells, but results were inconclusive (personal correspondence). The limitations of this analysis were that the U133 microarrays have less probe sets than the U133Plus2.0 microarrays (60 out of 80) and that it was challenging to normalise the U133A data to the U133APlus2.0 data. Though these are preliminary results, they are further independent exploratory confirmation of our findings.

Our data suggests a role for Wnt signalling in Tam-R cells. Published data supports a role for early Wnt signalling activation in the promotion of tamoxifen resistance. Schlange et al. (2007) showed that Wnt1 could rescue MCF-7 breast cancer cells from growth arrest following a seven day treatment with tamoxifen. This rescue was mediated by Wnt1 transactivation of EGFR activity via src, which our group has shown is also induced by tamoxifen (Gee et al. 2003, Borley et al. 2008). Tamoxifen treatment may thus induce signalling changes which make MCF-7 cells more sensitive to modulation by Wnt ligands (e.g. our Affymetrix data showed increased

LRP6 expression in Tam-R cells compared to MCF-7 cells). Wnt signalling may thus be an early target in helping to prevent acquired tamoxifen resistance. It also highlights an important potential interaction between Wnt and EGFR signalling. This interaction has been extensively described in the literature (although not in the setting of acquired tamoxifen resistance) and will be described in more detail in a later section.

Published clinical data further supports observations seen in these cellular models. Joo et al. (2011) showed that in patients with invasive ductal carcinoma of the breast, neo-adjuvant tamoxifen treatment for twenty-six days prior to surgery produced changes in Wnt signalling components as determined by immunocytochemistry. In contrast, treatment with anastrozole failed to induce Wnt pathway expression. This may have important clinical implications and parallels changes in Wnt signalling noted during tamoxifen treatment *in vitro* and ultimately in the acquired tamoxifen resistance model. Tamoxifen is often used as second line treatment following failure of aromatase inhibitors in the treatment of breast cancer. Targeting Wnt alongside treatment with tamoxifen may thus improve prognosis in this setting.

Differences between MCF-7 and Tam-R cells as evidenced by Western blotting and immunocytochemistry further supported a role for deregulated Wnt signalling in Tam-R cells. Western blot showed increased p-LRP6 and total  $\beta$ -catenin, and immunocytochemistry showed increased nuclear activated beta catenin in Tam-R cells. Exploration of baseline TCF/LEF reporter assay activity in MCF-7 and Tam-R cells provides scope for further work.

Guided by these changes, the impact of modulating Wnt signalling in MCF-7 and Tam-R cells was compared. Both Wnt activators and Wnt inhibitors were used to further determine the relevance of this pathway and hence gauge potential targeting value.

Wnt3a ligand is believed to play a key role in activating canonical Wnt signalling (Yamamoto H 2008) by binding to LRP6 (Yamamoto et al. 2006). Lithium Chloride inhibits GSK-3 activity (Stambolic et al. 1996) and has been extensively used to study modulation of  $\beta$ -catenin. When MCF-7 cells were treated with Wnt3a ligand, there was no change in GSK-3 $\alpha$  or active  $\beta$ -catenin expression. Total  $\beta$ -catenin expression fell at Wnt3a concentration of 100ng/ml. There was a fall in GSK-3 $\beta$  expression after treatment at Wnt3a concentrations of 100 and 200ng/ml. p-GSK-3 $\alpha$  expression fell at Wnt3a concentration of 200ng/ml; there was a rise in p-GSK-3 $\beta$  expression at Wnt3a concentrations of 50ng/ml and 100ng/ml and a fall at Wnt3a concentration of 200ng/ml. When Tam-R cells were treated with Wnt3a ligand, active  $\beta$ -catenin expression was increased, supporting Wnt signalling activation. Total  $\beta$ -catenin and total GSK-3 $\alpha/\beta$  expressions were unchanged, and expression of p-GSK-3 $\alpha/\beta$  differed with varying ligand concentrations.

Treatment of MCF-7 and Tam-R cells with LiCl resulted in increased expressions of p-GSK-3 $\alpha/\beta$  and active  $\beta$ -catenin which would support Wnt activation. Total  $\beta$ -catenin expression remained unchanged. Activation of Wnt signalling by LiCl in Tam-R cells was confirmed using a TCF/LEF (luciferase) reporter assay. However, there was no significant change in growth for both MCF-7 and Tam-R cells after

stimulation with Wnt3a ligand or LiCl. These preliminary findings suggest that canonical Wnt signalling can be further activated in both MCF-7 and Tam-R cell lines, but that this activation is not linked to increased cell growth. We propose that Wnt signalling is already maximal in Tam-R cells and so no further increase in growth is seen when cells are treated with LiCl and Wnt3a ligand. Wnt5b ligand has been shown to increase invasive properties in MCF-7 cells and this occurs through activation of the planar cell polarity pathway (Klemm et al. 2011). In addition, growth in MCF-7 cells has been reported to be independent of  $\beta$ -catenin (Covey et al. 2012) and this is in agreement with our findings with LiCl and Wnt3a.

Inhibition of Wnt signalling was explored using commercially available pharmacological inhibitors. LRP6 expression was increased in Tam-R cells compared to MCF-7 cells as evidenced by Western blot and Affymetrix data: IWP2 was chosen to inhibit the Wnt pathway at this level. IWP2 has been reported to inhibit porcupine, block Wnt- dependent phosphorylation of LRP6 receptor and Dvl2, and block  $\beta$ -catenin accumulation (Chen et al. 2009a) but this has not been explained in the context of Tam-R cells. Treatment of MCF-7 and Tam-R cells with IWP2 resulted in decreased expression of p-LRP6 as evidenced by Western blot. As  $\beta$ -catenin was increased in Tam-R cells, we also targeted nuclear transcriptional activity of  $\beta$ -catenin. PNU 74654 is reported to bind to  $\beta$ -catenin; inhibit the interaction between  $\beta$ -catenin and T cell factor 4 (TCF4) and disrupt the Wnt signalling pathway (Trosset et al. 2006). Expression of p-GSK-3 $\alpha/\beta$  was decreased in both MCF-7 and Tam-R cell lines after treatment with IWP2 ((at 1 hour) and PNU 74654 (at 5 minutes and 1 hour), but there was no consistent change in p- $\beta$ -catenin (S33/37/T41) expression for the two drugs. Unfortunately there was no reduction in

TCF/ LEF (luciferase) reporter assay activity in Tam-R cells following treatment with PNU 74654. Cyclin D1 and c-myc expression were reduced following treatment with PNU 74654 but these findings were not reproducible with RT-PCR. Another agent targeting the nuclear Wnt activity was therefore selected: iCRT14. This molecule is reported to inhibit  $\beta$ -catenin- responsive element (CRT), disrupting the interaction between  $\beta$ -catenin and TCF4 possibly by binding to  $\beta$ - catenin (Gonsalves et al. 2011). TCF/ LEF (luciferase) reporter assay activity in Tam-R cells was reduced following treatment with iCRT14.

When MCF-7 and Tam-R cells were treated with Wnt inhibitors some interesting differences emerged. Treatment with IWP2, PNU 74654 and iCRT14 decreased cell growth in Tam-R cells, but there was no significant effect in MCF-7 cells. This is supported by published data for IWP2 and iCRT14 activity on MCF-7 cells. Covey et al. (2012) showed that Wnt inhibition did not affect MCF-7 cell viability or cell growth. These findings were seen following treatment with IWP2 and knockdown of  $\beta$ -catenin respectively. Similarly, iCRT14 did not affect growth or proliferation in MCF-7 cells (Gonsalves et al. 2011). Preliminary growth data for Fas-R cells treated with iCRT14 shows that their response is similar to that seen in MCF-7 cells (see Appendix, Figure 9.6). Tam-R cells, however, appear to be growth- sensitive to Wnt inhibition and this is in contrast to lack of growth following further Wnt stimulation. Tam-R cells withdrawn from tamoxifen were equally susceptible to Wnt inhibition and Tam-R cells showed similar growth suppression. Inhibition of Wnt signalling is thus able to deplete tamoxifen agonistic effects in this model. These findings show that Wnt signalling appears to have a distinct role in Tam-R cells and the pathway may be targeted at the ligand/ receptor level (IWP2) and in the nucleus (PNU 74654

and iCRT14) to decrease cell growth. iCRT14 also decreased cellular proliferation in Tam-R cells as assessed by Ki-67 staining. This supports growth assay data for this compound and the importance of Wnt signalling to such cells.

Cell migration in Tam-R cells was also decreased following Wnt inhibition by IWP2, PNU 74654 and iCRT14. Inhibition of Wnt signalling by sFRP1 has been reported to decrease cell migration in MDA-MB-231 cells and this is in agreement with our findings with IWP2 in Tam-R cells (Matsuda et al. 2009). Wnt signalling modulates transcription of several genes and some of these are important for migration. Examples of such genes are: CD44, CTGF, EFNB1, EGFR, FGF7, FN1, GDNF, IGF1, IL6, IRS1, JAG1, MMP9 (Gelatinase B), NRCAM, NRP1, PDGFRA, PPAP2B, PPARD, SIX1, SMO, TWIST1, VEGFA some of which are increased in Tam-R cells (SABiosciences 2012). For example, EGFR and IGF signalling play key roles in tamoxifen resistance and contributes to their aggressive behaviour (Knowlden et al. 2008, Nicholson et al. 2007, Jones et al. 2006). Moreover, Tam-R cells show increased expression of CD44 (Hiscox et al. 2006) and this has been linked to a more aggressive phenotype. All three Wnt inhibitors inhibited migration and this would suggest that the Wnt pathway may be inhibited at multiple levels with similar effect on this end point. Treatment with IWP2 and PNU 74654 reduced expression of p-MAPK in Tam-R cells, an element which contributes to growth and migration in this model (Knowlden et al. 2003). These findings support decreased growth and migration following Wnt inhibition. Similar findings have been reported in other breast cancer cell lines following disruption of Wnt signalling at the receptor level, e.g. cellular proliferation was decreased and MAPK activity was reduced (Schlange et al. 2007).

Tam-R cells are ER positive but rely heavily on EGFR signalling for growth (Gee et al. 2005a). The interactions of activated growth factor pathways with ER function are important in understanding endocrine resistance in breast cancer. EGFR, HER2, phosphatidylinositol 3-kinase (PI3K) and insulin-like growth factor 1 receptor (IGF-1R) are recognised key players in this cross-talk (Knowlden et al. 2008, Nicholson et al. 2007, Jones et al. 2006). The role of Wnt signalling in established endocrine resistance is less clearly defined. However Wnt can interact with the oestrogen receptor (El-Tanani et al. 2001, Inadera et al. 2002, Mastroianni et al. 2010, Kouzmenko et al. 2004, Mulholland et al. 2005) and EGFR signalling (Hu and Li 2010) in this setting. Figure 7.1 summarises the key interactions between EGFR and Wnt signalling reported in cancer.

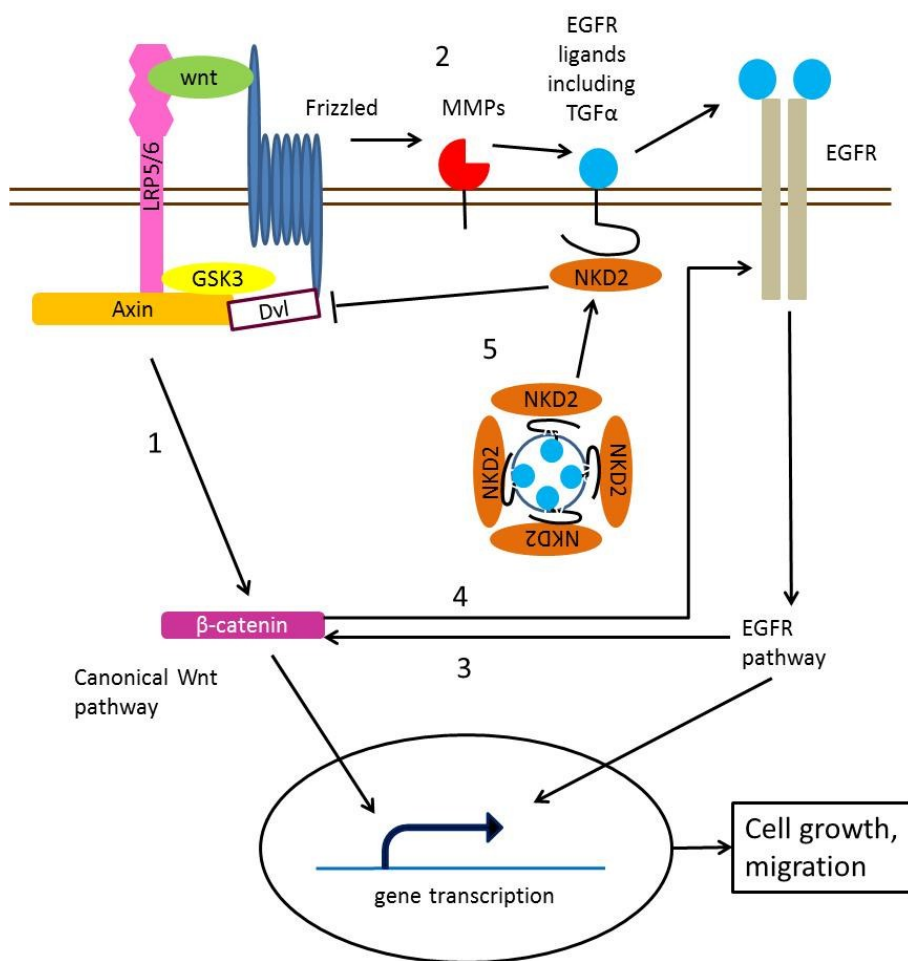


**Figure 7.1**  
**Five possible interactions between Wnt Signalling and EGFR pathway in cancer.**

(1) Wnt ligand binds to LRP6 and Frizzled to activate the Canonical Wnt pathway. (2) Frizzled activates EGFR signalling through metalloproteinase-mediated release of soluble EGFR ligands such as TGF $\alpha$ . (3) EGFR can activate  $\beta$ -catenin via AKT/PI3K pathway. (4)  $\beta$ -catenin can form a heterodimer with EGFR to activate the EGFR pathway. (5) NKD2 binds to TGF- $\alpha$  and escorts it to plasma membrane where it is released. NKD2 can then bind Dvl and the two are mutually degraded. Adapted from Hu et al. (2010).



In the next section, the evidence for Wnt and EGFR signalling cross talk within breast cancer is explored, with emphasis on the potential for this interaction in Tam-R cells. EGFR can be activated by the following ligands: EGF, transforming growth factor-  $\alpha$  (TGF- $\alpha$ ), amphiregulin, betacellulin, heparin-binding epidermal growth factor-like growth factor (HB-EGF) and epiregulin (Hynes and Lane 2005). Activated EGFR signalling in turn activates other pathways such as Ras-Raf-MAPK and PI3K/Akt which are important for cellular growth, proliferation, survival and motility (Hynes and Lane 2005). However, there is also literature evidence for activation of EGFR signalling by the Wnt pathway.

Activation of Wnt signalling increases phosphorylation of EGFR in breast cancer (Schlange et al. 2007) and this EGFR activation occurs via metalloproteinase (MMP) mediated release of soluble EGFR ligands (Musgrove 2004, Faivre and Lange 2007). Increased MAPK activity is downstream of EGFR activity and results in increased levels of cyclin D1 (Musgrove 2004, Civenni G 2003). One possible EGFR ligand target for MMP activity in breast cancer may be HB-EGF (Civenni G 2003). Work on prostate cancer showed that a target for MMP activity may be proHB-EGF (Prenzel et al. 1999); and work on squamous cell cancers showed that MMPs also cleave proamphiregulin by metalloprotease-disintegrin tumour necrosis factor- $\alpha$ -converting enzyme (TACE) (Gschwind et al. 2003). Amphiregulin is also highly expressed by Tam-R cells and drives an EGFR autocrine growth signalling loop in these cells (Britton et al. 2006). Contribution for Wnt in this remains unknown.

Schroeder et al. (2002) showed that  $\beta$ -catenin could directly bind to EGFR/HER2 heterodimers in MMTV-Wnt1 mammary tumours (mammary tumours in transgenic mice with expression of int-1 gene). In tumours driven by Wnt1, EGFR was always involved. However in tumours driven by EGFR,  $\beta$ -catenin was not always involved. Tam-R cells have upregulated  $\beta$ -catenin and EGFR activity (Hutcheson et al. 2006). There is also preferential EGFR/HER2 dimerization (Knowlden et al. 2003). Future work would thus be to look into identifying whether this dimerization could be disrupted by Wnt signalling inhibition as part of the growth inhibition mechanism.

Katoh (2001) showed that Naked 1 (NKD1) and Naked 2 (NKD2) were upregulated in gastrointestinal tumours. Once TGF- $\alpha$  was processed by the Golgi apparatus, the C-terminal end could interact with NKD2 (Li et al. 2004). Vesicles coating TGF- $\alpha$  were formed and these were then transported to the cell membrane (Li et al. 2007, Cao et al. 2008, Hu et al. 2006). NKD2 was then downregulated by Dvl in HEK293T cells (Hu et al. 2010). Tam-R cells have increased expression of TGF- $\alpha$  (Knowlden et al. 2003, Hiscox et al. 2006). Stimulation of Tam-R cells with TGF- $\alpha$  results in src dependent phosphorylation of EGFR (Y1068) (Knowlden et al. 2005) and increased p-AKT (Hiscox et al. 2006). Thus, it is possible that TGF- $\alpha$  may be the ligand linking Wnt and any activation of EGFR signalling.

Based on the considerable potential for Wnt/EGFR cross-talk in this setting, and having established that Wnt inhibition decreased cell growth in Tam-R cells, we thus wanted to begin to explore if these changes resulted from interaction of Wnt and EGFR signalling, or if there was independent pathway activity. As growth in MCF-7

cells is not affected by Wnt inhibition or TKI treatment (previous data from our lab) and has decreased Wnt and EGFR signalling compared to Tam-R, we did not explore dual inhibition in this model but focussed on the Tam-R model that shows deregulation of both Wnt and EGFR pathways.

IWP2 was used to target Wnt signalling at the ligand/ receptor and iCRT14 was used to target nuclear pathway activity. Interesting differences were noted on dual inhibition using TKI – IWP2 and TKI – iCRT14. In growth assays using IWP2, TKI and TKI – IWP2 growth suppression was greatest by TKI or combination TKI – IWP2. There was a significant difference in growth suppression between TKI and IWP2 and between IWP2 and TKI - IWP2 with superiority for the TKI subgroups. This suggested that EGFR activity was the dominant pathway. However, treatment with combination TKI – iCRT14 was significantly better than treatment with either agent alone and there was no significant difference in Tam-R growth inhibition following treatment with iCRT14 or TKI alone with both agents growth inhibitory. This suggested that targeting Wnt signalling at the nuclear level may be more effective than inhibition at the ligand/ receptor level and may be able to add to the EGFR blockade effect.

Dual Wnt and EGFR inhibition reduced cellular proliferation in Tam-R cells. Percentage positivity for Ki67 staining, assessed by immunocytochemistry, was lower for dual inhibition than for individual iCRT14 or TKI treatment. This again suggests that targeting Wnt signalling at the nuclear level may be more effective than inhibition at the ligand/ receptor level and supports our growth data.

When Wnt signalling is activated, resulting in effects at the nuclear level and Wnt regulated gene expression, there is increased transcription of growth factor genes including growth factor pathway elements (see Figure 7.2). EGFR and IGF-1R cross-talk are important for growth in Tam-R cells (Knowlden et al. 2008, Nicholson et al. 2007, Jones et al. 2006) with preferential recruitment of IRS1 to EGFR triggering the dominant EGFR growth mechanism in Tam-R cells. Nuclear inhibition of Wnt signalling may result in a more effective disruption of this mechanism.

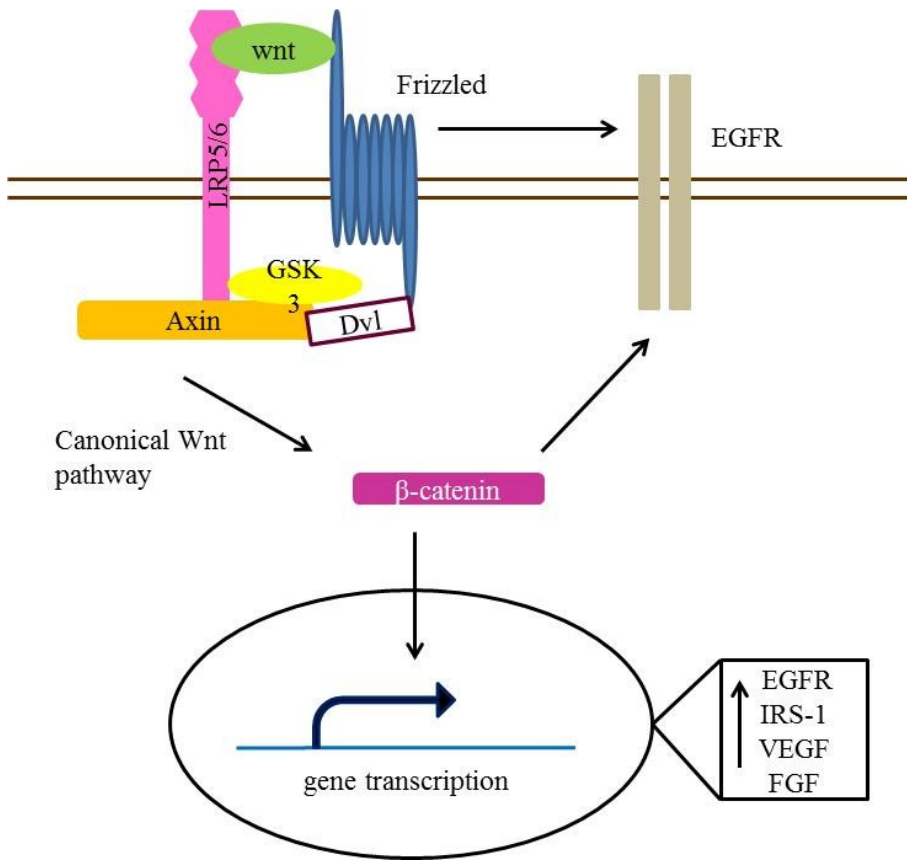


**Figure 7.2**  
**Wnt and crosstalk with other growth signalling pathways.**

Activation of Wnt signalling increases transcription of epidermal growth factor receptor (EGFR), insulin receptor substrate 1 (IRS-1), vascular endothelial growth factor (VEGF) and fibroblast growth factor (FGF). This results in crosstalk between Wnt and other growth signalling pathways: epidermal growth factor (EGF), insulin- like growth factor 1 (IGF-1), VEGF and FGF.

Adapted from Hu et al. (2010), Goss et al. (2011).

Signalling changes by Western blot also tentatively support interplay between Wnt and EGFR signalling. Treatment of Tam-R cells with TKI decreases MAPK and AKT phosphorylation (Hutcheson et al. 2006) which contribute to Tam-R growth. Our data suggest that MAPK and AKT activity is suppressed following treatment of Tam-R cells with IWP2, TKI or combination TKI – IWP2 suggesting significant pathway overlap at the level of these downstream kinases (Figure 6.7, Figure 6.8).

Further support for cross talk between the two signalling pathways in Tam-R cells comes from Affymetrix HGU-133A gene microarray data for Tam-R cells treated with gefitinib for 10 days, where changes support Wnt activation in Tam-R cells following treatment with gefitinib, and this activation was in addition to changes previously reported between Tam-R cells and MCF-7 cells. This signalling pathway interplay may be further explored through modulation of Wnt and EGFR activity in siRNA-mediated LRP6,  $\beta$ -catenin and EGFR knockdown models (Zhang et al. 2008, Zeng G 2007).

Interaction between Wnt and EGFR signalling may be important clinically. EGFR has been targeted in the context of tamoxifen resistance with limited success (Agrawal et al. 2005). Work on cellular models had suggested that combination gefitinib and tamoxifen was superior to tamoxifen treatment in MCF-7 cells as evidenced by cell growth inhibition (Gee et al. 2003). This has not been substantially replicated in phase II clinical trials. Though some success was reported in one study (Gutteridge et al. 2010), limited or no clinical benefit was generally reported following gefitinib treatment alone (Green et al. 2009) or treatment with tamoxifen

and gefitinib (Osborne et al. 2011). Work by Jones et al. (2006) has shown that MCF-7 cells develop resistance to sequential tamoxifen and gefitinib treatment and that this is coupled to increased IGF-1R activity. As Wnt can crosstalk with both EGFR and IGF-1R, targeting of Wnt alongside EGFR signalling may be a better approach in the context of tamoxifen resistance. Indeed Wnt inhibition is able to add to the effect of TKI in Tam-R cells.

However, the challenge to find the right Wnt inhibitor for clinical use is multifaceted. Wnt signalling is deregulated in several disease processes including several cancer types. The underlying mechanisms of action are diverse and often tissue dependent. Signalling may be altered as a result of genetic mutation (e.g. APC in colon cancer) or, more commonly, due to altered expression of various signalling components (e.g. downregulation of the negative Wnt regulator SFRP in breast cancer (Dahl et al. 2005)). Wnt signalling is also important for development and inhibition of some key functions and may not be compatible with normal physiological activity (Filipovich et al. 2011). It relies on a fine balance of negative and positive regulators making the choice of target level particularly challenging. Several Wnt modulators have been described in the literature but as yet none are in regular clinical use. It is estimated that 88 Wnt targeting drugs are currently being investigated for use in cancer (MarketResearch 2012). Some of these molecules are described in Table 7.1 and Table 7.2 (Nusse 2010).

<b>Drug</b>	<b>Action</b>	<b>Disease target</b>	<b>Types of studies</b>	<b>Reference</b>
Deoxycholic acid	$\beta$ -catenin activator	colon cancer	cell lines	(Pai et al. 2004)
WAY-316606	inhibits SFRP	osteoporosis	cell lines, animal models	(Bodine et al. 2009)
BIO (6-bromoindirubin-3'-oxime)	inhibits GSK3	stem cells	cell lines, animal models	(Sato et al. 2004)
SB-216763	inhibits GSK3		cell lines	(Coghlan et al. 2000)
RNF146	increases axin degradation		cell lines	(Zhang et al. 2011)

**Table 7.1**  
Wnt pathway activators.



<b>Drug</b>	<b>Action</b>	<b>Disease target</b>	<b>Types of studies</b>	<b>Reference</b>
ICG-001	CREB binding protein	colon cancer	cell lines, animal models	(Emami et al. 2004)
Ant1.4Br and Ant 1.4Cl	inhibits free Wnt ligands		cell lines, animal models	(Morrell et al. 2008)
Niclosamide	inhibits Fz		cell lines	(Chen et al. 2009b)
Apicularen and bafilomycin	inhibit vacuolar ATPase		animal models	(Cruciat et al. 2010)
IWR	activates Axin		cell lines, animal models	Chen et al. 2009a)
2,4-diamino-quinazoline	inhibits TCF/ $\beta$ -catenin	colon cancer	cell lines, animal models	(Chen et al. 2009c)
Quercetin	inhibits TCF	colon cancer	cell lines	(Park et al. 2005)
NSC668036	inhibits Dvl		animal models	(Shan et al. 2005)
OMP-18R5	antibody to Fz7	colon, breast, lung, pancreatic cancers	animal models	(Gurney et al. 2012)
Pyrvinium	inhibits CK1	colon cancer	cell lines	(Thorne et al. 2010)
XAV939	stabilizes actin		cell lines	(Huang et al. 2009)

**Table 7.2**  
Wnt pathway inhibitors.

A number of Wnt inhibitors are currently in Phase 1 clinical trials (see Table 7.3). BHQNVLP-LGK974 is being trialled in breast cancer and (like IWP2) it is a porcupine inhibitor.

<b>Drug</b>	<b>Action</b>	<b>Patient subgroup</b>	<b>Reference</b>
BHQ880	anti- DKK1 antibody	multiple myeloma	(Ettenberg S 2008)
BHQNVLP-LGK974	porcupine inhibitor	melanoma and lobular breast cancer	(Wang et al. 1993, Novartis 2011)
$\beta$ C2059	disrupts stabilization of $\beta$ -catenin		(The_ $\beta$ Catenin Company 2011)
OMP-18R5	antibody targeting Frizzled 7 receptor	solid tumours	(OncoMed_Pharmaceuticals 2011)

**Table 7.3**

Small molecule Wnt inhibitors currently in Phase I clinical trials.

Our data needs to be validated in the context of clinical material. Access to matched response clinical material may be challenging. Other labs are looking at ways of identifying Wnt pathway activation in clinical material using immunohistochemistry (personal communication with Dr A van de Stolpe, Philips Research Laboratories, Eindhoven, Netherlands): such a tool would allow us to further explore Wnt signalling in clinical relapse following tamoxifen treatment and EGFR inhibition. Work in our lab is currently underway to explore Wnt activity in other endocrine resistant breast cancer cell models.

In conclusion, our data appears to highlight an important role for Wnt signalling in the context of acquired tamoxifen- resistance. Targeting of the Wnt pathway alone, or particularly alongside the EGFR, appears an effective and selective strategy for suppressing proliferation of tamoxifen resistant cells, at least *in vitro*. The emergence of clinical Wnt inhibitors signals the start of an exciting phase in the fight against breast cancer and this project proposes these agents may be of benefit in the context of endocrine resistance.

# Chapter 8

## References

## 8 References

1. Abraham SC, Reynolds C, Lee J-H, Montgomery EA, Baisden BL, Krasinskas AM, et al. Fibromatosis of the breast and mutations involving the APC/[beta]-catenin pathway. *Human Pathology*. 2002;33(1):39-46.
2. Agrawal A, Gutteridge E, Gee JMW, Nicholson RI, Robertson JFR. Overview of tyrosine kinase inhibitors in clinical breast cancer. *Endocrine-Related Cancer*. 2005 July 1, 2005;12(Supplement 1):S135-S44.
3. Ahn Victoria E, Chu Matthew L-H, Choi H-J, Tran D, Abo A, Weis William I. Structural Basis of Wnt Signaling Inhibition by Dickkopf Binding to LRP5/6. *Developmental cell*. 2011;21(5):862-73.
4. Ai L, Tao Q, Zhong S, Fields CR, Kim W-J, Lee MW, et al. Inactivation of Wnt inhibitory factor-1 (WIF1) expression by epigenetic silencing is a common event in breast cancer. *Carcinogenesis*. [Research Support, N.I.H., Extramural Research Support, Non-U.S. Gov't]. 2006 Jul;27(7):1341-8.
5. Allred DC, Mohsin SK. Biological Features of Premalignant Disease in the Human Breast. *Journal of Mammary Gland Biology and Neoplasia*. 2000;5(4):351-64.
6. Bafico A, Liu G, Yaniv A, Gazit A, Aaronson SA. Novel mechanism of Wnt signalling inhibition mediated by Dickkopf-1 interaction with LRP6/Arrow. *Nat Cell Biol*. [10.1038/35083081]. 2001;3(7):683-6.
7. Baker R, Kent CV, Silbermann RA, Hassell JA, Young LJ, Howe LR. Pea3 transcription factors and wnt1-induced mouse mammary neoplasia. *PloS one*. 2010;5(1):e8854.
8. Bienz M, Clevers H. Armadillo/[beta]-catenin signals in the nucleus - proof beyond a reasonable doubt? *Nat Cell Biol*. [10.1038/ncb0303-179]. 2003;5(3):179-82.
9. Biosciences. [cited 2011 16 June ]; TCF/LEF reporter]. Available from: [http://www.sabiosciences.com/reporter\\_assay\\_product/HTML/CCS-018L.html](http://www.sabiosciences.com/reporter_assay_product/HTML/CCS-018L.html).

10. Bjorklund P, Svedlund J, Olsson AK, Akerstrom G, Westin G. The internally truncated LRP5 receptor presents a therapeutic target in breast cancer. *PloS one*. 2009;4 (1):e4243.
11. Björnström L, Sjöberg M. Mechanisms of Estrogen Receptor Signaling: Convergence of Genomic and Nongenomic Actions on Target Genes. *Molecular Endocrinology*. 2005 April 1, 2005;19(4):833-42.
12. Bocchinfuso WP, Hively WP, Couse JF, Varmus HE, Korach KS. A mouse mammary tumor virus Wnt-1 transgene induces mammary gland hyperplasia and tumorigenesis in mice lacking estrogen receptor- $\alpha$ . *Cancer Research*. 1999 Apr;59(8):1869-76.
13. Bodine PVN, Stauffer B, Ponce-de-Leon H, Bhat RA, Mangine A, Seestaller-Wehr LM, et al. A small molecule inhibitor of the Wnt antagonist secreted frizzled-related protein-1 stimulates bone formation. *Bone*. 2009;44(6):1063-8.
14. Borgquist S, Holm C, Stendahl M, Anagnostaki L, Landberg G, Jirstrom K. Oestrogen receptors  $\alpha$  and  $\beta$  show different associations to clinicopathological parameters and their co-expression might predict a better response to endocrine treatment in breast cancer. *Journal of Clinical Pathology*. 2008 February 1, 2008;61(2):197-203.
15. Borley A, Hiscox S, Gee J, Smith C, Shaw V, Barrett-Lee P, et al. Anti-oestrogens but not oestrogen deprivation promote cellular invasion in intercellular adhesion-deficient breast cancer cells. *Breast Cancer Research*. 2008;10(6):R103.
16. Bradford M. *Anal Biochem*. 1976;72(248).
17. Britton DJ, Hutcheson IR, Knowlden JM, Barrow D, Giles M, McClelland RA, et al. Bidirectional cross talk between ER $\alpha$  and EGFR signalling pathways regulates tamoxifen-resistant growth. *Breast Cancer Research and Treatment*. 2006;96(2):131-46.
18. Cancer\_Research\_UK. Cancer Research UK: breast cancer. 2012 [cited 2012 May]; Available from: <http://info.cancerresearchuk.org/cancerstats/types/breast/>.

19. Cao Z, Li C, Higginbotham JN, Franklin JL, Tabb DL, Graves-Deal R, et al. Use of Fluorescence-activated Vesicle Sorting for Isolation of Naked2-associated, Basolaterally Targeted Exocytic Vesicles for Proteomics Analysis. *Molecular & Cellular Proteomics*. 2008 September 2008;7(9):1651-67.
20. cell\_signalling. LRP6 (C5C7) Rabbit mAb. 2012 [cited 2102 8 May]; Available from: [www.cellsignal.com/pdf/2560.pdf](http://www.cellsignal.com/pdf/2560.pdf)
21. cell\_signalling. p-LRP6 Ser1490 antibody #2568. 2012 [cited 2012 8 May]; Available from: <http://www.cellsignal.com/products/2568.html>.
22. Chamorro MN, Schwartz DR, Vonica A, Brivanlou AH, Cho KR, Varmus HE. FGF-20 and DKK1 are transcriptional targets of [beta]-catenin and FGF-20 is implicated in cancer and development. *EMBO J*. [10.1038/sj.emboj.7600460]. 2005;24(1):73-84.
23. Chen B, Dodge ME, Tang W, Lu J, Ma Z, Fan C-W, et al. Small molecule-mediated disruption of Wnt-dependent signaling in tissue regeneration and cancer. *Nat Chem Biol*. [10.1038/nchembio.137]. 2009;5(2):100-7.
24. Chen M, Wang J, Lu J, Bond MC, Ren X-R, Lysterly HK, et al. The Anti-Helminthic Niclosamide Inhibits Wnt/Frizzled1 Signaling. *Biochemistry*. 2009/11/03;48(43):10267-74.
25. Chen S, Bubeck D, MacDonald Bryan T, Liang W-X, Mao J-H, Malinauskas T, et al. Structural and Functional Studies of LRP6 Ectodomain Reveal a Platform for Wnt Signaling. *Developmental cell*. 2011;21(5):848-61.
26. Chen Z, Venkatesan AM, Dehnhardt CM, Santos OD, Santos ED, Ayrall-Kaloustian S, et al. 2,4-Diamino-quinazolines as inhibitors of  $\beta$ -catenin/Tcf-4 pathway: Potential treatment for colorectal cancer. *Bioorganic & Medicinal Chemistry Letters*. 2009;19(17):4980-3.
27. Civenni G HT, and Hynes NE. Wnt1 and Wnt5a induce cyclin D1 expression through ErbB1 transactivation in HC11 mammary epithelial cells. *EBMO Reports*. 2003;Feb; 4(2):166-71.
28. Clevers H. Wnt Signaling: Ig-Norrin the Dogma. *Current biology : CB*. 2004;14(11):R436-R7.

29. Coghlan MP, Culbert AA, Cross DAE, Corcoran SL, Yates JW, Pearce NJ, et al. Selective small molecule inhibitors of glycogen synthase kinase-3 modulate glycogen metabolism and gene transcription. *Chemistry & biology*. 2000;7(10):793-803.
30. Collu GM, Brennan K. Cooperation between Wnt and Notch signalling in human breast cancer. *Breast Cancer Research*. [Research Support, Non-U.S. Gov't]. 2007;9(3):105.
31. Cong F, Varmus H. Nuclear-cytoplasmic shuttling of Axin regulates subcellular localization of  $\beta$ -catenin. *Proceedings of the National Academy of Sciences of the United States of America*. 2004 March 2, 2004;101(9):2882-7.
32. Corning. Transwell permeable supports selection and use guide. 2012 [cited 2012 19 April]; Available from: [http://catalog2.corning.com/Lifesciences/media/pdf/transwell\\_guide.pdf](http://catalog2.corning.com/Lifesciences/media/pdf/transwell_guide.pdf).
33. Covey TM, Kaur S, Tan Ong T, Proffitt KD, Wu Y, Tan P, et al. PORCN Moonlights in a Wnt-Independent Pathway That Regulates Cancer Cell Proliferation. *PloS one*. 2012;7(4):e34532.
34. Cruciat C-M, Ohkawara B, Acebron SP, Karaulanov E, Reinhard C, Ingelfinger D, et al. Requirement of Prorenin Receptor and Vacuolar H<sup>+</sup>-ATPase-Mediated Acidification for Wnt Signaling. *Science*. 2010 January 22, 2010;327(5964):459-63.
35. Dahl E, Veeck J, An H, Wiesmann F, Klopocki E, Sauter G, et al. Epigenetic inactivation of the WNT antagonist SFRP1 in breast cancer. *Epigenetische Inaktivierung des WNT-Antagonisten SFRP1 im Mammakarzinom*. 2005;89:169-77.
36. Dudoit S, Shaffer JP, Boldrick JC. Multiple Hypothesis Testing in Microarray Experiments. *Statistical Science*. 2003;18(1):71-103.
37. Dulaimi E, Hillinck J, de Caceres II, Al-Saleem T, Cairns P. Tumor Suppressor Gene Promoter Hypermethylation in Serum of Breast Cancer Patients. *Clinical Cancer Research*. 2004 September 15, 2004;10(18):6189-93.



38. Early Breast Cancer Trialists' Collaborative G. Relevance of breast cancer hormone receptors and other factors to the efficacy of adjuvant tamoxifen: patient-level meta-analysis of randomised trials. *The Lancet*. 2011;378(9793):771-84.
39. El-Tanani M, Fernig DG, Barraclough R, Green C, Rudland P. Differential Modulation of Transcriptional Activity of Estrogen Receptors by Direct Protein-Protein Interactions with the T Cell Factor Family of Transcription Factors. *Journal of Biological Chemistry*. 2001 November 9, 2001;276(45):41675-82.
40. Emami KH, Nguyen C, Ma H, Kim DH, Jeong KW, Eguchi M, et al. A small molecule inhibitor of  $\beta$ -catenin/cyclic AMP response element-binding protein transcription. *Proceedings of the National Academy of Sciences of the United States of America*. 2004 August 24, 2004;101(34):12682-7.
41. Ettenberg S CF, Shulok J, et al. BHQ880, a novel anti-DKK1 neutralizing antibody, inhibits tumor-induced osteolytic bone disease. *American Association for Cancer Research Annual Meeting*; April 12–16, 2008; San Diego, California 2008.
42. Faivre EJ, Lange CA. Progesterone Receptors Upregulate Wnt-1 To Induce Epidermal Growth Factor Receptor Transactivation and c-Src-Dependent Sustained Activation of Erk1/2 Mitogen-Activated Protein Kinase in Breast Cancer Cells. *Molecular and Cellular Biology*. 2007 January 15, 2007;27(2):466-80.
43. Fan P, Wang J, Santen RJ, Yue W. Long-term Treatment with Tamoxifen Facilitates Translocation of Estrogen Receptor  $\alpha$  out of the Nucleus and Enhances its Interaction with EGFR in MCF-7 Breast Cancer Cells. *Cancer Research*. 2007 February 1, 2007;67(3):1352-60.
44. Filipovich A, Gehrke I, Poll-Wolbeck SJ, Kreuzer K-A. Physiological inhibitors of Wnt signaling. *European Journal of Haematology*. 2011;86(6):453-65.
45. Forget MA, Turcotte S, Beauseigle D, Godin-Ethier J, Pelletier S, Martin J, et al. The Wnt pathway regulator DKK1 is preferentially expressed in hormone-resistant breast tumours and in some common cancer types. *British Journal of Cancer*. [Research Support, Non-U.S. Gov't]. 2007 Feb 26;96(4):646-53.
46. Fuqua SAW, Allred DC, Auchus RJ. Expression of estrogen receptor variants. *Journal of Cellular Biochemistry*. 1993;53(S17G):194-7.

47. Furuuchi K, Tada M, Yamada H, Kataoka A, Furuuchi N, Hamada J-i, et al. Somatic Mutations of the APC Gene in Primary Breast Cancers. *The American Journal of Pathology*. 2000;156(6):1997-2005.
48. Gan X-q, Wang J-y, Xi Y, Wu Z-l, Li Y-p, Li L. Nuclear Dvl, c-Jun,  $\beta$ -catenin, and TCF form a complex leading to stabilization of  $\beta$ -catenin–TCF interaction. *The Journal of Cell Biology*. 2008 March 24, 2008;180(6):1087-100.
49. Gee JM, Robertson JF, Gutteridge E, Ellis IO, Pinder SE, Rubini M, et al. Epidermal growth factor receptor/HER2/insulin-like growth factor receptor signalling and oestrogen receptor activity in clinical breast cancer. *Endocrine-Related Cancer*. 2005 July 1, 2005;12(Supplement 1):S99-S111.
50. Gee JMW, Harper ME, Hutcheson IR, Madden TA, Barrow D, Knowlden JM, et al. The Antiepidermal Growth Factor Receptor Agent Gefitinib (ZD1839/Iressa) Improves Antihormone Response and Prevents Development of Resistance in Breast Cancer in Vitro. *Endocrinology*. 2003 November 1, 2003;144(11):5105-17.
51. Gee JMW, Howell A, Gullick WJ, Benz CC, Sutherland RL, Santen RJ, et al. Consensus Statement. *Endocrine-Related Cancer*. 2005 July 1, 2005;12(Supplement 1):S1-S7.
52. GeneCards. GeneCards. 2012 [cited 2012 24 March ]; Available from: <http://www.genecards.org/index.php?path=/Search/keyword/>.
53. Girault I, Lerebours F, Amarir S, Tozlu S, Tubiana-Hulin M, Lidereau R, et al. Expression Analysis of Estrogen Receptor  $\alpha$  Coregulators in Breast Carcinoma. *Clinical Cancer Research*. 2003 April 1, 2003;9(4):1259-66.
54. Glinka A, Wu W, Delius H, Monaghan AP, Blumenstock C, Niehrs C. Dickkopf-1 is a member of a new family of secreted proteins and functions in head induction. *Nature*. [10.1038/34848]. 1998;391(6665):357-62.
55. Goetz M, Knox S, Suman V, Rae J, Safgren S, Ames M, et al. The impact of cytochrome P450 2D6 metabolism in women receiving adjuvant tamoxifen. *Breast Cancer Research and Treatment*. 2007;101(1):113-21.

56. Goetz MP, Rae JM, Suman VJ, Safgren SL, Ames MM, Visscher DW, et al. Pharmacogenetics of Tamoxifen Biotransformation Is Associated With Clinical Outcomes of Efficacy and Hot Flashes. *Journal of Clinical Oncology*. 2005 December 20, 2005;23(36):9312-8.
57. Gonsalves FC, Klein K, Carson BB, Katz S, Ekas LA, Evans S, et al. An RNAi-based chemical genetic screen identifies three small-molecule inhibitors of the Wnt/wingless signaling pathway. *Proceedings of the National Academy of Sciences of the United States of America*. 2011;108(15):5954-63.
58. Goss K KM, editor. *Targeting the Wnt Pathway in Cancer*: Springer; 2011.
59. Green MD, Francis PA, Gebiski V, Harvey V, Karapetis C, Chan A, et al. Gefitinib treatment in hormone-resistant and hormone receptor-negative advanced breast cancer. *Annals of Oncology*. 2009 November 1, 2009;20(11):1813-7.
60. Gschwind A, Hart S, Fischer OM, Ullrich A. TACE cleavage of proamphiregulin regulates GPCR-induced proliferation and motility of cancer cells. *EMBO J*. [10.1093/emboj/cdg231]. 2003;22(10):2411-21.
61. Gujral TS, MacBeath G. A System-Wide Investigation of the Dynamics of Wnt Signaling Reveals Novel Phases of Transcriptional Regulation. *PloS one*. 2010;5(4):e10024.
62. Gunnar Schulte JD, Matthias Lauth, Tilman Polonio. Frizzled receptors, introductory chapter. 2012 [updated 8 May 2009; cited 2012 7 March]; Available from: <http://www.iuphar-db.org/DATABASE/FamilyIntroductionForward?familyId=25>. .
63. Gurney A, Axelrod F, Bond CJ, Cain J, Chartier C, Donigan L, et al. Wnt pathway inhibition via the targeting of Frizzled receptors results in decreased growth and tumorigenicity of human tumors. *Proceedings of the National Academy of Sciences*. 2012 July 17, 2012;109(29):11717-22.
64. Gutteridge E, Agrawal A, Nicholson R, Leung Cheung K, Robertson J, Gee J. The effects of gefitinib in tamoxifen-resistant and hormone-insensitive breast cancer: A phase II study. *International Journal of Cancer*. 2010;126(8):1806-16.

65. Habas R, Dawid I. Dishevelled and Wnt signaling: is the nucleus the final frontier? *Journal of Biology*. 2005;4(1):2.
66. Hanahan D, Weinberg RA. The Hallmarks of Cancer. *Cell*. 2000;100(1):57-70.
67. Harris JL, ME; Morrow. M; Osborne, CK, editor. *Diseases of the Breast* (Harris). Third ed: Lippincott Williams & Wilkins; 2004.
68. Hayes MJ, Thomas D, Emmons A, Giordano TJ, Kleer CG. Genetic changes of Wnt pathway genes are common events in metaplastic carcinomas of the breast. *Clinical Cancer Research*. [Research Support, N.I.H., Extramural Research Support, Non-U.S. Gov't]. 2008 Jul 1;14(13):4038-44.
69. He X. Antagonizing Wnt and FGF Receptors: an Enemy from within (the ER). *Cell*. 2005;120(2):156-8.
70. Henderson BRF, F. The ins and outs of APC and  $\beta$ -catenin nuclear transport. *EBMO Reports*. 2002;3(9):834-9.
71. Hendriksen J, Fagotto F, van der Velde H, van Schie M, Noordermeer J, Fornerod M. RanBP3 enhances nuclear export of active  $\beta$ -catenin independently of CRM1. *The Journal of Cell Biology*. 2005 December 5, 2005;171(5):785-97.
72. Herynk MH, Fuqua SAW. Estrogen Receptor Mutations in Human Disease. *Endocrine Reviews*. 2004 December 1, 2004;25(6):869-98.
73. Heuberger J BW. Interplay of cadherin-mediated cell adhesion and canonical Wnt signaling. *Cold Spring Harb Perspect Biol*. 2010;Feb;2(2):a002915.
74. Hiscox S, Jiang WG, Obermeier K, Taylor K, Morgan L, Burmi R, et al. Tamoxifen resistance in MCF7 cells promotes EMT-like behaviour and involves modulation of  $\beta$ -catenin phosphorylation. *International Journal of Cancer*. 2006;118(2):290-301.
75. Hiscox S JN, Smith C, James M, Morgan L, Taylor KM, Green TP, Nicholson RI. Dual targeting of Src and ER prevents acquired antihormone resistance in breast cancer cells. *Breast Cancer Res Treat*. 2009;115(1):57-67.

76. Ho, Kalle, Lo, Lam, Tang. Reduced expression of APC and DCC gene protein in breast cancer. *Histopathology*. 1999;35(3):249-56.
77. Hopp TA, Weiss HL, Parra IS, Cui Y, Osborne CK, Fuqua SAW. Low Levels of Estrogen Receptor  $\beta$  Protein Predict Resistance to Tamoxifen Therapy in Breast Cancer. *Clinical Cancer Research*. 2004 November 15, 2004;10(22):7490-9.
78. Hu T, Krezel AM, Li C, Coffey RJ. Structural studies of human Naked2: A biologically active intrinsically unstructured protein. *Biochemical and Biophysical Research Communications*. 2006;350(4):911-5.
79. Hu T, Li C. Convergence between Wnt-beta-catenin and EGFR signaling in cancer. *Molecular Cancer*. 2010;9(1):236.
80. Hu T, Li C, Cao Z, Van Raay TJ, Smith JG, Willert K, et al. Myristoylated Naked2 Antagonizes Wnt- $\beta$ -Catenin Activity by Degrading Dishevelled-1 at the Plasma Membrane. *Journal of Biological Chemistry*. 2010 April 30, 2010;285(18):13561-8.
81. Huang S, Chen Y, Podsypanina K, Li Y. Comparison of expression profiles of metastatic versus primary mammary tumors in MMTV-Wnt-1 and MMTV-Nuc transgenic mice. *Neoplasia*. 2008;10(2):118-24.
82. Huang S, Podsypanina K, Chen Y, Cai W, Tsimelzon A, Hilsenbeck S, et al. Wnt-1 is dominant over neu in specifying mammary tumor expression profiles. *Technology in Cancer Research & Treatment*. [Research Support, N.I.H., Extramural]. 2006 Dec;5(6):565-71.
83. Huang S-MA, Mishina YM, Liu S, Cheung A, Stegmeier F, Michaud GA, et al. Tankyrase inhibition stabilizes axin and antagonizes Wnt signalling. *Nature*. [10.1038/nature08356]. 2009;461(7264):614-20.
84. Huguet EL, McMahon JA, McMahon AP, Bicknell R, Harris AL. Differential expression of human Wnt gene-2, gene-3, gene-4, and gene-7b in human breast cell- lines and normal and disease states of human breast tissue. *Cancer Research*. 1994 May;54(10):2615-21.

85. Hutcheson IR, Knowlden JM, Jones HE, Burmi RS, McClelland RA, Barrow D, et al. Inductive mechanisms limiting response to anti-epidermal growth factor receptor therapy. *Endocr Relat Cancer*. 2006 Dec;13 Suppl 1:S89-97.
86. Hutcheson IR, Knowlden JM, Madden T-A, Barrow D, Gee JMW, Wakeling AE, et al. Oestrogen Receptor-Mediated Modulation of the EGFR/MAPK Pathway in Tamoxifen-Resistant MCF-7 Cells. *Breast Cancer Research and Treatment*. 2003;81(1):81-93.
87. Hynes NE, Lane HA. ERBB receptors and cancer: the complexity of targeted inhibitors. *Nat Rev Cancer*. [10.1038/nrc1609]. 2005;5(5):341-54.
88. Inadera H, Dong H-Y, Matsushima K. WISP-2 is a secreted protein and can be a marker of estrogen exposure in MCF-7 cells. *Biochemical and Biophysical Research Communications*. 2002;294(3):602-8.
89. Iozzo RV, Eichstetter I, Danielson KG. Aberrant expression of the growth-factor Wnt-5a in human malignancy. *Cancer Research*. 1995 Aug;55(16):3495-9.
90. Jarno L. Studies of the activation of metabolism of Retinoic Acid in MCF-7 human breast cancer cells. Cardiff: University of Cardiff; 2003.
91. Jin Y, Desta Z, Stearns V, Ward B, Ho H, Lee K-H, et al. CYP2D6 Genotype, Antidepressant Use, and Tamoxifen Metabolism During Adjuvant Breast Cancer Treatment. *Journal of the National Cancer Institute*. 2005 January 5, 2005;97(1):30-9.
92. Jin Z, Tamura G, Tsuchiya T, Sakata K, Kashiwaba M, Osakabe M, et al. Adenomatous polyposis coli (APC) gene promoter hypermethylation in primary breast cancers. *Br J Cancer*. 2001;85(1):69-73.
93. Johnston SRD. New Strategies in Estrogen Receptor–Positive Breast Cancer. *Clinical Cancer Research*. 2010 April 1, 2010;16(7):1979-87.
94. Jones HE, Gee JMW, Hutcheson IR, Knowlden JM, Barrow D, Nicholson RI. Growth factor receptor interplay and resistance in cancer. *Endocrine-Related Cancer*. 2006 December 1, 2006;13(Supplement 1):S45-S51.

95. Jönsson M, Borg Å, Nilbert M, Andersson T. Involvement of adenomatous polyposis coli (APC)/ $\beta$ -catenin signalling in human breast cancer. *European journal of cancer* (Oxford, England : 1990). 2000;36(2):242-8.
96. Jordan NJ, Gee JMW, Barrow D, Wakeling AE, Nicholson RI. Increased Constitutive Activity of PKB/Akt in Tamoxifen Resistant Breast Cancer MCF-7 Cells. *Breast Cancer Research and Treatment*. 2004;87(2):167-80.
97. Jordan VC, Chen C. Metabolites of tamoxifen in animals and man: Identification, pharmacology, and significance. *Breast Cancer Research and Treatment*. 1982;2(2):123-38.
98. Kashiwaba M, Tamura G, Ishida M. Aberrations of the APC gene in primary breast carcinoma. *J Cancer Res Clin Oncol*. 1994;120(12):727-31.
99. Katanaev VL, Solis GP, Hausmann G, Buestorf S, Katanayeva N, Schrock Y, et al. Reggie-1/flotillin-2 promotes secretion of the long-range signalling forms of Wingless and Hedgehog in *Drosophila*. *EMBO J*. [10.1038/sj.emboj.7601981]. 2008;27(3):509-21.
100. Katoh M. Molecular cloning, gene structure, and expression analyses of NKD1 and NKD2. *Int J Oncol*. 2001;19(5):963-9.
101. Katoh M. Expression and regulation of WNT1 in human cancer: up-regulation of WNT1 by beta-estradiol in MCF-7 cells. *International Journal of Oncology*. [Research Support, Non-U.S. Gov't]. 2003 Jan;22(1):209-12.
102. Kawano Y, Kypta R. Secreted antagonists of the Wnt signalling pathway. *Journal of Cell Science*. 2003 July 1, 2003;116(13):2627-34.
103. Kazanskaya O, Glinka A, del Barco Barrantes I, Stanek P, Niehrs C, Wu W. R-Spondin2 Is a Secreted Activator of Wnt/ $\beta$ -Catenin Signaling and Is Required for *Xenopus* Myogenesis. *Developmental cell*. 2004;7(4):525-34.
104. Khan Z, Vijayakumar S, de la Torre TV, Rotolo S, Bafico A. Analysis of Endogenous LRP6 Function Reveals a Novel Feedback Mechanism by Which Wnt Negatively Regulates Its Receptor. *Molecular and Cellular Biology*. 2007 October 15, 2007;27(20):7291-301.

105. Khramtsov AI, Khramtsova GF, Tretiakova M, Huo D, Olopade OI, Goss KH. Wnt/ $\beta$ -catenin pathway activation is enriched in basal-like breast cancers and predicts poor outcome. *American Journal of Pathology*. 2010;176(6):2911-20.
106. Kim K-A, Wagle M, Tran K, Zhan X, Dixon MA, Liu S, et al. R-Spondin Family Members Regulate the Wnt Pathway by a Common Mechanism. *Molecular Biology of the Cell*. 2008 June 1, 2008;19(6):2588-96.
107. Kirkegaard T, McGlynn LM, Campbell FM, Müller S, Tovey SM, Dunne B, et al. Amplified in Breast Cancer 1 in Human Epidermal Growth Factor Receptor–Positive Tumors of Tamoxifen-Treated Breast Cancer Patients. *Clinical Cancer Research*. 2007 March 1, 2007;13(5):1405-11.
108. Kizildag S, Zengel B, Vardar E, Sakizli M. beta-catenin gene mutation in invasive ductal breast cancer. *J Buon*. 2008;13(4):533-6.
109. Klemm F, Bleckmann A, Siam L, Chuang HN, Rietkötter E, Behme D, et al.  $\beta$ -catenin-independent WNT signaling in basal-like breast cancer and brain metastasis. *Carcinogenesis*. 2011 March 1, 2011;32(3):434-42.
110. Knowlden J, Jones H, Barrow D, Gee J, Nicholson R, Hutcheson I. Insulin receptor substrate-1 involvement in epidermal growth factor receptor and insulin-like growth factor receptor signalling: implication for Gefitinib ('Iressa') response and resistance. *Breast Cancer Research and Treatment*. 2008;111(1):79-91.
111. Knowlden JM, Gee JMW, Robertson JFR, Ellis IO, Nicholson RI. A possible divergent role for the oestrogen receptor alpha and beta subtypes in clinical breast cancer. *International Journal of Cancer*. 2000;89(2):209-12.
112. Knowlden JM, Hutcheson IR, Barrow D, Gee JMW, Nicholson RI. Insulin-Like Growth Factor-I Receptor Signaling in Tamoxifen-Resistant Breast Cancer: A Supporting Role to the Epidermal Growth Factor Receptor. *Endocrinology*. 2005 November 1, 2005;146(11):4609-18.
113. Knowlden JM, Hutcheson IR, Jones HE, Madden T, Gee JMW, Harper ME, et al. Elevated Levels of Epidermal Growth Factor Receptor/c-erbB2 Heterodimers Mediate an Autocrine Growth Regulatory Pathway in Tamoxifen-Resistant MCF-7 Cells. *Endocrinology*. 2003 March 1, 2003;144(3):1032-44.



114. Kouzmenko AP, Takeyama K-i, Ito S, Furutani T, Sawatsubashi S, Maki A, et al. Wnt/ $\beta$ -Catenin and Estrogen Signaling Converge in Vivo. *Journal of Biological Chemistry*. 2004 September 24, 2004;279(39):40255-8.
115. Lacroix M LG. Relevance of breast cancer cell lines as models for breast tumours: an update. *Breast Cancer Res Treat*. 2004;83(3):249-89.
116. Landesman-Bollag E, Romieu-Mourez R, Song DH, Sonenshein GE, Cardiff RD, Seldin DC. Protein kinase CK2 in mammary gland tumorigenesis. *Oncogene*. [Research Support, Non-U.S. Gov't  
Research Support, U.S. Gov't, Non-P.H.S.  
Research Support, U.S. Gov't, P.H.S.]. 2001 May 31;20(25):3247-57.
117. Lawson JS, Glenn WK, Salmons B, Ye Y, Heng B, Moody P, et al. Mouse mammary tumor virus-like sequences in human breast cancer. *Cancer Research*. [Research Support, Non-U.S. Gov't]. 2010 May 1;70(9):3576-85.
118. Lejeune S, Huguet EL, Hamby A, Poulsom R, Harris AL. Wnt5a cloning, expression, and up-regulation in human primary breast cancers. *Clinical Cancer Research*. [Research Support, Non-U.S. Gov't]. 1995 Feb;1(2):215-22.
119. Lepourcelet M, Chen Y-NP, France DS, Wang H, Crews P, Petersen F, et al. Small-molecule antagonists of the oncogenic Tcf/ $\beta$ -catenin protein complex. *Cancer cell*. 2004;5(1):91-102.
120. Lewis JS, Jordan VC. Selective estrogen receptor modulators (SERMs): Mechanisms of anticarcinogenesis and drug resistance. *Mutation Research/Fundamental and Molecular Mechanisms of Mutagenesis*. 2005;591(1–2):247-63.
121. Li C, Franklin JL, Graves-Deal R, Jerome WG, Cao Z, Coffey RJ. Myristoylated Naked2 escorts transforming growth factor  $\alpha$  to the basolateral plasma membrane of polarized epithelial cells. *Proceedings of the National Academy of Sciences of the United States of America*. 2004 April 13, 2004;101(15):5571-6.
122. Li C, Hao M, Cao Z, Ding W, Graves-Deal R, Hu J, et al. Naked2 Acts as a Cargo Recognition and Targeting Protein to Ensure Proper Delivery and Fusion of

TGF- $\alpha$ -containing Exocytic Vesicles at the Lower Lateral Membrane of Polarized MDCK Cells. *Molecular Biology of the Cell*. 2007 August 1, 2007;18(8):3081-93.

123. Li X, Zhang Y, Kang H, Liu W, Liu P, Zhang J, et al. Sclerostin Binds to LRP5/6 and Antagonizes Canonical Wnt Signaling. *Journal of Biological Chemistry*. 2005 May 20, 2005;280(20):19883-7.

124. Li Y, Hively WP, Varmus HE. Use of MMTV-Wnt-1 transgenic mice for studying the genetic basis of breast cancer. *Oncogene*. [Research Support, U.S. Gov't, Non-P.H.S.

Review]. 2000 Feb 21;19(8):1002-9.

125. Lin SY, Xia WY, Wang JC, Kwong KY, Spohn B, Wen Y, et al. beta-catenin, a novel prognostic marker for breast cancer: Its roles in cyclin D1 expression and cancer progression. *Proceedings of the National Academy of Sciences of the United States of America*. 2000 Apr;97(8):4262-6.

126. Lin X. Functions of heparan sulfate proteoglycans in cell signaling during development. *Development*. 2004 December 15, 2004;131(24):6009-21.

127. Lindvall C, Zylstra CR, Evans N, West RA, Dykema K, Furge KA, et al. The Wnt Co-Receptor Lrp6 Is Required for Normal Mouse Mammary Gland Development. *PloS one*. 2009;4(6):e5813.

128. Liu C-C, Prior J, Piwnica-Worms D, Bu G. LRP6 overexpression defines a class of breast cancer subtype and is a target for therapy. *Proceedings of the National Academy of Sciences of the United States of America*. [Research Support, N.I.H., Extramural

Research Support, Non-U.S. Gov't]. 2010 Mar 16;107(11):5136-41.

129. Logan CY, Nusse R. The Wnt signaling pathway in development and disease. *Annual Review of Cell and Developmental Biology*. 2004;20(1):781-810.

130. López-Knowles E, Zardawi SJ, McNeil CM, Millar EKA, Crea P, Musgrove EA, et al. Cytoplasmic localization of  $\beta$ -catenin is a marker of poor outcome in breast cancer patients. *Cancer Epidemiology Biomarkers and Prevention*. 2010;19(1):301-9.

131. MacDonald BT, Tamai K, He X. Wnt/ $\beta$ -Catenin Signaling: Components, Mechanisms, and Diseases. *Developmental cell*. 2009;17(1):9-26.
132. Madden TA. Gene inhibition studies on estrogen receptor function in breast cancer. Cardiff: Cardiff University; 2004.
133. Maher MT, Mo R, Flozak AS, Peled ON, Gottardi CJ.  $\beta$ -Catenin Phosphorylated at Serine 45 Is Spatially Uncoupled from  $\beta$ -Catenin Phosphorylated in the GSK3 Domain: Implications for Signaling. *PloS one*. 2010;5(4):e10184.
134. Mai M, Qian C, Yokomizo A, Smith DI, Liu W. Cloning of the Human Homolog of Conductin (AXIN2), a Gene Mapping to Chromosome 17q23–q24. *Genomics*. 1999;55(3):341-4.
135. MarketResearch. Wnt Signaling Pathway in Oncology Drug Pipeline Update. 2012 [cited 2012 6 April]; Available from: <http://www.marketresearch.com/BioSeeker-Group-AB-v2583/Wnt-Signaling-Pathway-Oncology-Drug-6837266/>.
136. Mastroianni M, Kim S, Kim YC, Esch A, Wagner C, Alexander CM. Wnt signaling can substitute for estrogen to induce division of ER $\alpha$ -positive cells in a mouse mammary tumor model. *Cancer Letters*. 2010;289(1):23-31.
137. Matsuda Y, Schlange T, Oakeley E, Boulay A, Hynes N. WNT signaling enhances breast cancer cell motility and blockade of the WNT pathway by sFRP1 suppresses MDA-MB-231 xenograft growth. *Breast Cancer Research*. 2009;11(3):R32.
138. McClelland RA, Barrow D, Madden T-A, Dutkowski CM, Pamment J, Knowlden JM, et al. Enhanced Epidermal Growth Factor Receptor Signaling in MCF7 Breast Cancer Cells after Long-Term Culture in the Presence of the Pure Antiestrogen ICI 182,780 (Faslodex). *Endocrinology*. 2001 July 1, 2001;142(7):2776-88.
139. Molenaar M, van de Wetering M, Oosterwegel M, Peterson-Maduro J, Godsave S, Korinek V, et al. XTcf-3 Transcription Factor Mediates  $\beta$ -Catenin-Induced Axis Formation in *Xenopus* Embryos. *Cell*. 1996;86(3):391-9.

140. Morrell NT, Leucht P, Zhao L, Kim J-B, ten Berge D, Ponnusamy K, et al. Liposomal Packaging Generates Wnt Protein with In Vivo Biological Activity. *PloS one*. 2008;3(8):e2930.
141. Mulholland DJ, Dedhar S, Coetzee GA, Nelson CC. Interaction of Nuclear Receptors with the Wnt/ $\beta$ -Catenin/Tcf Signaling Axis: Wnt You Like to Know? *Endocrine Reviews*. 2005 December 1, 2005;26(7):898-915.
142. Musgrove E. Wnt signalling via the epidermal growth factor receptor: a role in breast cancer? *Breast Cancer Res*. 2004;6(2):65 - 8.
143. Nakopoulou L, Mylona E, Papadaki I, Kavantzias N, Giannopoulou I, Markaki S, et al. Study of phospho- $\beta$ -catenin subcellular distribution in invasive breast carcinomas in relation to their phenotype and the clinical outcome. *Modern Pathology*. 2006;19(4):556-63.
144. Nicholson R, Hutcheson I, Jones H, Hiscox S, Giles M, Taylor K, et al. Growth factor signalling in endocrine and anti-growth factor resistant breast cancer. *Reviews in Endocrine & Metabolic Disorders*. 2007;8(3):241-53.
145. Nicholson RI, Hutcheson IR, Hiscox SE, Knowlden JM, Giles M, Barrow D, et al. Growth factor signalling and resistance to selective oestrogen receptor modulators and pure anti-oestrogens: the use of anti-growth factor therapies to treat or delay endocrine resistance in breast cancer. *Endocrine-Related Cancer*. 2005 July 1, 2005;12(Supplement 1):S29-S36.
146. Nicholson RI, Staka C, Boyns F, Hutcheson IR, Gee JMW. Growth factor-driven mechanisms associated with resistance to estrogen deprivation in breast cancer: new opportunities for therapy. *Endocrine-Related Cancer*. 2004 December 1, 2004;11(4):623-41.
147. Normanno N, Di Maio M, De Maio E, De Luca A, de Matteis A, Giordano A, et al. Mechanisms of endocrine resistance and novel therapeutic strategies in breast cancer. *Endocrine-Related Cancer*. 2005 December 1, 2005;12(4):721-47.
148. Novartis. A Study of Oral LGK974 in Patients With Melanoma and Lobular Breast Cancer. 2011 [updated December 21, 2011 cited 2012 21 March];

- NCT01351103]. Available from: <http://clinicaltrials.gov/ct2/show/NCT01351103?intr=%22LGK974%22&rank=1>.
149. Nusse R, Varmus HE. Many tumors induced by the mouse mammary tumor virus contain a provirus integrated in the same region of the host genome. *Cell*. 1982;31(1):99-109.
150. Nusse RaL, X. The Wnt Homepage. 2010 [cited 2012 22 March]; Available from: <http://www.stanford.edu/group/nusselab/cgi-bin/wnt/smallmolecules>.
151. O'Brien W, Klein P. Validating GSK3 as an in vivo target of lithium action. *Biochem Soc Trans*. 2009;Oct(37(Pt 5)):1133-8.
152. OncoMed\_Pharmaceuticals. A Dose Escalation Study of OMP-18R5 in Subjects With Solid Tumors. 2011 [updated December 14, 2011; cited 2012 21 March]; Available from: <http://clinicaltrials.gov/ct2/show/record/NCT01345201>.
153. Osborne CK, Bardou V, Hopp TA, Chamness GC, Hilsenbeck SG, Fuqua SAW, et al. Role of the Estrogen Receptor Coactivator AIB1 (SRC-3) and HER-2/neu in Tamoxifen Resistance in Breast Cancer. *Journal of the National Cancer Institute*. 2003 March 5, 2003;95(5):353-61.
154. Osborne CK, Neven P, Dirix LY, Mackey JR, Robert J, Underhill C, et al. Gefitinib or Placebo in Combination with Tamoxifen in Patients with Hormone Receptor–Positive Metastatic Breast Cancer: A Randomized Phase II Study. *Clinical Cancer Research*. 2011 March 1, 2011;17(5):1147-59.
155. Osborne CK, Schiff R. Estrogen-Receptor Biology: Continuing Progress and Therapeutic Implications. *Journal of Clinical Oncology*. 2005 March 10, 2005;23(8):1616-22.
156. Osborne CK, Schiff R. Mechanisms of Endocrine Resistance in Breast Cancer. *Annual Review of Medicine*. 2011;62(1):233-47.
157. Osborne CK, Zhao H, Fuqua SAW. Selective Estrogen Receptor Modulators: Structure, Function, and Clinical Use. *Journal of Clinical Oncology*. 2000 September 17, 2000;18(17):3172-86.

158. Otton SV, Ball SE, Cheung SW, Inaba T, Rudolph RL, Sellers EM. Venlafaxine oxidation in vitro is catalysed by CYP2D6. *British Journal of Clinical Pharmacology*. 1996;41(2):149-56.
159. Ozaki S, Ikeda S, Ishizaki Y, Kurihara T, Tokumoto N, Iseki M, et al. Alterations and correlations of the components in the Wnt signaling pathway and its target genes in breast cancer. *Oncology Reports*. [Research Support, Non-U.S. Gov't]. 2005 Dec;14(6):1437-43.
160. Pai R, Tarnawski AS, Tran T. Deoxycholic Acid Activates  $\beta$ -Catenin Signaling Pathway and Increases Colon Cell Cancer Growth and Invasiveness. *Molecular Biology of the Cell*. 2004 May 1, 2004;15(5):2156-63.
161. Panakova D, Sprong H, Marois E, Thiele C, Eaton S. Lipoprotein particles are required for Hedgehog and Wntless signalling. *Nature*. [10.1038/nature03504]. 2005;435(7038):58-65.
162. Park CH, Chang JY, Hahm ER, Park S, Kim H-K, Yang CH. Quercetin, a potent inhibitor against  $\beta$ -catenin/Tcf signaling in SW480 colon cancer cells. *Biochemical and Biophysical Research Communications*. 2005;328(1):227-34.
163. Pettersson K DF, Gustafsson JA. Estrogen receptor beta acts as a dominant regulator of estrogen signaling. *Oncogene*. 2000;Oct 12(19 (43)):4970-80.
164. Prasad CP, Mirza S, Sharma G, Prashad R, DattaGupta S, Rath G, et al. Epigenetic alterations of CDH1 and APC genes: Relationship with activation of Wnt/[beta]-catenin Pathway in invasive ductal carcinoma of breast. *Life Sciences*. 2008;83(9-10):318-25.
165. Prasad CP, Rath G, Mathur S, Bhatnagar D, Parshad R, Ralhan R. Expression analysis of E-cadherin, Slug and GSK3 $\beta$  in invasive ductal carcinoma of breast. *BMC Cancer*. 2009;9:325.
166. Prenzel N, Zwick E, Daub H, Leserer M, Abraham R, Wallasch C, et al. EGF receptor transactivation by G-protein-coupled receptors requires metalloproteinase cleavage of proHB-EGF. *Nature*. [10.1038/47260]. 1999;402(6764):884-8.
167. Ravdin PM. A Review of the 1998 Overview Analysis of Randomized Adjuvant Tamoxifen Breast Cancer Trials. 1998 [cited 2012 21 May]; Available

from:

<http://www.adjuvantonline.com/breasthelp0306/OverviewOfTamoxifenCancerTrials.html>.

168. Reiner A, Yekutieli D, Benjamini Y. Identifying differentially expressed genes using false discovery rate controlling procedures. *Bioinformatics*. 2003 February 12, 2003;19(3):368-75.
169. Rijsewijk F, Schuermann M, Wagenaar E, Parren P, Weigel D, Nusse R. The *Drosophila* homology of the mouse mammary oncogene *int-1* is identical to the segment polarity gene *wingless*. *Cell*. 1987;50(4):649-57.
170. Ring A, Dowsett M. Mechanisms of tamoxifen resistance. *Endocrine-Related Cancer*. 2004 December 1, 2004;11(4):643-58.
171. Ryo A, Nakamura M, Wulf G, Liou YC, Lu KP. Pin1 regulates turnover and subcellular localization of beta-catenin by inhibiting its interaction with APC. *Nature Cell Biology*. [Research Support, Non-U.S. Gov't Research Support, U.S. Gov't, P.H.S.]. 2001 Sep;3(9):793-801.
172. SABiosciences. Wnt SignallingTargets 2012 [cited 2012 2 April]; Available from: [http://www.sabiosciences.com/rt\\_pcr\\_product/HTML/PAHS-243A.html](http://www.sabiosciences.com/rt_pcr_product/HTML/PAHS-243A.html).
173. SABiosciences. RT Profiler™ PCR Array Human Wnt Signaling Pathway ( PAHS-043A ). 2012 [cited 2012 March 2012]; Available from: <http://www.sabiosciences.com/genetable.php?pcatn=PAHS-043A>.
174. Saiki R, Gelfand D, Stoffel S, Scharf S, Higuchi R, Horn G, et al. Primer-directed enzymatic amplification of DNA with a thermostable DNA polymerase. *Science*. 1988;29(239):487-91.
175. Saiki R, Scharf S, Faloona F, Mullis K, Horn G, Erlich H, et al. Enzymatic amplification of beta-globin genomic sequences and restriction site analysis for diagnosis of sickle cell anemia. *Science*. 1985;20(230):1350-4.
176. Samarzija I, Sini P, Schlange T, MacDonald G, Hynes NE. Wnt3a regulates proliferation and migration of HUVEC via canonical and non-canonical Wnt signaling pathways. *Biochemical and Biophysical Research Communications*. 2009;386(3):449-54.

177. Sarrio D, Moreno-Bueno G, Hardisson D, Sanchez-Estevez C, Guo M, Herman JG, et al. Epigenetic and genetic alterations of APC and CDH1 genes in lobular breast cancer: relationships with abnormal E-cadherin and catenin expression and microsatellite instability. *International Journal of Cancer*. [Research Support, Non-U.S. Gov't]. 2003 Aug 20;106(2):208-15.
178. Sato N, Meijer L, Skaltsounis L, Greengard P, Brivanlou AH. Maintenance of pluripotency in human and mouse embryonic stem cells through activation of Wnt signaling by a pharmacological GSK-3-specific inhibitor. *Nat Med*. [10.1038/nm979]. 2004;10(1):55-63.
179. Schafer JM, Liu H, Bentrem DJ, Zapf JW, Jordan VC. Allosteric Silencing of Activating Function 1 in the 4-Hydroxytamoxifen Estrogen Receptor Complex Is Induced by Substituting Glycine for Aspartate at Amino Acid 351. *Cancer Research*. 2000 September 9, 2000;60(18):5097-105.
180. Schlange T, Matsuda Y, Lienhard S, Huber A, Hynes NE. Autocrine WNT signaling contributes to breast cancer cell proliferation via the canonical WNT pathway and EGFR transactivation. *Breast Cancer Research*. [Research Support, Non-U.S. Gov't]. 2007;9(5):R63.
181. Schroeder JA, Adriance MC, McConnell EJ, Thompson MC, Pockaj B, Gendler SJ. ErbB- $\beta$ -Catenin Complexes Are Associated with Human Infiltrating Ductal Breast and Murine Mammary Tumor Virus (MMTV)-Wnt-1 and MMTV-c-Neu Transgenic Carcinomas. *Journal of Biological Chemistry*. 2002 June 21, 2002;277(25):22692-8.
182. Shan J, Shi D-L, Wang J, Zheng J. Identification of a Specific Inhibitor of the Dishevelled PDZ Domain†. *Biochemistry*. 2005 2005/11/01;44(47):15495-503.
183. Sharma RP, Chopra VL. Effect of the wingless (wgl) mutation on wing and haltere development in *Drosophila melanogaster*. *Developmental Biology*. 1976;48(2):461-5.
184. Shou J, Massarweh S, Osborne CK, Wakeling AE, Ali S, Weiss H, et al. Mechanisms of Tamoxifen Resistance: Increased Estrogen Receptor-HER2/neu Cross-Talk in ER/HER2-Positive Breast Cancer. *Journal of the National Cancer Institute*. 2004 June 16, 2004;96(12):926-35.



185. Simstein R, Burow M, Parker A, Weldon C, Beckman B. Apoptosis, Chemoresistance, and Breast Cancer: Insights From the MCF-7 Cell Model System. *Experimental Biology and Medicine*. 2003 October 1, 2003;228(9):995-1003.
186. Smith CL, Nawaz Z, O'Malley BW. Coactivator and Corepressor Regulation of the Agonist/Antagonist Activity of the Mixed Antiestrogen, 4-Hydroxytamoxifen. *Molecular Endocrinology*. 1997 June 1, 1997;11(6):657-66.
187. Sommer S, Fuqua SAW. Estrogen receptor and breast cancer. *Seminars in Cancer Biology*. 2001;11(5):339-52.
188. Sonderegger S, Haslinger P, Sabri A, Leisser C, Otten JV, Fiala C, et al. Wingless (Wnt)-3A Induces Trophoblast Migration and Matrix Metalloproteinase-2 Secretion through Canonical Wnt Signaling and Protein Kinase B/AKT Activation. *Endocrinology*. 2010 January 1, 2010;151(1):211-20.
189. Staal FJ NMM, Strous GJ, Clevers HC. Wnt signals are transmitted through N-terminally dephosphorylated beta-catenin. *EBMO Reports*. 2002 Jan;3(1):63-8.
190. Stambolic V, Ruel L, Woodgett JR. Lithium inhibits glycogen synthase kinase-3 activity and mimics Wingless signalling in intact cells. *Current biology : CB*. 1996;6(12):1664-9.
191. Stearns V, Johnson MD, Rae JM, Morocho A, Novielli A, Bhargava P, et al. Active Tamoxifen Metabolite Plasma Concentrations After Coadministration of Tamoxifen and the Selective Serotonin Reuptake Inhibitor Paroxetine. *Journal of the National Cancer Institute*. 2003 December 3, 2003;95(23):1758-64.
192. Sugiura H, Toyama T, Hara Y, Zhang Z, Kobayashi S, Fujii Y, et al. Expression of Estrogen Receptor  $\beta$  Wild-type and its Variant ER $\beta$ cx/ $\beta$ 2 is Correlated with Better Prognosis in Breast Cancer. *Japanese Journal of Clinical Oncology*. 2007 November 1, 2007;37(11):820-8.
193. Suzuki H, Toyota M, Carraway H, Gabrielson E, Ohmura T, Fujikane T, et al. Frequent epigenetic inactivation of Wnt antagonist genes in breast cancer (*British Journal of Cancer* (2008) 98, (1147-1156) DOI: 10.1038/sj.bjc.6604259). *British Journal of Cancer*. 2008;99(2):384.

194. Teh L, Mohamed N, Salleh M, Rohaizak M, Shahrin N, Saladina J, et al. The Risk of Recurrence in Breast Cancer Patients Treated with Tamoxifen: Polymorphisms of CYP2D6 and ABCB1. *The AAPS Journal*. 2012;14(1):52-9.
195. The\_beta\_Catenin\_Company. The  $\beta$ C2059  $\beta$  catenin modulation opportunity. 2011 [cited 2012 21 March]; Available from: [http://www.pharmaconnections.com/Investment\\_Opps/BetaCat/Beta\\_Cat\\_BC2059\\_Opportunity\\_Investors.pdf](http://www.pharmaconnections.com/Investment_Opps/BetaCat/Beta_Cat_BC2059_Opportunity_Investors.pdf).
196. Thorne CA, Hanson AJ, Schneider J, Tahinci E, Orton D, Cselenyi CS, et al. Small-molecule inhibition of Wnt signaling through activation of casein kinase 1 $\alpha$ . *Nat Chem Biol*. [10.1038/nchembio.453]. 2010;6(11):829-36.
197. Thorpe S. Estrogen and progesterone receptor determinations in breast cancer. Technology, biology and clinical significance. *Acta Oncol*. 1988;27(1):1-19.
198. Thorpe SM RC. Oestrogen and progesterone receptor determinations in breast cancer: technology and biology. *Cancer Surv*. 1986;5(3):502-25.
199. Trosset J-Y, Dalvit C, Knapp S, Fasolini M, Veronesi M, Mantegani S, et al. Inhibition of protein-protein interactions: The discovery of druglike  $\beta$ -catenin inhibitors by combining virtual and biophysical screening. *Proteins: Structure, Function, and Bioinformatics*. 2006;64(1):60-7.
200. Ueda M, Gemmill RM, West J, Winn R, Sugita M, Tanaka N, et al. Mutations of the  $\beta$ - and  $\gamma$ -catenin genes are uncommon in human lung, breast, kidney, cervical and ovarian carcinomas. *British Journal of Cancer*. 2001;85(1):64-8.
201. Ugolini F, Charafe-Jauffret E, Bardou VJ, Geneix J, Adelaide J, Labat-Moleur F, et al. WNT pathway and mammary carcinogenesis: loss of expression of candidate tumor suppressor gene SFRP1 in most invasive carcinomas except of the medullary type. *Oncogene*. [Research Support, Non-U.S. Gov't]. 2001 Sep 13;20(41):5810-7.
202. Van der Auwera I, Van Laere SJ, Van den Bosch SM, Van den Eynden GG, Trinh BX, van Dam PA, et al. Aberrant methylation of the Adenomatous Polyposis Coli (APC) gene promoter is associated with the inflammatory breast cancer phenotype. *Br J Cancer*. 2008;99(10):1735-42.

203. Veeck J, Geisler C, Noetzel E, Alkaya S, Hartmann A, Knuechel R, et al. Epigenetic inactivation of the secreted frizzled-related protein-5 (SFRP5) gene in human breast cancer is associated with unfavorable prognosis. *Carcinogenesis* (Oxford). 2008 May;29(5):991-8.
204. Veeck J, Niederacher D, An H, Klopocki E, Wiesmann F, Betz B, et al. Aberrant methylation of the Wnt antagonist SFRP1 in breast cancer is associated with unfavourable prognosis. *Oncogene*. [Research Support, Non-U.S. Gov't]. 2006 Jun 8;25(24):3479-88.
205. Verhaegh W, Hatzis P, Clevers H, van de Stolpe A. Personalized Cancer Treatment Selection Using Computational Signaling Pathway Models. *Cancer Research*. 2012;71(24 Supplement (P5-04-03)).
206. Vincan E, editor. *Wnt signaling*; Springer Protocols; 2008.
207. Virmani AK, Rathi A, Sathyanarayana UG, Padar A, Huang CX, Cunningham HT, et al. Aberrant Methylation of the Adenomatous Polyposis Coli (APC) Gene Promoter 1A in Breast and Lung Carcinomas. *Clinical Cancer Research*. 2001 July 1, 2001;7(7):1998-2004.
208. Vlad A, Röhrs S, Klein-Hitpass L, Müller O. The first five years of the Wnt targetome. *Cellular Signalling*. 2008;20(5):795-802.
209. Wakeling AE, Guy SP, Woodburn JR, Ashton SE, Curry BJ, Barker AJ, et al. ZD1839 (Iressa). *Cancer Research*. 2002 October 15, 2002;62(20):5749-54.
210. Wang S-L, Huang J-D, Lai M-D, Liu B-H, Lai M-L. Molecular basis of genetic variation in debrisoquin hydroxylation in Chinese subjects: Polymorphism in RFLP and DNA sequence of CYP2D6. *Clin Pharm Ther*. 1993;53(4):410-8.
211. Watanabe O, Imamura H, Shimizu T, Kinoshita J, Okabe T, Hirano A, et al. Expression of twist and wnt in human breast cancer. *Anticancer Research*. 2004 Nov-Dec;24(6):3851-6.
212. Webster M-T, Rozycka M, Sara E, Davis E, Smalley M, Young N, et al. Sequence variants of the Axin gene in breast, colon, and other cancers: An analysis

of mutations that interfere with GSK3 binding. *Genes Chromosomes and Cancer*. 2000 August;28(4):443-53.

213. Wiecezorek M, Paczkowska A, Guzenda P, Majorek M, Bednarek AK, Lamparska-Przybysz M. Silencing of Wnt-1 by siRNA induces apoptosis of MCF-7 human breast cancer cells. *Cancer Biology & Therapy*. 2008;7(2):268-74.

214. Wolf DM, Jordan VC. The estrogen receptor from a tamoxifen stimulated MCF-7 tumor variant contains a point mutation in the ligand binding domain. *Breast Cancer Research and Treatment*. 1994;31(1):129-38.

215. Wong SCC, Lo SFE, Lee KC, Yam JWP, Chan JKC, Wendy Hsiao WL. Expression of frizzled-related protein and Wnt-signalling molecules in invasive human breast tumours. *Journal of Pathology*. [Research Support, Non-U.S. Gov't]. 2002 Feb;196(2):145-53.

216. Wu X, Tu X, Joeng KS, Hilton MJ, Williams DA, Long F. Rac1 Activation Controls Nuclear Localization of  $\beta$ -catenin during Canonical Wnt Signaling. *Cell*. 2008;133(2):340-53.

217. Yamamoto H, Komekado H, Kikuchi A. Caveolin Is Necessary for Wnt-3a-Dependent Internalization of LRP6 and Accumulation of  $\beta$ -Catenin. *Developmental cell*. 2006;11(2):213-23.

218. Yamamoto H SH, Yamamoto H, Michiue T, Kikuchi A. Wnt3a and Dkk1 regulate distinct internalization pathways of LRP6 to tune the activation of beta-catenin signaling. *Dev Cell*. 2008;July, 15(1):37-48.

219. Yarden RI, Wilson MA, Chrysogelos SA. Estrogen suppression of EGFR expression in breast cancer cells: A possible mechanism to modulate growth\*. *Journal of Cellular Biochemistry*. 2001;81(S36):232-46.

220. Yue W, Wang JP, Li Y, Fan P, Liu G, Zhang N, et al. Effects of estrogen on breast cancer development: Role of estrogen receptor independent mechanisms. *International journal of cancer Journal international du cancer*. 2010;127(8):1748-57.

221. Yun M-S, Kim S-E, Jeon SH, Lee J-S, Choi K-Y. Both ERK and Wnt/ $\beta$ -catenin pathways are involved in Wnt3a-induced proliferation. *Journal of Cell Science*. 2005 January 15, 2005;118(2):313-22.

222. Zanger U, Raimundo S, Eichelbaum M. Cytochrome P450 2D6: overview and update on pharmacology, genetics, biochemistry. *Naunyn-Schmiedeberg's Archives of Pharmacology*. 2004;369(1):23-37.
223. Zeng G AU, Cieply B, Singh S, Monga SP. siRNA-Mediated  $\beta$ -Catenin Knockdown in Human Hepatoma Cells Results in Decreased Growth and Survival. *Neoplasia*. 2007;9(11):951-0.
224. Zhang D, Pal A, Bornmann WG, Yamasaki F, Esteva FJ, Hortobagyi GN, et al. Activity of lapatinib is independent of EGFR expression level in HER2-overexpressing breast cancer cells. *Molecular Cancer Therapeutics*. 2008 July 1, 2008;7(7):1846-50.
225. Zhang Y, Liu S, Mickanin C, Feng Y, Charlat O, Michaud GA, et al. RNF146 is a poly(ADP-ribose)-directed E3 ligase that regulates axin degradation and Wnt signalling. *Nat Cell Biol*. [10.1038/ncb2222]. 2011;13(5):623-9.
226. Zilli M, Grassadonia A, Tinari N, Di Giacobbe A, Gildetti S, Giampietro J, et al. Molecular mechanisms of endocrine resistance and their implication in the therapy of breast cancer. *Biochimica et Biophysica Acta (BBA) - Reviews on Cancer*. 2009;1795(1):62-81.

# Chapter 9

## Appendix

## 9 Appendix

### 9.1 Affymetrix

**Table 9.1**

**Heatmap data for MCF-7 cells versus Tam-R cells.**

Rows 1-22 and rows 96 onwards show > 1.5 fold change.

Note: row 96 = 1.5 fold difference

Row	Other ID	Gene Name	Gene ID	Multiple probes	Significance by t-test
1	208606_s_at	wingless-type MMTV integration site family, member 4	WNT4	1,,,,,,,,,	*
2	221609_s_at	wingless-type MMTV integration site family, member 6	WNT6	2,,,,,,,,,	*
3	221558_s_at	lymphoid enhancer-binding factor 1	LEF1	3,81,,,,,,,,,	
4	203525_s_at	adenomatous polyposis coli	APC	4,40,65,91,,,,,,,,,	*
5	220277_at	CXXC finger 4	CXXC4	5,,,,,,,,,	
6	205990_s_at	wingless-type MMTV integration site family, member 5A	WNT5A	6,14,,,,,,,,,	*
7	201533_at	catenin (cadherin-associated protein), beta 1, 88kDa	CTNNB1	7,,,,,,,,,	*
8	200951_s_at	cyclin D2	CCND2	8,37,,,,,,,,,	*
9	204420_at	FOS-like antigen 1	FOSL1	9,,,,,,,,,	*
10	212073_at	casein kinase 2, alpha 1 polypeptide /// casein kinase 2, alpha 1 polypeptide pseudogene	CSNK2A1	10,48,62, ,,,,,,	
11	34697_at	low density lipoprotein receptor-related protein 6	LRP6	11,,,,,,,,,	
12	221455_s_at	wingless-type MMTV integration site family, member 3	WNT3	12,,,,,,,,,	

13	202210_x_at	glycogen synthase kinase 3 alpha	GSK3A	13,63,,,,,, ,,,	
14	213425_at	wingless-type MMTV integration site family, member 5A	WNT5A	6,14,,,,,, ,	
15	206459_s_at	wingless-type MMTV integration site family, member 2B	WNT2B	15,53,,,,, ,,,	
16	201700_at	cyclin D3	CCND3	16,,,,,,	
17	204129_at	B-cell CLL/lymphoma 9	BCL9	17,,,,,,	
18	219993_at	SRY (sex determining region Y)-box 17	SOX17	18,,,,,,	
19	208867_s_at	casein kinase 1, alpha 1	CSNK1A1	19,23,33, 35,,,,,	
20	203698_s_at	frizzled-related protein	FRZB	20,92,,,,, ,,,	
21	209468_at	low density lipoprotein receptor-related protein 5	LRP5	21,,,,,,	
22	221245_s_at	frizzled homolog 5 (Drosophila)	FZD5	22,49,,,,, ,,,	
23	206562_s_at	casein kinase 1, alpha 1	CSNK1A1	19,23,33, 35,,,,,	
24	208652_at	protein phosphatase 2 (formerly 2A), catalytic subunit, alpha isoform	PPP2CA	24,,,,,,	
25	214724_at	DIX domain containing 1	DIXDC1	25,,,,,,	*
26	205254_x_at	transcription factor 7 (T-cell specific, HMG-box)	TCF7	26,82,,,,, ,,,	
27	218318_s_at	nemo-like kinase	NLK	27,,,,,,	*
28	203705_s_at	frizzled homolog 7 (Drosophila)	FZD7	28,,,,,,	
29	40837_at	transducin-like enhancer of split 2 (E(sp1) homolog, Drosophila)	TLE2	29,,,,,,	
30	215517_at	pygopus homolog 1 (Drosophila)	PYGO1	30,,,,,,	
31	210248_at	wingless-type MMTV	WNT7A	31,,,,,,	



		integration site family, member 7A			
32	204712_at	WNT inhibitory factor 1	WIF1	32,,,,,,,,,	
33	213086_s_at	casein kinase 1, alpha 1	CSNK1A1	19,23,33, 35,,,,,,,,	
34	202431_s_at	v-myc myelocytomatosis viral oncogene homolog (avian)	MYC	34,,,,,,,,,	
35	208865_at	casein kinase 1, alpha 1	CSNK1A1	19,23,33, 35,,,,,,,,	
36	203230_at	dishevelled, dsh homolog 1 (Drosophila) /// hypothetical LOC642469	DVL1	36,,,,,,,,,	*
37	200952_s_at	cyclin D2	CCND2	8,37,,,,,,,, ,	
38	212863_x_at	C-terminal binding protein 1	CTBP1	38,46,,,,,,,, ,,,	
39	203987_at	frizzled homolog 6 (Drosophila)	FZD6	39,,,,,,,,,	
40	203526_s_at	adenomatous polyposis coli	APC	4,40,65,9 1,,,,,,,,	
41	204451_at	frizzled homolog 1 (Drosophila)	FZD1	41,85,,,,,,,, ,,,	
42	209456_s_at	F-box and WD repeat domain containing 11	FBXW11	42,47,,,,,,,, ,,,	*
43	218122_s_at	SUMO1/sentrin/SMT 3 specific peptidase 2	SENP2	43,,,,,,,,,	
44	203081_at	catenin, beta interacting protein 1	CTNNBIP 1	44,,,,,,,,,	
45	219483_s_at	porcupine homolog (Drosophila)	PORCN	45,,,,,,,,,	
46	213980_s_at	C-terminal binding protein 1	CTBP1	38,46,,,,,,,, ,,,	
47	209455_at	F-box and WD repeat domain containing 11	FBXW11	42,47,,,,,,,, ,,,	
48	212072_s_at	casein kinase 2, alpha 1 polypeptide	CSNK2A1	10,48,62, ,,,,,,	
49	206136_at	frizzled homolog 5 (Drosophila)	FZD5	22,49,,,,,,,, ,,,	

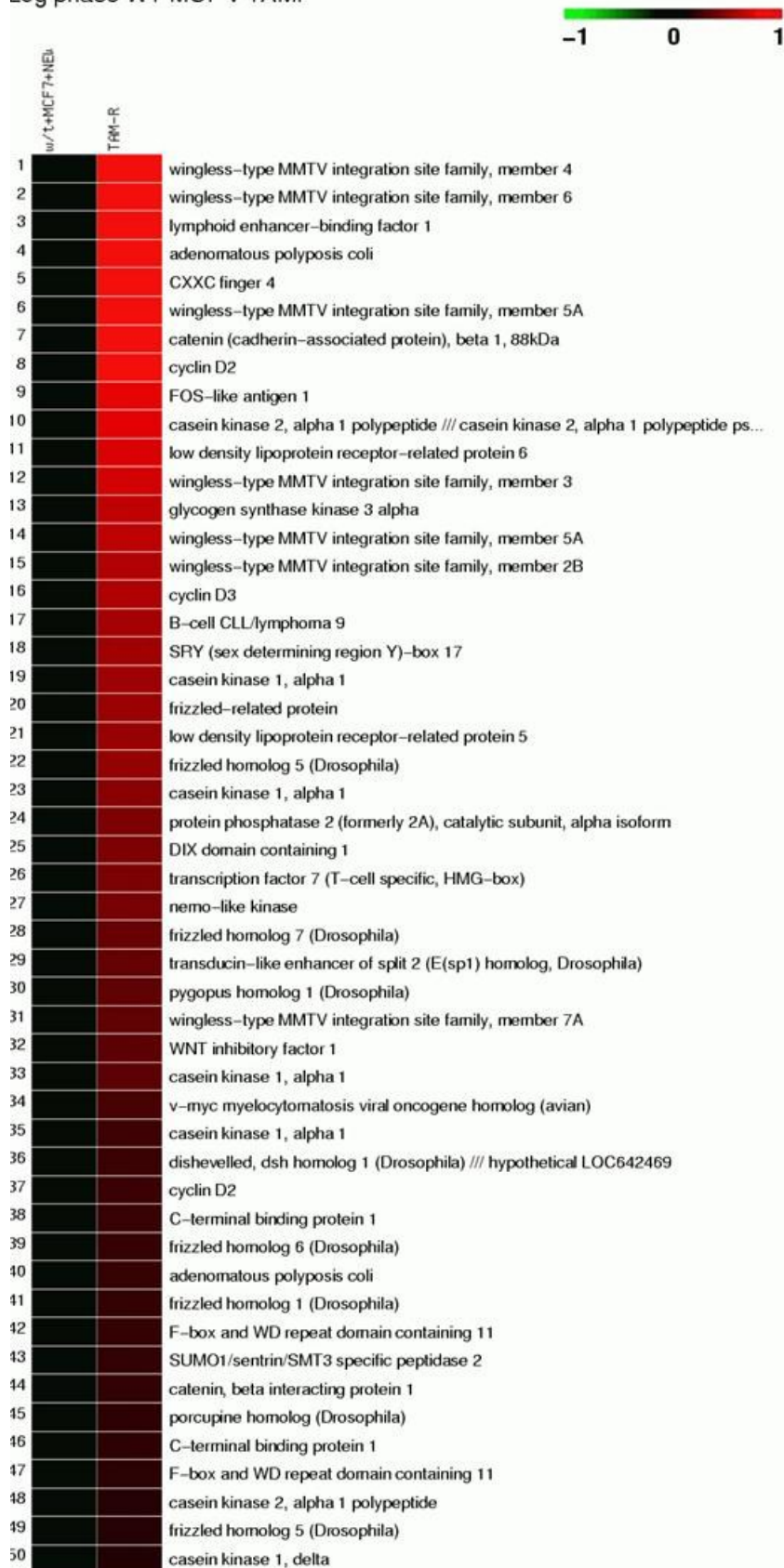
50	208774_at	casein kinase 1, delta	CSNK1D	50,75,,,,,, ,,,	
51	221673_s_at	casein kinase 1, gamma 1	CSNK1G1	51,105,,,, ,,,,,	
52	217729_s_at	amino-terminal enhancer of split	AES	52,,,,,,,,,	
53	206458_s_at	wingless-type MMTV integration site family, member 2B	WNT2B	15,53,,,,, ,,,	
54	221016_s_at	transcription factor 7- like 1 (T-cell specific, HMG-box)	TCF7L1	54,,,,,,,,,	
55	207558_s_at	paired-like homeodomain 2	PITX2	55,,,,,,,,,	
56	209630_s_at	F-box and WD repeat domain containing 2	FBXW2	56,99,,,,, ,,,	
57	210554_s_at	C-terminal binding protein 2	CTBP2	57,80,84, 101,,,,,	
58	206524_at	T, brachyury homolog (mouse)	T	58,,,,,,,,,	
59	221113_s_at	wingless-type MMTV integration site family, member 16	WNT16	59,,,,,,,,,	
60	213579_s_at	E1A binding protein p300	EP300	60,96,,,,, ,,,	
61	209945_s_at	glycogen synthase kinase 3 beta	GSK3B	61,,,,,,,,,	
62	206075_s_at	casein kinase 2, alpha 1 polypeptide	CSNK2A1	10,48,62, ,,,,,	
63	632_at	glycogen synthase kinase 3 alpha	GSK3A	13,63,,,,, ,,,	
64	208712_at	cyclin D1	CCND1	64,93,,,,, ,,,	
65	215310_at	adenomatous polyposis coli	APC	4,40,65,9 1,,,,,	
66	202036_s_at	secreted frizzled- related protein 1	SFRP1	66,76,,,,, ,,,	
67	204052_s_at	secreted frizzled- related protein 4	SFRP4	67,68,,,,, ,,,	
68	204051_s_at	secreted frizzled- related protein 4	SFRP4	67,68,,,,, ,,,	
69	219683_at	frizzled homolog 3 (Drosophila)	FZD3	69,,,,,,,,,	

70	201349_at	solute carrier family 9 (sodium/hydrogen exchanger), member 3 regulator 1	SLC9A3R1	70,,,,,,,,,	
71	216587_s_at	frizzled homolog 8 (Drosophila)	FZD8	71,,,,,,,,,	
72	201219_at	C-terminal binding protein 2	ZRANB1	72,,,,,,,,,	
73	207683_at	forkhead box N1	FOXN1	73,,,,,,,,,	
74	200695_at	protein phosphatase 2 (formerly 2A), regulatory subunit A, alpha isoform	PPP2R1A	74,,,,,,,,,	
75	207945_s_at	casein kinase 1, delta	CSNK1D	50,75,,,,,, ,,,	
76	202037_s_at	secreted frizzled-related protein 1	SFRP1	66,76,,,,,, ,,,	
77	219889_at	frequently rearranged in advanced T-cell lymphomas	FRAT1	77,,,,,,,,,	
78	206737_at	wingless-type MMTV integration site family, member 11	WNT11	78,,,,,,,,,	
79	217681_at	wingless-type MMTV integration site family, member 7B	WNT7B	79,,,,,,,,,	
80	210835_s_at	C-terminal binding protein 2	CTBP2	57,80,84, 101,,,,,,	
81	221557_s_at	lymphoid enhancer-binding factor 1	LEF1	3,81,,,,,, ,	
82	205255_x_at	transcription factor 7 (T-cell specific, HMG-box)	TCF7	26,82,,,,,, ,,,	
83	205648_at	wingless-type MMTV integration site family member 2	WNT2	83,,,,,,,,,	
84	201220_x_at	C-terminal binding protein 2	CTBP2	57,80,84, 101,,,,,,	
85	204452_s_at	frizzled homolog 1 (Drosophila)	FZD1	41,85,,,,,, ,,,	
86	216091_s_at	beta-transducin repeat containing	BTRC	86,100,,,, ,,,,,	
87	210220_at	frizzled homolog 2	FZD2	87,,,,,,,,,	

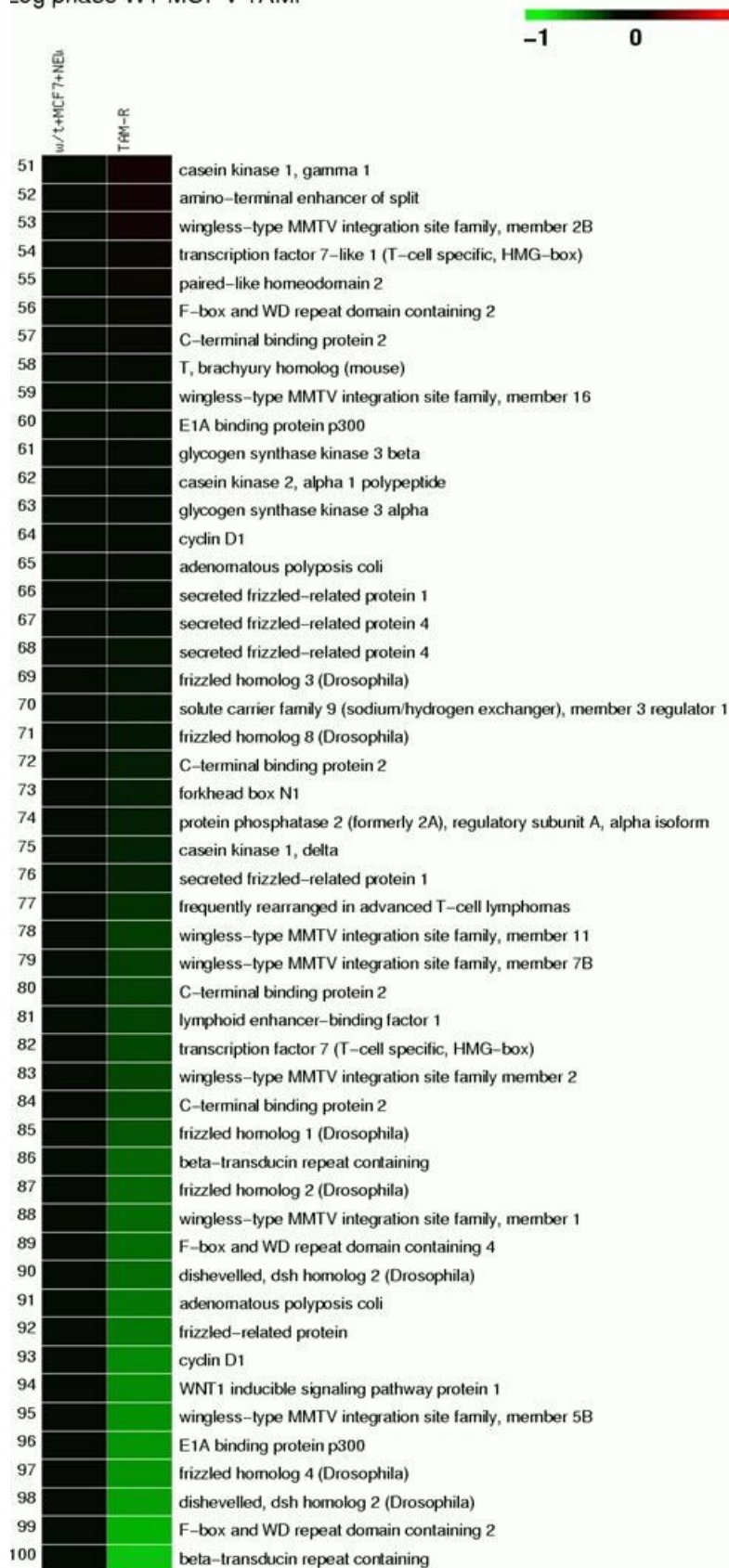
		(Drosophila)			
88	208570_at	wingless-type MMTV integration site family, member 1	WNT1	88,,,,,,,,,	
89	221519_at	F-box and WD repeat domain containing 4	FBXW4	89,,,,,,,,,	
90	57532_at	dishevelled, dsh homolog 2 (Drosophila)	DVL2	90,98,,,,, ,,,	
91	216933_x_at	adenomatous polyposis coli	APC	4,40,65,91,,,,,	
92	203697_at	frizzled-related protein	FRZB	20,92,,,,, ,,,	
93	208711_s_at	cyclin D1	CCND1	64,93,,,,, ,,,	
94	211312_s_at	WNT1 inducible signaling pathway protein 1	WISP1	94,102,,,, ,,,,,	
95	221029_s_at	wingless-type MMTV integration site family, member 5B	WNT5B	95,,,,,,,,,	
96	202221_s_at	E1A binding protein p300	EP300	60,96,,,,, ,,,	*
97	218665_at	frizzled homolog 4 (Drosophila)	FZD4	97,,,,,,,,,	
98	218759_at	dishevelled, dsh homolog 2 (Drosophila)	DVL2	90,98,,,,, ,,,	
99	218941_at	F-box and WD repeat domain containing 2	FBXW2	56,99,,,,, ,,,	
100	204901_at	beta-transducin repeat containing	BTRC	86,100,,,, ,,,,,	
101	215377_at	C-terminal binding protein 2	CTBP2	57,80,84, 101,,,,,	
102	206796_at	WNT1 inducible signaling pathway protein 1	WISP1	94,102,,,, ,,,,,	
103	212849_at	axin 1	AXIN1	103,,,,,,,, ,	*
104	201466_s_at	jun oncogene	JUN	104,110,, ,,,,,	
105	220640_at	casein kinase 1, gamma 1	CSNK1G1	51,105,,,, ,,,,,	

106	214489_at	follicle stimulating hormone, beta polypeptide	FSHB	106,,,,,,,,, ,	
107	216060_s_at	dishevelled associated activator of morphogenesis 1	DAAM1	107,,,,,,,,, ,	
108	204602_at	dickkopf homolog 1 (Xenopus laevis)	DKK1	108,,,,,,,,, ,	*
109	203220_s_at	transducin-like enhancer of split 1 (E(sp1) homolog, Drosophila)	TLE1	109,111,, ,,,,,,	*
110	201465_s_at	jun oncogene	JUN	104,110,, ,,,,,,	*
111	203222_s_at	transducin-like enhancer of split 1 (E(sp1) homolog, Drosophila)	TLE1	109,111,, ,,,,,,	*

Log phase WT MCF v TAMr



\_log phase WT MCF v TAMr



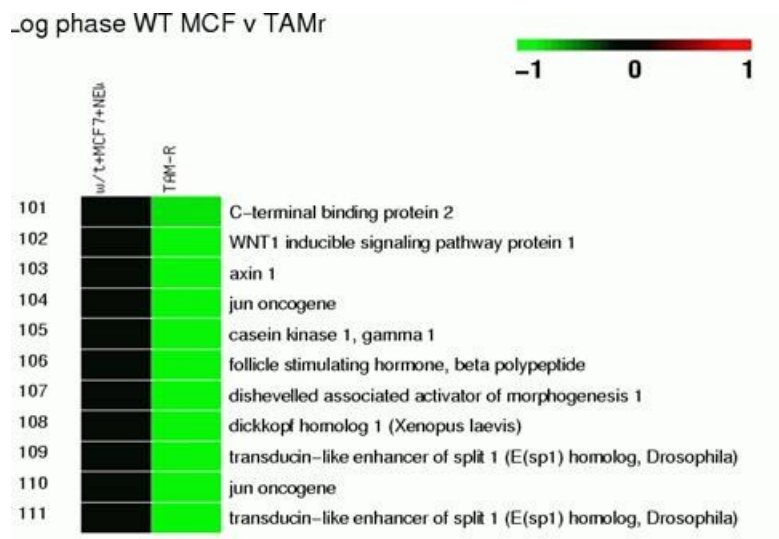


**Figure 9.1**  
**Heatmap for Wnt signalling probe set showing changes in gene expression between MCF-7 and Tam-R cells.**

Rows 1-22 and rows 96 onwards show >1.5 fold change. Note: row 96 = 1.5 fold difference.

Red signalled increased expression; green showed decreased expression of mRNA compared to MCF-7 controls (black).



**Table 9.2**

**Heatmap data for MCF-7 cells versus MCF-7 cells treated with tamoxifen [10<sup>-7</sup>M] for 10 days.**

Rows 1-19 and rows 89 onwards show >1.5 fold change.

Note: row 19 = 1.5 fold difference.

Row	Other ID	Gene Name	Gene ID	Multiple probes	Significance by t-test
1	221558_s_at	lymphoid enhancer-binding factor 1	LEF1	1,56,,,,,,,,,	*
2	203525_s_at	adenomatous polyposis coli	APC	2,25,33,63,,,,,,,,,	
3	214724_at	DIX domain containing 1	DIXDC1	3,,,,,,,,,	
4	216060_s_at	dishevelled associated activator of morphogenesis 1	DAAM1	4,,,,,,,,,	*
5	203987_at	frizzled homolog 6 (Drosophila)	FZD6	5,,,,,,,,,	
6	209630_s_at	F-box and WD repeat domain containing 2	FBXW2	6,80,,,,,,,,,	
7	201465_s_at	jun oncogene	JUN	7,29,,,,,,,,,	
8	212073_at	casein kinase 2, alpha 1 polypeptide /// casein kinase 2, alpha 1 polypeptide pseudogene	CSNK2A1	8,37,78,,,,,,,,,	
9	34697_at	low density lipoprotein receptor-related protein 6	LRP6	9,,,,,,,,,	
10	213425_at	wingless-type MMTV integration site family, member 5A	WNT5A	10,83,,,,,,,,,	
11	200951_s_at	cyclin D2	CCND2	11,39,,,,,,,,,	*
12	219683_at	frizzled homolog 3 (Drosophila)	FZD3	12,,,,,,,,,	
13	201219_at	C-terminal binding	ZRANB1	13,,,,,,,,,	*

		protein 2			
14	201349_at	solute carrier family 9 (sodium/hydrogen exchanger), member 3 regulator 1	SLC9A3R1	14,,,,,,,,,	*
15	208865_at	casein kinase 1, alpha 1	CSNK1A1	15,20,22,28,,,,,	
16	208606_s_at	wingless-type MMTV integration site family, member 4	WNT4	16,,,,,,,,,	
17	202431_s_at	v-myc myelocytomatosis viral oncogene homolog (avian)	MYC	17,,,,,,,,,	*
18	215517_at	pygopus homolog 1 (Drosophila)	PYGO1	18,,,,,,,,,	
19	206524_at	T, brachyury homolog (mouse)	T	19,,,,,,,,,	
20	206562_s_at	casein kinase 1, alpha 1	CSNK1A1	15,20,22,28,,,,,	
21	221245_s_at	frizzled homolog 5 (Drosophila)	FZD5	21,96,,,,,,,,,	
22	213086_s_at	casein kinase 1, alpha 1	CSNK1A1	15,20,22,28,,,,,	
23	208652_at	protein phosphatase 2 (formerly 2A), catalytic subunit, alpha isoform	PPP2CA	23,,,,,,,,,	
24	201533_at	catenin (cadherin-associated protein), beta 1, 88kDa	CTNNB1	24,,,,,,,,,	*
25	203526_s_at	adenomatous polyposis coli	APC	2,25,33,63,,,,,	
26	204451_at	frizzled homolog 1 (Drosophila)	FZD1	26,30,,,,,,,,,	
27	208712_at	cyclin D1	CCND1	27,44,,,,,,,,,	
28	208867_s_at	casein kinase 1, alpha 1	CSNK1A1	15,20,22,28,,,,,	
29	201466_s_at	jun oncogene	JUN	7,29,,,,,,,,,	
30	204452_s_at	frizzled homolog 1	FZD1	26,30,,,,,,,,,	*

	at	(Drosophila)			
31	209945_s_at	glycogen synthase kinase 3 beta	GSK3B	31,,,,,,,,,	
32	210554_s_at	C-terminal binding protein 2	CTBP2	32,36,38,45,,,,, ,,,	
33	216933_x_at	adenomatous polyposis coli	APC	2,25,33,63,,,,,, ,	
34	218318_s_at	nemo-like kinase	NLK	34,,,,,,,,,	
35	209455_at	F-box and WD repeat domain containing 11	FBXW11	35,81,,,,,,,,,	
36	210835_s_at	C-terminal binding protein 2	CTBP2	32,36,38,45,,,,, ,,,	
37	212072_s_at	casein kinase 2, alpha 1 polypeptide	CSNK2A1	8,37,78,,,,,,,,	
38	201220_x_at	C-terminal binding protein 2	CTBP2	32,36,38,45,,,,, ,,,	
39	200952_s_at	cyclin D2	CCND2	11,39,,,,,,,,,	
40	203705_s_at	frizzled homolog 7 (Drosophila)	FZD7	40,,,,,,,,,	
41	207558_s_at	paired-like homeodomain 2	PITX2	41,,,,,,,,,	
42	202036_s_at	secreted frizzled-related protein 1	SFRP1	42,90,,,,,,,,,	
43	204712_at	WNT inhibitory factor 1	WIF1	43,,,,,,,,,	
44	208711_s_at	cyclin D1	CCND1	27,44,,,,,,,,,	
45	215377_at	C-terminal binding protein 2	CTBP2	32,36,38,45,,,,, ,,,	
46	218122_s_at	SUMO1/sentrin/SM T3 specific peptidase 2	SENP2	46,,,,,,,,,	
47	218759_at	dishevelled, dsh homolog 2 (Drosophila)	DVL2	47,89,,,,,,,,,	
48	221519_at	F-box and WD repeat domain containing 4	FBXW4	48,,,,,,,,,	
49	206796_at	WNT1 inducible signaling pathway	WISP1	49,82,,,,,,,,,	

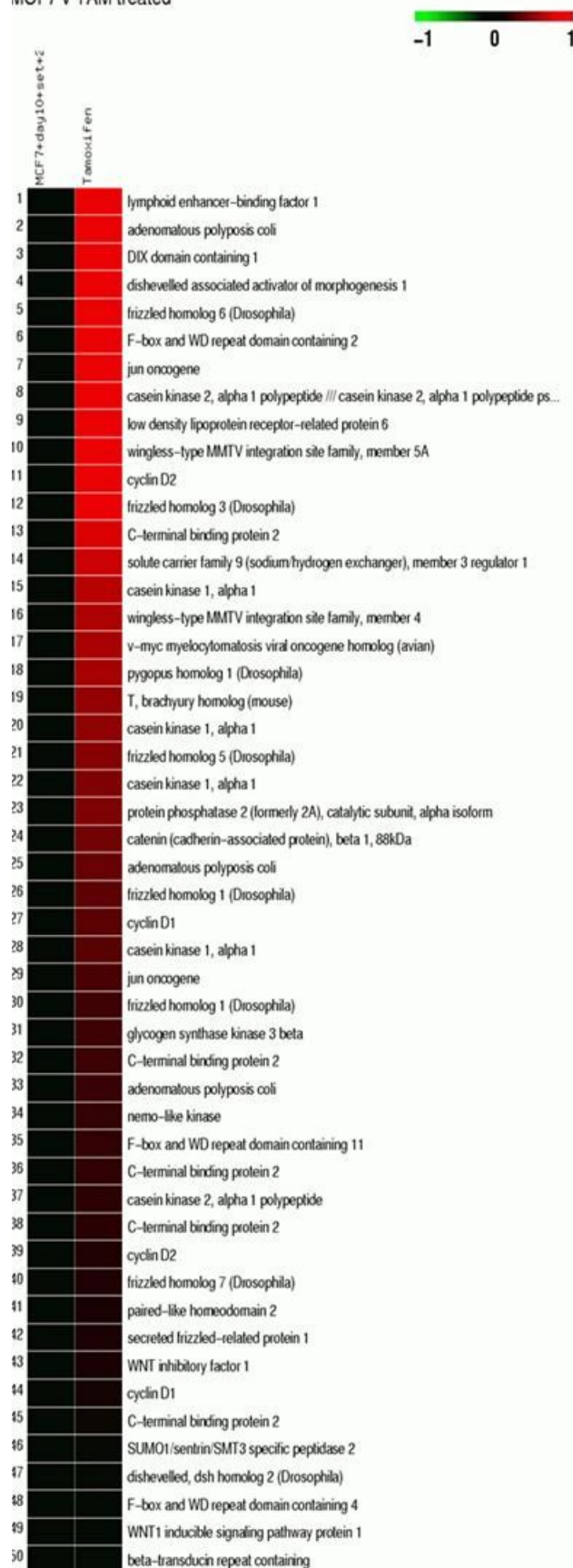
		protein 1			
50	204901_at	beta-transducin repeat containing	BTRC	50,65,,,,,,,,	
51	213579_s_at	E1A binding protein p300	EP300	51,68,,,,,,,,	
52	219483_s_at	porcupine homolog (Drosophila)	PORCN	52,,,,,,,,	
53	206458_s_at	wingless-type MMTV integration site family, member 2B	WNT2B	53,100,,,,,,,,	
54	219993_at	SRY (sex determining region Y)-box 17	SOX17	54,,,,,,,,	
55	221455_s_at	wingless-type MMTV integration site family, member 3	WNT3	55,,,,,,,,	
56	221557_s_at	lymphoid enhancer-binding factor 1	LEF1	1,56,,,,,,,,	
57	632_at	glycogen synthase kinase 3 alpha	GSK3A	57,106,,,,,,,,	
58	204129_at	B-cell CLL/lymphoma 9	BCL9	58,,,,,,,,	
59	201700_at	cyclin D3	CCND3	59,,,,,,,,	
60	205648_at	wingless-type MMTV integration site family member 2	WNT2	60,,,,,,,,	
61	219889_at	frequently rearranged in advanced T-cell lymphomas	FRAT1	61,,,,,,,,	
62	203230_at	dishevelled, dsh homolog 1 (Drosophila) /// hypothetical LOC642469	DVL1	62,,,,,,,,	
63	215310_at	adenomatous polyposis coli	APC	2,25,33,63,,,,,, ,	
64	221673_s_at	casein kinase 1, gamma 1	CSNK1G1	64,110,,,,,,,,	
65	216091_s_at	beta-transducin	BTRC	50,65,,,,,,,,	

	at	repeat containing			
66	205254_x_at	transcription factor 7 (T-cell specific, HMG-box)	TCF7	66,70,,,,,,,,	
67	203220_s_at	transducin-like enhancer of split 1 (E(sp1) homolog, Drosophila)	TLE1	67,105,,,,,,,,	
68	202221_s_at	E1A binding protein p300	EP300	51,68,,,,,,,,	
69	217681_at	wingless-type MMTV integration site family, member 7B	WNT7B	69,,,,,,,,	
70	205255_x_at	transcription factor 7 (T-cell specific, HMG-box)	TCF7	66,70,,,,,,,,	
71	216587_s_at	frizzled homolog 8 (Drosophila)	FZD8	71,,,,,,,,	
72	218665_at	frizzled homolog 4 (Drosophila)	FZD4	72,,,,,,,,	
73	204052_s_at	secreted frizzled-related protein 4	SFRP4	73,95,,,,,,,,	
74	212863_x_at	C-terminal binding protein 1	CTBP1	74,76,,,,,,,,	
75	207945_s_at	casein kinase 1, delta	CSNK1D	75,91,,,,,,,,	
76	213980_s_at	C-terminal binding protein 1	CTBP1	74,76,,,,,,,,	
77	210220_at	frizzled homolog 2 (Drosophila)	FZD2	77,,,,,,,,	
78	206075_s_at	casein kinase 2, alpha 1 polypeptide	CSNK2A1	8,37,78,,,,,,,,	*
79	206737_at	wingless-type MMTV integration site family, member 11	WNT11	79,,,,,,,,	
80	218941_at	F-box and WD repeat domain containing 2	FBXW2	6,80,,,,,,,,	*
81	209456_s_at	F-box and WD repeat domain containing 11	FBXW11	35,81,,,,,,,,	

82	211312_s_at	WNT1 inducible signaling pathway protein 1	WISP1	49,82,,,,,,,,,	
83	205990_s_at	wingless-type MMTV integration site family, member 5A	WNT5A	10,83,,,,,,,,,	
84	200695_at	protein phosphatase 2 (formerly 2A), regulatory subunit A, alpha isoform	PPP2R1A	84,,,,,,,,,	
85	208570_at	wingless-type MMTV integration site family, member 1	WNT1	85,,,,,,,,,	
86	204602_at	dickkopf homolog 1 (Xenopus laevis)	DKK1	86,,,,,,,,,	
87	221113_s_at	wingless-type MMTV integration site family, member 16	WNT16	87,,,,,,,,,	
88	207683_at	forkhead box N1	FOXN1	88,,,,,,,,,	
89	57532_at	dishevelled, dsh homolog 2 (Drosophila)	DVL2	47,89,,,,,,,,,	*
90	202037_s_at	secreted frizzled-related protein 1	SFRP1	42,90,,,,,,,,,	*
91	208774_at	casein kinase 1, delta	CSNK1D	75,91,,,,,,,,,	
92	212849_at	axin 1	AXIN1	92,,,,,,,,,	
93	203081_at	catenin, beta interacting protein 1	CTNNB1	93,,,,,,,,,	
94	221609_s_at	wingless-type MMTV integration site family, member 6	WNT6	94,,,,,,,,,	
95	204051_s_at	secreted frizzled-related protein 4	SFRP4	73,95,,,,,,,,,	*
96	206136_at	frizzled homolog 5 (Drosophila)	FZD5	21,96,,,,,,,,,	*
97	217729_s_at	amino-terminal enhancer of split	AES	97,,,,,,,,,	
98	210248_at	wingless-type	WNT7A	98,,,,,,,,,	

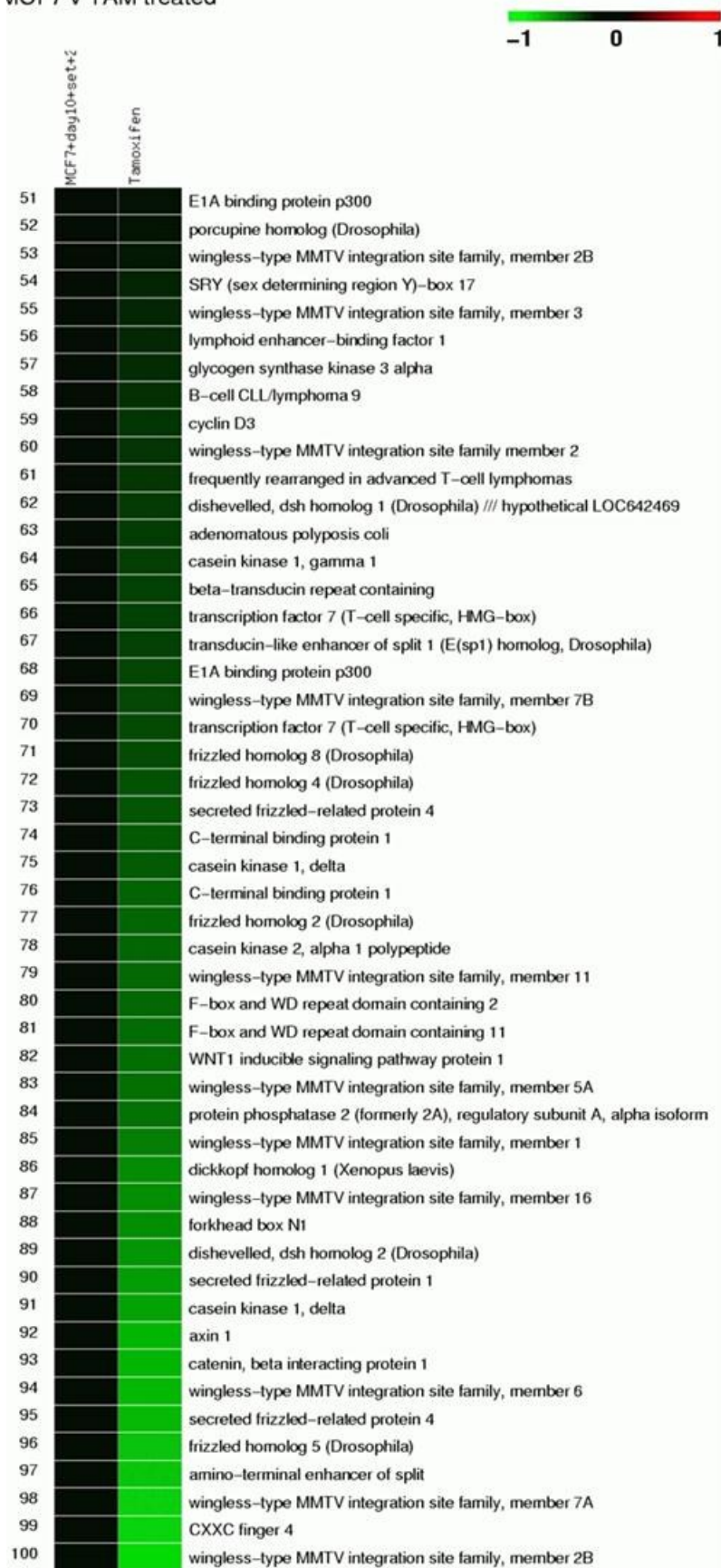
		MMTV integration site family, member 7A			
99	220277_at	CXXC finger 4	CXXC4	99,,,,,,,,,,,,,	
100	206459_s_at	wingless-type MMTV integration site family, member 2B	WNT2B	53,100,,,,,,,,,,,,,	
101	204420_at	FOS-like antigen 1	FOSL1	101,,,,,,,,,,,,,	*
102	209468_at	low density lipoprotein receptor-related protein 5	LRP5	102,,,,,,,,,,,,,	*
103	203698_s_at	frizzled-related protein	FRZB	103,107,,,,,,,,,,,,,	
104	221016_s_at	transcription factor 7-like 1 (T-cell specific, HMG-box)	TCF7L1	104,,,,,,,,,,,,,	*
105	203222_s_at	transducin-like enhancer of split 1 (E(sp1) homolog, Drosophila)	TLE1	67,105,,,,,,,,,,,,,	
106	202210_x_at	glycogen synthase kinase 3 alpha	GSK3A	57,106,,,,,,,,,,,,,	*
107	203697_at	frizzled-related protein	FRZB	103,107,,,,,,,,,,,,,	
108	40837_at	transducin-like enhancer of split 2 (E(sp1) homolog, Drosophila)	TLE2	108,,,,,,,,,,,,,	*
109	221029_s_at	wingless-type MMTV integration site family, member 5B	WNT5B	109,,,,,,,,,,,,,	*
110	220640_at	casein kinase 1, gamma 1	CSNK1G1	64,110,,,,,,,,,,,,,	
111	214489_at	follicle stimulating hormone, beta polypeptide	FSHB	111,,,,,,,,,,,,,	*

## MCF7 v TAM treated





MCF7 v TAM treated



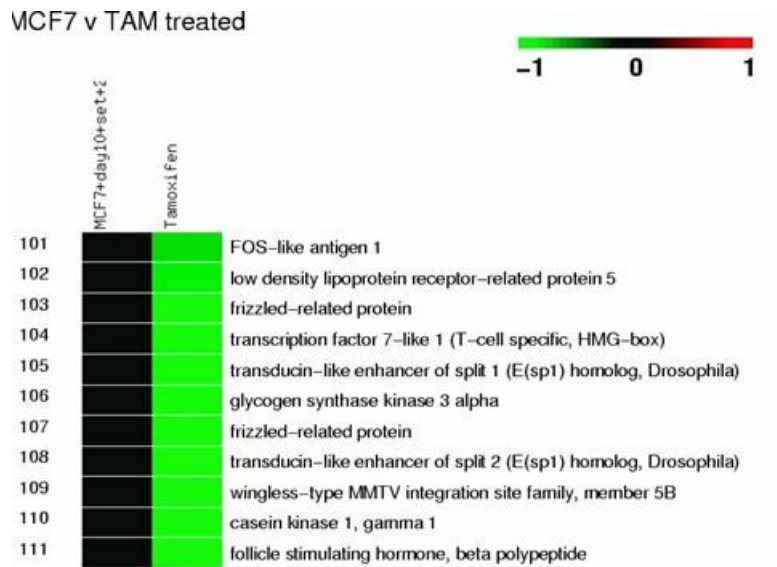


**Figure 9.2**  
**Heatmap for Wnt signalling probe set showing changes in gene expression between MCF-7 cells and MCF-7 cells treated with tamoxifen for 10 days.**

Rows 1-19 and rows 89 onwards show >1.5 fold change.

Note: row 19 = 1.5 fold difference.

Red signalled increased expression; green showed decreased expression of mRNA compared to MCF-7 controls (black).

**Table 9.3****Heatmap data for MCF-7 cells versus Fas-R cells**

Rows 1-14 and rows 86 onwards show &gt;1.5 fold change

Note: row 86 to 88 = 1.5 fold difference

Row	Other ID	Gene Name	Gene ID	Multiple probes	Significance by t-test
1	201700_at	cyclin D3	CCND3	1,,,,,,,,,	*
2	204712_at	WNT inhibitory factor 1	WIF1	2,,,,,,,,,	
3	221609_s_at	wingless-type MMTV integration site family, member 6	WNT6	3,,,,,,,,,	
4	208606_s_at	wingless-type MMTV integration site family, member 4	WNT4	4,,,,,,,,,	
5	40837_at	transducin-like enhancer of split 2 (E(sp1) homolog, Drosophila)	TLE2	5,,,,,,,,,	
6	215310_at	adenomatous polyposis coli	APC	6,13,15,54,,,,,,,,,	
7	206737_at	wingless-type MMTV integration site family, member 11	WNT11	7,,,,,,,,,	*
8	210248_at	wingless-type MMTV integration site family, member 7A	WNT7A	8,,,,,,,,,	
9	212073_at	casein kinase 2, alpha 1 polypeptide /// casein kinase 2, alpha 1 polypeptide pseudogene	CSNK2A1	9,48,57,,,,,,,,,	
10	201533_at	catenin (cadherin-associated protein), beta 1, 88kDa	CTNNB1	10,,,,,,,,,	*
11	208652_at	protein phosphatase 2 (formerly 2A), catalytic subunit,	PPP2CA	11,,,,,,,,,	

		alpha isoform			
12	220277_at	CXXC finger 4	CXXC4	12,,,,,,,,,	
13	203525_s_at	adenomatous polyposis coli	APC	6,13,15,54,,,,,, ,	
14	209630_s_at	F-box and WD repeat domain containing 2	FBXW2	14,76,,,,,,,,,	*
15	203526_s_at	adenomatous polyposis coli	APC	6,13,15,54,,,,,, ,	*
16	206562_s_at	casein kinase 1, alpha 1	CSNK1A1	16,19,22,33,,,, ,,,	*
17	206459_s_at	wingless-type MMTV integration site family, member 2B	WNT2B	17,74,,,,,,,,,	
18	203987_at	frizzled homolog 6 (Drosophila)	FZD6	18,,,,,,,,,	
19	208867_s_at	casein kinase 1, alpha 1	CSNK1A1	16,19,22,33,,,, ,,,	
20	213579_s_at	E1A binding protein p300	EP300	20,94,,,,,,,,,	
21	203697_at	frizzled-related protein	FRZB	21,96,,,,,,,,,	
22	208865_at	casein kinase 1, alpha 1	CSNK1A1	16,19,22,33,,,, ,,,	
23	205990_s_at	wingless-type MMTV integration site family, member 5A	WNT5A	23,34,,,,,,,,,	
24	200952_s_at	cyclin D2	CCND2	24,39,,,,,,,,,	
25	218122_s_at	SUMO1/sentrin/SM T3 specific peptidase 2	SENP2	25,,,,,,,,,	
26	218318_s_at	nemo-like kinase	NLK	26,,,,,,,,,	*
27	217729_s_at	amino-terminal enhancer of split	AES	27,,,,,,,,,	
28	209456_s_at	F-box and WD repeat domain containing 11	FBXW11	28,46,,,,,,,,,	
29	201219_at	C-terminal binding protein 2	ZRANB1	29,,,,,,,,,	

30	210835_s_at	C-terminal binding protein 2	CTBP2	30,50,55,93,,,,,	
31	205254_x_at	transcription factor 7 (T-cell specific, HMG-box)	TCF7	31,70,,,,,,,,,	
32	221245_s_at	frizzled homolog 5 (Drosophila)	FZD5	32,64,,,,,,,,,	
33	213086_s_at	casein kinase 1, alpha 1	CSNK1A1	16,19,22,33,,,,,	
34	213425_at	wingless-type MMTV integration site family, member 5A	WNT5A	23,34,,,,,,,,,	
35	214724_at	DIX domain containing 1	DIXDC1	35,,,,,,,,,	
36	221673_s_at	casein kinase 1, gamma 1	CSNK1G1	36,103,,,,,,,,,	
37	201466_s_at	jun oncogene	JUN	37,92,,,,,,,,,	
38	219993_at	SRY (sex determining region Y)-box 17	SOX17	38,,,,,,,,,	
39	200951_s_at	cyclin D2	CCND2	24,39,,,,,,,,,	
40	205648_at	wingless-type MMTV integration site family member 2	WNT2	40,,,,,,,,,	
41	218665_at	frizzled homolog 4 (Drosophila)	FZD4	41,,,,,,,,,	
42	206796_at	WNT1 inducible signaling pathway protein 1	WISP1	42,88,,,,,,,,,	
43	217681_at	wingless-type MMTV integration site family, member 7B	WNT7B	43,,,,,,,,,	
44	204602_at	dickkopf homolog 1 (Xenopus laevis)	DKK1	44,,,,,,,,,	
45	204451_at	frizzled homolog 1 (Drosophila)	FZD1	45,89,,,,,,,,,	
46	209455_at	F-box and WD repeat domain	FBXW11	28,46,,,,,,,,,	

		containing 11			
47	204052_s_at	secreted frizzled-related protein 4	SFRP4	47,77,,,,,,,,	
48	206075_s_at	casein kinase 2, alpha 1 polypeptide	CSNK2A1	9,48,57,,,,,,,,	
49	221113_s_at	wingless-type MMTV integration site family, member 16	WNT16	49,,,,,,,,	
50	210554_s_at	C-terminal binding protein 2	CTBP2	30,50,55,93,,,,,	
51	34697_at	low density lipoprotein receptor-related protein 6	LRP6	51,,,,,,,,	
52	221557_s_at	lymphoid enhancer-binding factor 1	LEF1	52,98,,,,,,,,	
53	200695_at	protein phosphatase 2 (formerly 2A), regulatory subunit A, alpha isoform	PPP2R1A	53,,,,,,,,	
54	216933_x_at	adenomatous polyposis coli	APC	6,13,15,54,,,,,, ,	
55	201220_x_at	C-terminal binding protein 2	CTBP2	30,50,55,93,,,,,	
56	202037_s_at	secreted frizzled-related protein 1	SFRP1	56,69,,,,,,,,	
57	212072_s_at	casein kinase 2, alpha 1 polypeptide	CSNK2A1	9,48,57,,,,,,,,	
58	219889_at	frequently rearranged in advanced T-cell lymphomas	FRAT1	58,,,,,,,,	
59	632_at	glycogen synthase kinase 3 alpha	GSK3A	59,67,,,,,,,,	
60	216587_s_at	frizzled homolog 8 (Drosophila)	FZD8	60,,,,,,,,	
61	221519_at	F-box and WD repeat domain containing 4	FBXW4	61,,,,,,,,	
62	204901_at	beta-transducin repeat containing	BTRC	62,71,,,,,,,,	
63	201349_at	solute carrier family	SLC9A3R	63,,,,,,,,	

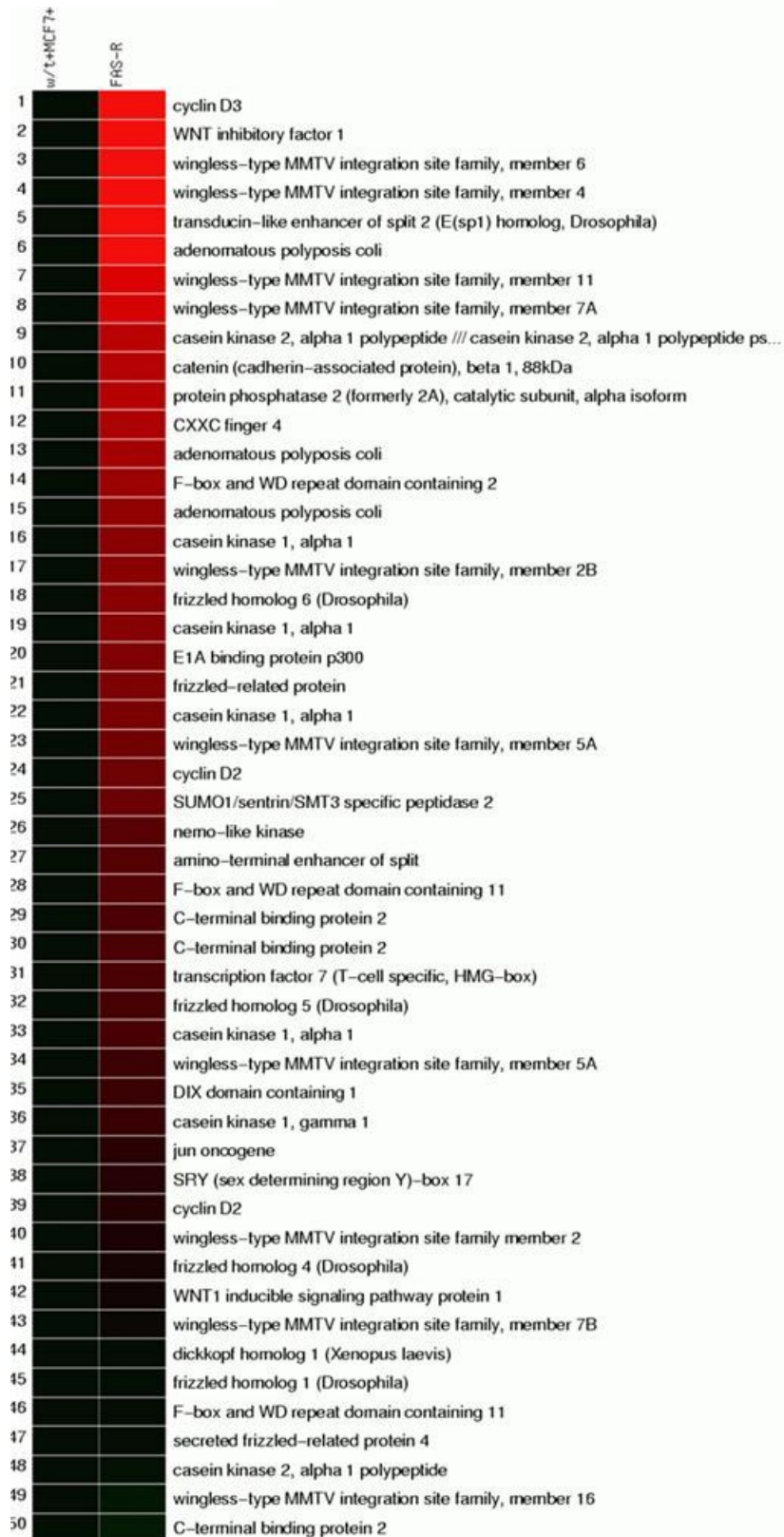
		9 (sodium/hydrogen exchanger), member 3 regulator 1	1		
64	206136_at	frizzled homolog 5 (Drosophila)	FZD5	32,64,,,,,,,,	
65	204129_at	B-cell CLL/lymphoma 9	BCL9	65,,,,,,,,	
66	207558_s_at	paired-like homeodomain 2	PITX2	66,,,,,,,,	
67	202210_x_at	glycogen synthase kinase 3 alpha	GSK3A	59,67,,,,,,,,	
68	221029_s_at	wingless-type MMTV integration site family, member 5B	WNT5B	68,,,,,,,,	
69	202036_s_at	secreted frizzled-related protein 1	SFRP1	56,69,,,,,,,,	
70	205255_x_at	transcription factor 7 (T-cell specific, HMG-box)	TCF7	31,70,,,,,,,,	
71	216091_s_at	beta-transducin repeat containing	BTRC	62,71,,,,,,,,	
72	221016_s_at	transcription factor 7-like 1 (T-cell specific, HMG-box)	TCF7L1	72,,,,,,,,	
73	208570_at	wingless-type MMTV integration site family, member 1	WNT1	73,,,,,,,,	
74	206458_s_at	wingless-type MMTV integration site family, member 2B	WNT2B	17,74,,,,,,,,	
75	203230_at	dishevelled, dsh homolog 1 (Drosophila) /// hypothetical LOC642469	DVL1	75,,,,,,,,	
76	218941_at	F-box and WD repeat domain containing 2	FBXW2	14,76,,,,,,,,	
77	204051_s_at	secreted frizzled-	SFRP4	47,77,,,,,,,,	

	at	related protein 4			
78	219483_s_at	porcupine homolog (Drosophila)	PORCN	78,,,,,,,,,	*
79	212863_x_at	C-terminal binding protein 1	CTBP1	79,100,,,,,,,,	
80	203081_at	catenin, beta interacting protein 1	CTNNB1	80,,,,,,,,,	
81	209945_s_at	glycogen synthase kinase 3 beta	GSK3B	81,,,,,,,,,	
82	202431_s_at	v-myc myelocytomatosis viral oncogene homolog (avian)	MYC	82,,,,,,,,,	
83	215517_at	pygopus homolog 1 (Drosophila)	PYGO1	83,,,,,,,,,	
84	209468_at	low density lipoprotein receptor-related protein 5	LRP5	84,,,,,,,,,	
85	219683_at	frizzled homolog 3 (Drosophila)	FZD3	85,,,,,,,,,	
86	221455_s_at	wingless-type MMTV integration site family, member 3	WNT3	86,,,,,,,,,	
87	206524_at	T, brachyury homolog (mouse)	T	87,,,,,,,,,	
88	211312_s_at	WNT1 inducible signaling pathway protein 1	WISP1	42,88,,,,,,,,	
89	204452_s_at	frizzled homolog 1 (Drosophila)	FZD1	45,89,,,,,,,,	
90	57532_at	dishevelled, dsh homolog 2 (Drosophila)	DVL2	90,102,,,,,,,,	*
91	207683_at	forkhead box N1	FOXN1	91,,,,,,,,,	
92	201465_s_at	jun oncogene	JUN	37,92,,,,,,,,	
93	215377_at	C-terminal binding protein 2	CTBP2	30,50,55,93,,,,,	
94	202221_s_at	E1A binding protein p300	EP300	20,94,,,,,,,,,	*
95	214489_at	follicle stimulating	FSHB	95,,,,,,,,,	

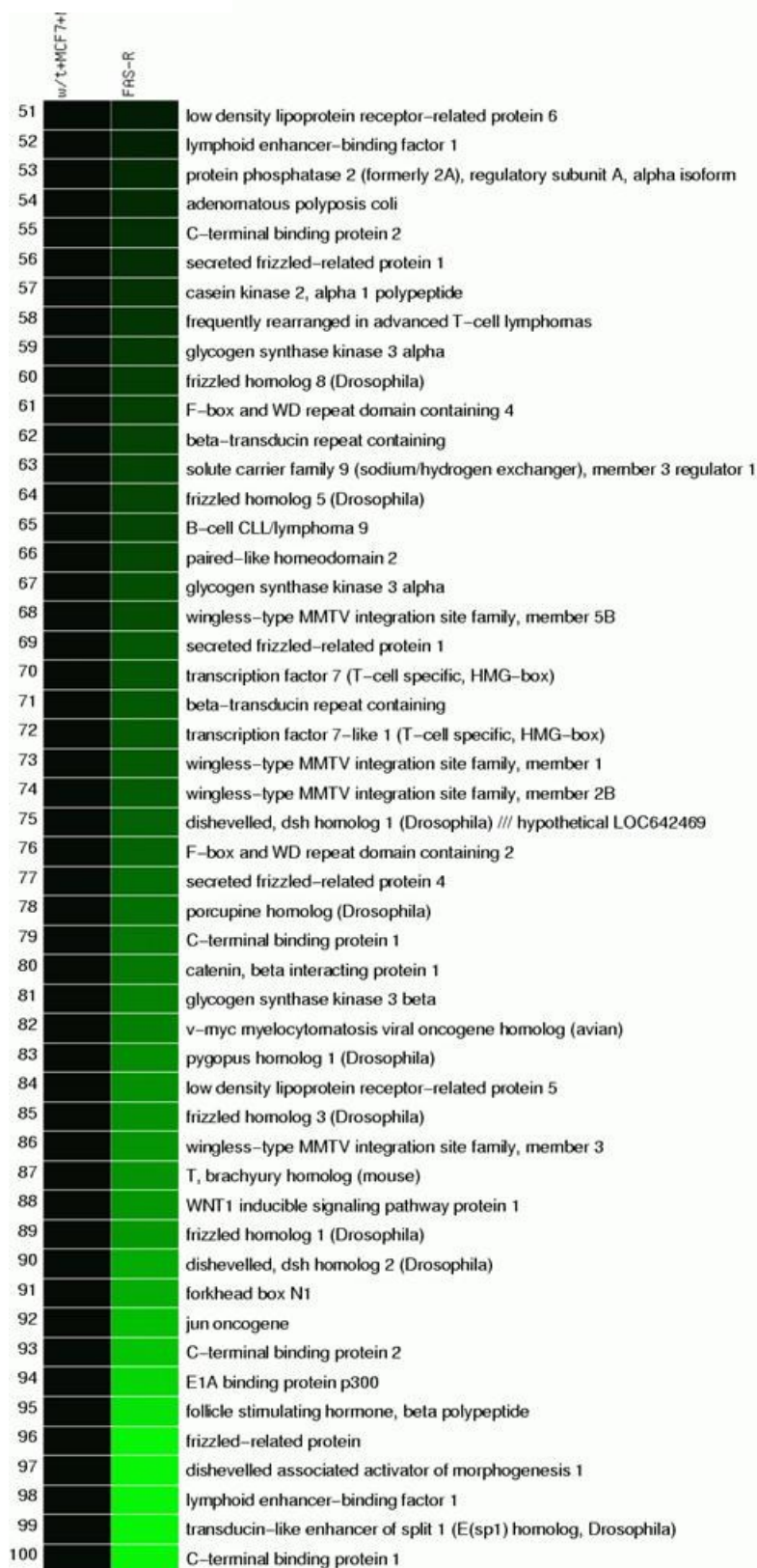


		hormone, beta polypeptide			
96	203698_s_at	frizzled-related protein	FRZB	21,96,,,,,,,,,	
97	216060_s_at	dishevelled associated activator of morphogenesis 1	DAAM1	97,,,,,,,,,	*
98	221558_s_at	lymphoid enhancer-binding factor 1	LEF1	52,98,,,,,,,,,	
99	203220_s_at	transducin-like enhancer of split 1 (E(sp1) homolog, Drosophila)	TLE1	99,108,,,,,,,,,	*
100	213980_s_at	C-terminal binding protein 1	CTBP1	79,100,,,,,,,,,	
101	208774_at	casein kinase 1, delta	CSNK1D	101,105,,,,,,,,,	*
102	218759_at	dishevelled, dsh homolog 2 (Drosophila)	DVL2	90,102,,,,,,,,,	*
103	220640_at	casein kinase 1, gamma 1	CSNK1G1	36,103,,,,,,,,,	
104	212849_at	axin 1	AXIN1	104,,,,,,,,,	*
105	207945_s_at	casein kinase 1, delta	CSNK1D	101,105,,,,,,,,,	*
106	208712_at	cyclin D1	CCND1	106,110,,,,,,,,,	*
107	203705_s_at	frizzled homolog 7 (Drosophila)	FZD7	107,,,,,,,,,	*
108	203222_s_at	transducin-like enhancer of split 1 (E(sp1) homolog, Drosophila)	TLE1	99,108,,,,,,,,,	
109	210220_at	frizzled homolog 2 (Drosophila)	FZD2	109,,,,,,,,,	*
110	208711_s_at	cyclin D1	CCND1	106,110,,,,,,,,,	*
111	204420_at	FOS-like antigen 1	FOSL1	111,,,,,,,,,	*

# MCF-7 vs log phase Fas-R



# MCF-7 vs log phase Fas-R



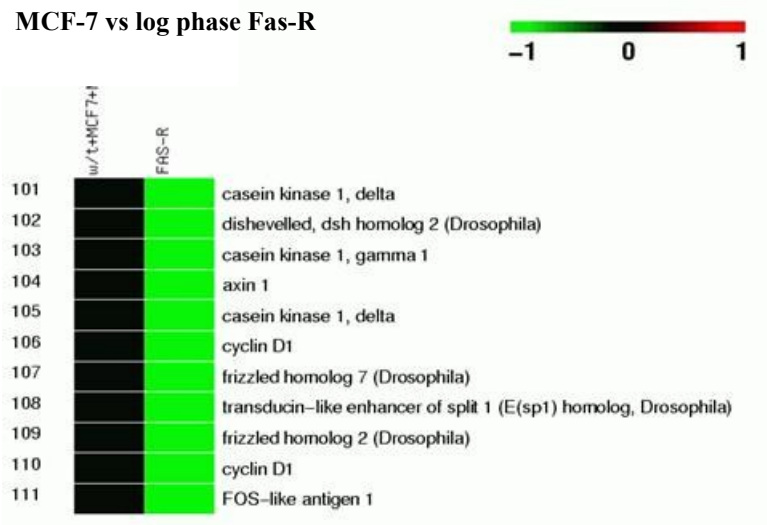


**Figure 9.3**  
**Heatmap for Wnt signalling probe set showing**  
**changes in gene expression between MCF-7 and**  
**Fas-R cells.**

Rows 1-14 and rows 86 onwards show >1.5 fold change.

Note: row 86 to 88 = 1.5 fold difference.

Red signalled increased expression; green showed decreased expression of mRNA compared to MCF-7 controls (black).

**Table 9.4**

**Heatmap data for MCF-7 cells versus MCF-7 cells treated with E2 [ $10^{-9}$ M] for 10 days**

Rows 1-19 and rows 82 onwards show > 1.5 fold change.

Note: row 81 = 1.5 fold difference.

Row	Other ID	Gene Name	Gene ID	Multiple probes	Sig by t-test
1	201465_s_at	jun oncogene	JUN	1,9,,,,,,,,	*
2	203525_s_at	adenomatous polyposis coli	APC	2,27,65,70,,,,,,,,	
3	34697_at	low density lipoprotein receptor-related protein 6	LRP6	3,,,,,,,,	
4	208712_at	cyclin D1	CCND1	4,8,,,,,,,,	*
5	213425_at	wingless-type MMTV integration site family, member 5A	WNT5A	5,110,,,,,,,,	
6	203987_at	frizzled homolog 6 (Drosophila)	FZD6	6,,,,,,,,	*
7	200952_s_at	cyclin D2	CCND2	7,45,,,,,,,,	*
8	208711_s_at	cyclin D1	CCND1	4,8,,,,,,,,	
9	201466_s_at	jun oncogene	JUN	1,9,,,,,,,,	*
10	202431_s_at	v-myc myelocytomatosis viral oncogene homolog (avian)	MYC	10,,,,,,,,	*
11	212073_at	casein kinase 2, alpha 1 polypeptide /// casein kinase 2, alpha 1 polypeptide pseudogene	CSNK2 A1	11,28,54, ,,,,,,	
12	216060_s_at	dishevelled associated activator of morphogenesis 1	DAAM1	12,,,,,,,,	*
13	206562_s_at	casein kinase 1, alpha 1	CSNK1 A1	13,15,17,19,,,,,,,,	
14	209630_s_at	F-box and WD repeat domain containing 2	FBXW2	14,84,,,,,,,,	
15	208865_at	casein kinase 1, alpha 1	CSNK1 A1	13,15,17,19,,,,,,,,	
16	201219_at	C-terminal binding protein 2	ZRANB 1	16,,,,,,,,	*
17	213086_s_at	casein kinase 1, alpha 1	CSNK1 A1	13,15,17,19,,,,,,,,	
18	201349_at	solute carrier family 9 (sodium/hydrogen exchanger), member 3 regulator 1	SLC9A3 R1	18,,,,,,,,	*
19	208867_s_at	casein kinase 1, alpha 1	CSNK1	13,15,17,	

			A1	19,,,,,,	
20	208652_at	protein phosphatase 2 (formerly 2A), catalytic subunit, alpha isoform	PPP2CA	20,,,,,,	
21	220277_at	CXXC finger 4	CXXC4	21,,,,,,	
22	218759_at	dishevelled, dsh homolog 2 (Drosophila)	DVL2	22,63,,,,, ,,,	
23	218318_s_at	nemo-like kinase	NLK	23,,,,,,	*
24	201533_at	catenin (cadherin-associated protein), beta 1, 88kDa	CTNNB1	24,,,,,,	
25	219683_at	frizzled homolog 3 (Drosophila)	FZD3	25,,,,,,	
26	209945_s_at	glycogen synthase kinase 3 beta	GSK3B	26,,,,,,	
27	203526_s_at	adenomatous polyposis coli	APC	2,27,65,70,,,,,	
28	212072_s_at	casein kinase 2, alpha 1 polypeptide	CSNK2A1	11,28,54, ,,,,,	
29	215377_at	C-terminal binding protein 2	CTBP2	29,30,31,32,,,,,	
30	210835_s_at	C-terminal binding protein 2	CTBP2	29,30,31,32,,,,,	
31	210554_s_at	C-terminal binding protein 2	CTBP2	29,30,31,32,,,,,	
32	201220_x_at	C-terminal binding protein 2	CTBP2	29,30,31,32,,,,,	
33	221558_s_at	lymphoid enhancer-binding factor 1	LEF1	33,73,,,,, ,,,	
34	221609_s_at	wingless-type MMTV integration site family, member 6	WNT6	34,,,,,,	
35	218122_s_at	SUMO1/sentrin/SMT3 specific peptidase 2	SEN2	35,,,,,,	
36	204451_at	frizzled homolog 1 (Drosophila)	FZD1	36,49,,,,, ,,,	
37	203230_at	dishevelled, dsh homolog 1 (Drosophila) /// hypothetical LOC642469	DVL1	37,,,,,,	
38	214724_at	DIX domain containing 1	DIXDC1	38,,,,,,	
39	221519_at	F-box and WD repeat domain containing 4	FBXW4	39,,,,,,	
40	203705_s_at	frizzled homolog 7 (Drosophila)	FZD7	40,,,,,,	
41	221673_s_at	casein kinase 1, gamma 1	CSNK1G1	41,107,,,, ,,,,,	
42	209456_s_at	F-box and WD repeat domain containing 11	FBXW11	42,48,,,,, ,,,	
43	204420_at	FOS-like antigen 1	FOSL1	43,,,,,,	
44	217681_at	wingless-type MMTV	WNT7B	44,,,,,,	

		integration site family, member 7B			
45	200951_s_at	cyclin D2	CCND2	7,45,,,,,,,,, ,	
46	210248_at	wingless-type MMTV integration site family, member 7A	WNT7A	46,,,,,,,,,	
47	201700_at	cyclin D3	CCND3	47,,,,,,,,,	
48	209455_at	F-box and WD repeat domain containing 11	FBXW1 1	42,48,,,,,, ,,,	
49	204452_s_at	frizzled homolog 1 (Drosophila)	FZD1	36,49,,,,, ,,,	
50	632_at	glycogen synthase kinase 3 alpha	GSK3A	50,98,,,,, ,,,	
51	206524_at	T, brachyury homolog (mouse)	T	51,,,,,,,,,	
52	216091_s_at	beta-transducin repeat containing	BTRC	52,56,,,,, ,,,	
53	219993_at	SRY (sex determining region Y)-box 17	SOX17	53,,,,,,,,,	
54	206075_s_at	casein kinase 2, alpha 1 polypeptide	CSNK2 A1	11,28,54, ,,,,,,	
55	211312_s_at	WNT1 inducible signalling pathway protein 1	WISP1	55,109,,,, ,,,,,	
56	204901_at	beta-transducin repeat containing	BTRC	52,56,,,,, ,,,	
57	213579_s_at	E1A binding protein p300	EP300	57,82,,,,, ,,,	
58	216587_s_at	frizzled homolog 8 (Drosophila)	FZD8	58,,,,,,,,,	
59	206459_s_at	wingless-type MMTV integration site family, member 2B	WNT2B	59,74,,,,, ,,,	
60	212863_x_at	C-terminal binding protein 1	CTBP1	60,64,,,,, ,,,	*
61	203081_at	catenin, beta interacting protein 1	CTNBNB P1	61,,,,,,,,,	
62	221245_s_at	frizzled homolog 5 (Drosophila)	FZD5	62,80,,,,, ,,,	
63	57532_at	dishevelled, dsh homolog 2 (Drosophila)	DVL2	22,63,,,,, ,,,	*
64	213980_s_at	C-terminal binding protein 1	CTBP1	60,64,,,,, ,,,	
65	216933_x_at	adenomatous polyposis coli	APC	2,27,65,7 0,,,,,,	
66	203220_s_at	transducin-like enhancer of split 1 (E(sp1) homolog, Drosophila)	TLE1	66,106,,,, ,,,,,	
67	206737_at	wingless-type MMTV	WNT11	67,,,,,,,,,	

		integration site family, member 11			
68	221455_s_at	wingless-type MMTV integration site family, member 3	WNT3	68,,,,,,,,,	
69	219483_s_at	porcupine homolog (Drosophila)	PORCN	69,,,,,,,,,	
70	215310_at	adenomatous polyposis coli	APC	2,27,65,7 0,,,,,	
71	204052_s_at	secreted frizzled-related protein 4	SFRP4	71,79,,,,, ,,,	
72	200695_at	protein phosphatase 2 (formerly 2A), regulatory subunit A, alpha isoform	PPP2R1 A	72,,,,,,,,,	*
73	221557_s_at	lymphoid enhancer-binding factor 1	LEF1	33,73,,,,, ,,,	
74	206458_s_at	wingless-type MMTV integration site family, member 2B	WNT2B	59,74,,,,, ,,,	
75	221113_s_at	wingless-type MMTV integration site family, member 16	WNT16	75,,,,,,,,,	
76	205255_x_at	transcription factor 7 (T-cell specific, HMG-box)	TCF7	76,89,,,,, ,,,	
77	207945_s_at	casein kinase 1, delta	CSNK1 D	77,86,,,,, ,,,	*
78	204129_at	B-cell CLL/lymphoma 9	BCL9	78,,,,,,,,,	*
79	204051_s_at	secreted frizzled-related protein 4	SFRP4	71,79,,,,, ,,,	
80	206136_at	frizzled homolog 5 (Drosophila)	FZD5	62,80,,,,, ,,,	
81	202037_s_at	secreted frizzled-related protein 1	SFRP1	81,104,,,, ,,,	
82	202221_s_at	E1A binding protein p300	EP300	57,82,,,,, ,,,	
83	208606_s_at	wingless-type MMTV integration site family, member 4	WNT4	83,,,,,,,,,	
84	218941_at	F-box and WD repeat domain containing 2	FBXW2	14,84,,,,, ,,,	
85	212849_at	axin 1	AXIN1	85,,,,,,,,,	
86	208774_at	casein kinase 1, delta	CSNK1 D	77,86,,,,, ,,,	*
87	215517_at	pygopus homolog 1 (Drosophila)	PYGO1	87,,,,,,,,,	*
88	219889_at	frequently rearranged in advanced T-cell lymphomas	FRAT1	88,,,,,,,,,	*
89	205254_x_at	transcription factor 7 (T-cell specific, HMG-box)	TCF7	76,89,,,,, ,,,	



90	207683_at	forkhead box N1	FOXN1	90,,,,,,,,,,	
91	204712_at	WNT inhibitory factor 1	WIF1	91,,,,,,,,,,	
92	218665_at	frizzled homolog 4 (Drosophila)	FZD4	92,,,,,,,,,,	*
93	208570_at	wingless-type MMTV integration site family, member 1	WNT1	93,,,,,,,,,,	
94	205648_at	wingless-type MMTV integration site family member 2	WNT2	94,,,,,,,,,,	
95	209468_at	low density lipoprotein receptor-related protein 5	LRP5	95,,,,,,,,,,	*
96	217729_s_at	amino-terminal enhancer of split	AES	96,,,,,,,,,,	*
97	221029_s_at	wingless-type MMTV integration site family, member 5B	WNT5B	97,,,,,,,,,,	
98	202210_x_at	glycogen synthase kinase 3 alpha	GSK3A	50,98,,,,,, ,,,	
99	221016_s_at	transcription factor 7-like 1 (T-cell specific, HMG-box)	TCF7L1	99,,,,,,,,,,	*
100	203698_s_at	frizzled-related protein	FRZB	100,103,, ,,,,,,	
101	207558_s_at	paired-like homeodomain 2	PITX2	101,,,,,,,,, ,	*
102	210220_at	frizzled homolog 2 (Drosophila)	FZD2	102,,,,,,,,, ,	*
103	203697_at	frizzled-related protein	FRZB	100,103,, ,,,,,,	
104	202036_s_at	secreted frizzled-related protein 1	SFRP1	81,104,,,, ,,,,,	
105	40837_at	transducin-like enhancer of split 2 (E(sp1) homolog, Drosophila)	TLE2	105,,,,,,,,, ,	*
106	203222_s_at	transducin-like enhancer of split 1 (E(sp1) homolog, Drosophila)	TLE1	66,106,,,, ,,,,,	*
107	220640_at	casein kinase 1, gamma 1	CSNK1 G1	41,107,,,, ,,,,,	
108	214489_at	follicle stimulating hormone, beta polypeptide	FSHB	108,,,,,,,,, ,	*
109	206796_at	WNT1 inducible signalling pathway protein 1	WISP1	55,109,,,, ,,,,,	
110	205990_s_at	wingless-type MMTV integration site family, member 5A	WNT5A	5,110,,,,, ,,,	
111	204602_at	dickkopf homolog 1 (Xenopus laevis)	DKK1	111,,,,,,,,, ,	*

## **9.2 Growth assays**

Wnt inhibitors were prepared by dissolving the powdered drug in DMSO. We wanted to show that DMSO did not affect MCF-7 or Tam-R growth. Dose response MTT growth assays were done using the two cell lines.

### **9.2.1 DMSO does not affect cell growth of MCF-7 and Tam-R cells in concentrations below 5 $\mu$ M**

MCF-7 and Tam-R cells were treated with DMSO (0 to 20 $\mu$ M concentrations) for 6 days and MTT assay was done as described in the materials and methods section. There was no significant change in cell growth with DMSO concentrations up to 5 $\mu$ M (Figure 9.4, Figure 9.5). Maximum DMSO concentration used in experiments was 2 $\mu$ M.

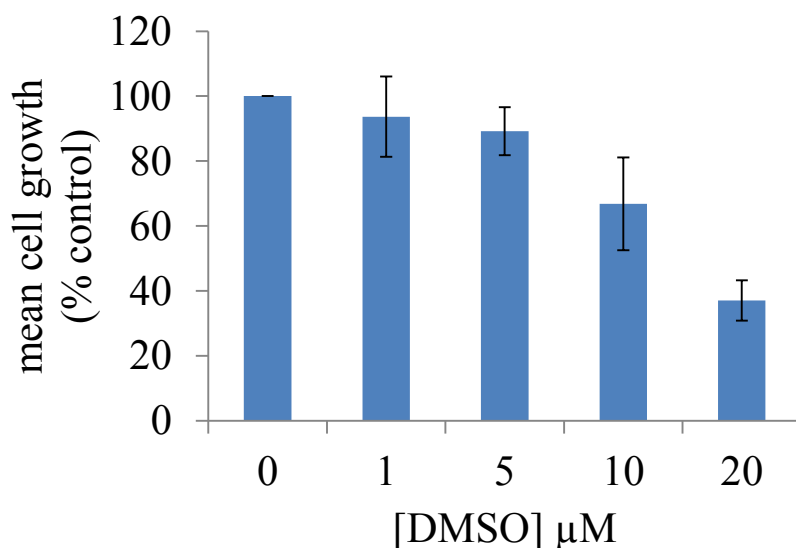


**Figure 9.4**  
**Effects of DMSO (6 days) on growth of MCF-7 cells**  
**as determined by MTT assay.**

MTT assay using MCF-7 cells treated with DMSO (0- 20  $\mu\text{M}$  concentrations) for 6 days was done as described in materials and methods section. There is no significant change in cell growth with DMSO concentrations up to 5 $\mu\text{M}$ . Error bars show SD (n=3, 24 wells).

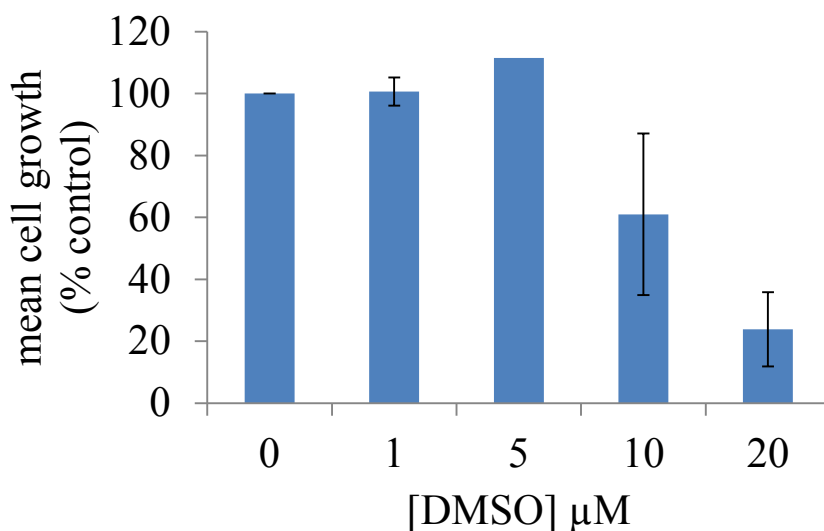


**Figure 9.5**  
**Effects of DMSO (6 days) on growth of Tam-R cells as determined by MTT assay.**

MTT assay using Tam-R cells treated with DMSO (0- 20  $\mu\text{M}$  concentrations) for 6 days was done as described in materials and methods section. There is no significant change in cell growth with DMSO concentrations up to 5 $\mu\text{M}$ . Error bars show SD (n=2, 16 wells except for DSMO 5 $\mu\text{M}$  where n=1; 8 wells).

**9.2.2 Dose effects of iCRT14 on growth of MCF-7 and Fas-R cell lines were determined by MTT assays**

Fas-R and MCF-7 cells show a similar growth response when treated with iCRT14 (Figure 9.6). There is some growth inhibition above iCRT14 concentrations of 12.5 $\mu$ M.

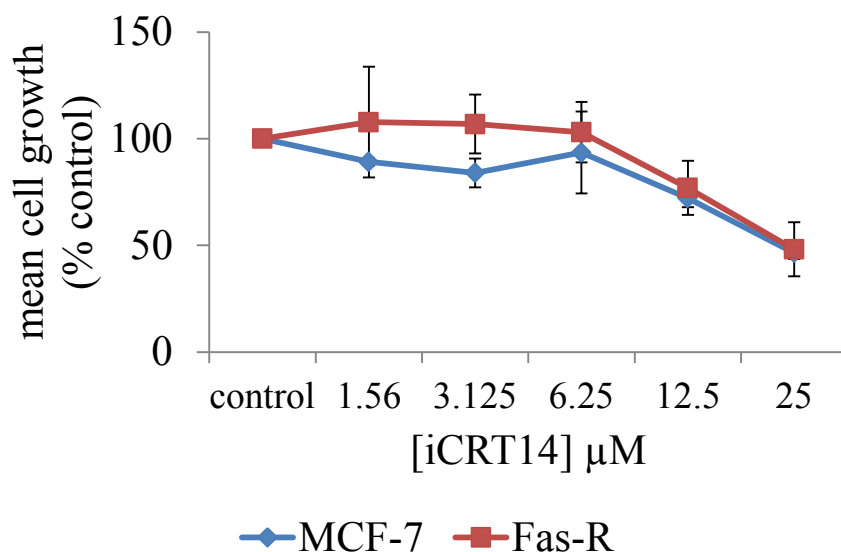


**Figure 9.6**  
**Effects of iCRT14 (6 days) on growth of MCF-7**  
**and Fas-R cells as determined by MTT assay.**

MTT assays using MCF-7 and Fas-R cells treated with iCRT14 (0- 25μM concentrations) for 6 days were done as described in materials and methods section. Fas-R cells and MCF-7 cells show similar inhibition of cell growth following treatment with iCRT14.

Error bars show SD (n=3, 24 wells for MCF-7 cells; n=2, 16 samples for Fas-R cells).